PTFE INITIATORS: THEIR INFLUENCE ON THE POLYMER PHYSICAL PROPERTIES

William Victor Venner

Faculty of Engineering, Built environment and Information Technology

Department of Chemical Engineering

University of Pretoria

A Dissertation Submitted in Partial Fulfilment of the Degree

Master of Engineering in Chemical Engineering

Supervisors:

Prof. Philip Crouse

Dr. Gerard Puts

December 2018

Acknowledgements

I would like to acknowledge, first and foremost, my supervisors Prof Philip Crouse and Dr Gerard Puts who, besides facilitating this research, prepared me for the rigours and challenges of the real world, which he must now enter, willingly or not.

I would like to especially acknowledge the technical and academic assistance of Dr Gerard Puts, who showed great patience and trust, even when it was clear I had no idea what I was doing. I also acknowledge and thank Mrs Suzette Seymore, as without her, the procurement processes would have been an insurmountable nightmare.

I would also like to thank the various funding bodies, including the FEI program, the Department of Science and Technology and The National Research Foundation, for contributing the funds and materials by which this research was conducted.

Executive Summary

The Fluorochemical Expansion Initiative (FEI) program was implemented to encourage the local beneficiation of South Africa's abundant fluorspar resources for the benefit of the economy. Fluoropolymer production was identified as an area in which technical expertise was decidedly lacking and which promised many opportunities for research and skills development.

Polytetrafluoroethylene (PTFE), also commonly referred to by its DuPont trade name, Teflon™, is the most well-known of the fluoropolymers. It is decidedly beneficial to develop expertise in the area of synthesis and characterisation of fluoropolymers, particularly PTFE. This polymer is synthesised *via* free radical polymerisation of TFE and can be initiated by a number of free radical initiators. A commonly used initiator is ammonium persulfate (APS). PTFE produced in this way experiences significant discolouration when subjected to temperatures in the region of 380 °C during the moulding process. The cause of the discolouration is unreported in the scientific literature, despite this discolouration being general knowledge within the fluoropolymer industry.

The research detailed herein was aimed at determining the cause of colour changes in thermally processed PTFE homopolymers. The research started with an in-depth review of the literature regarding the homopolymerisation of tetrafluoroethylene and included the types of end groups that could be formed from initiators as well as the infrared- and Raman spectroscopic identification of these end groups.

PTFE was synthesised in an autoclave *via* aqueous conventional radical polymerisation using ammonium- and metal persulfates, H_2O_2, $KMnO_4$ and di-tert-butyl peroxide, benzoyl peroxide as well as azo-based initiators. The synthesised PTFE was then subjected to differential scanning calorimetry, thermogravimetric analysis and Fourier-transform infrared- and Raman spectroscopy both before and after sintering. Care was taken to ensure the polymers were not contaminated with any initiator- or buffer residues.

It was found that the discolouration is caused by the decomposition of carboxylate end groups at elevated temperatures which deposit carbon into the polymer matrix. It was found to be generally true that higher initiator concentrations lead to more discolouration, because of more carbon being deposited into the matrix by eliminated end groups. It was also found that the use of buffering agents and the type of buffering agent used influence the type of end groups formed on the polymer chains.

Table of Contents

List of Abbreviations

Monomers

TFE	Tetrafluoroethylene	$CF_2=CF_2$

Polymers

PTFE	Polytetrafluoroethylene	$-(CF_2-CF_2)_n-$
PE	Polyethylene	$-(CH_2-CH_2)_n-$
PP	Polypropylene	$-(CH_2-CH(CH_3))_n-$

Initiators

APS	Ammonium persulfate
DTBP	Di-tertiary butyl peroxide
SPS	Sodium persulfate

Characterisation techniques

ATR	Attenuated total reflectance
FTIR	Fourier transform infrared spectroscopy
SS NMR	Solid state nuclear magnetic resonance spectroscopy
DSC	Differential scanning calorimetry
TGA	Thermogravimetric analysis
GPC	Gel permeation chromatography

Electromagnetic spectra

UV	Ultra-violet
IR	Infrared
Vis	Visible

Other abbreviations

FEI	Fluorochemical Expansion Initiative
FMG	Fluoro-Materials Group

List of Figures

List of Tables

Research outputs

Publications in peer-reviewed journals:

G.J. Puts, V. Venner, B. Ameduri, and P.L. Crouse (2018) Conventional and RAFT Copolymerization of Tetrafluoroethylene with Isobutyl Vinyl Ether. *Macromolecules,* **51 (17)**, 6724-6739. http://dx.doi.org/10.1021/acs.macromol.8b01286.

V. Venner, G.J. Puts, and P.L. Crouse (2018) Influence of initiators on the sintering discolouration of PTFE. *Journal of Fluorine Chemistry*, https://doi.org/10.1016/j.jfluchem.2018.10.017.

Conference contributions:

W.V. Venner en P.L. Crouse, Die effek van inisiatore op die fisiese eienskappe van politetrafluoroetileen, SAAWK Studentesimposium, Pretoria, 2-3 November 2017. (awarded 3rd place).

Chapter 1
General Introduction

Fluoro-compounds play a prominent, if somewhat unappreciated role in today's world. Fluorine containing compounds are everywhere, from the non-stick coating on your frying pan, to the medicines you take to improve your health. Apart from these everyday household uses, fluoro-materials are used in a diverse range of applications such as electronics, refrigeration, lubricants; and most relevant to this dissertation, engineering plastics.

Most fluorine that is used in a commercial capacity is obtained from the mineral fluorspar (CaF_2). This mineral is abundant in South Africa, which possesses the world's largest reserves, approximately 41 million tons. Currently, most of the fluorspar mined in South Africa is exported to China, where it is processed into higher value materials and products. South Africa then re-imports these materials and products at great cost. Therefore there is significant incentive to develop a beneficiation chain for fluorspar in South Africa, where the mined mineral can be processed into hydrogen fluoride (HF) and subsequently into fluorine gas (F_2) which can then be processed further to deliver high value materials for use in the South African commercial environment.

It is for this reason that the South African Government has initiated the Fluorochemical Expansion Initiative (FEI) program. This program hopes to encourage the local beneficiation of South Africa's abundant fluorspar resources for the benefit of the economy on a local and national level [1]. Fluoropolymers was identified as an area in which technical expertise was decidedly lacking and with many opportunities for research and skills development.

Probably the most well-known of the fluoropolymers is polytetrafluoroethylene (PTFE), also commonly referred to by its DuPont trade name, Teflon™. Ever since its accidental discovery in 1941 [2], a significant amount of research has been directed towards developing and understanding the synthetic pathways to prepare PTFE and its bulk physical properties [3]. Even though research in the field of fluoropolymers has shifted away from PTFE in recent years towards new growth fields such as TFE copolymers and the like, PTFE remains an important polymer in the worldwide commercial environment. Therefore it is decidedly beneficial to develop expertise in the area of synthesis and characterisation of fluoropolymers, particularly PTFE.

PTFE is synthesised by polymerising tetrafluoroethylene (TFE) gas. This is accomplished *via* free radical polymerisation which can be initiated by a number of free radical initiators. These initiators include, but are not limited to: persulfate compounds, strong oxidisers, redox compounds *etc.*

While the polymerisation of TFE using any of these types of initiators has been reported for well over half a century, there is a definite lack in the available literature of reports that document the

effects different initiators have on the polymer. Generally it is believed that with high molecular weight polymers such as PTFE that the type of initiator does not play a significant role in the mechanical properties of the polymer, because the end groups (functional groups present on the end of the polymer chains caused by the initiator) are present in such minute concentrations of the polymer overall.

However, PTFE produced by using initiators such as ammonium persulfate (APS) experiences significant discolouration when subjected to elevated temperatures in the region of 380 °C during sintering. Sintering is part of the special moulding processes PTFE must undergo to be formed into shapes. Unlike other polymers such as polypropylene (PP) or polyethylene (PE), PTFE cannot be injection moulded because of its extremely high melt viscosity. Therefore it must undergo special moulding processes to be formed into shapes. Besides the product colour, the choice of initiator also affects the thermal stability of the polymer. The patent literature indicates that the fluoropolymer industry employs perhalogenated initiators in PTFE synthesis to ensure the maximum thermal stability. The perhalogenated initiators also has the advantage of eliminating the discolouration phenomenon. Unfortunately, such perhalogenated initiators are expensive to produce.

It is believed the discolouration is caused by a chemical reaction or some form of a structural change within the end groups of the polymer chains at the elevated temperatures. The discolouration detrimentally impacts the commercial value of the PTFE. Very few, if any, commercial users of PTFE will purchase a yellow-brown product. For applications where thermal stability is not an issue, PTFE sealing tape used in domestic water supply systems being one example, the use of inexpensive initiators that are amenable to aqueous polymerisation may be preferred.

It is unlikely that the industry mindset will change regarding discoloured PTFE. Therefore, if the discolouration phenomenon could be understood and a mitigating strategy developed for initiators such as APS, a definite commercial advantage could be gained by small-scale PTFE producers who do not have the facilities to produce perhalogenated initiators.

The goal of this research was to determine whether it was in fact a change in the end groups which led to the discolouration of PTFE at elevated temperatures and which terminal structures resulted in the discolouration phenomenon.

PTFE was synthesised in an autoclave *via* aqueous conventional radical polymerisation using ammonium- and metal persulfates, H_2O_2, $KMnO_4$ and di-tert-butyl peroxide, benzoyl peroxide as

well as azo-based initiators. The virgin polymer was pressed into 20 mm discs at 160 MPa and then subjected to differential scanning calorimetry, thermogravimetric analysis and Fourier-transform infrared- and Raman spectroscopy both before and after sintering. Care was taken to ensure the polymers were not contaminated with any initiator- or buffer residues.

Chapter 2

Literature Review

Notes on literature review strategy

The Chemical Abstracts Service (CAS) SciFinder database, Scopus, Elsevier Reaxys, Google Scholar, Science Direct, SpringerLink, Wiley Online Library and Google Patents were employed to search for literature pertaining to the polymerisation of tetrafluoroethylene with particular focus on different initiators and end groups. Key phrases used included: "homopolymerisation of tetrafluoroethylene"; "polymerisation of tetrafluoroethylene"; "tetrafluoroethylene polymerisation"; "PTFE synthesis"; "PTFE end groups" and "end groups in PTFE".

Although there were some peer-reviewed research articles available in the open literature, many of them were written in either Russian, Mandarin or Japanese. Article in English were sparse, particularly in the early literature, with most of the English language, publically accessible literature consisting of patents or technical reports. The author realizes that patent documents are not good primary sources of scientific and technical data as they are not peer reviewed and specific technical data may be omitted or they may contain wilful falsification of results for the sake of misleading the competition. Nonetheless, the author has consulted them as primary literature due to the dearth of proper peer reviewed articles and due to the fact that the patent literature is the primary indicator of the research direction within the major commercial entities whom have been virtually the sole drivers of research into tetrafluoroethylene polymerisation.

There is considerable duplication in the literature, with patents being initially filed in the country of the originating commercial entity and subsequently in other countries, most commonly the US and the UK. In such cases the author consulted the earliest English language version of the publication, or, the earliest US Patent document were such a document is the only English version.

2.1 Polymerisation of TFE

Fluoropolymers exhibit unique and remarkable properties, largely due to the properties of fluorine. These include: high electronegativity, low polarisability, small van der Waals radius (1.32 Å) and the strong C−F bonds (485 $kJ \cdot mol^{-1}$) [4, 5]. Their applications span engineering thermoplastics and elastomers for chemical processes, automotive and aeronautics industries, weather-proof coatings, biomedical materials, membranes for use in lithium batteries, membranes in fuel cells, and many more.

Tetrafluoroethylene (TFE) is the monomer that is polymerised to deliver polytetrafluoroethylene (PTFE). PTFE was first reported by Plunkett [2]. The PTFE was produced under autogenous pressure at 25°C. TFE was found to autopolymerise inside its storage vessel over a number of days, forming a white powder. It was also reported that it formed low molecular weight waxes in

the presence of $AgNO_3$. Plunkett's patent also contained the first known report of PTFE depolymerisation, stating that the foamy product formed in the presence of $AgNO_3$ decomposed to TFE, leaving behind only a small amount of proper polymer.

PTFE and its marginally modified derivatives comprised approximately 60 % of the total international fluoropolymer market in 2015 [6, 7]. These polymers, both high molecular-mass materials and waxes, are chemically inert, hydrophobic, and exhibit superb thermal stability as well as an exceptionally low coefficient of friction. These polymers find use in applications ranging from coatings and lubrication to pyrotechnics, and an extensive industry (electronic, aerospace, wires and cables, as well as textiles) has been built around them.

The first method for free radical polymerisation of PTFE using ammonium persulfate was subsequently published by Brubaker [8] and since then, numerous methods have been reported whereby PTFE may be produced. Free radical polymerisation remains the most commonly employed methods for synthesising high molecular weight PTFE.

A large number of publications on the homo- and copolymerisation of TFE followed [9-26]), spanning processes such as free-radical-, co-ordination- [27] and electrochemical polymerisation [28, 29], with even plasma-type polymerisation being reported [30-33],

Because of the large volume of literature regarding the subject of TFE homopolymerisation, many contradictions exist in the literature regarding the most effective initiators and reaction conditions required to achieve the desired polymer properties. It must be noted here that the publications originating from universities and other academic institutions are done mostly in collaboration with commercial entities. As far as the author is aware, only Clemson University in the USA and the University of Pretoria in South Africa have direct access to multi-gram quantities of tetrafluoroethylene and operate independently from commercial entities

2.1.1 TFE

Tetrafluoroethylene (CAS No: 116-14-3) is an odourless, colourless and flammable gas with a density greater than air. TFE is highly unstable and the monomer may undergo auto-decomposition to carbon and CF_4 if heated to above 380 °C [34] and may self-polymerize under pressure. A summary of its properties is shown in Table 1.

Table 1: *Summary of the physical and chemical properties of tetrafluoroethylene [35].*

Property	Unit and numerical value			Reference
Molar mass	($g \cdot mol^{-1}$)		100.016	
Heat of formation	($MJ \cdot mol^{-1}$)		-63.31	[36]
Heat of combustion	($kJ \cdot mol^{-1}$)		-674	[36]
Heat of polymerisation	($kJ \cdot mol^{-1}$)		-196	[37]
Melting point	(°C)		-142.5	[38]
Boiling point	(°C)	[101.325 kPa]	-76.3	[38]
Triple point	(°C)		-131.2	[39]
Solid density	($g \cdot cm^{-3}$)	[-173.15 °C]	2.1	[40]
Liquid density	($g \cdot cm^{-3}$)	[-76.3 °C]	1.519	[41]
		[-142.5 °C]	1793	[41]
Critical temperature	(°C)		33.3	[42]
Critical pressure	(Bar)		39.44	[42]
Critical density	($g \cdot cm^{-3}$)		0.5815	[42]
Acentric factor			0.226	[42]
Solubility		Water at 25 °C	153 $mg \cdot L^{-1}$	[43]

Tetrafluoroethylene cannot be obtained easily from commercial sources, although small quantities can be purchase from speciality chemical suppliers.

There are numerous methods to produce TFE with the most salient examples being ultra-fast pyrolysis of chlorodifluoromethane, ultra-fast plasma pyrolysis of tetrafluoromethane [44, 45], dechlorination of CF_2Cl-CF_2Cl , or the debromination of CF_2Br-CF_2Br , pyrolysis of trifluoroacetic acid or the alkali salts of perfluoropropanoic acid [46] and the pyrolysis of polytetrafluoroethylene under vacuum [47]. These methods have been extensively reviewed elsewhere [48] and are summarised in Figure 1, so the following discussion is only a brief overview of the synthetic routes for TFE production. The various methods will not be discussed in detail here. For more detail, the doctoral thesis of Dr. GJ Puts [35] may be consulted.

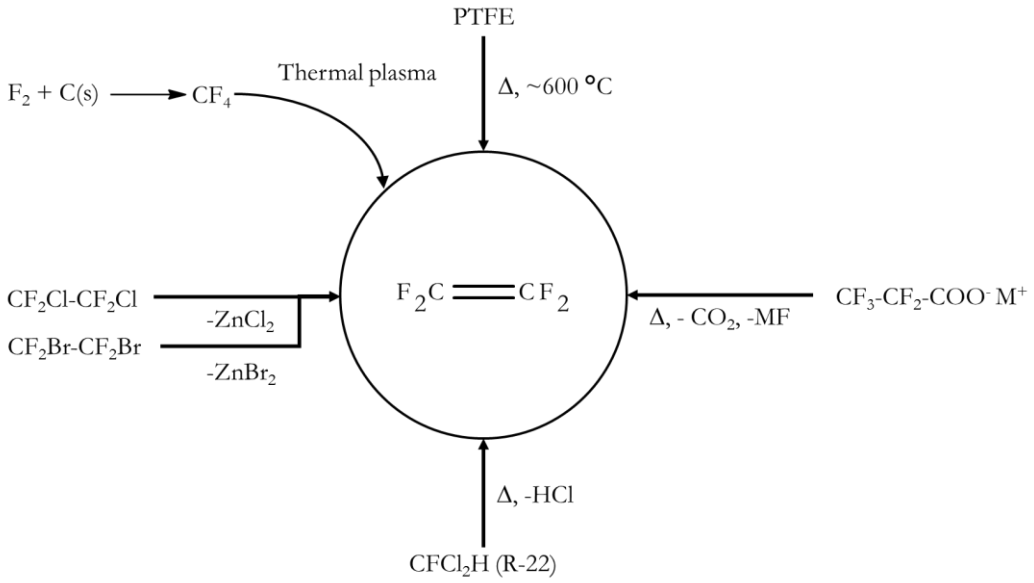

Figure 1: *Summary of the common synthetic routes for the production of TFE [35].*

PTFE may be pyrolysed under a vacuum of around 1 Pa at 600°C, to yield nearly pure (99.5 %) TFE, with minor amounts of HFP, OFCB and PFIB [49]. This method is practically achievable with the available resources at the FMG and does not require any expensive reagents or complex equipment. Such a system was designed and constructed at the University of Pretoria [35]. The pyrolysis reactions are summarised in Figure 2 and Figure 3.

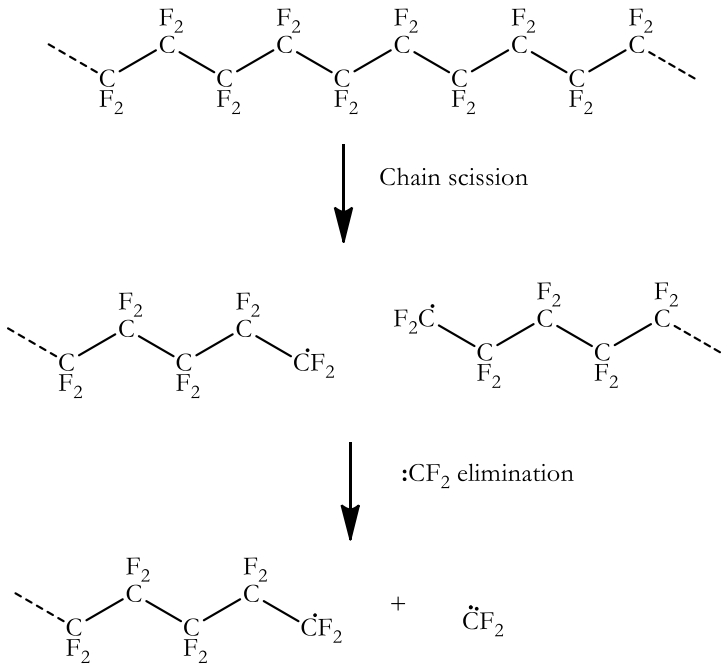

Figure 2: *Mechanism of PTFE breakdown by thermal chain scission to eliminate difluorocarbene [35].*

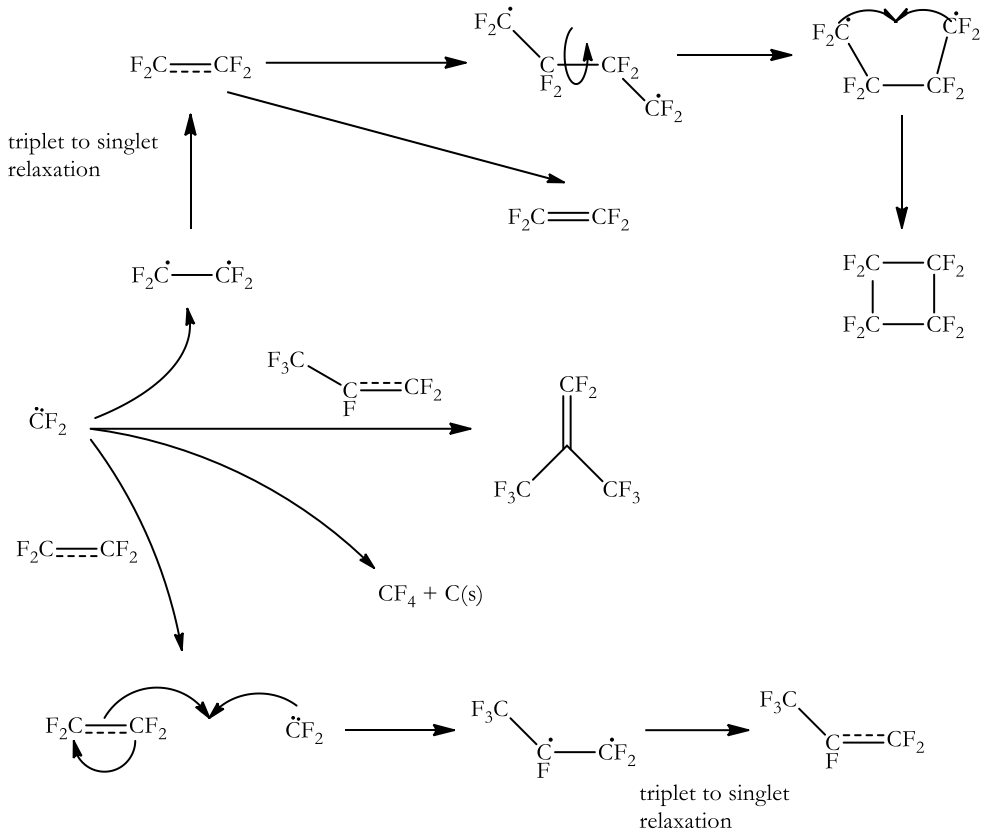

Figure 3*:* *Gaseous radical reactions occurring during PTFE pyrolysis which lead to the formation of TFE and fluorocarbon byproducts [35].*

2.1.2 Process safety

Safety is paramount when considering working with tetrafluoroethylene as it can and often does explode. This is usually due to lack of caution on the part of the people working with the substance. While 1 or 2 g quantities may burst a tube or a cylinder, larger amounts tend to do significant damage to infrastructure and at the 10 or 20 g scale, the detonating power of enclosed TFE is truly frightening and should give anyone pause for thought.

The companies and public entities who engage in working with TFE have developed facilities and expertise through long years of trial and error, many times at the cost of human life [35]. The Thrasher Group at Clemson University has spent years developing academic barricades to permit the safe use of large quantities of TFE in their facilities and their recent publication on the topic is well worth the read [50].

The safety aspects detailed here are meant to guide and inform, but are no substitutes for experience and all work done with TFE should be carried out in sub gram quantities before being scaled up to any size. Tetrafluoroethylene is dangerous to work with and care must be taken to avoid subjecting TFE to conditions where it may auto-polymerise or auto-decompose. The

mechanism of decomposition has been discussed in detail elsewhere [34, 49, 51-55] and Puts [35] gives a very good summary of these findings.

Institutions working with TFE have all developed their own rules for the handling of TFE, and some rules of thumb have been extracted from both the literature as well as other people's years of experience developed at the Nuclear Energy Corporation of South Africa.

A good rule of thumb gathered from the literature is: **Do not heat TFE above 100 °C when the gas is under a pressure of greater than 15 Bar**. The second rule of thumb is: **Do not subject TFE to large pressure changes at any temperature**. A technical implication of this rule is that TFE should not be subjected to sudden, drastic changes in flowpath diameter. This means that tubing should be of a consistent size throughout and any valves employed should have internal diameters of size similar to the tubing employed. In a similar vein, the flow of TFE through a valve should be sufficiently slow to ensure that there is little frictional heating of the gas.

The author's own experience with TFE, as well as conventional wisdom employed at the Nuclear Energy Corporation of South Africa's Applied Chemistry Laboratories, teaches that TFE should preferably not be pressurised to greater than 20 Bar when doing polymerisation experiments [35].

Also oxygen normally acts as an inhibitor to polymerisation, but in the case of TFE, the presence of oxygen will not only inhibit polymerisation, but will also worsen any decomposition reaction [55]. Indeed, if sufficient oxygen is present alongside TFE, it may initiate a spontaneous decomposition under pressure.

Therefore, a third good rule of thumb is: **Rigorously scrub free oxygen from any closed system containing TFE.**

The polymerisation reaction itself is also highly exothermic (ΔH_R = -196 kJ/mol) [37], and care must be taken to ensure that the heat generated be quickly removed. Therefore, jacketed reactors are not recommended as the thermal lag in a jacketed system is sufficiently large to permit the system to reach deflagration temperatures. Rather, an immersed cooling coil should be used, or preferably, a jacket and coil system should be used to ensure that the reaction medium is cool and that there are no severe thermal gradients in the polymerisation reactor.

The use of additives also plays a role in the removal of the heat of reaction, as in large polymerisation kettles, there is a noticeable improvement in heat transfer within the reactor if emulsion polymerisation is employed (as compared to precipitation polymerisation) [56].

Solvents other than water may be used as reaction medium. Although TFE is only sparingly soluble in water, it is easily solubilised in fluorinated and partially fluorinated solvents. A danger exists here in that if the concentration of the TFE in the solvent is sufficiently high, local hotspots may develop even in the presence of proper cooling, leading to runaway reactions and an explosion.

Experience at the Nuclear Energy Corporation of South Africa shows that performing batch polymerisation reactions (*i.e.* 20 g of TFE in a 330 ml autoclave) using perfluorodecalin as solvent always leads to a runaway reactions and explosions [35].

For this reason, use of solvents other than water should be avoided when performing batch reactions and, when solvents in which TFE is highly soluble are employed, it should rather be done in a continuous monomer and initiator dosing mode, with strict control over the amount of TFE present in the kettle at any given time.

There are a variety of methods by which TFE may be prepared, not all of them suited to a laboratory setting, and while some synthesis routes are facile and inexpensive, the use of tetrafluoroethylene brings with it significant risk to the researcher. Importantly, care should be exercised regarding selection and sizing of gas handling equipment as well as the amount of TFE stored and its storage location, with a make-and-use strategy being preferred over make-and-store.

2.1.3 PTFE synthesis

Tetrafluoroethylene is gaseous at standard conditions and is sparingly soluble in water, so high pressure equipment must be employed in the polymerisation process. Laboratory scale work may take place in thick glass ampoules or in stainless steel autoclaves; however, industrial scale polymerisation primarily takes place in large, high-pressure, stirred tank reactors.

TFE is usually polymerised in water in the presence of an initiator, a surfactant and other additives [4]. Two different regimes of polymerisation are common for production of different types of PTFE. These are suspension/precipitation and dispersion/emulsion polymerisation.

Suspension polymerisation is the route to production of coarse or granular resins and has been known for a long time, first being described in US patent 2 393 967 in 1946 [8]. It retains the majority of today's market. In this regime TFE is polymerised aqueously in the presence of water-soluble initiators such as ammonium persulfates, percarbonates, perphosphates, perborates or water-soluble redox initiators, accompanied by vigorous agitation. Buffers and precipitants are also usually added in the course of polymerisation. If appropriate, the aqueous polymerisation medium can also contain small amounts of perfluorinated emulsifiers which are inactive to

polymerisation, such as salts of perfluorocarboxylic acids. This prevents the polymer produced from remaining as a colloidal dispersion in the aqueous medium [57].

Dispersion or emulsion polymerisation is the method by which fine powder products are manufactured. Fine powder resins are also called coagulated dispersions, which is descriptive of their production method. Milder agitation, a dispersion agent (or surfactant) and an anti-coagulant set the dispersion polymerisation apart from the suspension method. The product often comes out as a waxy substance. Finishing processes convert the waxy substance to dispersion and fine powder products [4].

Homopolymers of PTFE are completely linear without detectable branches, unlike polyethylene. TFE polymerises linearly without branching which gives rise to a virtually perfect chain structure up to rather high molecular weights. The chains have minimal interactions and crystallise to form a nearly completely crystalline structure [4]. This highly crystalline form of PTFE is undesirable for commercial applications. The only way to counteract this is by increasing the molecular weight of the polymer. This is done by controlling the crystallinity of the polymer upon recrystallization after it has been remelted. The extremely long chains of PTFE have a much better probability of chain entanglement in the molten phase and little chance to crystallise to the same extent as before remelting. It is for this reason that commercial PTFE is polymerised to $10^6 – 10^7$ [4]. The molecular weight of PTFE can be controlled by means of polymerisation parameters such as initiator content, telogens and chain transfer agents.

Ordinary suspension polymerisation is not employed in industry as the properties of the product polymer cannot meet current product specifications. All polymerisation used to date is some form of dispersion polymerisation, but, with granular PTFE grades produced by a process bordering on the suspension precipitation method, as only a tiny amount (2 to 200 ppm) of dispersive agent is employed [35].

Furthermore, most of the polymerisation processes, as practiced, do not produce a true TFE homopolymer, but rather a "modified PTFE". This entails adding a small amount($\leq$ 0.6 mol %) of a fluorinated comonomer, such as perfluoromethyl vinyl ether, to produce a TFE high polymer containing small amounts of modifier, just sufficient to impart the mechanical properties required for the moulding process [58].

The granular grades are employed in powder moulding processes whereas the fine suspensions are employed in dispersion coating of metals and other substrates, impregnation of textiles and fibres, the preparation of films and varnish as well as paste extrusion fabrication processes [35].

A consequence of the high molecular weight of PTFE is its immense melt viscosity. Its melt viscosity is far too high for melt processing in extrusion or injection moulding.

Generally PTFE is produced by batch polymerisation under elevated pressure in specially designed reactors. The polymerisation media (the solvent) is high purity water, which is devoid of inorganic and organic impurities that impact the reaction by inhibition and retardation of the free radical polymerisation. It can also lead to chain transfer which yields products with undesirable properties. The surfactant of choice in these reactions is anionic. A perfluorinated carboxylic ammonium salt containing 7 - 20 carbon atoms is often used [5]. The dispersant is usually added in concentrations of 5 – 500 ppm, which is sufficient to cause formation of colloidal polymer particles [4].

TFE easily polymerises at moderate pressures and temperatures. The reaction is highly exothermic and it is therefore necessary to control the rate of reaction and to transfer the heat generated by the reaction.

Relatively inert organic compounds such as saturated hydrocarbons inhibit the polymerisation reaction unless their solubility in water is very low. Paraffins up to C_{12} inhibit, while longer paraffins are less inhibitive due to their low aqueous solubility [4].

2.1.4 Reaction kinetics

Tetrafluoroethylene may be polymerised batch wise, semi-batch wise, or continuously, with semi-batch using continuous dosing of TFE as the preferred industrial method. Some reaction kinetics have been reported, but there remains a dearth of information on the temperature dependence of the propagation and termination rates. Significant research scope exists in terms of determining the kinetics of polymerisation and, in particular, the effects of temperature and pressure on the molecular weight distribution of PTFE.

In the absence of chain transfer agents or other materials which may prematurely terminate the growing macroradical, the only kinetic parameters are initiation (k_i), propagation (k_p) and mutual termination (k_{td}). Measurement of the propagation and termination parameters are somewhat difficult as PTFE cannot be subjected to GPC, but there are scattered reports in the literature.

Plyusnin and Chirkov [59] estimated the elementary rate constants for free-radical polymerisation in water at 40 °C by measuring the active chain end concentrations using 2,2,6,6-tetramethyl-4-piperidinol and found the rates of propagation dead-end termination (k_p and k_t) to be 7400 and 74 $L \cdot mol^{-1} \cdot s^{-1}$, respectively. These parameters correspond to the well-known variables in Tobolsky's relation [60].

Xu *et al* [61] reports a $k_p \cdot k_t^{-0.5}$ of 0.38, but no further kinetic data is given.

2.1.5 Reaction conditions

TFE monomer purity

Tetrafluoroethylene used in polymerisation should be as pure as possible, with a 99.99 % pure material classified as "polymerisation grade". Impurities usually come from the production process, with substances such as CF_4, HFP, $C_2F_3H_3$, $C_2F_2H_4$ and C_2F_6 *etc.* being the typical contaminants. The contaminants either affect the solubility of TFE in the reaction medium or act as chain transfer agents. Both have deleterious effects on the reaction rate, product yield, molecular mass and thermal stability of the final product. Specifically in the case of HFP, the contaminant may co-polymerise with TFE, but the reaction rate is so low that most of the HFP simply remains unreacted, crowding the TFE out of the reaction medium and blanketing the gas-liquid interface, forming an additional layer through which TFE must diffuse before it reaches the actual reaction zone, *etc.*

Solvents

Tetrafluoroethylene may be polymerised either in the gas- or liquid phase, both autogenously [62], or in the presence of a suitable radical source, but because this bulk reaction cannot be easily controlled, it is preferred to polymerise TFE in the presence of a liquid carrier. As pointed out by Brubaker [8], the choice of solvent depends on the initiator used, heat transfer considerations and inertness to the polymerisation process as well as the solubility of the monomer.

Solvents may be completely avoided if gaseous photoinitiators are used in conjunction with UV light, but, as with bulk free radical polymerisation, removal of the heat of reaction is an issue that limits the commercial feasibility [35].

A large number of solvents can be used for polymerisation. However, owing to the electron withdrawing effects of fluorine, the radical chain ends of the fluoromacroradical are highly electrophilic and proton transfer occurs readily between the macroradical and conventional polymerisation solvents [63]. Therefore, hydrocarbon solvents cannot be used for the synthesis of perfluorinated high polymers by free radical mechanism. Of the conventional solvents employed in polymer synthesis, only water seems to be completely inert toward the radicals of fully fluorinated monomers [35].

Temperature and Pressure

The temperature and pressure conditions inside the polymerisation kettle are of utmost importance, as the kinetics of reaction, and consequently, polymer yield and molecular weights are dependent thereon. Furthermore, operating temperature and pressure need to be taken into account when designing the reactor system in order to ensure the process operates within safety limits. In general, the operating pressure is determined by the equipment employed. TFE may spontaneously decompose under pressure, resulting in a pressure spike within the reactor and may result in an explosion. The upper pressure limit is determined by temperature and the vessel size, but is generally set at 90 bar [35].

In free-radical polymerisation the operating temperature is selected based on the decomposition kinetics of the initiator, but in general, the polymerisation temperatures do not exceed 150 °C. For example, Brubaker reports that, for optimal results, the free-radical polymerisation should be carried out at 20 atm or higher of TFE pressure and at temperatures around 80 °C. He reports polymer yields in the range of 80 % to 100 % at these conditions. Polymerisation may be performed at ambient temperatures using photoinitiation methods such Gamma or UV light, with the temperature of a UV photoinitiated polymerisation reaction being determined by the temperature required to keep the initiator and other additives in the gas phase.

TFE will polymerise even at low pressures but in the case of gas phase polymerisation such as photoinitiation by UV, the kinetics and therefore, the molecular mass of the PTFE obtained, as well as the yield, is determined by the partial pressure of TFE. The higher the pressure, the greater the yield and molecular mass. For liquid phase polymerisation and in particular, polymerisation in water, the concentration of TFE in the aqueous phase is determined by the pressure of TFE above it according to Henry's law. Naturally, the solubility of TFE is also determined by the reactor temperature.

The greater majority of polymerisation operations are isothermal in nature, with the reactors starting at some ambient temperature, being ramped up to the reaction temperature and then maintained at this temperature for the duration of the operation.

pH Buffering Agents

As previously stated, pH controllers include borax [64, 65], NaOH, HCl, acetic acid, K_2CO_3, NH_4CO_3 [66] or buffer mixtures. The role of the pH controller is primarily to ensure that the aqueous polymerisation medium does not adversely affect the initiator performance and that

metals from the materials of construction are not leached into the reaction mixture, with typical pH values range from 7 to 11 [67]. In non-aqueous media, buffering agents are not required.

The choice of buffering agent must be carefully considered as it not only adds to the cost of the polymer, but may contaminate the polymer and cause problems in the end application, may undergo proton transfer leading to premature termination and low molecular masses.

Summary

The PTFE synthesis process is highly sensitive to factors such as monomer purity and the presence of chain transfer agents and one is restricted to a narrow range of solvents. For any kind of polymerisation, perfluorinated liquids are the solvent of choice, with water following after them as the most stable solvent. The future of PTFE production resides in supercritical carbon dioxide as this solvent negates much of the problems associated with perfluorinated surfactants as well as the concerns over water wastage.

2.1.6 Initiators

The initiators used in TFE polymerisation are crucial to thermal stability, colour and molecular weight. All these attributes are in some way, functions of the initiator and its subsequent end group.

Polymerisation of TFE proceeds by a free radical mechanism. The reaction is initiated either by a catalyst or by an initiator, depending on the reaction temperature. If polymerisation is carried out at low temperatures (<30°C), a redox catalyst is used. These compounds ionise into charged fragments such as $KMnO_4 \rightarrow K^+ + MnO_4^-$ [68]. Bisulfites, persulfates or other organic compounds are the typical initiators for higher temperature TFE polymerisation. At lower temperatures the effectiveness of the organic compounds is diminished due to insufficient decomposition rate.

Free radical initiators

Peroxy compounds are often used for free radical polymerisation, particularly those that can be thermally activated. The reaction scheme for a persulfate initiator is described as follows [4]:

The persulfate degrades under heat to form free radicals:

$$K_2S_2O_8 \xrightarrow{\Delta} 2S\dot{O}_4^- + 2K^+$$

Initiation takes place by formation of new free radicals when the persulfate radicals react with TFE dissolved in the aqueous phase:

$$S\dot{O}_4^- + CF_2{=}CF_2 \rightarrow SO_4(CF_2\text{-}CF_2)\cdot$$

Propagation takes place by further addition of TFE:

$$SO_4^-(CF_2\text{-}CF_2)\cdot + n\ CF_2{=}CF_2 \rightarrow SO_4^-(CF_2\text{-}CF_2)_n\text{-}(CF_2\text{-}CF_2)\cdot$$

Free radicals undergo hydrolysis where a hydroxyl end group replaces the sulfate:

$$SO_4^-(CF_2\text{-}CF_2)_n\text{-}(CF_2\text{-}CF_2)\cdot + H_2O \rightarrow HO(CF_2\text{-}CF_2)_n\text{-}(CF_2\text{-}CF_2)\cdot + H^+ + HSO_4^-$$

$$HO(CF_2\text{-}CF_2)_n\text{-}(CF_2\text{-}CF_2)\cdot + H_2O \rightarrow COOHCF_2\text{-}(CF_2\text{-}CF_2)_n\cdot + 2HF$$

Termination takes place when two of these free radicals combine:

$$COOHCF_2\text{-}(CF_2\text{-}CF_2)_n\cdot + COOHCF_2\text{-}(CF_2\text{-}CF_2)_m\cdot \rightarrow COOH\text{-}(CF_2\text{-}CF_2)_{m+n}\text{-}COOH$$

There are alternative courses of hydrolysis that can affect the end group at a different stage of the polymerisation. However, the key point is that there is no sulfur when persulfate is the initiator [69]. Bisulfite initiators form sulfonic acid end groups [70]. The reactions of free radicals with saturated molecules have appreciable activation energies and negative entropies of activation. It is for this reason that termination by disproportionation and transfer to monomer and polymer are not favourable [71].

Ideally, a thermal free radical initiator should be relatively stable at room temperature but should decompose rapidly enough at the polymerisation reaction temperature to ensure a practical reaction rate. In addition to the temperature, the decomposition rate (k_d) of the initiator depends on the solvent used. The decomposition rate is affected by what is known as the *cage effect*.

Cage effect

The *cage effect* describes how the properties of a molecule are affected by its surroundings. First introduced by Franck and Rabinowitch in 1934 [72, 73] the cage effect suggest that molecules in solvents are more accurately described as an encapsulated particle [74, 75]. It is this confining effect of solvent molecules that causes secondary reactions which may include the recombination of radicals to regenerate the initiator. In order to interact with other molecules, the caged particle must diffuse from its solvent cage. The typical lifetime of a solvent cage is 10^{-11} s [76]. In free radical polymerisation, radicals formed from the decomposition of an initiator molecule are surrounded by a cage consisting of solvent and/or monomer molecules [74]. Within the cage, the free radicals undergo many collisions leading to their recombination or mutual deactivation [74, 75, 77]. After recombination, free radicals can either react with monomer molecules within the cage walls or diffuse out of the cage. This is shown in Figure 4.

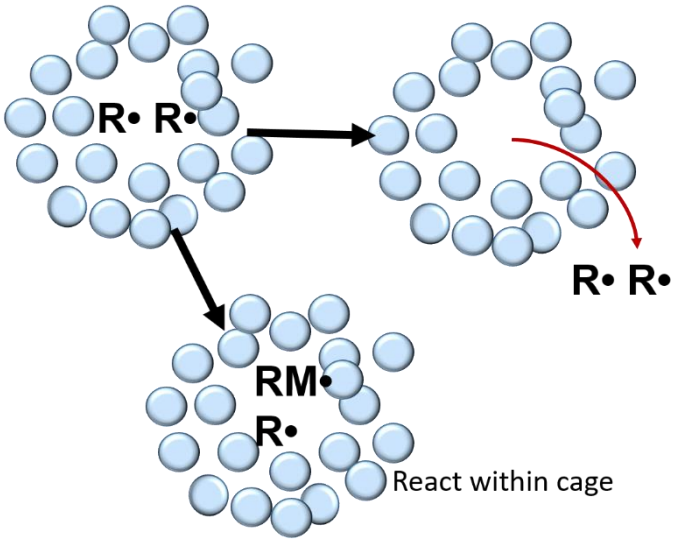

Figure 4: *Free radicals in solvent can potentially react with a monomer within the solvent cage or diffuse out.*

In polymers, the probability of a free radical pair to escape recombination in the cage is 0.1 – 0.01 [75]. The cage effect is dependent on changes in several parameters including radical size, shape and solvent viscosity [77-79]. These sources report that the cage effect will increase with an increase in radical size and a decrease in radical mass.

In free radical polymerisation, the rate of initiation is dependent on how effective the initiator is. Low initiator efficiency is largely attributed to the cage effect [74]. Initiator efficiency represents the fraction of primary radicals, R·, that actually contribute to chain initiation. Due to the cage effect, free radicals can undergo mutual deactivation which produces stable products instead of initiating propagation, reducing the initiator efficiency [74].

The most important indicator of activity of an initiator is its half-life ($t_{1/2}$). This is the time required to reduce the original initiator content of a solution by 50 % at a given temperature. Most free radical organic initiators conform to first order decomposition kinetics. Therefore the half-life is related to the initiator decomposition rate as follows:

$$t_{1/2} = \frac{\ln(2)}{k_d} \quad (1)$$

Inorganic initiators

The most common inorganic free-radical generating initiators employed with tetrafluoroethylene are the various persulfate initiators, with sodium, potassium and ammonium persulfate the most common initiators. Ammonium persulfate is preferred as any residual initiator not washed out of the polymer is decomposed and evaporated during the sintering steps for PTFE, leaving no residual inorganic contamination in the polymer. Typical concentrations of persulfate initiators

required to produce high polymers fall in the range of 2 ppm to 500 ppm based as calculated on the mass of water with polymerisation continued until the reactor contains ~30 % solids [80]

There is some dispute as to whether molecular oxygen could be used to polymerise TFE. Joyce [81] indicated that it could indeed be used, but this goes against what is reported elsewhere in the literature [22, 82, 83]. Oxygen is known to act as an inhibitor to polymerisation and must be rigorously extracted from the polymerisation system if any appreciable polymer yield is desired.

Strong oxidizers, such as $KMnO_4$ in water [58, 66] have also been cited as initiators for the low temperature (10–50 °C) polymerisation of tetrafluoroethylene, giving high molecular mass polymers. The claim was made that any of the salts of permanganic, manganic and manganous acid can be used in this fashion.

Furthermore, fluorine radicals may be generated by the heating of certain metal fluorides like CrF_3 and AgF_2 in the presence of tetrafluoroethylene and polymerisation may be initiated in this manner to produce a high polymer [84].

Organic initiators

Organic free-radical generating initiators have been the mainstay initiators for commercial PTFE product and the most common types are of the peroxide class. Since nearly all PTFE production occurs in aqueous medium, those compounds that can dissolve well in water are most preferred, with disuccinic acid peroxide and diglutaric acid peroxide being the most cited initiators. Water insoluble compounds such has benzoyl peroxide can be used, but their application is limited to situations where organic solvents or water/organic biphasic systems are employed [35].

The selection of initiator is based primarily on solubility and half-life, but there are limitations on the chemistry and size of the initiators owing to the possibility of atom transfer from the initiator to the fluoromacroradicals. Lauroyl peroxide is an example of an organic initiator that will also act as a chain transfer agent.

Importantly, azo-initiators have been found to not be very effective in initiating TFE polymerisation, with azo-bis(isobutyronitrile) (AIBN) and similar initiators producing no polymer at all, irrespective of concentration or reaction temperature.

Normally, organic peroxydicarbonates, such as bis(tert-butylcyclohexyl) peroxydicarbonate do not initiate the polymerisation of tetrafluoroethylene, but Scoggins and Mahan [85] demonstrated that organic peroxydicarbonates, specifically di(saturated hydrocarbyl)s with carbon atom count of 1 to 4, can initiate the polymerisation of tetrafluoroethylene, either carried in finely divided PTFE

powder or as neat powders with no solvent. In the cases of di-(isopropyl) and di(sec-butyl) peroxydicarbonates, TFE high polymer was obtained.

Fluorinated initiators

Peroxy or similar compounds are often used as TFE polymerisation initiators. However, from the author's own experience, persulfate initiators cause discolouration in the polymer, especially once the polymer has been sintered. For this reason, persulfate initiators have been largely replaced by organic peroxides, especially perfluorinated peroxide initiators, such as HFPO dimer peroxide or Di(perfluoro-2-methyl-3-oxahexanoyl) peroxide.

Certain fluorinated initiators such as di-(perfluoroacyl) peroxide have a tendency to hydrolyse when used in systems containing water, reducing the initiator efficiency and slowing the polymerisation rate [86]. They also result in unstable end groups. Using more sterically hindered initiators tends to overcome this problem.

Redox initiators

According to Myers [22], when using a redox initiator with TFE systems, a redox system comprising an organic peroxide, a divalent metal and a reducing agent gives the best results. While nickel, copper, cobalt, manganes and iron may be used, iron compounds are most preferred. While most inorganic metal salts may be used, organic salts and chelates that are soluble in the polymerisation medium as well as the monomer are preferred. Many reducing agents can be used, but bisulfites are preferred. The redox initiation of TFE polymerisation has one major drawback, *viz.*,the discolouration of the polymer due to metal deposits in the produced polymer. However, the redox system does result in a more controlled reaction, and a polymer with a higher M_n [22].

Photoinitiators

Polymerisation of TFE and other fluoromonomers can be initiated by UV irradiation of a suitable initiator in a batch process [87]. Most compounds that produce free-radicals by UV induced bond cleavage may be used as photoinitiators with salient examples being Cl_2, F_2, SF_5Cl [88], N_2O [89] and short chain acyl halides [90].

Hydrogen peroxide is an example of such a compound and has been used successfully by the author to achieve polymerisation of TFE. UVC (280 - 100 nm) and UVB (300 - 280 nm) radiation is typically employed, with monochromatic light at 253.7 nm being the wavelength of choice [35].

There has also been a report concerning the use of fluorinated azoalkanes like perfluoroazoethane as photoinitiators [91].

Polymerisation of TFE in supercritical carbon dioxide

According to US patent 6 103 844 [92] TFE can be polymerised in supercritical CO_2 when azo type initiators are used, with dialkyl(2,2-azobisisobutyrate) being especially effective.

Azo initiators are desirable because of their predictable kinetics. They do not undergo radical induced decomposition [93]. Furthermore, their decomposition rates are not affected by the environment.

Other initiators

Other inorganic initiators include neat, anhydrous CsF [94] in contact with tetrafluoroethylene gas at temperatures in the region of 150 °C. This reaction can produce both polytetrafluoroethylene waxes and high polymer with properties comparable to high polymers obtained by free-radical mechanisms.

Electrons have also been used to directly initiate the homopolymerisation of TFE.

Summary of initiators

Tetrafluoroethylene may be polymerised *via* free-radical polymerisation. This may be initiated with well-known substances such as persulfates and organic acylperoxides as well as azo based initiators in special instances. In particular, numerous water soluble organic peroxides, such as disuccinic acid peroxide, have been developed. Fluorinated organic initiators have been specially developed by commercial entities for use with TFE, permitting polymerization in fluorinated solvents *etc.* Photochemical initiation as well as a variety of special inorganic initiators have also been investigated for use with tetrafluoethylene. Initiator chemistry is all important for the thermal and chemical stability of the endgoups, which in turn, to a large extent determines the thermal and chemical stability of PTFE.

Table 2 shows a summation of some of the initiators that have been used in TFE polymerisation.

Table 2: *Initiators used for tetrafluoroethylene polymerisation.*

Initiator	Structure	Reference
Ammonium persulfate	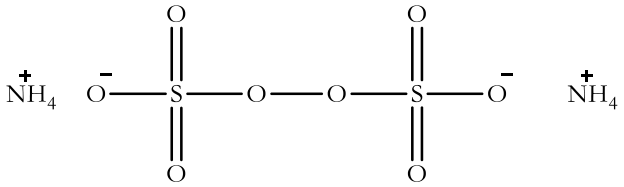	[8, 10, 81]
Sodium bisulfite / $FeSO_4$	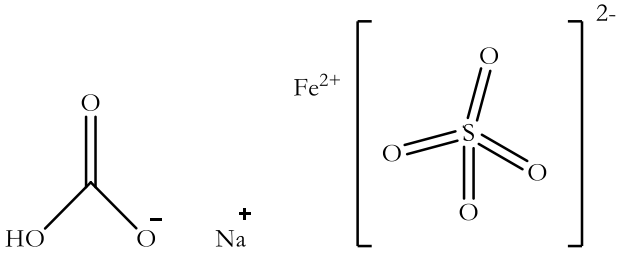	[70]
Hydrogen peroxide	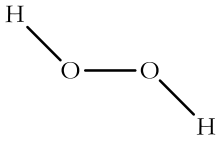	[8, 10, 81]
Benzoyl peroxide	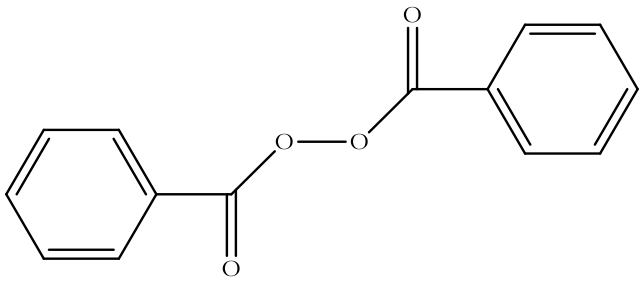	[95]
Dimethylamine oxide	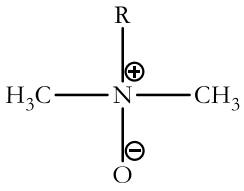	[96]
Disccinic acid peroxide	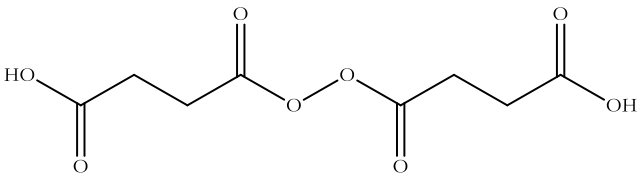	[97, 98]

Monosuccinic acid peroxide	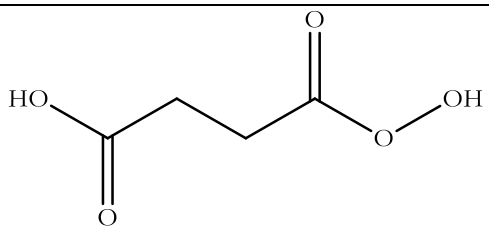	[98]
Diglutaric acid peroxide	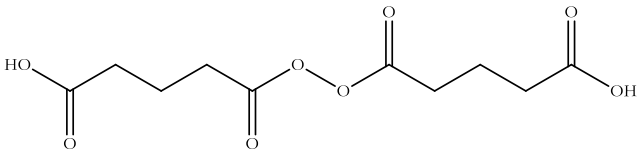	[98]
Perfluorodipropionyl peroxide	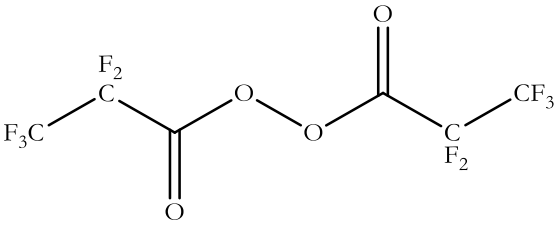	[99]
Di(perfluoro-2-methyl-3-oxahexanoyl) peroxide	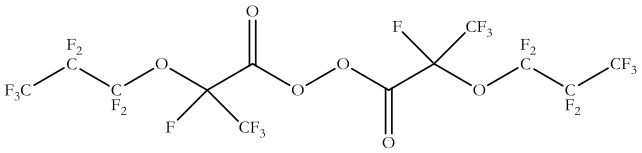	[100]
Bis(3-chloro-2, 2, 3, 3-tetrafluoro-1-oxopropyl) peroxide	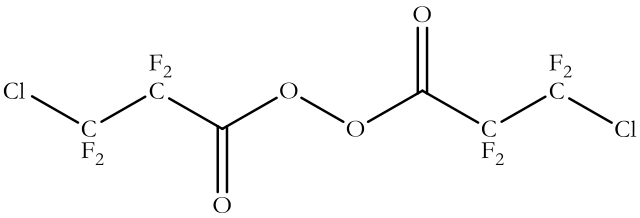	[86]
Tert-butyl peroxybenzoate	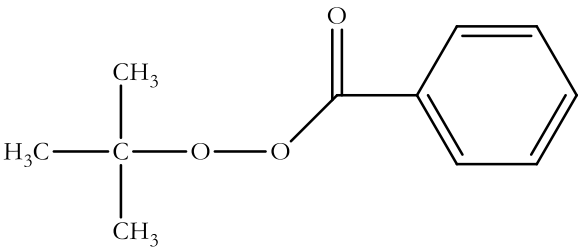	[22]
Bistrichloroacetyl peroxide	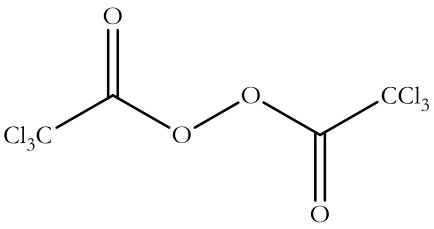	[101]

Di-tert-butyl peroxide	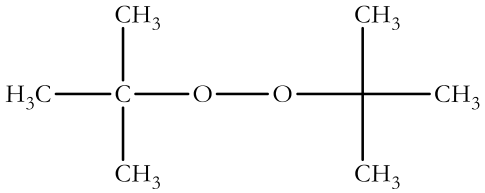	[102]
Tert-butyl peracetate	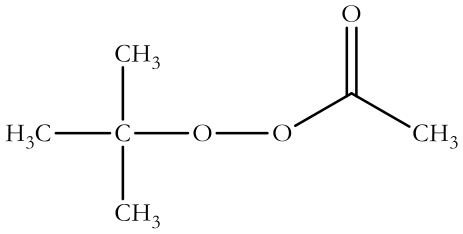	[102]
Diisopropyl peroxydicarbonate	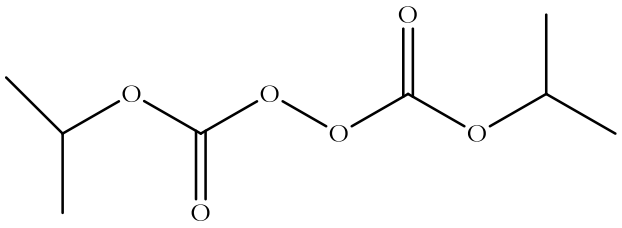	[85]
Di(sec-butyl) peroxydicarbonate	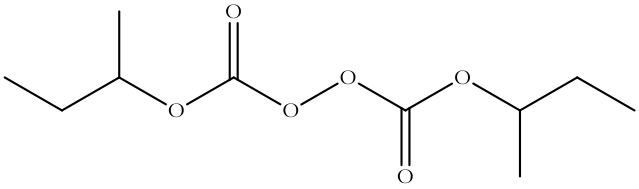	[85]
Potassium permanganate	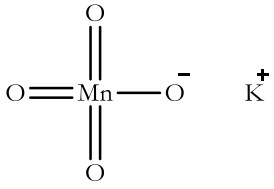	[68]
Silver(II) fluoride	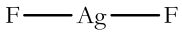	[84]
Chromium trifluoride		[84]

2.2 PTFE processing

2.2.1 Suspension polymerised (granular) PTFE

In aqueous, free-radical precipitation polymerisation the polymer is usually isolated from the reactor as clumps of coarse, compacted, granular material of irregular shape or as stringy particles, with the degree of clumping and the size of granules depending on the vigour of the agitation in the reactor, as well as the molecular mass of the polymer and the fraction of solids reached in the reactor, but not on the temperature or the pressure [58, 65, 103]. These irregular particles are too coarse for most processing purposes. This crude polymer powder can only be processed further with difficulty because of poor flowability, low bulk density and large average particle diameter. In most cases these crude polymers are subjected to grinding down to smaller particle diameters, greatly improving their workability. Fabricating this kind of PTFE is done by compression moulding.

PTFE does not exhibit a melt phase like PE does; rather, the high polymers have a transition point at ~335 °C where the chains move more freely. PTFE composites manufactured by powder processing techniques are "sintered" at or slightly above this temperature in order to coalesce the agglomerate particle. This melting point is a strong function of the molecular weight and the crystallinity of the polymer, with the melting point usually falling in the range 320 to 350 °C, depending on the initial crystallinity of the polymer [35].

During the sintering process, the PTFE powder is compressed into a 'preform' at ambient temperature. The preform is still rather brittle, but has sufficient strength to be handled. After removal from the preform mould, the preform is heated in an oven above its melting point and is sintered. Sintering of PTFE is a thermal treatment during which the polymer is melted, coalesced and recrystallized during cooling. The consolidation of particles during sintering is referred to as coalescence, which produces a homogenous and strong structure. Variation of the cooling rate controls the crystallinity of the final product.

2.2.2 Sintering

The commonest way of sintering PTFE preforms is by a batch process in an electrically heated oven. Sintering is normally carried out at temperatures between 360 °C and 380 °C [104]. These temperatures are well above the traditionally quoted melting point of 327 °C. However, this melting point is only true once PTFE has been melted for the first time. Before the first melt, the crystalline melting point of 340 °C must be exceeded until the PTFE particles coalesce and lose

their identity. The time required to complete the sintering process depends on the following factors [104]:

- Maximum temperature reached
- Rate of heating
- Rate of cooling
- Thickness of PTFE through which heat has to pass

In general, the higher the maximum sintering temperature, the quicker sintering can be completed. However, the sintering temperature should not exceed 380 °C, as this may lead to some degree of thermal degradation, especially in thicker parts. The heating rate is limited by the need to minimise stresses set up in the moulding as it expands on heating. This is especially true in thicker parts. For very thin mouldings, it is possible to use very fast heating rates, or even to place the moulding in an oven pre-heated to 380 °C.
For very thin mouldings, the rate of cooling is governed mainly by the crystallinity required in the finished product, with slow cooling giving maximum crystallinity and quench cooling giving minimum crystallinity. Different processing conditions such as the length of exposure to sintering temperatures affect some of the properties of the part.

2.3 Degradation of PTFE

Heat or radiation are capable of degrading PTFE if they are supplied in sufficient quantities to reach the temperature or radiation dose at which the polymer chain degrades [4]. A common conclusion from multiple studies is that PTFE degrades more at a lower temperature and more rapidly in the presence of oxygen or air. Under vacuum or in an inert atmosphere, decomposition delivers mostly TFE and other small molecules. Under oxygen or air, smaller polymer chains are the product [4]. Polymer structure and monomer type influence thermal degradation.

In addition to thermal decomposition, exposure of PTFE to high energy radiation breaks down carbon-carbon bonds in the polymer chain, leading to degradation. PTFE radicals react with oxygen the same way regardless of whether they have been produced by thermal decomposition or irradiation. The following reaction scheme has been widely accepted for the degradation of PTFE [4]:

$$\text{-CF}_2\text{-CF}_2\text{-CF}_2\text{-CF}_2\text{-CF}_2\text{-} + \text{heat or irradiation} \rightarrow \text{-CF}_2\text{-CF}_2\cdot + \text{-CF}_2\text{-}\dot{\text{C}}\text{F}_2\text{-CF}_2\text{-}$$

$$\text{-CF}_2\text{-CF}_2\cdot + \text{O}_2 \rightarrow \text{-CF}_2\text{-CFO}$$

$$-CF_2-CF_2-CF_2 + O_2 \rightarrow -C\dot{O}F_2-CF_2-CF_2- \rightarrow -CF_2-CF_2\cdot + -CF_2CFO$$

The end group of degraded PTFE is acyl fluoride (-CFO) which reacts with water and forms carboxylic acid group (-COOH) and evolves HF [4]. End groups are usually identified by infrared spectroscopy.

The end groups can have an effect on the properties of the polymer such as discolouration. In some cases, the end groups can even promote adhesion of micropowders to metals.

In the particular case of PTFE initiated by persulfate, the sulfate group is hydrolysed to OH in the aqueous polymerisation medium [19]. The unstable 1,1-difluorocarbinol end group reacts to form carboxyl groups, so ultimately, PTFE produced from persulfate initiators ends up terminated by fluorocarboxyl end groups. These end groups may eliminate CO_2 and HF, even at moderate temperatures, to from unsaturated end group structures which, being much less stable than the PTFE backbone, are eliminated first at elevated temperatures, followed by the unzipping of the chain from the end. Furthermore, the presence of unsaturated chain ends produces a discolouration of the polymer. Initiation using sodium bisulfite does not produce hydrolysable end groups, with the chain being terminated by a more stable bisulfite end group and, concomitantly, the chain is more thermally stable [19]. Pianca *et al.* [105] gives an overview of the end groups present in fluoropolymers as well as their mechanisms of elimination.

2.4 IR spectroscopy of PTFE

Infrared spectroscopy involves the interaction of infrared radiation with matter. It is conducted with an instrument called an infrared spectrometer to produce an infrared (IR) spectrum. An IR spectrum is essentially a graph of infrared light absorbance (or transmittance) on the vertical axis vs. frequency or wavelength on the horizontal axis. Typical units of frequency used in IR spectra are reciprocal centimeters (sometimes called wave numbers), with the symbol cm^{-1}. A common laboratory instrument that uses this technique is a Fourier transform infrared (FTIR) spectrometer. Infrared spectroscopy exploits the fact that molecules absorb frequencies that are characteristic of their structure. These absorptions occur at resonant frequencies, *i.e.* the frequency of the absorbed radiation matches the vibrational frequency. The energies are affected by the shape of the molecular potential energy surfaces, the masses of the atoms, and the associated vibronic coupling.

The vast majority of functional groups in polymers give rise to bands in the infrared region [106]. Therefore vibrational spectra can be used to identify polymers through the use of group frequencies or simply by attempting to compare the spectrum to reference spectra. The latter approach can run into difficulties when dealing with copolymers or polymers that have been

modified in some way. However, this was not a problem in this case, because only PTFE homopolymer was studied. Besides providing the analyst with the means to identify polymers, vibrational spectroscopy can also yield valuable information on the structure of a polymer. This includes configurational and conformational information on the structure and identification of end groups and defects [106].

The most widely used region is mid-IR, which extends from about 670 to 4000 cm^{-1}. In this region, absorption, reflection and emission spectra are employed for both qualitative and quantitative analysis. Most organic compounds exhibit numerous absorption bands throughout the mid-IR region. When analysing solids, the solid sample must be ground until its particle size is less than the wavelength of the radiation to avoid the effects of scattered radiation.

Qualitative analysis when using mid-IR is generally a two-step process. The first step involves determining what functional groups are most likely present by examining the group frequency region which encompasses radiation from about 3600 cm^{-1} to approximately 1250 cm^{-1}. The second step involves a detailed comparison of the spectrum of the unknown with the spectra of pure compounds that contain all of the functional groups found in the first step. Here the fingerprint region, which ranges from 1200 to 600 cm^{-1} is particularly useful, because small differences in the structure and constitution of a molecule result in significant changes in the appearance and distribution of absorption bands in this region. Consequently, a close match between two spectra in the fingerprint region constitutes almost certain evidence that the compounds are identical [107]. The difference between the group frequency region and the fingerprint region can be seen in Figure 5. More detail regarding IR spectroscopy can be found in Appendix A.1.

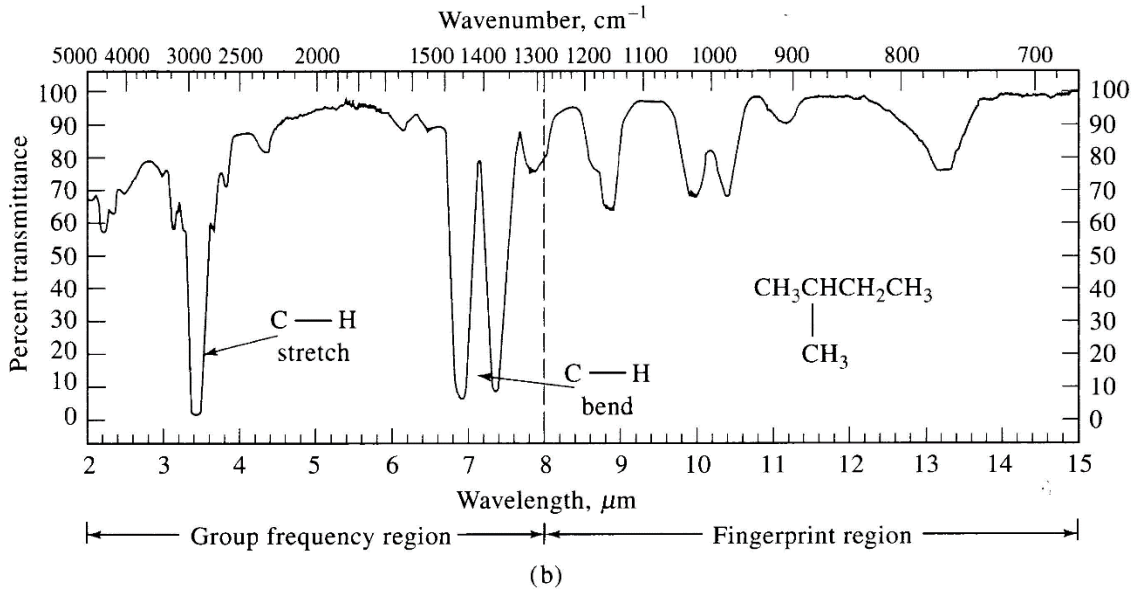

Figure 5: *The group frequency region (3600 – 1250 cm^{-1}) of the mid-IR is used to identify common functional groups. The fingerprint region (1200 – 600 cm^{-1}) is used to identify compounds [107].*

2.5 Raman Spectroscopy of PTFE

Infrared and Raman spectroscopy are extremely powerful analytical techniques for qualitative and quantitative analysis. These techniques are best used in tandem, because one may yield important complementary and/or confirmatory information regarding the sample. The infrared and Raman spectra of a given sample usually differ considerably. Therefore each technique can provide additional, complimentary information regarding the sample [106]. Bands of importance to a particular study may occur in regions where they are overlapped by the bands due to other groups. Therefore, by making use of the other technique (Raman or infrared) it is often possible to observe the bands of importance in interference-free regions.

Raman spectroscopy relies on inelastic scattering, or Raman scattering, of monochromatic light, usually from a laser in the visible, near infrared, or near ultraviolet range. The laser light interacts with molecular vibrations, phonons or other excitations in the system, resulting in the energy of the laser photons being shifted up or down. The shift in energy gives information about the vibrational modes in the system.

The Raman effect should not be confused with emission (fluorescence or phosphorescence), where a molecule in an excited electronic state emits a photon and returns to the ground electronic state. Raman scattering also contrasts with infrared absorption, where the energy of the absorbed photon matches the difference in energy between the initial and final states. Raman activity requires

polarizability of the analyte molecule, while IR requires a changing electric dipole moment. This contrasting feature allows transitions that might not be active in IR to be analysed using Raman spectroscopy. Transitions which have large Raman intensities often have weak IR intensities and vice versa. More detail regarding Raman spectroscopy can be found in Appendix A.2. Figure 6 shows the IR and Raman spectra of a high molecular weight PTFE.

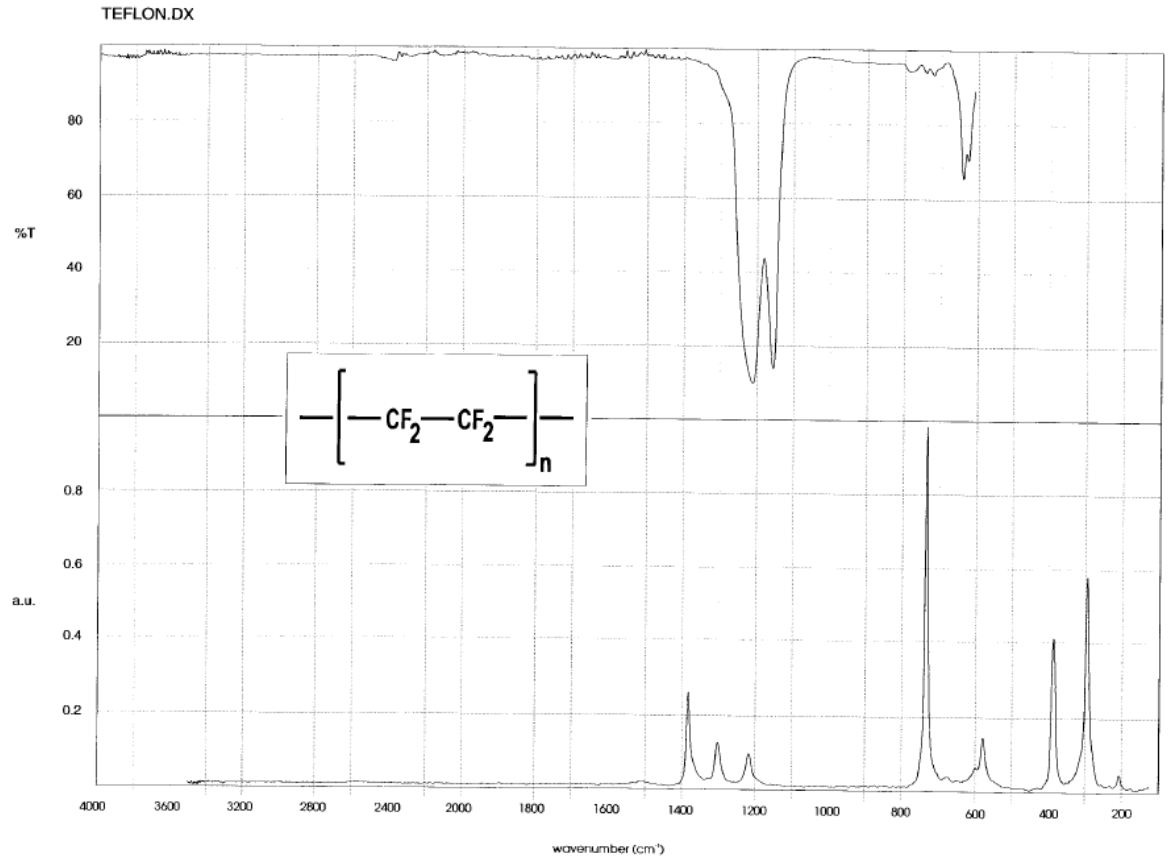

Figure 6: *The transmission IR spectra (top) and Raman spectra of high-molecular weight PTFE [108].*

According to Kuptsov *et al.* [108], there are some generalisations of the common observations about Raman spectral intensities:

- Stretching vibrations associated with chemical bonds should be more intense than deformation vibrations.
- Multiple bonds should give rise to more intense stretching modes. For example, a Raman band corresponding to a C=C (or C≡C) vibration should be more intense than that from a C-C vibration.
- Bonds involving atoms of large atomic mass are expected to give rise to stretching vibrations of high Raman intensity.

Vibrational spectroscopy allows investigation of polymers virtually without any form of pre-treatment. Pre-treatments are extremely difficult when it comes to poorly soluble and poorly dispersible specimens such as PTFE. Moreover, pre-treatment can distort the initial structure of specimens. This makes Raman spectroscopy an ideal method to analyse PTFE.

According to Firsov *et. al* [109], Raman spectral bands caused by vibrations of the structure of the PTFE chains are the most intense. These bands occur at 1382, 734, 385 and 290 cm^{-1} and can be assigned to symmetric stretching vibrations of CF_2, symmetric stretching vibrations of C-C and deformation and torsional vibrations of CF_2, respectively [110]. There are also bands of medium intensity at 1302 and 1218 cm^{-1}. They are assigned to asymmetric stretching vibrations of CF_2. All these bands can clearly be seen in Figure 6.

The regions from 1300 to 1400 cm^{-1} and 500 to 700 cm^{-1} are structurally sensitive. The intense band at 1382 cm^{-1}, as well as a low intensity band at 1335 cm^{-1} caused by asymmetric stretching vibrations of CF_2 groups, are located in the first region. The band at 1335 cm^{-1} is especially clear in the Raman spectra of PTFE specimens with high crystallinity (>90 %) [109]. However, it is also reported that at lower temperatures, the band at 1335 cm^{-1} is overlapped by a much more intense band at 1381 cm^{-1}, which narrows and shifts to lower frequency as the temperature decreases. The frequencies in the 500 to 700 cm^{-1} region are assigned to plane pendulum vibrations of the CF_2 group. These frequencies are especially sensitive to conformational changes in the PTFE macromolecule chain.

2.6 NMR spectroscopy of PTFE

Recently, it has been demonstrated that high-resolution solid-state NMR is a powerful tool for elucidating the structure and dynamics of polymers in the solid state. However, conventional high-resolution solid-state NMR often fails to obtain useful information about the structure of fluoropolymer such as PTFE, because they give rise to a broad, featureless spectrum [111]. This is mainly due to dipolar coupling and shielding anisotropy. The high speed magic angle spinning (MAS) method leads to significant reduction in such broadening [112].

A major advantage of ^{19}F NMR in polymer studies is the large chemical shift range for this nucleus. The effect of nearest and next-nearest neighbours on the chemical shift of a particular fluorine is readily measured [113]. Therefore, it is possible to determine the number and type of monomer sequences present in a fluorocarbon polymer [112].

The need for a practical high resolution technique for solid samples of these kinds of polymers is underscored by the fact that most known solvents must either be used at high temperature or

cause a spectral overlap [114, 115]. Furthermore, the ability to obtain spectra of undissolved polymers allows one to examine a polymer directly in the state in which its common structural applications depend [112]. The high density of fluorine atoms in fluorocarbon polymers yields strong and homogenous ^{19}F-^{19}F dipolar interactions. Therefore, ^{19}F MAS NMR spectra are still severely broadened at high sample spinning speeds. In order to effectively average the strong homonuclear dipole-dipole interactions present in these systems and obtain high resolution solid state ^{19}F MAS NMR, higher spinning speeds are required [112].

An example of the effect of higher spinning speeds can be seen in Figure 7, which shows the ^{19}F MAS NMR spectra of VDF-TFE copolymer. It shows three very broad features. The large band widths of the peaks are due to a number of effects, namely [112]:

- range of isotropic chemical shifts
- chemical shift anisotropies
- ^{19}F-^{19}F dipolar interactions
- ^{19}F-^{1}H dipolar interactions

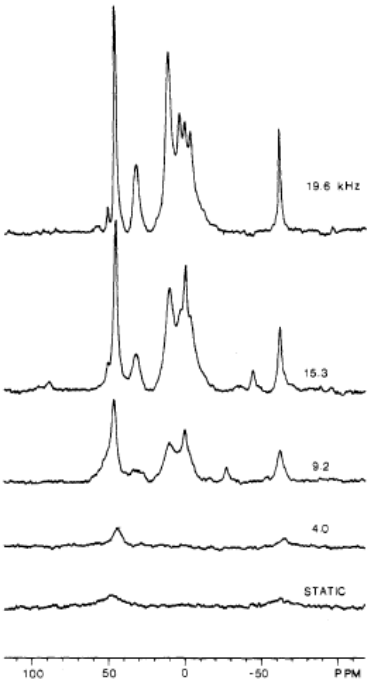

Figure 7: *338.7 MHz ^{19}F MAS NMR spectra of a VDF-TFE copolymer as a function of MAS speed [112].*

Dec *et al.* [112], came to the conclusion that high-speed magic-angle spinning permits the direct observation of high-resolution ^{19}F NMR spectra of solid fluorocarbon polymers. The detail

provided in these spectra allows the direct assignment of individual resonances associated with specific carbon pentad structures and provides a powerful approach for the structural characterisation of such systems. In addition, the nature of the dominant anisotropic interactions present in these systems indicates that improved results should be obtained by using higher MAS spinning frequencies and larger magnetic fields [112].

The low concentration of chain end units, which have much weaker signals than resonances from main chain sequences, makes NMR studies of the detailed structures of chain end units very difficult. Pianca [105] reported the use of IR and NMR spectroscopies together to identify the possible chain end groups in TFE and VDF based fluoropolymers. Since such polymers contain both proton and fluorine atoms, the couplings between these nuclei made the 1-D NMR spectra very complicated when observing one nucleus without decoupling the other [116]. The ability to apply ^{19}F decoupling during ^{1}H detected experiments (and vice versa) provides considerable spectral simplification [116]. Additional information regarding SS NMR spectroscopy can be found in Appendix A.3.

2.7 End groups

2.7.1 Importance of end groups

The importance of fluoropolymers in high-performance applications such as in the aerospace, aircraft, chemical, petroleum and energy industries has stimulated much research in their synthesis and characterisation [117]. It is generally accepted that end groups have no significant effect on the macroscopic properties of most polymers. This is because of their negligible weight when compared to the whole mass of polymer and because energy values for the bonds in end groups and those in the constitutive units are practically equal [105]. However, this is not true for perfluoropolymers where hydrogen containing end groups (produced by persulfate initiators) do have definite influences on the performance and stability. This can be expected when the bond strength of C-H and C-F (410 and 460 $kJ.mol^{-1}$) are compared [105]. With hydrogen and fluorine containing polymers, such as PVDF, it has been shown that thermal stability and fire resistance are influenced by the end groups generated in the presence of different initiators. In this case the relative strength of C-H to C-F bonds cannot be the determining factor. This unexpected behaviour was attributed to different degradation mechanisms induced by the nature of the end groups [118]. In addition to the thermal stability, other properties such as fluidity and electrical conductivity were demonstrated to be significantly influenced by end groups.

In addition a knowledge of the type and number of chain end units can reveal information about the mechanisms and relative rates of chain transfer and termination processes [116]. Characterising chain ends of a polymer is important to optimise the polymer's performance. However, the low concentration of chain end structures in high molecular weight polymers makes their characterisation challenging [117].

End groups can also determine the crystallisation kinetics from the melt of thermoplastic fluoropolymers, and hence the processing and end-use properties [119]. The importance of end groups in determining the properties of fluoropolymers cannot be understated.

The end groups in thermoplastic fluoropolymers can be generated during the polymerisation process by the initiator, transfer agent, solvent, contaminants *etc.* or during handling of the polymer by ageing, heating, extrusion, chemical reactions *etc.* The identification and quantitative determination of these end groups is of paramount importance. IR spectroscopy is a particularly useful technique in the determination of end groups in TFE based polymers, since they are insoluble in common solvents. Moreover, many functional groups show absorptions in spectral regions that are free from the main absorption bands of the polymer. One of the major features of Fourier transform infrared (FTIR) spectroscopy is the high sensitivity due to the high energy available and the possibility to enhance the signal to noise ratio by increasing the number of scans. It is possible to evaluate end groups concentration in the range 10^{-3} to 10^{-5} mol·kg^{-1} [4].

A wide variety of initiators have been suggested for the polymerisation of TFE. Two of the most common groups of compounds suggested are inorganic peroxy compounds such as potassium persulfate in combination with reducing agents such as sodium bisulfite, and organic peroxides such as dibenzoyl peroxide and acetyl peroxide. According to US patent 3 193 539 [120], organic catalysts provide higher quality polymer than the inorganic type, the organic peroxy catalysts having been found to provide polymers of considerably higher thermal stability and processability. While organic peroxy catalysts generally provide better polymers, catalysts of this type generally require extremely high pressures in the region of 70 MPa to produce appreciable yields of polymer [120]. Even at these high pressures, the yields of polymer are still often relatively poor, between 10 and 20 %. The cost of carrying out polymerisation at such high pressures is exorbitantly high. One organic initiator, di-tertiary-butyl peroxide, has been found to be capable of providing excellent yields of high quality polymer. According to US patent 3 193 539 [120], di-tertiary-butyl peroxide (DTBP) is unique among organic catalysts in providing high conversions under mild pressures. Numerous attempts to obtain similar results with other organic initiators, even with initiators as similar as tertiary-butyl hydroperoxide, tertiary-butyl perbenzoate and tertiary butyl

peracetate, have been unsuccessful, while tertiary butyl peracetate gave polymers of poor quality [120].

Commonly used polymers such as polyethylene and polypropylene form hydroperoxide groups as a result of thermal degradation. These groups are not easy to detect by IR, because the O-O stretching vibrations result in a very weak band and the concentration of the hydroperoxide groups is very low [106]. The OH stretching band may also be difficult to observe as it only results in a medium intensity band. Hydroperoxide groups however, react to form a variety of carbonyl containing compounds. It is usually possible to detect these bands due to ketones (~1720 cm^{-1}), aldehydes (~1735 cm^{-1}) and carboxylic acids (~1710 cm^{-1}). In the case of photochemically decomposed samples, bands due to the vinyl group are observed near 910 cm^{-1} and 990 cm^{-1} in addition to the carbonyl groups.

2.7.2 IR spectra of PTFE end groups

The absorption bands of the distinctive functional groups was obtained from various literature sources [69, 105, 121-129]. However, this review focuses on the identification of the end groups, the frequencies of which were summarised as follows by Pianca and co-workers [105]:

Carboxylic groups

Carboxylic groups are identified by IR spectroscopy by the following group frequencies due to O-H and C=O stretching:

- 3557 cm^{-1} (sharp, O-H stretching free)
- 3300-3000 cm^{-1} (broad, O-H stretching, bonded)
- 1813 cm^{-1} (sharp, C=O stretching, free)
- 1775 cm^{-1} (C=O stretching, bonded)

The IR spectra for carboxylic groups in a PFA polymer can be seen in Figure 8. The spectra shows the C=O stretching region before and after exposure to ammonia. The exposure to ammonia is to verify the nature of the observed bands, because it leads to the disappearance of the O-H and C=O stretching bands and to the appearance of new bands due to the in-phase and out-of-phase $–COO^-$ stretching vibration [105].

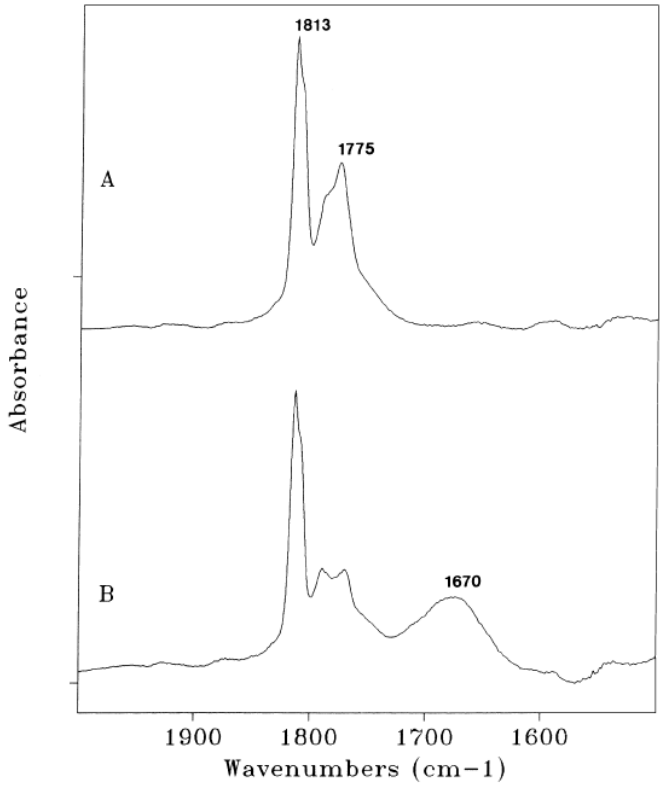

Figure 8: *(A) IR absorption bands in the C=O stretching region due to carboxylic end groups in a PFA polymer. (B) The same region after exposure to ammonia [105].*

Carboxylic groups can decompose by thermal treatment following different mechanisms [105]:

a) $–CF_2-CF_2-COOH \rightarrow -CF=CF_2 + CO_2 + HF$

b) $–CF_2-CF_2-COOH \rightarrow -CF_2-COF + HF + CO$

c) $–CF_2-CF_2-COOH \rightarrow -CF_2-CF_2H + CO_2$

Mechanism a) is observed during press treatment at 380 °C for some minutes. It is characterised by a decrease of the absorptions due to carboxylic groups and the formation of a band at 1784 cm^{-1} due to perfluorovinyl ($-CF=CF_2$) groups [105].

Mechanism b) has been observed during industrial extrusions of perfluoropolymers manufactured by aqueous emulsion polymerisation with $K_2S_2O_8$ as initiator. In the IR spectra of the extruded items, a substantial decrease of the absorptions due to carboxylic groups and the formation of a band at 1884 cm^{-1} attributable to the acyl fluoride ($-CF_2-COF$) end group, was observed. Because the carboxylic groups could be present either as K^+ salts or in the protonated form, the unimolecular reaction pathway shown in Scheme 1 was proposed [105]:

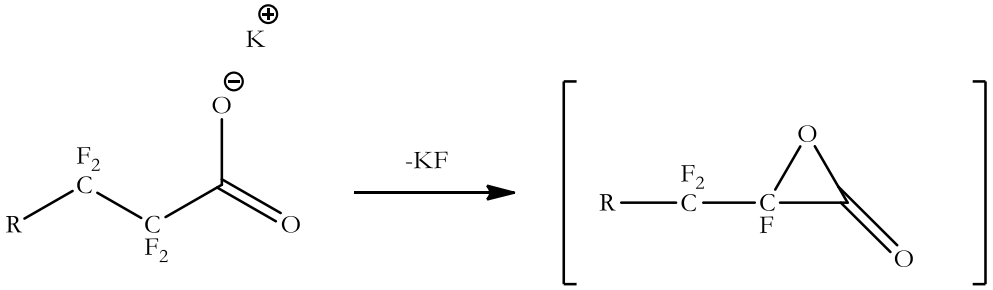

Scheme 1: *Unimolecular reaction pathway proposed for intermediate which leads to acyl fluoride or perfluorovinyl end groups.*

KF, eliminated α to the carbonyl, results in a zwitterionic intermediate which can evolve into a cyclic form. Upon heating, loss of CO from the cyclic intermediate results in the observed end groups [105]. This mechanism is not unusual and closely resembles the thermal extrusion difluorocarbene from hexafluoropropene oxide to give acetyl fluoride.

Mechanism c) is followed when the carboxylate end group is in ionic form and the polymer is treated with water at 210 – 250 °C [121, 122, 125, 130].

Amide groups

Amide groups can be generated during the polymerisation step when ammonium salts are used as initiators. The structure of the proposed amide end group can be seen in Figure 9.

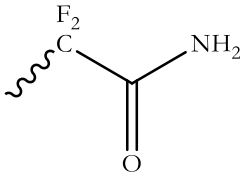

Figure 9: *Structure of amide end group.*

Their presence is revealed by four bands at 3555, 3438, 1768 and 1587 cm^{-1} [105]. The two high frequencies (3555 and 3438 cm^{-1}) are assigned to asymmetric and symmetric NH_2 stretching of R_fCONH_2 groups and can be seen in Figure 10. The 1768 cm^{-1} band to C=O stretching and the 1587 cm^{-1} to the N-H deformation and can be seen in Figure 11. These assignments were confirmed by Pianca *et al.*, by means of acid hydrolysis.

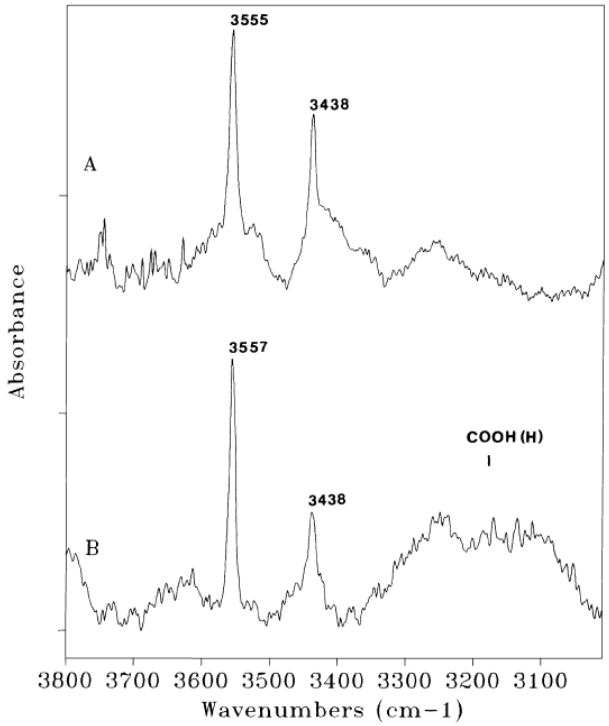

Figure 10: *(A) IR absorbtion bands in the N-H stretching region due to amidic end groups in a PFA polymer. (B) The same spectral regions observed after acid hydrolysis [105].*

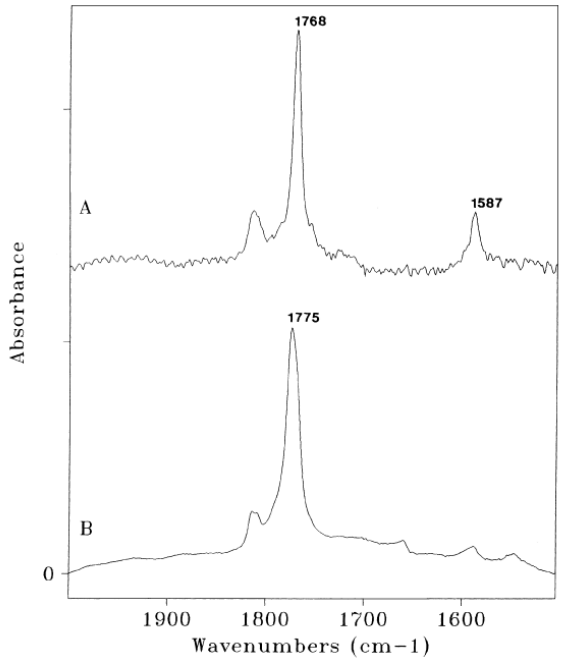

Figure 11: *(A) IR absorbtion bands in the C=O stretching region due to amidic end groups in a PFA polymer. (B) The same spectral regions observed after acid hydrolysis [105].*

Perfluorovinyl groups

The IR spectra of some PFA polymers show a band at 1784 cm^{-1} and can be seen in Figure 13.

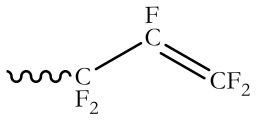

Figure 12: *Structure of the perfluorovinyl end group.*

This same absorption was observed during the thermal degradation of –COOH end groups. Pianca *et al.*, 1999, attributed it to perfluorovinyl double bond stretching.

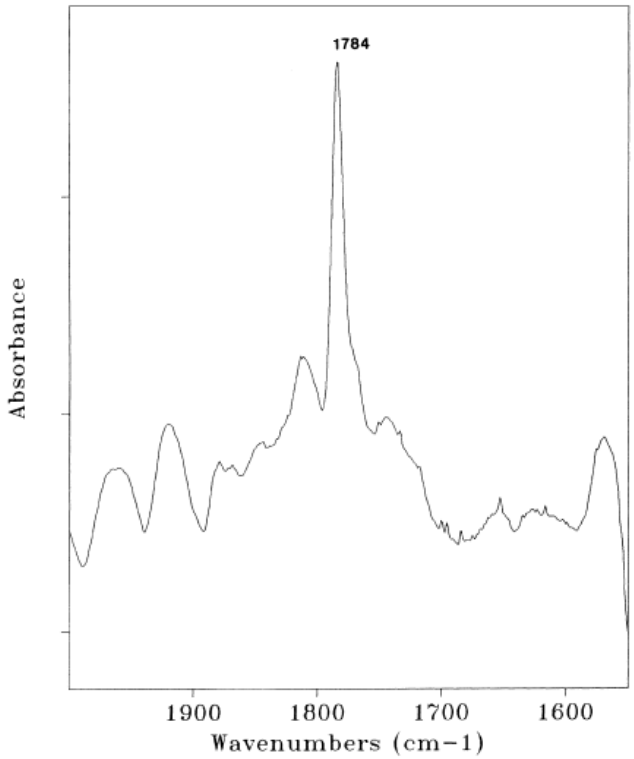

Figure 13: *IR spectrum in the C=C stretching region of a PFA polymer indicating perfluorovinyl end groups [105].*

Acyl fluoride groups

The IR spectra of some extruded TFE perfluorinated copolymers revealed a band at 1884 cm^{-1} which can be seen in Figure 15.

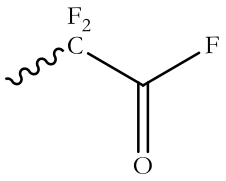

Figure 14: *Structure of acyl fluoride group.*

This group was assigned to C=O stretching in R_fCOF groups [105]. In PFA copolymers, -CF_2COF end groups can also be generated during polymerisation through the radical rearrangement shown in Scheme 2 [105]:

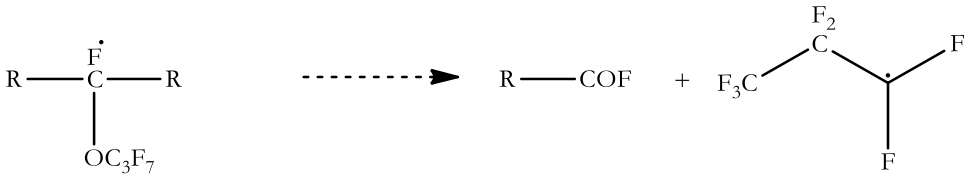

Scheme 2: Radical rearrangement to form –CF_2COF end groups.

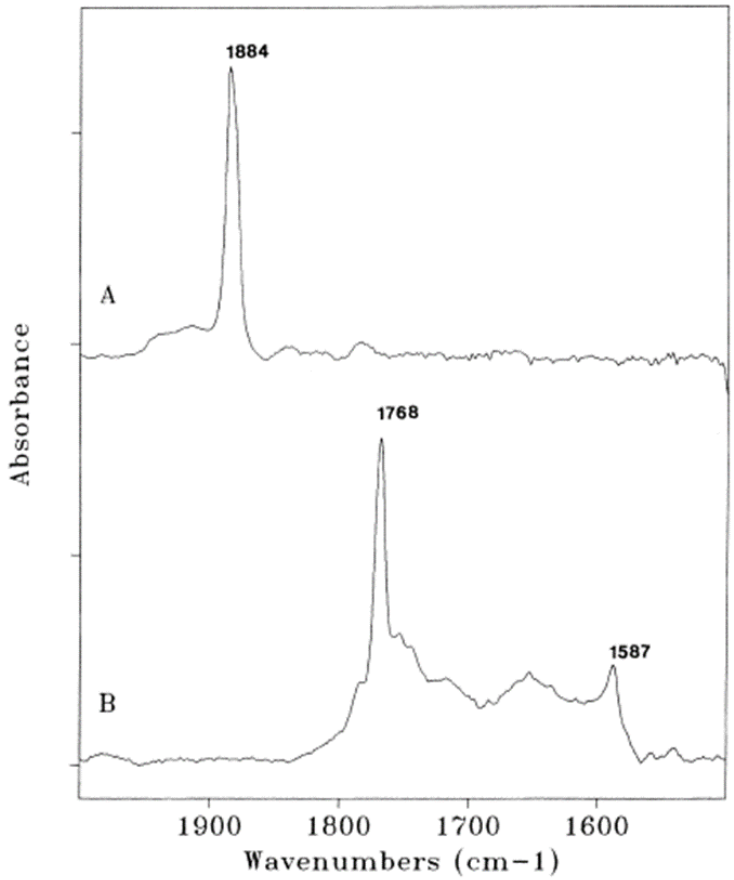

Figure 15: *(A) IR spectrum in the C=O stretching region of a PFA polymer indicating acyl fluoride end groups. (B) The same spectral regions observed after exposure to ammonia and water vapours [105].*

Difluoromethyl groups

When difluoromethyl groups, shown in Figure 16, are present, they give rise to weak absorptions in the CH stretching region [121, 122, 125, 130]. Pianca *et al.* report two bands at 3005 and 2970 cm^{-1}. The presence of two bands is justified by the existence of two different conformers and has been confirmed recording IR spectra at different temperatures.

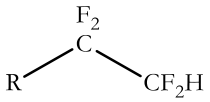

Figure 16: *Structure of the difluoromethyl group.*

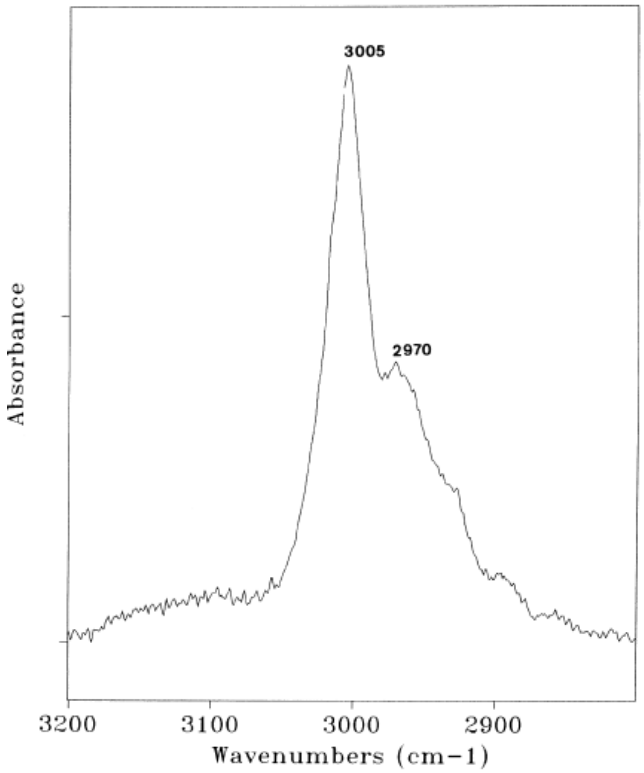

Figure 17: *IR spectrum in the C-H stretching region of a PFA sample indicating difluoromethyl end groups [105].*

Ethyl groups

By using ethane as a chain transfer agent in the emulsion polymerisation of TFE based thermoplastic fluoropolymers, Pianca *et al.* obtained the following end groups, whose structure can be seen in Figure 18.

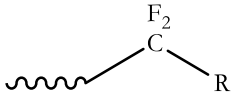

Figure 18: *Structure of ethyl-like groups found in TFE based copolymers.*

Three bands were identified at 3003, 2960 and 2900 cm^{-1} respectively and assigned to the ethyl end group.

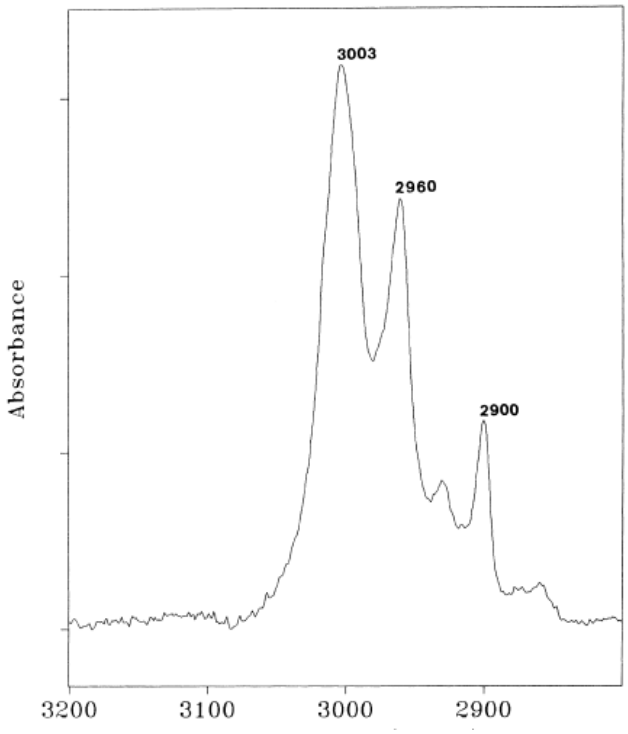

Figure 19: *IR spectrum C-H stretching region of a PFA sample indicating ethyl end groups [105].*

Alkane groups

Four types of vibrations are normally observed with alkane groups, namely the stretching and deformation of the C-C and C-H bonds [106]. The C-H vibration frequencies of methyl and methylene groups fall in narrow ranges for saturated hydrocarbons. Atoms directly attached to $-CH_3$ or $-CH_2-$ groups may result in relatively large shifts in the absorption frequencies. In general, electronegative groups or atoms increase the C-H absorption frequency. CH stretching vibrations occur from 3000 cm^{-1} to 2800 cm^{-1} in bands of medium-to-strong intensity as do the CH_3 and CH_2 deformation vibrations which occur from 1470 cm^{-1} to 1400 cm^{-1} [106]. The CH_3 symmetric deformation vibration generally gives medium-to-strong bands. The C-C deformation vibrations occur between 400 cm^{-1} and 250 cm^{-1} but are generally weak in IR spectra.

Tertiary butyl peroxide groups

Most tert-butyl compounds have three moderate-to-strong absorption bands in the region between 2990 cm^{-1} and 2930 cm^{-1} due to the asymmetric stretching vibrations. The symmetric stretching vibrations occur in the region 2950 cm^{-1} to 2850 cm^{-1} [106].

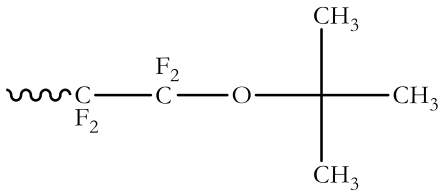

Figure 20: *Structure of tertiary butyl peroxide end group.*

Frequency tables

Table 3 shows IR signal assignments for possible end-groups of PTFE, as reported by various authors. Table 4 shows the Raman signal assignments.

Table 3: *Assignments of IR signals for PTFE and possible end groups as reported by various authors.*

Frequency (cm^{-1})	Group	Assignment	Reference
3557	COOH	OH stretching	[105]
3555	$CONH_2$	NH_2 asymmetric stretching	[105]
3438	$CONH_2$	NH_2 symmetric stretching	[105]
3300 - 3000	COOH (Hydrogen bonded)	OH stretching	[105]
3005	CF_2H	CH stretching	[105]
3003	CH_2CH_3	CH stretching	[105]
2465	C≡C-F	C≡C skeletal vibration	Ab initio calculations
2367	CF_2	CF_2 stretching overtone	[131]
2330	CF_2	CF_2 stretching overtone	[106]
1884	COF	CO stretching	[105]
1813	COOH	CO stretching	[105]
1800-1780	$CF=CF_2$	$=CF_2$ end-group due to C=C stretching	[106]
1792	CF_2	CF_2 combination band	[131]
1784	$CF=CF_2$	CC stretching	[105]

1775	COOH (Hydrogen bonded)	CO stretching	[105]
1768	$CONH_2$	CO stretching	[105]
1670 (broad)	COO^-X^+	COO asymmetrical stretching	[105]
1587	$CONH_2$	NH_2 deformation motion	[105]
1545	CF_2	CF_2 perpendicular band	[131]
1451	CF_2	CF_2 combination band	[131]
1420	CF_2	CF_2 combination band	[131]
~1400, 1300, 1200	$C\equiv C\text{-}CF_3$	C≡C and C-F vibrational bands	Ab initio calculations
1365-1325	$CF_2\text{-}CF_3$	CF_3 end-group due to C-F stretching	[106]
1340-1300	$CF=CF_2$	$=CF_2$ end-group due to C-F stretching	[106]
~1300	C≡N	C≡N vibrational band	Ab initio calculations
1245, 1210, 1155	CF_2	CF_2 groups in amorphous area	[132]
1180, 1100	CF_3	CF_3 stretching vibrations	[133]
935, 835 (very narrow)	CF_2	CF_2 groups in amorphous area	[132]
778, 738, 718	CF_2	CF_2 amorphous bands	[131]
745-730	$CF_2\text{-}CF_3$	CF_3 end-group due to C-F stretching	[106]
700, 520	CF_3	CF_3 deformation vibrations	[133]
638, 625	CF_2	CF_2 groups in crystallised area	[132]

Table 4: PTFE Raman assignments as reported by various authors.

Frequency (cm^{-1})	Group	Assignment	Reference
3774, 3555	$CONH_2$	NH_2 stretching	Ab initio calculations
3744, 750	COOH	OH stretching	Ab initio calculations
3005-2975	CHF_2	Asymmetrical stretching	[106]
3000-2960	CH_2CH_3	Asymmetrical CH_3 stretching	[106]
2465	C≡C-F	C≡C skeletal vibrations	Ab initio calculations
2403	C≡C-CF_3	C≡C skeletal vibrations	Ab initio calculations
2388	C≡N	C≡N skeletal vibrations	Ab initio calculations
1800-1780	CF=CF_2	=CF_2 end-group due to C=C stretching	[106]
1790-1755	COOH	CO stretching vibration	[106]
1380, 1299, 1218 triplet	CF_2	Splitting of F_2 symmetry band	[132]
1365-1325	CF_2-CF_3	CF_3 end-group due to C-F stretching	[106]
1340-1300	CF=CF_2	=CF_2 end-group due to C-F stretching	[106]
1281, 628	CF_2	F_2 symmetry	[109, 132]
908	CF_2	A_1 symmetry	[109, 132]
792	CF_2	C-F stretching	[109, 132]
745-730	CF_2-CF_3	CF_3 end-group due to C-F stretching	[106]
590, 579, 560 triplet	CF_2	Splitting of F_2 symmetry band	[132]
435	CF_2	E symmetry	[109, 132]
384, 291	CF_2	Splitting of E symmetry mode	[132]

End groups with conjugated bonds

Conjugated double bonds in a molecule mean that the single and double bonds alternate. This enables the electrons to be delocalised over the whole system and so be shared by many atoms, *i.e.* the delocalised electrons may move around the whole system. Conjugated double bonds may be the cause of discolouration in the PTFE post-sintering [134]. Figure 21 shows some possible configurations of conjugated end groups that could be the cause of discolouration in the PTFE samples.

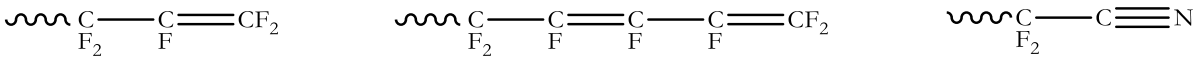

Figure 21: *Possible configurations of conjugated end groups in PTFE.*

Alkyne containing end groups

End groups that contain alkynes (C≡C) bonds could be present in the chains and may lead to conjugation and subsequent colour changes.

Socrates reports that the peaks for central C≡C bonds are weak in the IR spectrum and are therefore difficult to identify. However, according to Socrates [106], terminal alkyne groups give strong peaks in the region of ~2100 cm^{-1} in Raman and IR spectra, due to C≡C stretching vibrations. When the triple bond is moved to an internal position, its intensity becomes less. Conjugation increases the intensity and the frequency of the C≡C stretching vibration. In the Raman spectra of disubstituted alkynes, there are often two closely spaced bands near ~2280 cm^{-1}. The additional band has been attributed to an overtone/combination band enhanced by Fermi resonance [106].

Socrates reports the regions for peaks of conjugated alkynes, where the alkyne carbon atom is bonded to a halogen group. However, the frequencies were only published for cases where the attached halogen was I, Br or Cl and none for F. From the published frequencies, it can be surmised that with increasing electron negativity, I<Br<Cl<F, the frequency seems to shift to higher values. The frequency for C≡C stretching vibrations, where the alkyne group is attached to a Cl group is reported as 2190 – 2270 cm^{-1}. Socrates also reports that this bond will have a strong band due to C-Cl stretching in the region of 430 – 760 cm^{-1}. Similarly to the C≡C stretching vibrations, this frequency becomes higher with increasing electron negativity of the attached halogen group. This lead to the conclusion that for an alkyne group with an F attached, the stretching frequencies would be in the region ~2250 – 2450 cm^{-1} and ~500 – 800 cm^{-1}.

In addition to the stretching vibrations, monosubstituted acetylenes, in which the substituent is not an alkyl group, absorb in the region 260 – 510 cm^{-1}as a result of deformation vibrations [106].

Nitrile containing end groups

According to Socrates, nitrile containing compounds normally have a sharp absorption in the region 2260-2200 cm^{-1}. These can be difficult to identify, because C≡C stretching vibrations also absorb in this region, as well as compounds with cumulative double bonds. In IR spectra, the C≡N stretching band may be of variable intensity. Oxygen atoms on neighbouring carbons tend to reduce the intensity, whereas conjugation appears to increase the intensity of the band. The intensity is also reduced by electron withdrawing atoms or groups. In Raman spectra, the band is of medium-to-strong intensity.

In general, aliphatic nitriles have a medium band at ~360 cm^{-1} in IR and Raman spectra; and a very strong band at ~180 cm^{-1} in Raman [106].

Isonitriles (-N≡C) have strong absorptions in similar regions to nitriles. However, they have a characteristic band, not found for nitriles near ~1595 cm^{-1}.

2.8 *Ab initio* calculations for end group IR and Raman spectra

To assist in determining the structures of alkyne end groups, *ab initio* calculations were conducted, using the SPARTAN software package [135], to determine the predicted Raman and Infrared frequencies for several possible configurations where an alkyne bonded to an F or similar configuration is present. Information regarding the expected spectral regions was difficult to find in the literature and where sparse information regarding halogens bonded to alkynes was found, F was not covered. Therefore several assumptions had to be made to extrapolate the information about the other halogens, I, Br and Cl, to arrive at expected values for the IR and Raman spectra of F bonded to alkynes. This led to the decision to utilise *ab initio* calculations to simulate expected structures and to calculate the IR and Raman spectra of these structures.

The compounds modelled, as well as their respective Raman and IR spectra can be seen in the following section:

2.8.1 Terminal alkyne end group

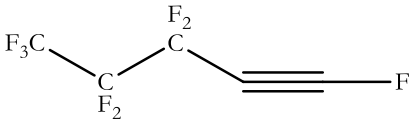

Figure 22: *Structure of the proposed terminal alkyne group for ab initio calculations.*

Figure 22 shows the structure of the proposed end group that is believed to be present in the PTFE chains. The structure was modelled with only 3 carbon backbone atoms in the chain to limit calculation time. Adding more would have constituted a better representation of a PTFE chain, but would have significantly increased calculation time. It is believed that the modelled compound provided an accurate depiction for the purpose of identifying end groups. As can be seen Figure 23, the Raman spectra calculated by *ab initio* corresponds very well with the frequencies predicted for these groups with the help of the publication by Socrates. The very large peak in Figure 23 at 2465 cm^{-1} is only slightly higher than the estimated value of ~2450 cm^{-1}. The higher than expected frequency is likely because of the highly electron negative nature of the F atom. There is also a medium intensity peak at 612 cm^{-1} which coincides with the predicted range of 500 – 800 cm^{-1}.

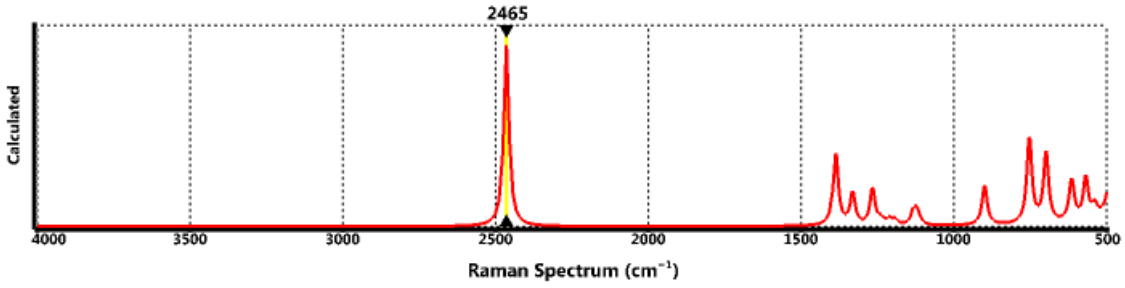

Figure 23: *Predicted Raman spectra of the proposed terminal alkyne group, according to ab initio calculations.*

Figure 24, clearly shows a very strong band at 2465 cm^{-1} in the IR spectrum which is assigned to the terminal C≡C group.

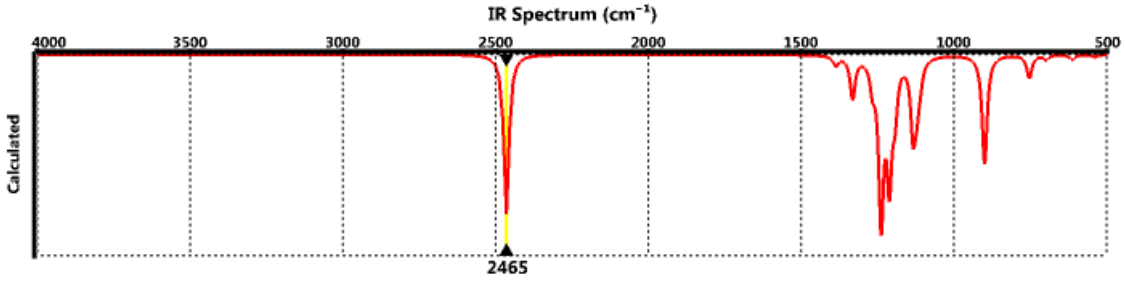

Figure 24: *Predicted IR spectra of the proposed terminal alkyne group, according to ab initio calculations.*

2.8.2 Inner alkyne end group

Figure 25 shows the structure of another possible end group that could be present in the PTFE chains. It was modelled in a similar fashion to the previous structure. As can be seen in Figure 26, the Raman spectra calculated by *ab initio* coincides with the values predicted with the help of Socrates. The intense peak at 2403 cm^{-1}, as well as the less intense peak at ~600 cm^{-1}, fall into the predicted ranges.

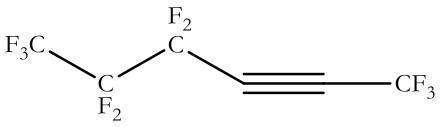

Figure 25: *Structure of the proposed inner (non-terminal) alkyne group for ab initio calculations.*

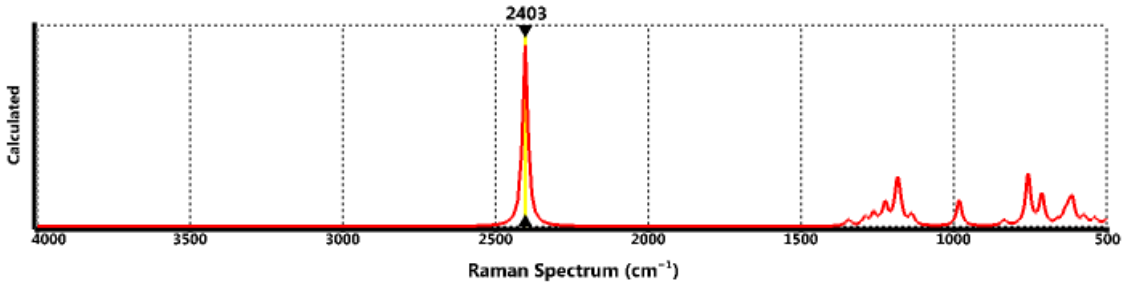

Figure 26: *Predicted Raman spectra of the proposed inner alkyne group, according to ab initio calculations.*

Figure 27 shows the clear absence of any band in the region of ~2450 cm^{-1}. This is because of the inner position of the C≡C bond which lessens the intensity of the band in the IR spectrum.

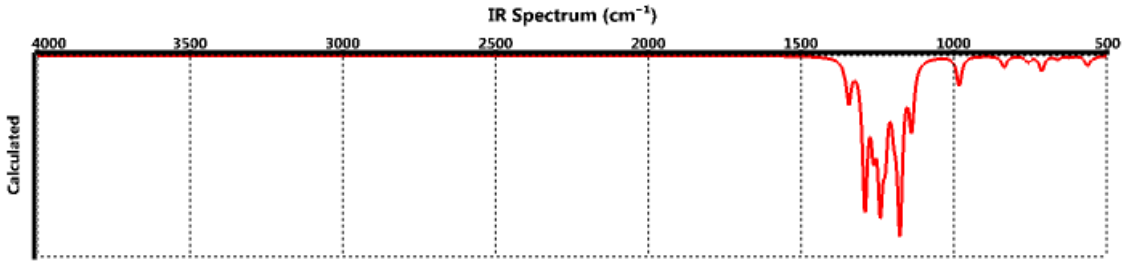

Figure 27: *Predicted IR spectra of the proposed inner alkyne group, according to ab initio calculations.*

2.8.3 Double alkyne end group

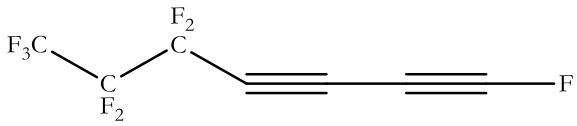

Figure 28: *Structure of the proposed double alkyne group for ab initio calculations.*

Figure 28 shows the structure of another possible end group that could be present in the PTFE chains. It was modelled in a similar fashion to the previous structure. As can be seen in Figure 29, the Raman spectra calculated by *ab initio* shows a very intense peak at ~2440 cm^{-1}, which is due to the C≡C stretching vibration. This coincides well with the value predicted with the help of Socrates. However, there is another well defined peak at 2326 cm^{-1}, which is likely due to an overtone/combination band enhanced by Fermi resonance, due to the disubstituted nature of the alkyne.

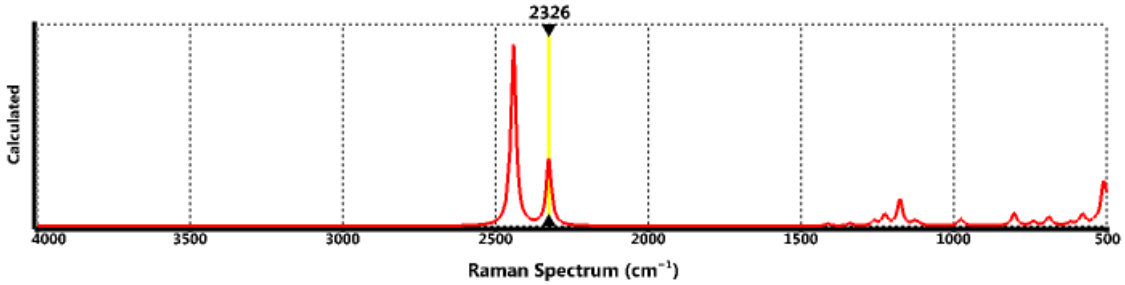

Figure 29: *Predicted Raman spectra of the proposed double alkyne group, according to ab initio calculations.*

Similarly to the IR spectra of the terminal alkyne group, the double alkyne group in Figure 30 shows a very strong peak at 2441 cm^{-1}, which indicates the terminal C≡C bond.

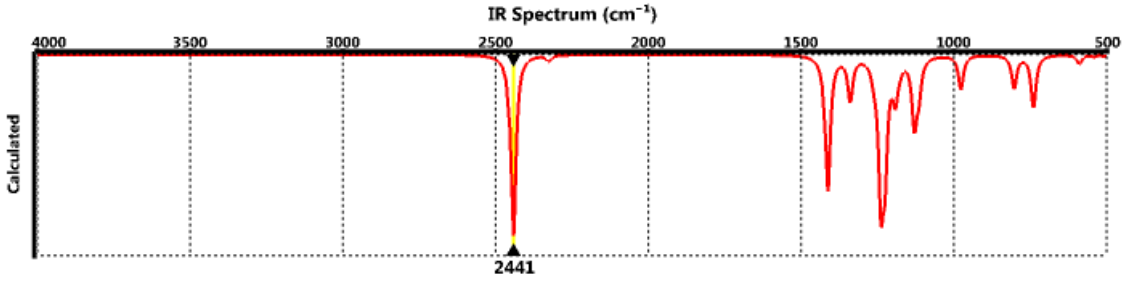

Figure 30: *Predicted IR spectra of the proposed double alkyne group, according to ab initio calculations.*

2.8.4 Perfluorocarboxylic acid end group

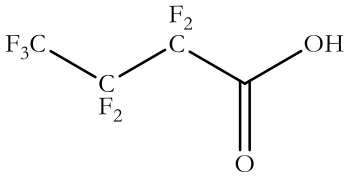

Figure 31: *Structure of the proposed perfluorocarboxylic acid end group for ab initio calculations.*

The sharp, medium intensity band at ~1900 cm^{-1} shown in Figure 32 is likely due to the C=O stretching vibration which has been shifted higher than normal (~1700 cm^{-1}) due to the electronegative fluorine atoms. Once again the sharp bands at ~750 cm^{-1} are in a region that is densely populated by PTFE vibrations and will therefore be very difficult to identify in sampled spectra. The band at 3744 cm^{-1} is unexpected and unassigned in Socrates and Pianca.

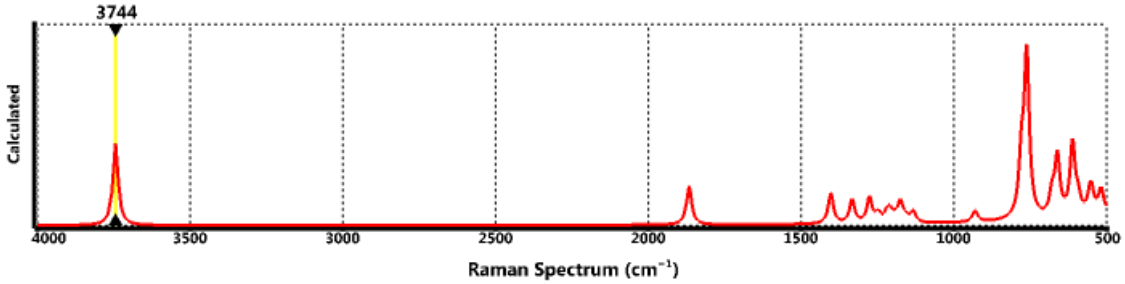

Figure 32: *Predicted Raman spectra of the proposed prefluorocarboxylic acid end group, according to ab initio calculations.*

From Figure 33, it can be seen that the broad band at 3300 – 2500 cm^{-1} due to hydrogen bonding of the OH groups reported by Socrates is completely absent. Though this is likely because the compound was only modelled as a single molecule and therefore no hydrogen bonding between molecules could occur. Socrates reports that the C=O group absorbs very strongly in the region ~1720 cm^{-1} and this frequency is heightened by electronegative substituents, which is in agreement with Figure 33. It is unclear what the sharp, medium intensity band at 3744 cm^{-1} indicates.

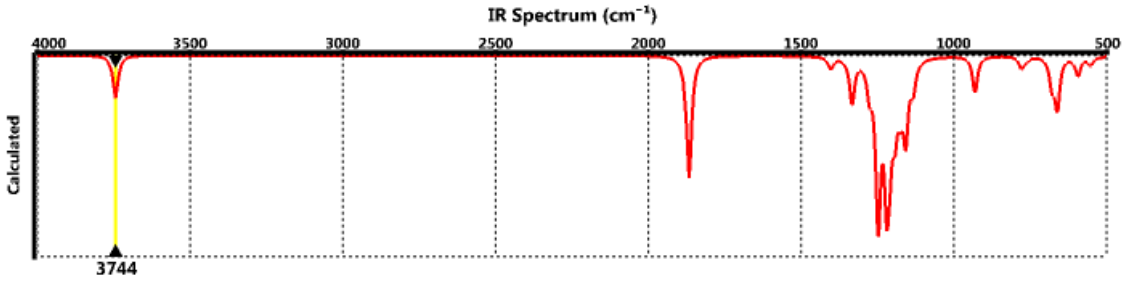

Figure 33: *Predicted IR spectra of the proposed prefluorocarboxylic acid end group, according to ab initio calculations.*

2.8.5 Perfluoronitrile end group

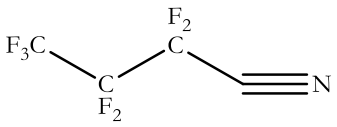

Figure 34: *Structure of the proposed perfluoronitrile end group for ab initio calculations.*

The calculated Raman spectra, shown in Figure 35 agree with the predicted sharp band in the region of ~2250 cm^{-1}, though this band is at a somewhat higher frequency due to the highly electronegative nature of the nitrile group's substituents. Socrates also reports medium bands in the region ~560 cm^{-1} which are present in Figure 35. The band at ~750 cm^{-1} is not assigned to any stretching vibration of a nitrile group by Socrates.

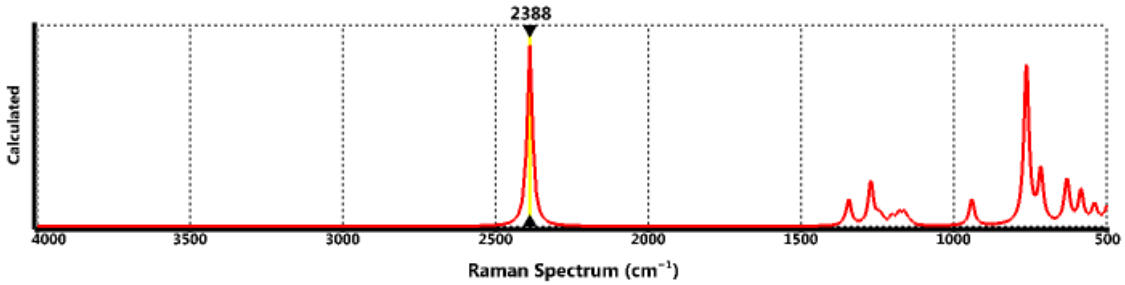

Figure 35: *Predicted Raman spectra of the proposed prefluoronitrile end group, according to ab initio calculations.*

From Figure 36 it is apparent that the sharp absorption band predicted by Socrates at ~2250 cm^{-1} is of a very weak intensity and at a higher frequency closer to ~2400 cm^{-1}. The higher frequency and weak intensity are expected due to the highly electronegative nature of the nitrile group's substituents. The sharp bands shown in Figure 36 all occur in the same region as PTFE's strong

structural vibrational bands. This will make them very difficult if not impossible to identify when interpreting the results.

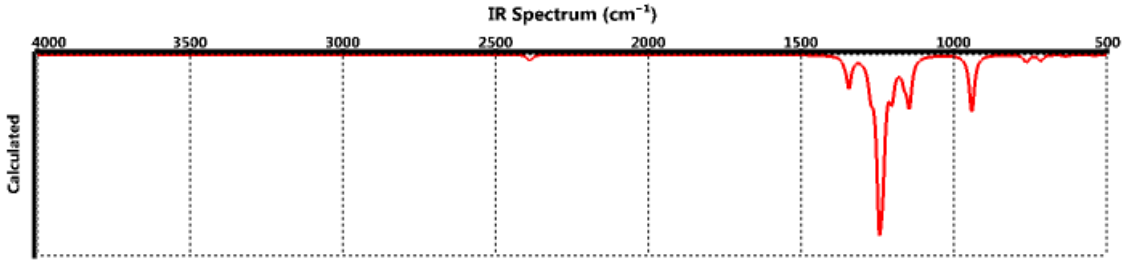

Figure 36: *Predicted IR spectra of the proposed prefluoronitrile end group, according to ab initio calculations.*

2.8.6 Perfluoro amide end group

The structure of the proposed amidic end group can be seen in Figure 37.

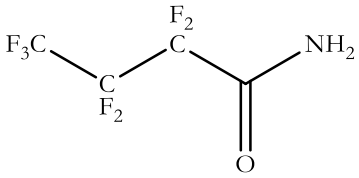

Figure 37: *Structure of the proposed perfluoro amide end group for SPARTAN calculations.*

From Figure 38 it is clear that the predicted calculated Raman spectra is somewhat different than the spectra predicted by Socrates and Pianca. The two bands at ~1768 and 1587 cm^{-1} are present and of weak intensity, as expected. However, the two bands that were predicted at 3555 and 3438 cm^{-1} seems to have shifted to significantly higher frequencies of ~3700 and 3600 cm^{-1}. This could be because of the electronegative nature of the fluorine atoms shifting the frequencies higher. Similar peaks can be seen in the IR spectrum in Figure 39.

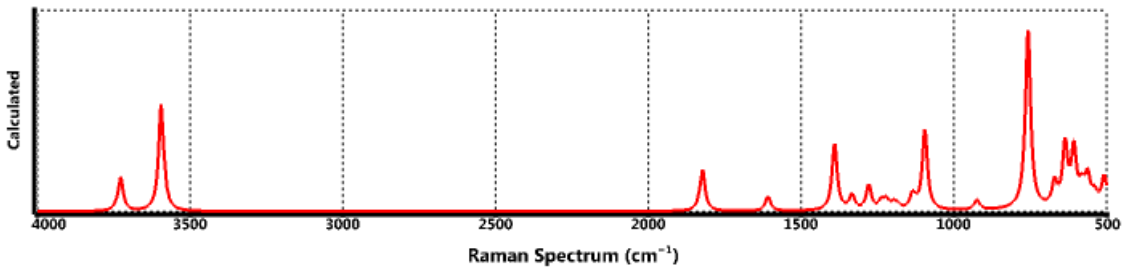

Figure 38: *Predicted Raman spectra of the proposed prefluoro amide end group, according to ab initio calculations.*

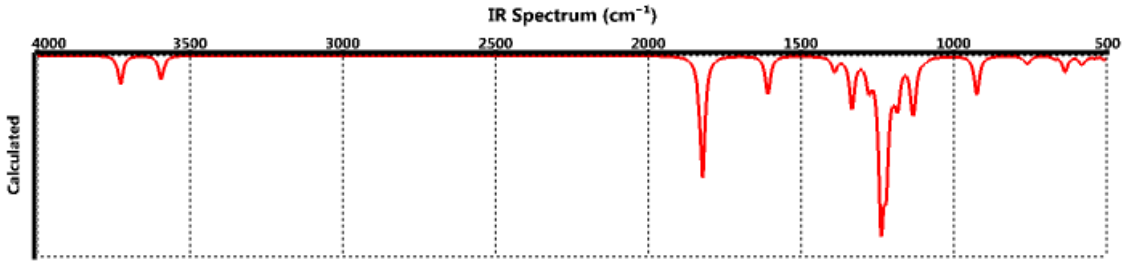

Figure 39: *Predicted IR spectra of the proposed prefluoro amide end group, according to ab initio calculations.*

2.9 Molecular weight

Aqueous free-radical polymerisation (both precipitation and emulsion) may yield molecular masses anywhere from 300 Da to 10^7 Da, depending on the initiator concentration, temperature and reaction pressure. Higher TFE partial pressures, low initiator concentrations and low temperatures generally result in higher molecular masses. Commercial PTFE is marketed with a reported number average molecular mass range of 10^6 – 10^7 Da [35]. Liquid medium photoinitiation usually produces a waxy, low-molecular weight polymer, however, the Ausimont corporation has indicated that high polymers with thermal and mechanical properties similar to those produced by conventional free-radical methods can be obtained at low temperatures (~ 15 °C) when combining photoinitiation of peroxide initiators with emulsion polymerisation techniques [56].

It has been well established that PTFE is insoluble in all known solvents. Therefore the usual methods for measuring molecular weight such as gel-permeation column (GPC) are not applicable. A method for measuring the molecular weight was presented by Sperati *et al.,* [71]. This method uses the specific gravity to determine the molecular weight. This method, while practical, presents several problems. It is complicated to execute and possible micro-voids in the sample tend to cause a lower specific gravity reading than the actual value, resulting in inaccurate molecular weight results [136]. Suwa and co-workers [136] found that the heat of crystallisation of the polymer melt is closely related to its molecular weight. Based on their findings, a simple and reliable method for measuring the molecular weight from the heat of crystallisation which can be obtained from a differential scanning calorimeter (DSC) curve.

According to their results, a virgin polymer (polymer which has not been exposed to any elevated temperatures since polymerisation) has two melting peaks, while a sample crystallised from that same polymer melt shows a single melting peak at a much lower temperature than the virgin polymer. The heat of fusion for the virgin polymer was also shown to be larger than the sample crystallised from the melt. These findings indicate that the polymer has a high level of crystallinity

as polymerised because of its entirely linear structure and that the sample cooled from the melt has lower crystallinity because the polymer chains of very high molecular weight cannot completely crystallise during cooling [137, 138]. Therefore some polymer chains remain in the amorphous state [136].

Their results show the crystallisation peak is remarkably affected by the polymer molecular weight. The larger the molecular weight, the smaller and broader the crystallisation peak is. This means that a higher molecular weight polymer, when crystallised from the melt, gives a lower level of crystallinity. This makes sense when considering that the longer polymer chain has greater difficulty in arranging itself regularly during the solidification because of smaller mobility and greater entanglement [136].

The heat of crystallisation calculated from DSC curves was plotted against the number average molecular weight on a logarithmic scale. The straight line that was obtained can be plotted by Equation 1 [136]:

$$\bar{M}_n = 2.1 \times 10^{10} \Delta H_c^{-5.16} \quad (1)$$

Here ΔH_c is the heat of crystallisation in cal·g^{-1}. The advantages of this method are that it is simple, quick, reproducible and only requires a small amount of sample. Suwa's method was modified by Wiegel [139] to give Equation 2:

$$\bar{M}_n = 3.5 \times 10^{11} \times \Delta H_c^{-5.16} \quad (2)$$

It must be noted that these correlations can be trusted only if the calculated M_n falls between 10^5 and 10^7 g·mol^{-1}.

Little is known in the literature about the weight average molecular mass of PTFE.

2.10 Thermal stability

PTFE exhibits excellent thermal stability, being inert to over 400 °C even under pure oxygen. Pure PTFE will exhibit nearly the same degradation temperature under air and nitrogen, while modified and filled PTFE will generally exhibit a lower oxidative stability due to catalytic effects. Smith and co-workers have discussed the mechanism of TFE polymer breakdown [49].

The intrinsic thermal stability of PTFE is measured *via* thermogravimetric analysis, or TGA [49], using the standard ASTM method for polymer analysis, which follows a heating program from

ambient (~25 °C) to 850 °C at a rate of 10 °C·min^{-1} under a nitrogen atmosphere flowing at 50 mL.min^{-1} [35]. Oxidative thermal stability follows the same method, but, substituting oxygen or air for nitrogen. Typically, 25 mg of polymer is used in the analysis and α-alumina crucibles are employed, although, platinum or any other high-temperature material may be specified as crucible material. Depending on the reaction conditions in the instrument, mixtures of PTFE with certain metals may undergo runaway reaction and care must be taken to ensure that these compositions do not destroy the instrument [140].

While the intrinsic thermal stability of PTFE is determined by the end group or the CF_2 backbone, any real TFE homopolymer exhibits a pseudo-thermal stability [35]. Low-molecular-weight PTFE or PTFE with a large polydispersity tends to evaporation off the low molecular mass chains from 300 °C to the bulk breakdown temperature. In these cases, thermogravimetric experiments may show total polymer mass loss before the bulk breakdown temperature, even though no chain breakage has occurred.

2.11 Melting point

Melting point is determined using either a DTA or a DSC, running approximately 5 mg of polymer at 10 °C·min^{-1} from ambient to 400 °C and back again under a nitrogen atmosphere flowing a 50 mL·min^{-1} [141]. Typically, aluminium or platinum pans are used for the melting point determination. Accuracy requires that the polymer be cycled through at least two, but preferably three thermal cycles to remove any thermal history, with the melting point determined from the data of the third thermal cycle.

2.12 Photoinitiated PTFE

2.12.1 Introduction

As an offshoot to the originally intended purpose of this dissertation, additional work was carried out concerning the photoinitiation of PTFE using H_2O_2 as initiator. The work was carried out to determine which part of the electromagnetic spectrum is responsible for the photoinitiation of PTFE and whether synergistic effects between different regions of the spectrum *i.e.* UV, IR and the visible light spectrum have an effect.

2.12.2 Electromagnetic spectrum

Regions of the spectrum

The electromagnetic spectrum is a collective term referring to the entire range and scope of frequencies of electromagnetic radiation and their respective, associated photon wavelengths.

The electromagnetic spectrum extends from below the low frequencies used for modern radio communication to gamma radiation at the short-wavelength (high-frequency) end. Visible light lies toward the shorter end, with wavelengths from 400 to 700 nm.

The types of electromagnetic radiation are broadly classified into the following classes:

- Gamma radiation
- X-ray radiation
- Ultraviolet radiation
- Visible radiation
- Infrared radiation
- Terahertz radiation
- Microwave radiation
- Radio waves

This literature review focuses on three of these regions, namely infrared, visible light and the ultra-violet spectrum, because these are the three regions of the electromagnetic spectrum that were used in the work done by the author, the relevance of which will become clear in due course.

Infrared

The infrared part of the electromagnetic spectrum covers the range from roughly 1 mm - 750 nm. It can be divided into three parts [142]:

- Far-infrared, from 1000 – 10 μm. This radiation is typically absorbed by rotational modes in gas-phase molecules, by molecular motions in liquids, and by phonons in solids.
- Mid-infrared, from 10 – 2.5 μm. This radiation is absorbed by molecular vibrations, where the different atoms in a molecule vibrate around their equilibrium positions. This range is sometimes called the fingerprint region, since the mid-infrared absorption spectrum of a compound is very specific for that compound, which is why it is used in FTIR spectroscopy.

- Near-infrared, from 2,500 –750 nm. Physical processes that are relevant for this range are similar to those for visible light. The highest frequences in this region can be detected directly by some types of photographic film, and by many types of solid state image sensors for infrared photography and videography.

Visible light

By definition, visible light is the part of the electromagnetic spectrum the human eye is the most sensitive to. The sun emits its peak power in the visible region. Visible light (and near-infrared light) is typically absorbed and emitted by electrons in molecules and atoms that move from one energy level to another. This action allows the chemical mechanisms that underlie human vision and plant photosynthesis. The light that excites the human visual system is a very small portion of the electromagnetic spectrum.

Electromagnetic radiation with a wavelength between 380 and 760 nm is perceived as visible light. Other wavelengths, especially near infrared (longer than 760 nm) and ultraviolet (shorter than 380 nm) are also sometimes referred to as light, especially when the visibility to humans is not relevant. White light is a combination of lights of different wavelengths in the visible spectrum. Passing white light through a prism splits it up into the several colours of light observed in the visible spectrum between 400 and 780 nm. At most wavelengths, however, the information carried by electromagnetic radiation is not directly detected by human senses. Natural sources produce electromagnetic radiation across the spectrum, and technology can also manipulate a broad range of wavelengths.

Ultra violet region

The wavelength of UV rays is shorter than the violet end of the visible spectrum but longer than the X-ray. About 10 % of the power emitted by the sun is UV radiation.

The UV range spans a range of 100 to 400 nm. The UV range can be further divided into three sub-regions. These are the UVA, UVB and UVC regions. The UVC range spans 100 to 280 nm. Due to absorption by the atmosphere very little reaches Earth's surface. These wavelengths are mostly absorbed by nitrogen and, at longer wavelengths, by simple diatomic oxygen in the air.. The UVB range spans 280 to 315 nm and is mostly blocked by the ozone layer. UVA spans 315 to 400 nm, is the lowest energy range of UV and is not blocked well by the atmosphere. Commonly called "black light", this is actually the most abundant component of solar ultraviolet radiation,

accounting for approximately 95 % of the ultraviolet energy striking the earth's surface at the equator.

All the aforementioned absorbances leave less than 3 % of sunlight at sea level in UV, with all of the remainder being at the lower energies (longer wavelengths). UV rays can break chemical bonds, making molecules unusually reactive. An example of this is being able to initiate polymerisation reactions.

Sunlight

Sunlight is a portion of the electromagnetic radiation given off by the sun, in particular infrared, visible, and ultraviolet light. On Earth, sunlight is filtered through Earth's atmosphere, and is obvious as daylight when the sun is above the horizon. When the direct solar radiation is not blocked by clouds, it is experienced as sunshine, a combination of bright light and radiant heat. When it is blocked by clouds or reflects off other objects, it is experienced as diffused light.

The spectrum of the sun's solar radiation is close to that of a black body with a temperature of about 5,800 K [143]. The sun emits electromagnetic radiation across most of the electromagnetic spectrum. The sun emits X-rays, ultraviolet, visible light, infrared, and even radio waves. The spectrum of nearly all solar electromagnetic radiation striking the Earth's atmosphere spans a range of 100 nm to about 1 mm (1,000,000 nm). The total irradiance of the sun on the earth is represented in Figure 40.

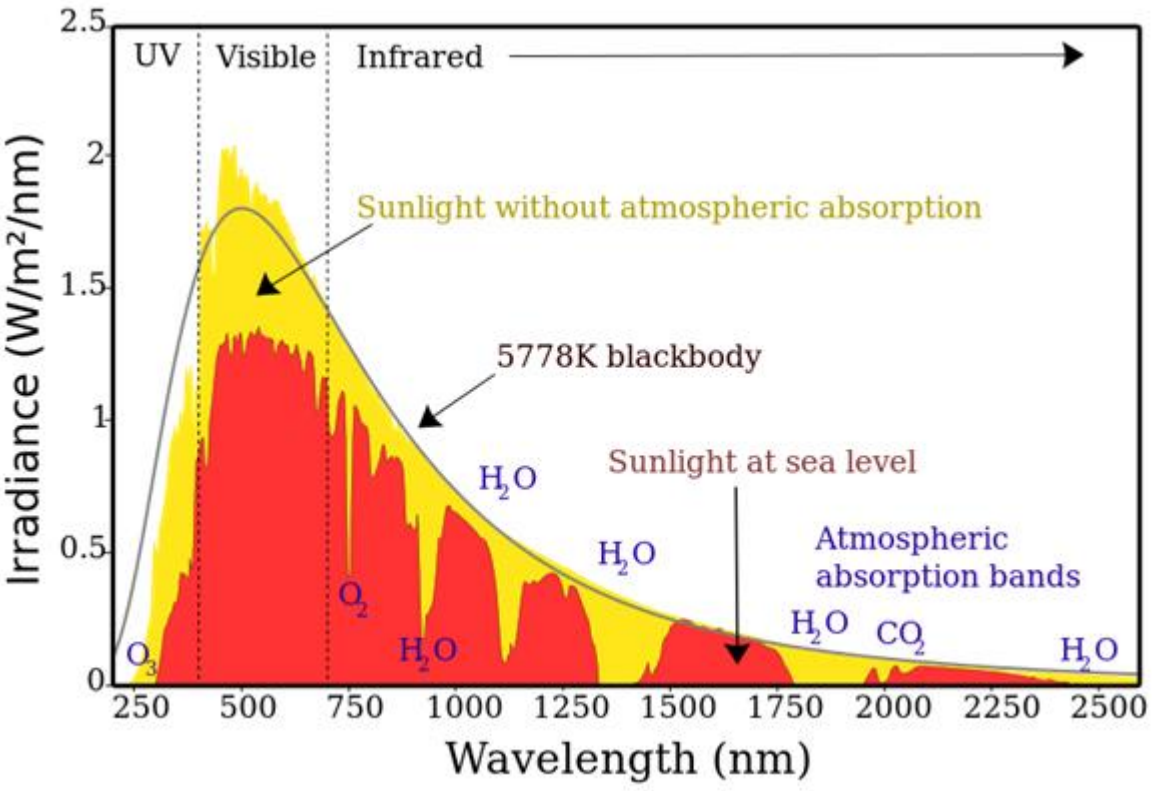

Figure 40: *The solar radiation spectrum for direct light at both the top of the Earth's atmosphere (represented by yellow area) and at sea level (red area) [144].*

The sun produces light with a distribution similar to what would be expected from a 5525 K (5250 °C) blackbody, which is approximately the sun's surface temperature. As light passes through the atmosphere, some is absorbed by gases with specific absorption bands. Additional light is redistributed by Raleigh scattering, which is responsible for the atmosphere's blue colour. These curves are based on the American Society for Testing and Materials (ASTM) Terrestrial Reference Spectra, which are standards adopted by the photovoltaics industry to ensure consistent test conditions and are similar to the light that could be expected in North America. Regions for ultraviolet, visible and infrared light are indicated [144].

The spectrum of surface illumination depends upon solar elevation due to atmospheric effects, with the blue spectral component dominating during twilight before and after sunrise and sunset, respectively, and red dominating during sunrise and sunset. when illumination is indirect, Rayleigh scattering in the upper atmosphere will lead blue wavelengths to dominate. Water vapour in the lower atmosphere produces further scattering and ozone, dust and water particles will also absorb selective wavelengths [145, 146]. The spectrum of the visible wavelengths during different times of day are represented in Figure 41.

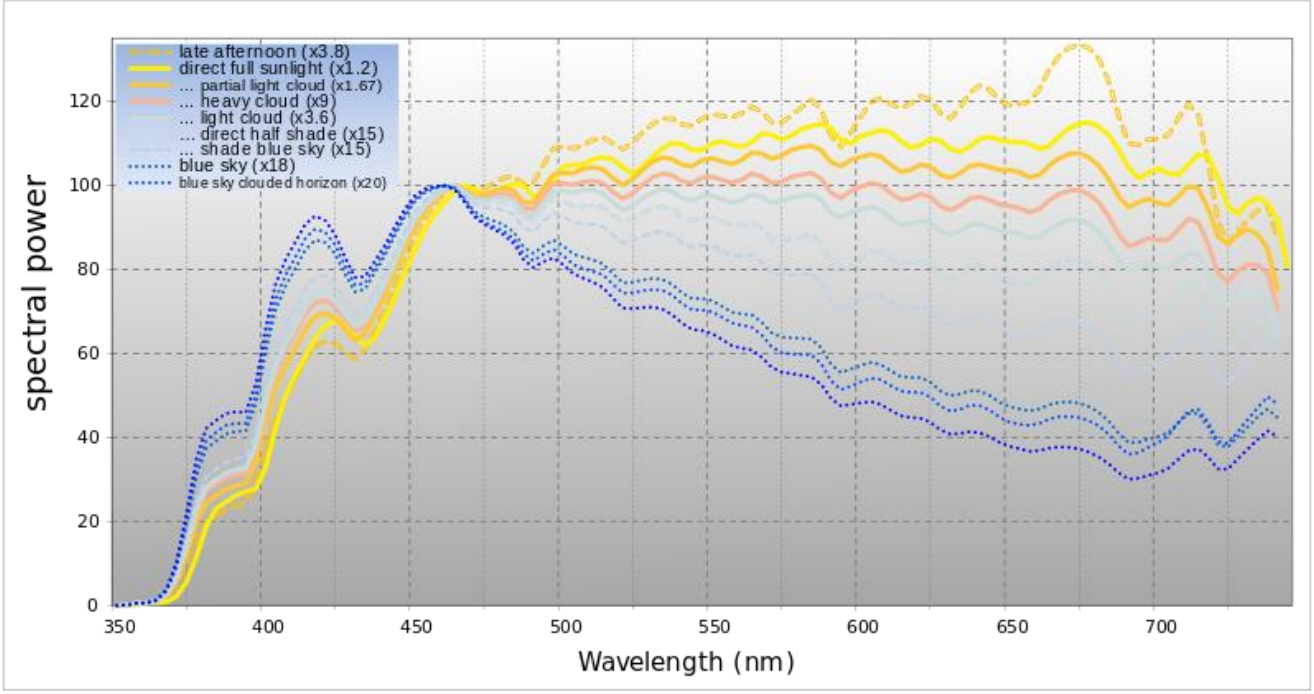

Figure 41: *Spectrum of the visible wavelengths at approximately sea level; illumination by direct sunlight compared with direct sunlight scattered by cloud cover and with indirect sunlight by varying degrees of cloud cover. The yellow line shows the spectrum of direct illumination under optimal conditions. The other illumination conditions are scaled to show their relation to direct illumination. The units of spectral power are simply raw sensor values with a linear response at specific wavelengths [147].*

2.13 Colour theory

A modest understanding of colour theory was helpful during the work conducted as discussed in this report.

Colouring of a compound is due to the way that electromagnetic energy interacts with matter and the way that human visual senses (the human eye and brain) perceives these interactions. The portion of the electromagnetic spectrum that is of interest to this discussion is the visible portion, or what is commonly known as *light*. This visible light includes all the colours that humans perceive: violet, blue, green, yellow, orange, red, and the various combinations thereof. Light can interact with matter in several different ways including: absorption, reflection, transmission and scattering. Several things can happen when light strikes an object, namely:

- All wavelengths of the light may be entirely reflected from the surface, which would result in what we perceive as the colour" white.

- All wavelengths may be entirely absorbed by the object, which could result in what we perceive as the "colour" black.
- The light may be completely transmitted through the object, with little interaction, resulting in what we call a colourless object. Glass is an example of this.
- Some wavelengths can be reflected and others absorbed, resulting in the appearance of the different colours.

The three components of the vision system are the object being viewed, the light, and the eye. When light strikes an object, a portion of the visible spectrum may be absorbed by the molecules comprising the object. Some portion that is not absorbed reflects off the object and strikes the eye, interacting with the molecules that make up the light sensors in the eye. A signal is sent to the brain and colour is perceived.

Colour is perceived because certain portions of the spectrum are absorbed by an object and others are not. As with many properties of compounds, this is determined by the structure of the molecules comprising the compound. Most simple organic compounds, having few multiple bonds and few functional groups, do not absorb visible light, and therefore appear as being colourless or white. More complex molecules, having several multiple bonds that are conjugated appear as being coloured. For multiple bonds to be conjugated, they must be in an alternating double bond–single bond–double bond, *etc.* arrangement. Figure 42 shows the difference between a conjugated and an unconjugated system.

Figure 42: *A conjugated system (left) versus an unconjugated system (right). Note that the compound on the left has an alternating single-double-single bond system, where the bonds can alternate, whereas the compound on the right does not.*

Such conjugation allows absorption of visible light because of the following: When ultraviolet or visible light (UV-Vis) is absorbed by a molecule, the energy goes into increasing the energy levels of valence, or outer shell electrons. In other words when light is absorbed by the molecule, these electrons, which normally reside in the ground state, are pushed up to higher energy levels or to an excited state. If the energy level of the excited state is much higher than that of the ground state, a large amount of light energy is required to push the electrons up to the higher level, and a correspondingly higher energy of light is needed to do this. If the excited state is closer in energy to the ground state, a correspondingly lower energy of light is needed.

For molecules having conjugated systems of electrons, the ground states and excited states of the electrons are closer in energy than for non-conjugated systems. This means that lower energy light is needed to excite electrons in conjugated systems, which means that lower energy light is absorbed by conjugated systems. The degree of conjugation determines the actual energy difference between the ground and excited states. The more highly conjugated the system the lower the energy difference and the lower the required energy of light needed to excite the electrons. In other words molecules having more conjugated multiple bonds absorb lower energies of light than do molecules having fewer conjugated multiple bonds.

The energy of the various colours in the visible spectrum differs. Energy of visible light increases in the following order: red, orange yellow, green, blue, violet. A highly conjugated system absorbs the lower energy portions of the light and reflect what is not absorbed. It is this reflected portion that the eye will perceive as the colour of that object. A less highly conjugated system will require the absorption of the higher energy part of the spectrum, allowing the lower energy parts to be reflected to the eye.

The colour that is reflected is the complementary colour of the colour that is absorbed. For example if the high energy violet portion of the spectrum is absorbed, its complementary colour of yellow is what is observed. If the lower energy blue or green colours are absorbed, the colours orange or red would be observed. To illustrate this, consider the structure of a few molecules. retinol, or vitamin A, has five conjugated double bonds and absorbs the violet part of the spectrum, therefore appearing as yellow. The structure for retinol can be seen in Figure 43.

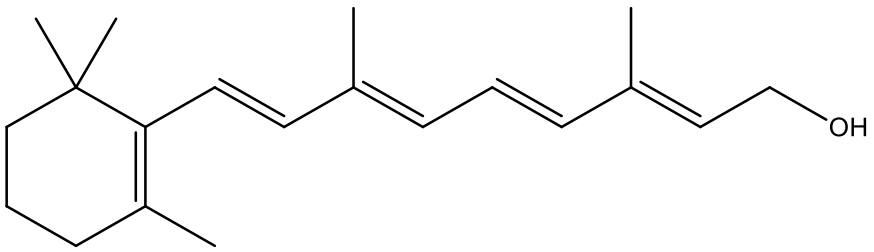

Figure 43: *Structure of retinol.*

The more highly conjugated β-carotene and lycopene, each having eleven conjugated double bonds absorb in the lower energy blue and green portions of the spectrum and appear as orange and red. β-carotene and lycopene's structures can be seen in Figure 44 and Figure 45 respectively.

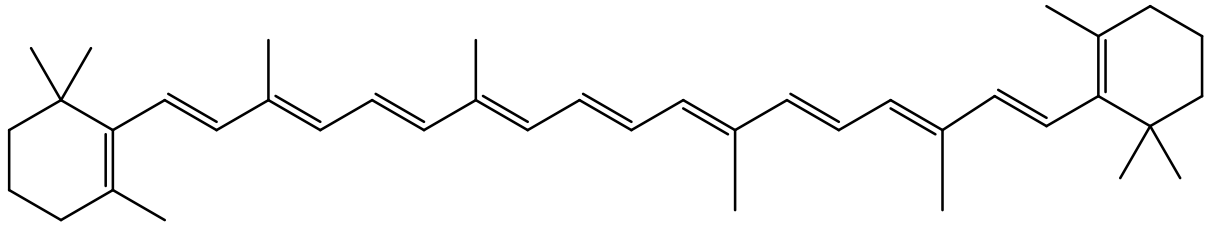

Figure 44: *Structure of β-carotene.*

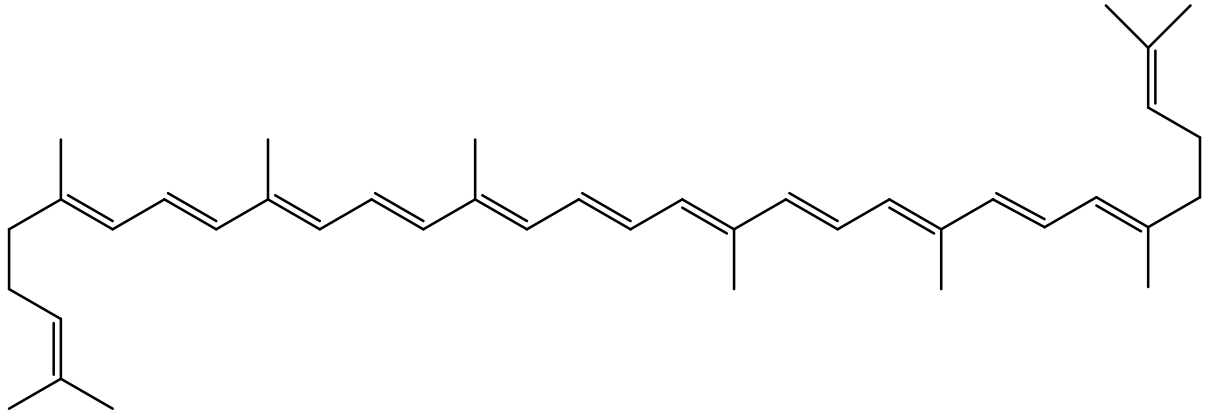

Figure 45: *Structure of lycopene.*

Chapter 3

Experimental

3.1 Depolymerisation of PTFE

TFE, because of its explosive potential, is not available commercially. The FMG gets its TFE by the vacuum pyrolysis of PTFE, which depolymerises PTFE into TFE. The design and construction of the system to depolymerise PTFE has already been well described [35] and will therefore not be repeated in this document. A short description of the operation of this system follows:

A stainless steel tube serves as the depolymerisation vessel, *i.e.* the vessel in which depolymerisation takes place. The appropriate amount of PTFE, usually 15 g, is poured into this vessel, which is then inserted into a tube furnace. Once secure in the furnace, the depolymerisation vessel is coupled to the cold trap system, which gathers the gaseous TFE and by-products once pyrolysis has taken place. The cold trap is a sealed stainless steel cylinder, which is placed in a bath of liquid nitrogen. Once coupled, the entire system is placed under vacuum using a vacuum pump. Once securely coupled to the cold trap system, the furnace is switched on and programmed to reach a temperature of 700 °C and to hold that temperature for approximately 1 hour. The gaseous products from depolymerisation flow from the depolymerisation vessel into the cold trap. The cold trap is then sealed and allowed to defrost, which yields approximately 15 g of gaseous TFE ready to be used for polymerisation. A schematic representation of this system is shown in Figure 46 and a photo of the working system can be seen in Figure 47.

According to GC-MS analysis conducted on a sample of the depolymerisation products, the products obtained from depolymerisation contain 93 % TFE, 6 % HFP and trace amounts of OFCB and PFIB. This was still deemed acceptable, as HFP does not readily polymerise [148] and the other compounds were present in such small amounts so as not to adversely affect polymerisation.

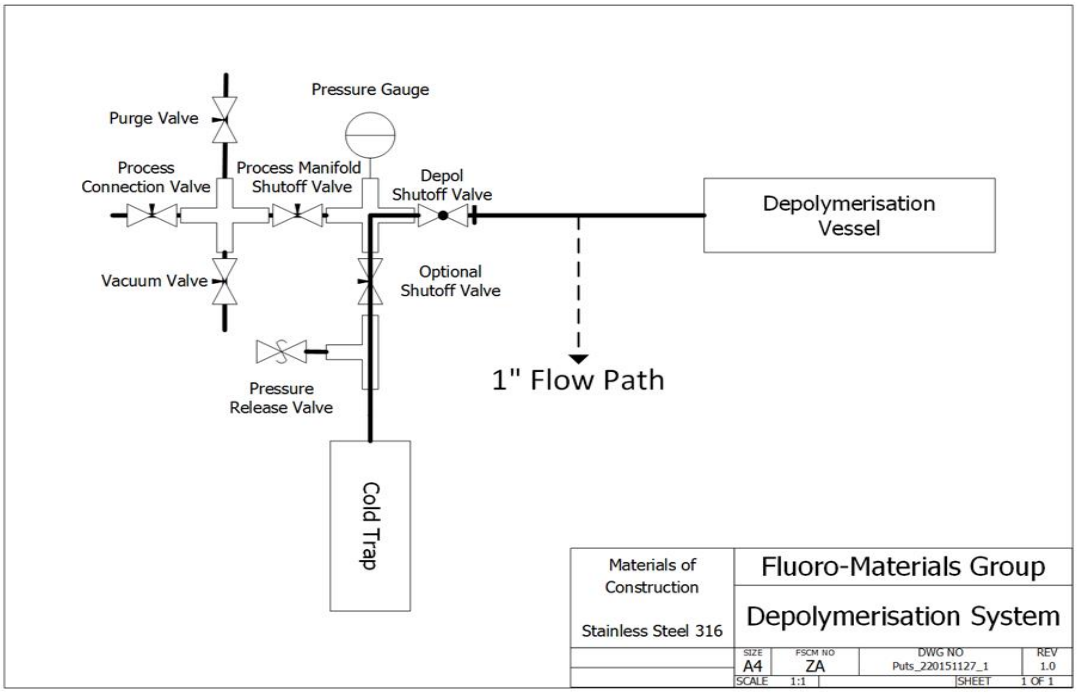

Figure 46: *Piping diagram for the depolymerisation system [35].*

Figure 47: *The depolymerisation system setup in the FMG laboratory.*

3.2 Thermally initiated polymerisation of TFE

Polymerisation was conducted either in a Parr Instruments Pressure Reactor (autoclave), or in borosilicate glass tubes, otherwise known as Carius tubes.

The autoclave has an internal volume of 250 ml and can handle pressures up to 250 bar. This makes it suitable for larger scale polymerisation reactions, in the region of 5-10 g of polymer. The major drawback of the autoclave polymerisation system is that only one polymerisation can be carried out at a time. In most cases, the reaction is left to run for at least 12 hours (overnight). This means that only one polymerisation can be performed daily.

Although very different in construction and operation from the autoclave, the Carius tube manifold fulfils the same need, *i.e.* to facilitate polymerisation of gaseous monomers. The major difference is that with the Carius tube Manifold, the polymerisation takes place inside a sealed glass tube, with mixing being obtained by placing the tube inside an orbital shaking oven, instead of an internal mixing apparatus.

The Carius tube system is useful for smaller scale polymerisations in the region of 1 g. This is advantageous in terms of the amount of expensive monomers used, but means the analyst must be careful when analysing the polymer, as there will be a very limited amount of sample. Another major advantage of the Carius tube system is that because the orbital shaker has the capacity to contain several Carius tubes at the same time, many polymerisations can be done simultaneously, the only limit being the number of Carius tubes one can fit into the shaker. Currently, the operators at the FMG can do up to six polymerisations simultaneously, using the Carius tube system.

3.2.1 TFE polymerisation using ammonium persulfate as initiator

TFE was polymerised in the Parr instruments autoclave using APS as initiator, water as solvent and sodium tetraborate decahydrate (Borax) as the alkali buffer, as per Brubaker's patent [8]. The autoclave was charged with the APS, water and borax, sealed and subsequently frozen using liquid nitrogen allowing the atmospheric gases to be evacuated from it. It was then allowed to defrost and the process was repeated. Once the autoclave was defrosted for the second time, it was frozen again. Once frozen, the correct amount of gaseous TFE was added from the aforementioned cold trap vessel. The still-frozen autoclave was then moved to the reactor cradle and connected to the reactor controller. Once the reactor was defrosted, the impeller and heater were activated. The impeller speed was set at a constant rate of 700 rpm. The temperatures and initiator concentrations were varied for the experiments, to ascertain the effect these parameters have on the polymer molecular weight and which end groups the APS introduce onto the polymer chains. The

temperatures and initiator concentrations used can be seen in Table 5. The reaction was left to run overnight, with the temperature and pressure being recorded at 1 s intervals. The PTFE formed was a fine white powder suspended in water. This powder was then filtered and washed three times to ensure all impurities were removed. The filtered and washed powders were dried overnight at 80 °C. The samples were then ready for weighing and analysis.

Table 5: *TFE polymerisations using APS as initiator.*

Exp. number	Initiator %	Temp. (°C)	Mass TFE (g)	Mass Borax (g)	Vol. water (mL)	Time (h)
1	5,52	65	5	0.48	100	12
2	5,52	65	5	0	100	12
3	5,52	50	5	0.48	100	12
4	2,30	55	5	0.48	100	12
5	5,52	55	5	0.48	100	12
6	8,68	55	5	0.48	100	12
7	1,00	65	5	0.48	100	12
8	2,03	65	5	0.48	100	12
9	5,52	65	5	0.48	100	12
10	8,68	65	5	0.48	100	12
11	9,99	65	5	0.48	100	12
12	19,99	65	5	0.48	100	12
13	2,02	75	5	0.48	100	12
14	5,52	75	5	0.48	100	12
15	8,68	75	5	0.48	100	12
16	9,99	75	5	0.48	100	12
17	5,52	80	5	0.48	100	12
18	9,99	80	5	0.48	100	12
19	5,52	65	5	0.48	100	12

3.2.2 TFE polymerisation using potassium carbonate as buffer

TFE was successfully polymerised in exactly the same way as described above, except that the equivalent molar amount of K_2CO_3 was used as the buffer instead of borax. This was done to determine whether the different buffers used had an effect on the polymer.

3.2.3 TFE polymerisation using sodium persulfate as initiator

TFE was successful polymerised using the same methodology as previously described, with the exception of sodium persulfate being used as initiator instead of ammonium persulfate. This was done to determine whether the different persulfate salts had an effect on the polymer.

3.2.4 TFE polymerisation using potassium permanganate as initiator

TFE was successfully polymerised using the same methodology as previously described, with the exception of a strong oxidising agent, in this case potassium permanganate, being used as initiator. This was done to determine whether using a strong oxidiser had an effect on the polymer, specifically what kind of end groups it would form.

3.2.5 TFE polymerisation using di-tertiary-butyl peroxide as initiator

TFE was successfully polymerised using the same methodology as previously described, with the exception of a different peroxide compound, in this case di-tertiary-butyl peroxide, being used as initiator. This was done to determine whether using a different peroxide compound had an effect on the polymer, specifically what kind of end groups it would form.

3.2.6 TFE polymerisation using various other initiators

The polymerisation of TFE was attempted with various other initiators and solvents, according to various publications and patents. However, many of these methods proved unsuccessful when attempted. These methods include:

- TFE polymerisation with azo-compounds as initiators. These compounds included 4,4-azobis(4-cyanovaleric acid) and 2,2-azobis(2-methylpropionamidine), both of which are commonly used free radical polymerisation initiators. These polymerisations were attempted firstl with water as solvent and later with supercritical carbon dioxide as solvent. None of the attempts delivered any polymer.

- TFE polymerisation with benzoyl peroxide was attempted. Benzoyl peroxide is water insoluble. Therefore dimethyl carbonate was used as solvent, with a sodium lauryl sulfate used as surfactant. This attempt was also unsuccessful.
- TFE polymerisation with lauroyl peroxide was attempted. Similarly to benzoyl peroxide, lauroyl peroxide is water insoluble and was also used with DMC as solvent and sodium lauryl sulfate as surfactant. This too proved unsuccessful.

The recipes used for all polymerisations can be seen in Table 6.

Table 6: *TFE polymerisations using various thermally activated initiators.*

Exp. number	Initiator	Initiator %	Temp. (°C)	Mass TFE (g)	Vol. water (mL)	Time (h)
20	SPS	5.5	65	5	100	12
21	SPS	30	65	5	100	12
22	$KMnO_4$	1	35	5	100	12
23	$KMnO_4$	10	35	5	100	12
24	$KMnO_4$	30	35	5	100	12
25	DTBP	1	135	5	100	12
26	DTBP	10	135	5	100	12
27	DTBP	30	135	5	100	12
28	H_2O_2	10	80	5	100	12
29	ACPA	10	80	5	100	12
30	AAPH	10	80	5	100	12
31	BPO	10	85	5	100	12
32	LPO	10	85	5	100	12
33	ACPA	0.5	55	5	100	12
34	AAPH	0.5	55	5	100	12

3.3 Photo-initiated polymerisation of TFE

3.3.1 Sunlight initiated polymerisations

H_2O_2 as initiator

The first attempts to use hydrogen peroxide as an initiator for TFE polymerisation in the autoclave *via* thermal initiation proved unsuccessful. However when the polymerisation was photoinitiated,

it proved successful. The photoinitiated runs were carried out using Carius tubes. Initially, a single Carius tube was filled with 5 ml of a 37 % hydrogen peroxide solution, to which was added 0.5 g of TFE *via* the Carius tube manifold according to the freeze-thaw cycle described earlier. The Carius tube was frozen, flame-sealed and left to thaw. Once it had reached room temperature, it was placed on the roof of Engineering 2 on a sunny day and left there for approximately 6 hours. This first run was merely a proof of concept to determine whether photoinitiation of PTFE was plausible as described in the literature. After 6 hours the tube was removed from the rooftop. Inside the tube a fine white powder had formed. FTIR analysis of this powder proved that it was in fact PTFE.

Other initiators

Upon the success of this first run, several more runs were conducted with some of the other initiators mentioned previously. Three tubes were filled with solutions that contained by molar weight 5 % of 4,4'-azobis(4-cyanovaleric acid), APS and H_2O_2 respectively. These tubes were then also filled with TFE as previously described and flame sealed. Similarl to the initial run, they were left on the rooftop in direct sunlight for approximately 6 hours. The tubes containing H_2O_2 and APS as initiators both contained a fine white powder, indicating polymerisation had successfully taken place. Unfortunately the tube containing the 4,4'-azobis(4-cyanovaleric acid) seemed to have exploded while on the rooftop. It was concluded that the build-up of nitrogen gas by the decomposition of the initiator had increased the pressure inside the tube to the point where it surpassed the tensile strength of the glass. From the glass shards that were recovered, it was apparent that no PTFE had formed before the tube ruptured. No further experiments were conducted with either of the azo compounds.

3.3.2 Controlled photo-initiated polymerisations

Following the success of the initial photo-initiation experiments, it was decided to determine which region of the electromagnetic spectrum was responsible for the successful initiation and to investigate whether there were any synergistic effects. The decision was made to use H_2O_2 in these experiments, because thermal initiation using H_2O_2 had been unsuccessful.

The experimental setup was as follows: A single Carius tube was filled with 5 ml of a 37 % H_2O_2 solution. It was then filled with 0.5 g of TFE gas using the Carius tube manifold according to the process as previously described. A cardboard box was used as the "isolation chamber" to seal off the Carius tube from any external radiation. Three off-the-shelf light fittings were installed inside

the box and wired so that each could be switched on/off individually of the others. The three light fittings were fitted with the following lamps respectively:

- A fluorescent tube that imitates the natural visible spectrum (400 – 700 nm)
- A fluorescent tube that emitted only UV light (10 – 400 nm)
- A powerful incandescent bulb that emitted mostly IR radiation (1 mm – 750 nm)

A single Carius tube, filled with 5 ml of the 37 % H_2O_2 solution and 0.5 g TFE, was placed inside the isolation chamber and subsequently exposed to the different parts of the electromagnetic radiation spectrum (UV, IR, Visible) both individually and in combination to determine the effect this had on the polymerisation of PTFE. The list of the different combinations of radiation the tube was exposed to is as follows:

- IR
- Visible
- UV
- IR, Visible
- UV, Visible
- UV, IR
- UV, IR, Visible

The spectrum delivered by the lamp meant to imitate visible light can be seen in Figure 48 and the spectrum delivered by the UV lamp can be seen in Figure 49.

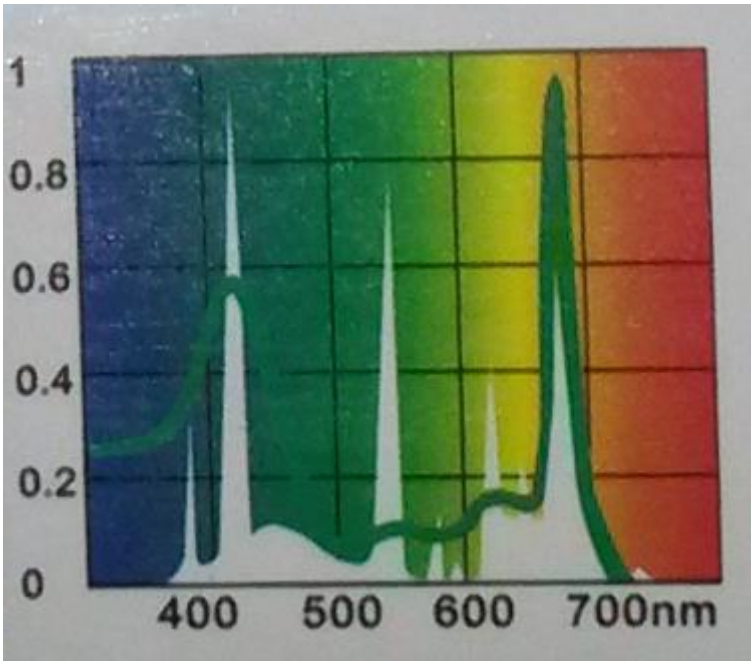

Figure 48: *Spectrum delivered by lamp to imitate the visible spectrum, as reported by the lamp manufacturer.*

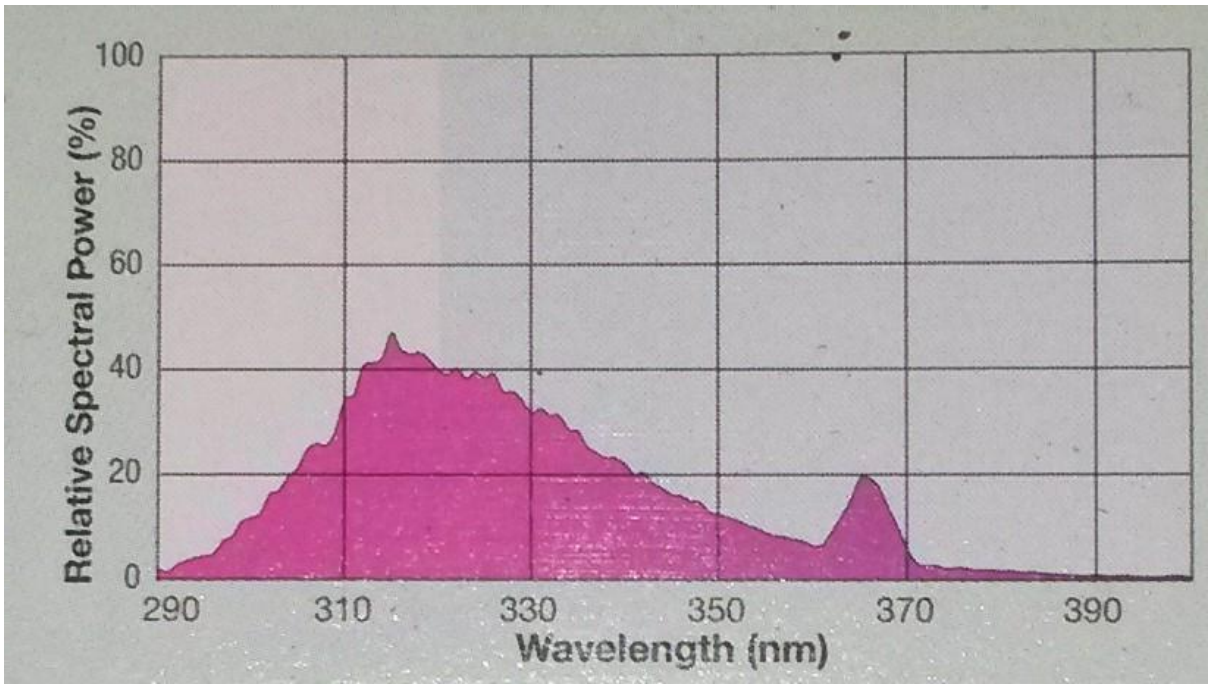

Figure 49: *Spectrum delivered by lamp to imitate the UV spectrum, as reported by the manufacturer.*

3.4 Pressing of PTFE discs

If the polymeric specimen being examined is a sufficiently thin film, then it may be introduced directly into the sample compartment with no further preparation to be examined by infrared

transmission techniques. Furthermore, if it is a thermoplastic then it is possible to use a hot press to prepare a thin film which may then be directly examined [106].

Several sources [131, 149] report pressing powders at room temperature to give transparent films for the study of highly crystalline samples. Moynihan [131] also reports studying strong absorption in the 1200 cm^{-1} and 650 – 400 cm^{-1} regions by suspending powdered polymer in KBr. When replicating these methods, several problems were encountered.

The PTFE powders, commercially obtained or produced in-house, were pressed into thin discs using a custom made stainless steel die and a workbench press. Approximately 250 mg of powder was weighed for each disc and pressed under 8 metric tons of pressure. The die produced discs with a diameter of 25 mm. The thickness of the discs varied, but on average the thickness was approximately 300 μm.

Firstly, when pressing the in-house produced PTFE powders at room temperature, the resulting films were not transparent and very brittle, making FTIR measurements very difficult, if not impossible. Most, but not all, of the pressed discs of the APS initiated experiments were yellow in colour. This is a stark contrast to the pure white colour and high ductility of pressed discs of commercial PTFE from DuPont and BFluor. It was believed that the yellow colour and brittleness of the produced PTFE samples was caused by different end groups than the commercial PTFE samples, as well as shorter chain lengths (therefore lower M_n), resulting in the end groups having a greater effect on the properties of the produced polymer.

When these powders were suspended in KBr and then pressed, the resulting spectra did not give a clear indication of the end groups as the spectral region where the signals of end groups were expected to be found was obscured by what was believed to be water adsorbed onto the KBr. Drying the KBr overnight in an oven alleviated the problem slightly, but did not eliminate it altogether. To render the process facile and more repeatable, the PTFE powders were eventually pressed at an elevated temperature of approximately 180 °C. This temperature is well below the melting point of PTFE and did not cause any additional discolouration of the discs. This resulted in transparent discs that were ductile enough to undergo the FTIR spectroscopy.

3.5 Sintering

Sintering was carried out in a Waltech Instruments muffle furnace. The furnace was allowed to reach a temperature of 380 °C and the temperature was held there. The pressed PTFE discs were placed inside an α-alumina crucible which was then placed inside the oven. Initially the discs were sintered for intervals of 2, 5, and 30 min respectively. However, this proved too time consuming

to replicate with all the produced discs, because after each sintering the discs had to be analysed with the FTIR spectrometer. It was decided to continue sintering the remaining discs only once for 30 min. This was carried out where possible. A problem arose with some of the lower molecular weight discs, where they partially melted when subjected to 380 °C. Once melted, the discs were impossible to extract from the crucible without destroying them, rendering them useless for transmission FTIR spectroscopy. This was because the discs had to have a minimum diameter of approximately 10 mm to cover the aperture in the instrument's sample holder. Powders of the samples that melted at 380 °C were re-pressed into discs and subjected to a lower temperature of 360 °C. Temperatures lower than this fall outside the temperature ranges at which sintering normally takes place and were therefore avoided. Most of the discs were usable after this treatment and still showed discolouration.

3.6 FTIR spectra measurements

3.6.1 ATR FTIR spectra measurements

Some of the pressed discs were initially analysed in a Perkin Elmer Spectrum 100 FTIR spectrometer using its ATR module. The samples were scanned from 4000 to 450 cm^{-1} at a resolution of 2 cm^{-1}, with 32 accumulations being done for each sample.

3.6.2 Transmission FTIR spectra measurements

The pressed discs, unsintered and sintered, were analysed in the same Perkin Elmer Spectrum 100 FTIR spectrometer using the transmission module. The samples were scanned from 4000 to 450 cm^{-1} at a resolution of 2 cm^{-1}, with 32 accumulations being done for each sample.

3.7 Raman spectra measurements

Raman analysis was performed using a WITec Alpha 300R Confocal Raman Spectroscopy instrument. The laser operated at an excitation wavelength of 532 nm and power of 6 W. The samples were scanned using various combinations of different scan times and accumulations, the most common configuration being 20 accumulations of 20 s each.

3.8 SS NMR spectra measurements

The NMR facility at the University of Pretoria is not capable of performing SS NMR measurements. Several facilities in South Africa and abroad were contacted to provide assistance. While a facility with a working ^{19}F SS probe could not be found, the NMR facility at the University of Stellenbosch offered to help with ^{13}C SS NMR spectroscopy. A single sample of low molecular

weight (and therefore high end group concentration) was sent to determine whether there was a signal present in the sample that would indicate the presence of alkyne end groups. Approximately 150 mg of the thermally initiated sample, initiated with 30 % $KMnO_4$ was sent for analysis using DP ^{13}C SS NMR using a MAS rotor spinning at 12 MHz.

3.9 TGA measurements

Thermogravimentric analysis was performed using a Hitachi STA7300 TGA-DTA instrument. Approximately 10 mg of sample was used for each run. Each sample was heated from 30 °C to 1000 °C at a rate of 10 °C·min^{-1} under and nitrogen atmosphere flowing at 200 mL·min^{-1}.

3.10 DSC measurements

Differential scanning calorimetry was performed on a Perkin Elmer DSC 4000 with ~12 mg of dried polymer sample. The samples were heated from 20 °C to 430 °C at a rate of 10 °C·min^{-1} before being cooled to 20 °C at a rate of 10 °C·min^{-1}, all under a nitrogen atmosphere flowing at a rate of 20 mL·min^{-1}. Each sample was subjected to three of these heating/cooling cycles to erase any thermal history in the sample. The heat of crystallisation determined by integrating the crystallisation peak on the third cycle. The heat of crystallisation was then used to determine the number average molecular mass of the polymer, according to the correlations of Suwa *et al.* and Wiegel *et al.* as recommended by Lappan *et al.* [149].

Chapter 4

Results and discussion

4.1 Unprocessed PTFE results

4.1.1 Thermally initiated PTFEs

Results of spectroscopic and thermal analysis

Figure 50 shows the ATR FTIR spectrum of commercial PTFE obtained from DuPont. What is immediately apparent from the spectrum is that it only shows bands associated with the structure of PTFE chains, namely the strong bands at 1198 and 1144 cm^{-1} and the weaker bands at 635 and 556 cm^{-1}. No other bands, especially bands that could indicate the end groups of the PTFE chains, are visible. This is likely because ATR FTIR spectroscopy only penetrates approximately 2 µm into the particle, which leads to reduced sensitivity. Transmission FTIR measurements proved much more useful and will be discussed hereafter.

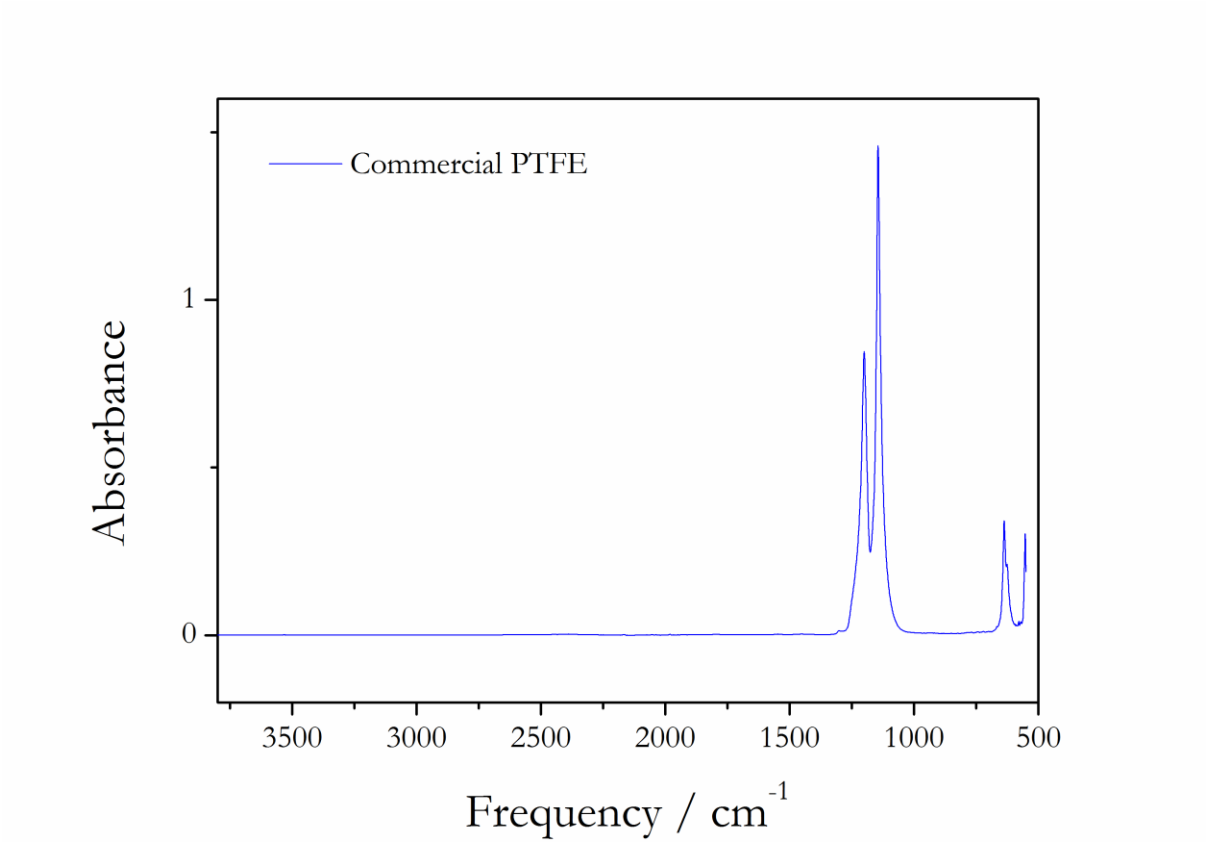

Figure 50: *ATR FTIR spectrum of commercial PTFE.*

Commercial PTFE obtained from DuPont was used as the baseline/reference material for comparison with in-house produced PTFEs. Its annotated transmission FTIR spectrum can be seen in Figure 51.

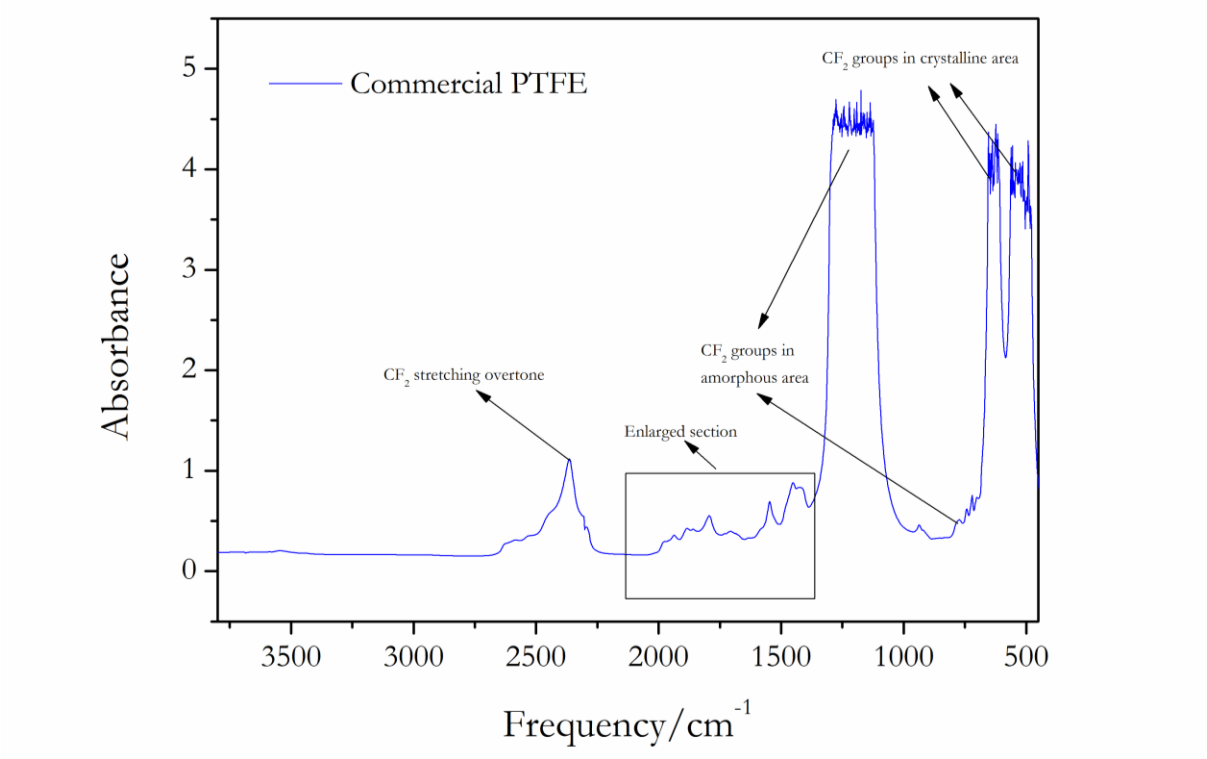

Figure 51: *Transmission FTIR spectra of commercial PTFE, DuPont. The enlarged section can be seen in Figure 52.*

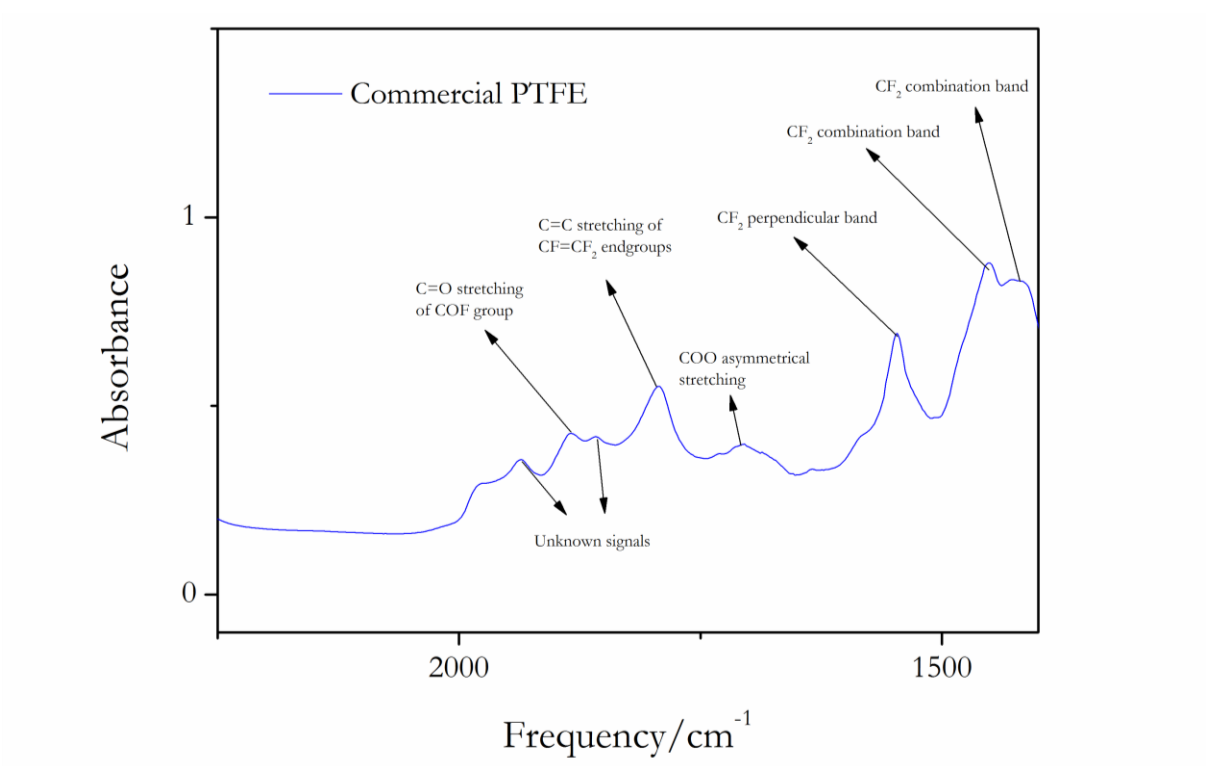

Figure 52: *Annotated enlarged section of Figure 51.*

What is immediately clear is that the transmission FTIR measurement provides much more detail than the ATR FTIR measurement.

According to Socrates, [106], PTFE has a strong absorption in the region 1250 – 1100 cm^{-1} apart from which the region above 650 cm^{-1} is relatively free of absorptions. This does not seem to be the case here, because there is a strong absorption at ~2400 cm^{-1} which Socrates did not predict. After consulting several sources including Socrates and Moynihan [106, 131], it was initially believed that the medium intensity band at ~2400 cm^{-1} was due to the overtone of the CF_2 stretching vibration [106]. However, the *ab initio* calculations indicated that this signal was due to the stretching vibrations of an alkyne (C≡C) group. This supported the presence of an alkyne containing end-group as discussed in the literature review section of this document.

After the band at ~2400 cm^{-1}, no peaks are evident up to the end of the spectrum at 4000 cm^{-1}. This could be because there are no end groups whose peaks would appear in this region, or more likely that the PTFE is of such high molecular weight (very long chains) that the concentration of the end groups is too low to appear on the spectrum.

Similarly to the FTIR spectra, commercial PTFE obtained from DuPont was used as the baseline/reference material to compare with the Raman results of the in-house produced PTFEs. The annotated Raman spectra for the commercial PTFE can be seen in Figure 53.

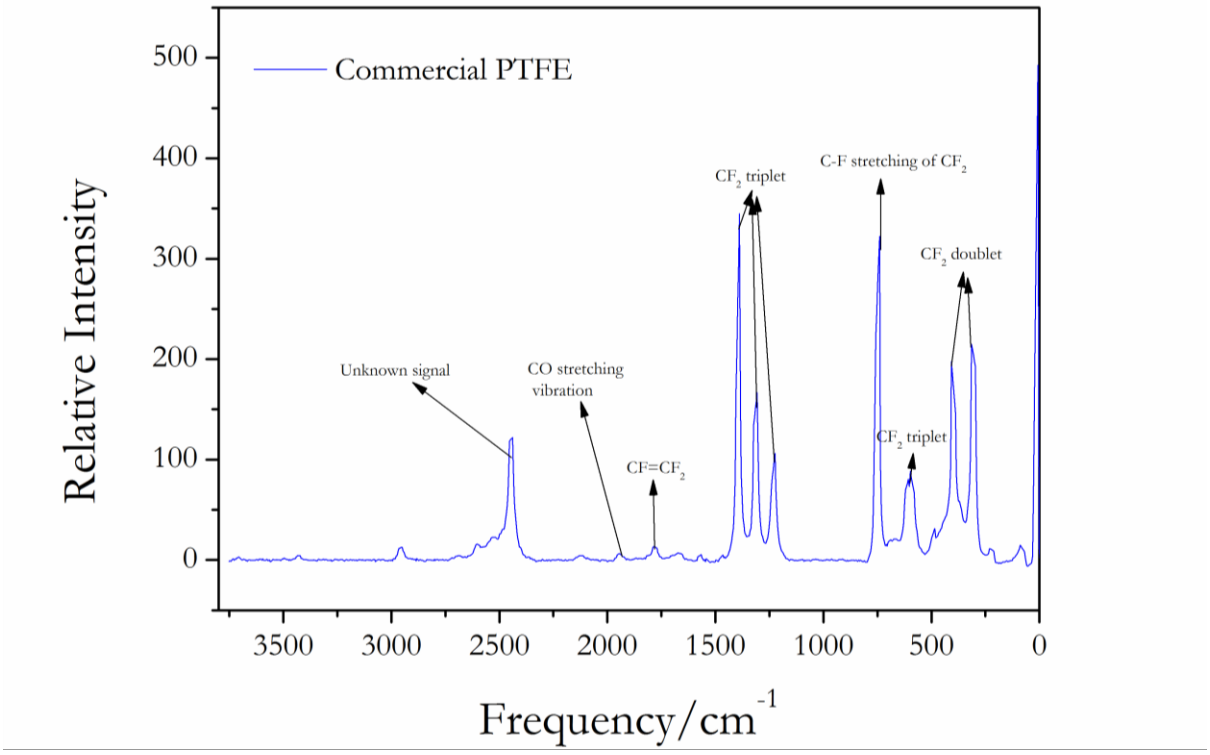

Figure 53: *Raman Spectrum of Commercial PTFE.*

From Figure 53, it can be seen that the commercial PTFE obtained from DuPont is high molecular mass, because of the high intensity of the peaks characteristic of the structure of PTFE. To reiterate, these intense peaks are seen at 1382, 734, 385 and 290 cm^{-1}. There are also bands of medium intensity at 1302 and 1218 cm^{-1}. However, there is a very definite peak at ~2450 cm^{-1}, as well as one at ~600 cm^{-1}, both of which are not classified in the literature and therefore could not be assigned with certainty. No clear indication of what these peaks may be could be found in previous papers on the subject of Raman analyses of PTFE [109, 110]. However, the Raman spectra predicted by *ab initio* calculations for a terminal alkyne end-group, shown in Figure 23, indicates that the band at ~2450 cm^{-1} is indicative of the C≡C stretching of an alkyne group.

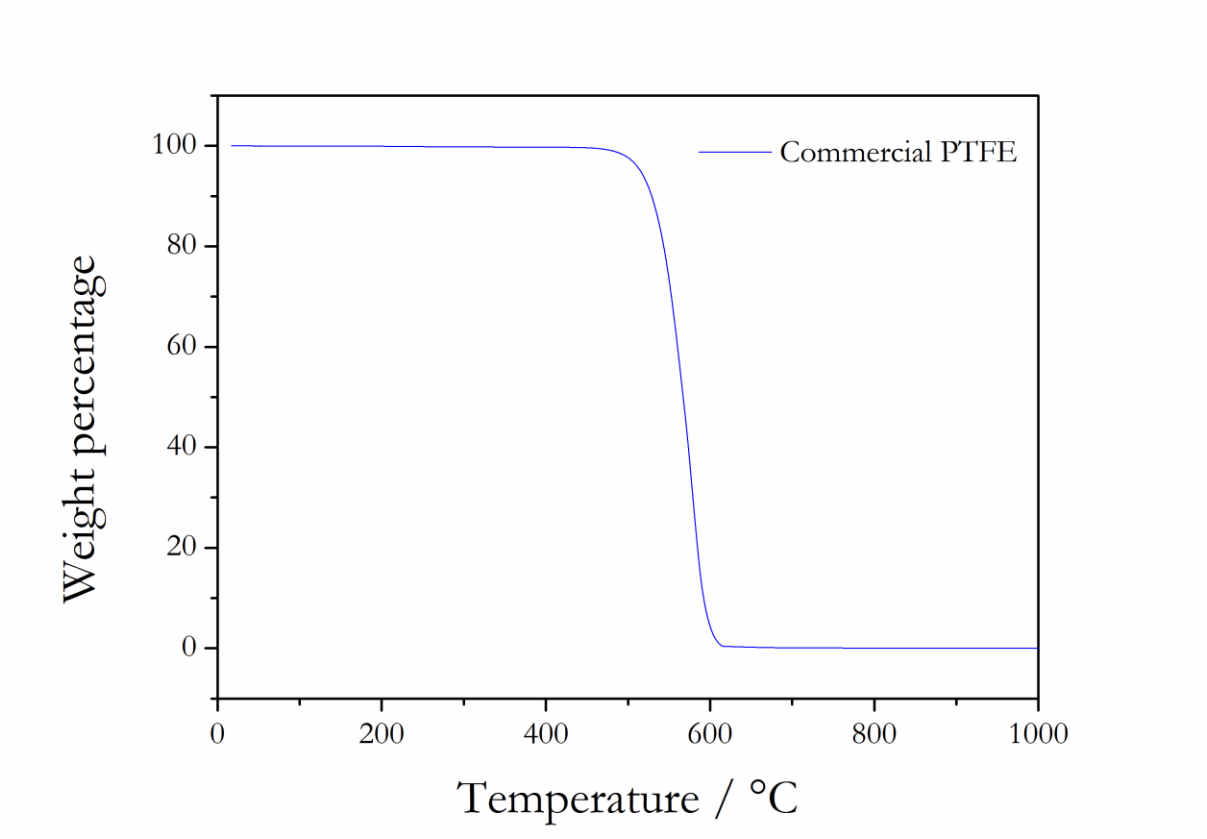

Figure 54: *TGA curve for commercial PTFE.*

The TGA curve for the commercial PTFE is shown in Figure 54. The commercial PTFE is of a very high molecular weight and therefore only starts to decompose at very high temperatures. However, once started, this decomposition proceeds very rapidly with increasing temperature due to the unzipping of the PTFE molecules.

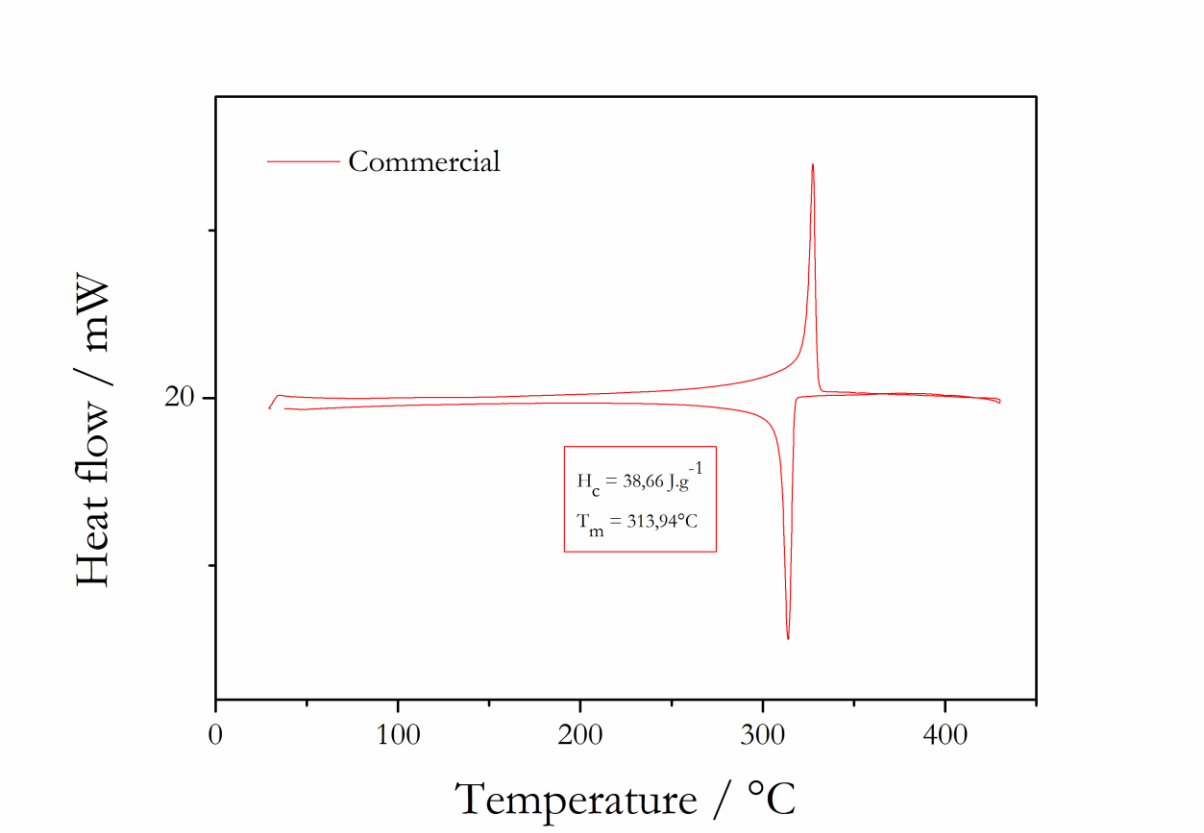

Figure 55: *DSC curve for commercial PTFE.*

The DSC curve for commercial PTFE, shown in Figure 55 shows that it has a ΔH_c of 38.66 J·g^{-1}. This value is used to calculate the number average molecular weight (M_n) according to Suwa's and Wiegel's methods [139]. These results for all the thermally initiated samples are tabulated in Table 7, along with the yields for the same samples. The results for the commercial PTFE show that it has an M_n of 2.19 x 10^6 or 3.65 x 10^7 Da, according to Suwa and Wiegel's methods respectively. Ignoring the fact that these values differ by an order of magnitude, it is apparent that even the lower value predicted by Suwa's method still indicates a very high molecular weight polymer.

In addition to the APS initiated experiments, PTFE was synthesised with different buffers to determine whether this had an effect on the polymer end groups.

Figure 56 shows the ATR FTIR measurement for experiment 6 from Table 5. Similarly to the commercial PTFE sample, it only shows the four bands associated with the structure of PTFE chains and none that indicate end groups or other structural moieties. Because of the lack of sensitivity provided by the FTIR ATR measurements, only transmission FTIR spectra was used from this point on.

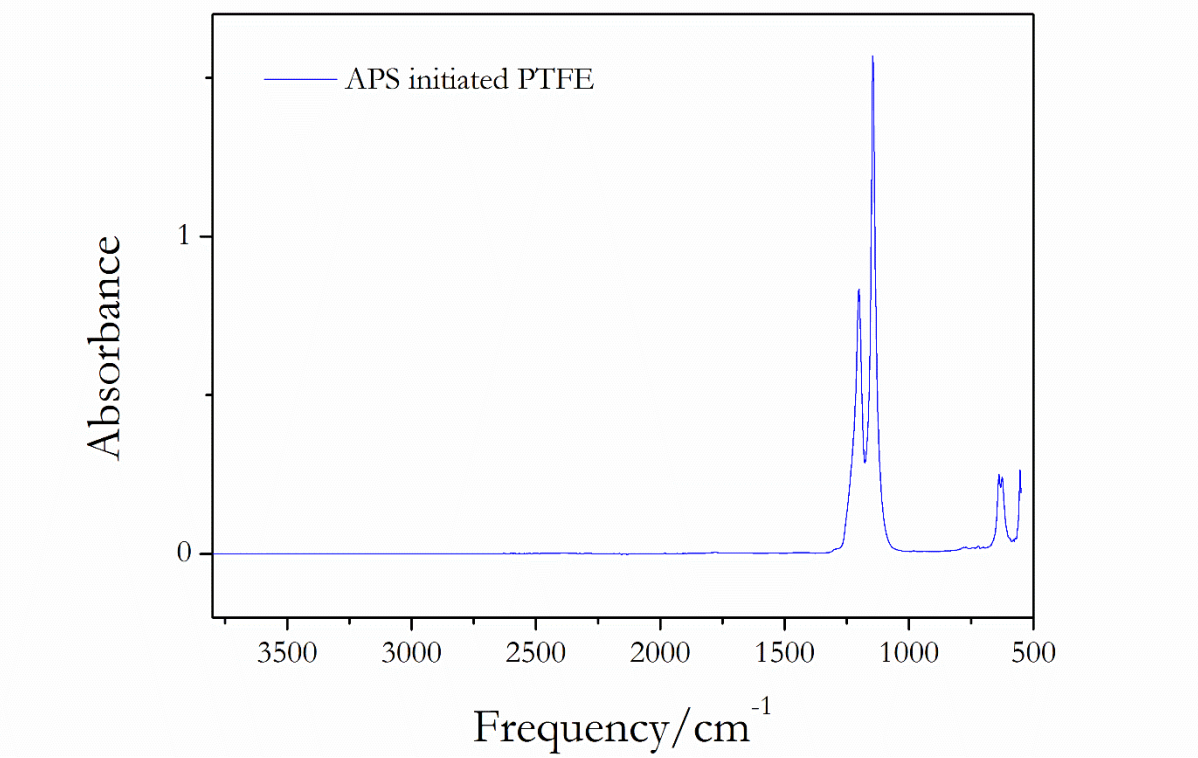

Figure 56: *ATR FTIR spectrum of APS initiated PTFE, experiment 6 from Table 5.*

The APS initiated PTFE experiments, were analysed by transmission FTIR spectroscopy as described in the experimental section of this document. As expected, the spectra of the APS initialised PTFE samples had identical configurations, albeit with differences in peak intensities. This was no surprise however, as the differing molecular weights due to different experimental conditions for the samples meant that the peak intensities were always likely to differ. These spectra can be seen in Figure 57.

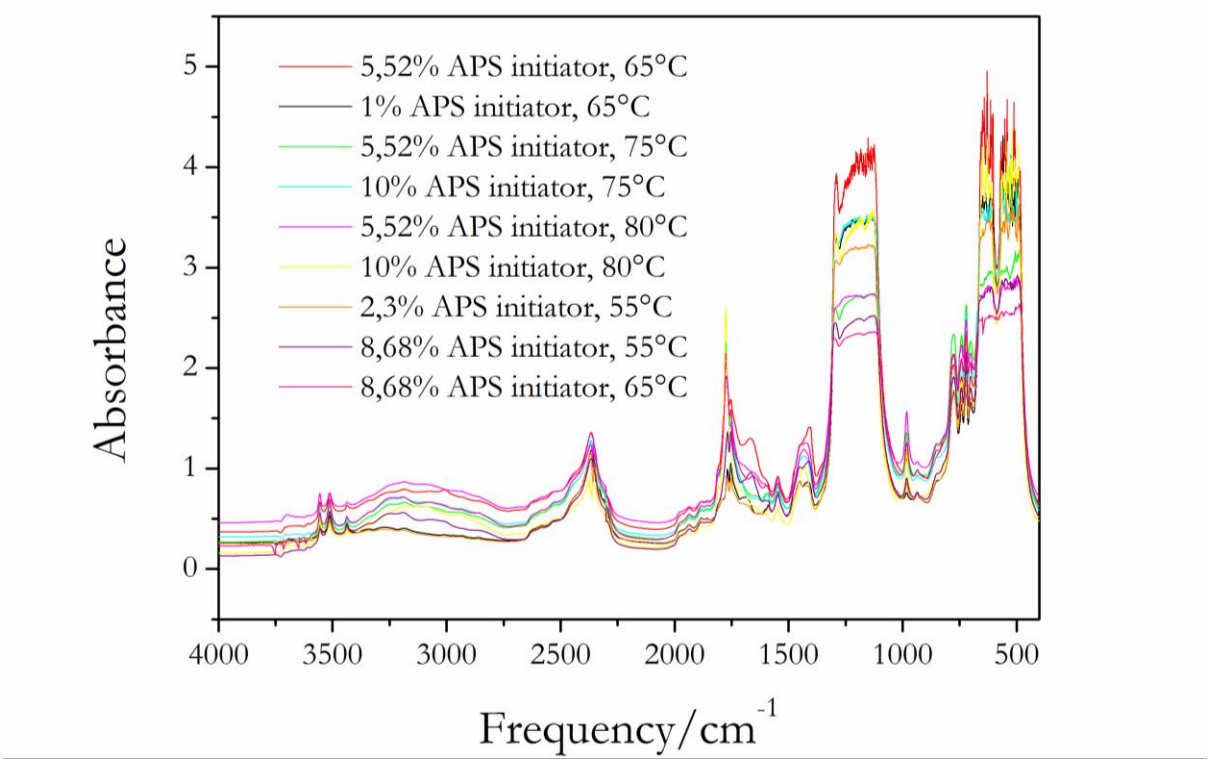

Figure 57: *Overlaid transmission FTIR spectra of the APS initiated PTFE experiments.*

The in-house produced PTFE samples were analysed and compared to the commercial sample, to determine any structural differences in the polymer molecules. The end groups of the different samples were identified by comparing their spectra to reference spectra identified in the literature. Pianca's paper [105] served as the *de facto* reference for FTIR reference spectra, though it was found to be somewhat lacking as the research detailed in this document progressed. The text of Socrates [106] was consulted extensively. The spectra of experiment 1 of Table 5 can be seen in Figure 58.

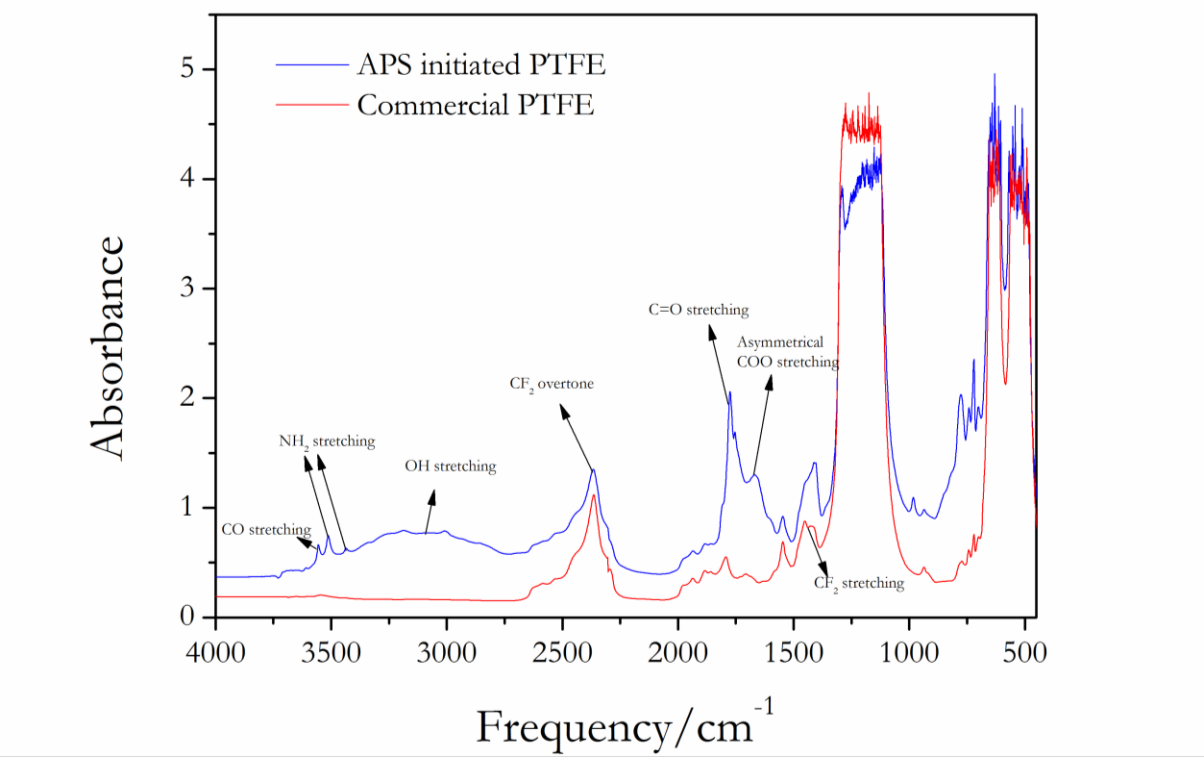

Figure 58: *Overlaid spectra of produced PTFE initiated by APS and commercial PTFE (DuPont).*

From Figure 58 it can be seen that while the structural frequencies (in the region of 400 cm^{-1} to 1500 cm^{-1}) are identical, albeit with differences in peak heights, there are three small peaks present in the APS initiated PTFE in the region of 3500 cm^{-1} that are clearly absent from the commercial PTFE. The very broad peak between approximately 3500 cm^{-1} and 2700 cm^{-1} is indicative of bonded OH stretching, which could indicate carboxylic acid groups. The difference in several of the peak heights between the produced and commercial PTFEs can be attributed to the fact that the APS initiated PTFE is of a much lower molecular weight than the commercial DuPont product. Therefore, certain structural moieties such as end groups are present in higher concentrations and have larger peak heights/intensities.

The APS initiated sample has a very definite peak at 1775 cm^{-1} as well as an additional peak at 1754 $cm^{-1}$and a broad peak from approximately 1680 cm^{-1} to 1640 cm^{-1}. According to Pianca [105], the peak at 1775 cm^{-1} is caused by bonded C=O stretching and is indicative of COOH end groups. According to Socrates [106], α-halo-carboxylic acids exhibit two bands due to the C=O stretching vibration, caused by partially restricted rotation [106]. The broad, medium intensity band from 3300 cm^{-1} to 2700 cm^{-1} also indicates COOH groups. There is no sign of the sharp band at 3744 cm^{-1} predicted by the *ab initio* calculations due to COOH groups.

Pianca states that COOH groups should show a sharp band at 3557 cm^{-1} due to free OH stretching and another at 1813 cm^{-1} because of free C=O stretching. In this case there is only a small intensity band at 3555 cm^{-1}, which is indicative of an amide group. There is possibly an obscured band at 1813 cm^{-1}. The broad peak between 1680 cm^{-1} and 1600 cm^{-1} is indicative of asymmetric COO stretching and indicates COO^-X^+ groups, where X^+ is NH_4^+ in this case.

Furthermore, according to Pianca and co-workers [105], the peak at 3438 cm^{-1} corresponds to an amide end group. This would be supported by additional peaks at 1768 cm^{-1} and 1587 cm^{-1} which all correspond to amide ($CONH_2$) groups. However, there is no clearly visible peak at 1768 cm^{-1}, but this could be because it is being obscured by the broad COOH peak at 1775 cm^{-1}. This is possibly because the COOH groups are in a much higher concentration than the $CONH_2$ groups and because the bands occur so close to each other that the higher concentration of the one obscures the other. The same can be said for the band at 1587 cm^{-1} which is not clearly visible, but could be obscured because it is present in a low concentration. However, according to Moynihan [131], this peak is due a structural PTFE vibration, specifically a CF_2 overtone from the polymer backbone. It is unclear which is correct.

Lastly the IR spectrum of the APS initiated sample shows a very strong, broad peak at ~2450 cm^{-1}. According to the *ab initio* calculated IR spectra, this is indicative of an alkyne containing end group, specifically the terminal alkyne end group, as the inner alkyne end group does not have a peak in its IR spectra in this region.

These observations are contrary to what has been reported in the literature. According to the literature, when a persulfate initiator is used, only carboxylic acid end groups are formed [105]. However, these findings would seem to indicate that there is more than one method of termination at work here. It seems there is indeed a termination step as predicted by the literature where carboxylic acid end groups are formed, but there seems to be two, possibly three termination reactions. These additional reactions form amidic end-groups, as well as end-groups where ionic bonds with the salt used in the initiator form. If the *ab initio* calculations are correct, terminal alkyne end-groups form on some of the polymer chains as well.

As a control experiment, no pH buffer was used in experiment 2 from Table 5. This was done to compare to the rest of the APS initiated experiments which all had borax as the buffering agent. The resultant spectra can be seen in Figure 59.

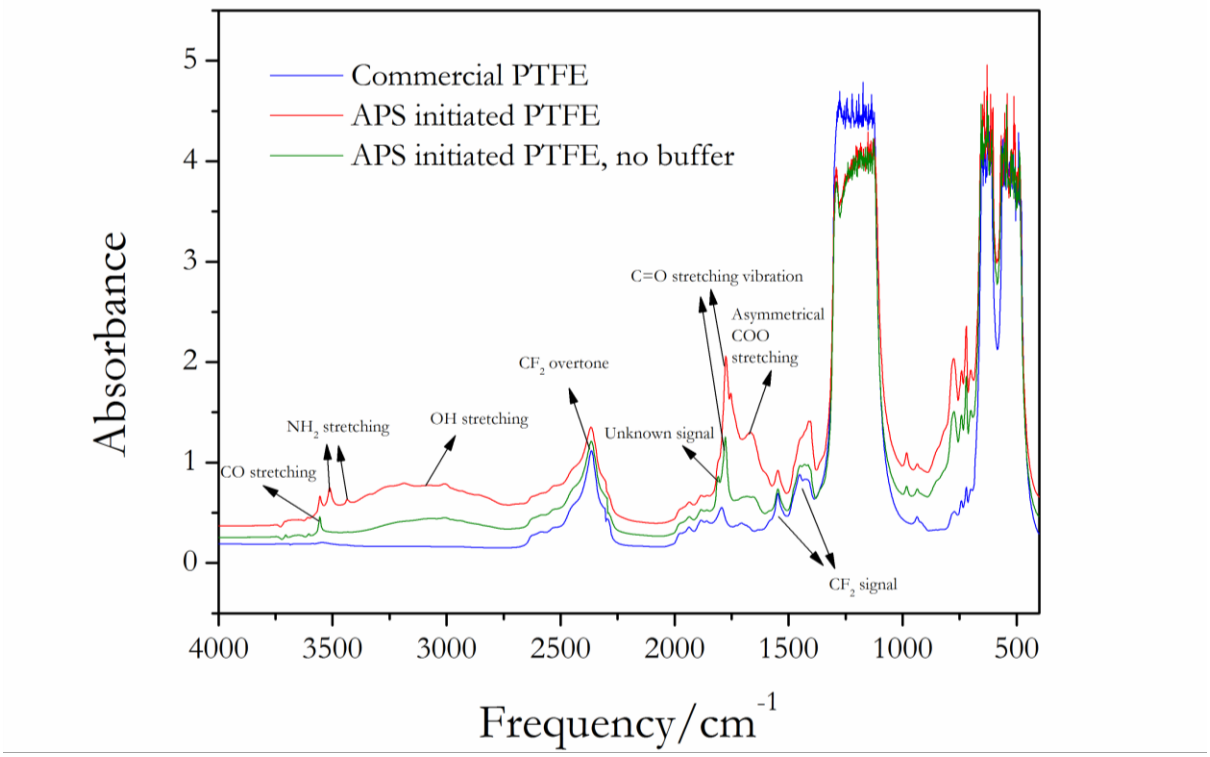

Figure 59: *Overlaid transmission FTIR spectra of PTFE initiated by APS, with and without buffering agents.*

Besides the differences in some intensities, the spectra of the PTFE polymerised with- and without buffering agents appear to be identical, except for the absence of the two small peaks at 3438 cm^{-1} and 3512 cm^{-1}. The left-most peak of the buffer-less sample also appears to be 3557 cm^{-1} where the buffered sample's left-most peak is at 3555 cm^{-1}. This would seem to indicate the absence of $CONH_2$ groups in the buffer-less sample. The significantly lower intensity of the broad peak at ~1670 cm^{-1}, which is indicative of COO^-X^+ groups, also indicates that less NH_4^+ has bonded with the polymer chains. Because the same amount of initiator was used in these two experiments, this result suggests that the buffer is somehow involved in the reaction, which leads to the formation of amide groups.

The peak at 3557 cm^{-1} along with the other characteristic peak at 1775 cm^{-1} indicates the presence of COOH groups and the almost identical peak at ~2450 cm^{-1} indicates the presence of the alkyne end groups in the buffer-free sample.

An experiment was conducted where potassium carbonate was used as a buffering agent instead of borax. The resultant FTIR spectra can be seen in Figure 60.

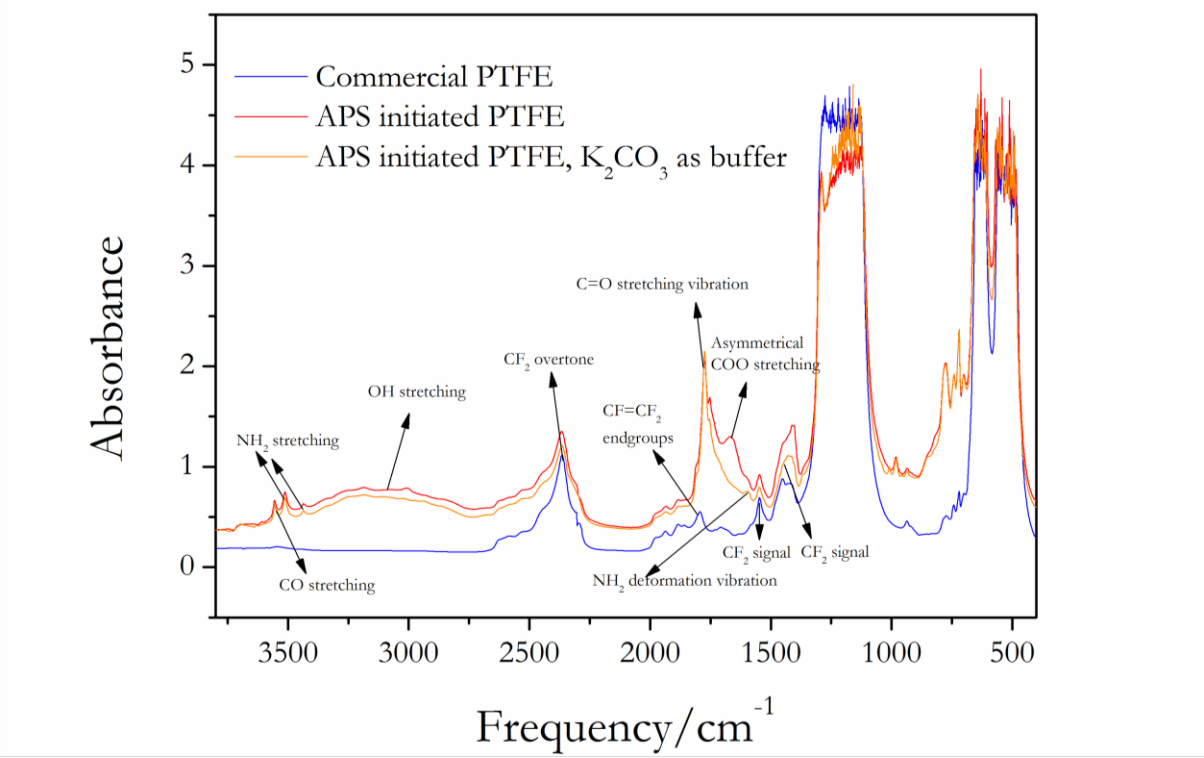

Figure 60: *Overlaid transmission FTIR spectra of PTFE initiated by APS with borax and K_2CO_3 as buffering agents.*

The spectra of APS initiated PTFE polymerised with different buffers appears to be identical, except for the broad peak shown by the borax buffer sample at approximately 1670 cm^{-1}. This peak is notably absent in the spectra of the K_2CO_3 sample. This indicates that while the borax buffer sample contains $COO^-NH_4^+$ groups, the K_2CO_3 sample does not.

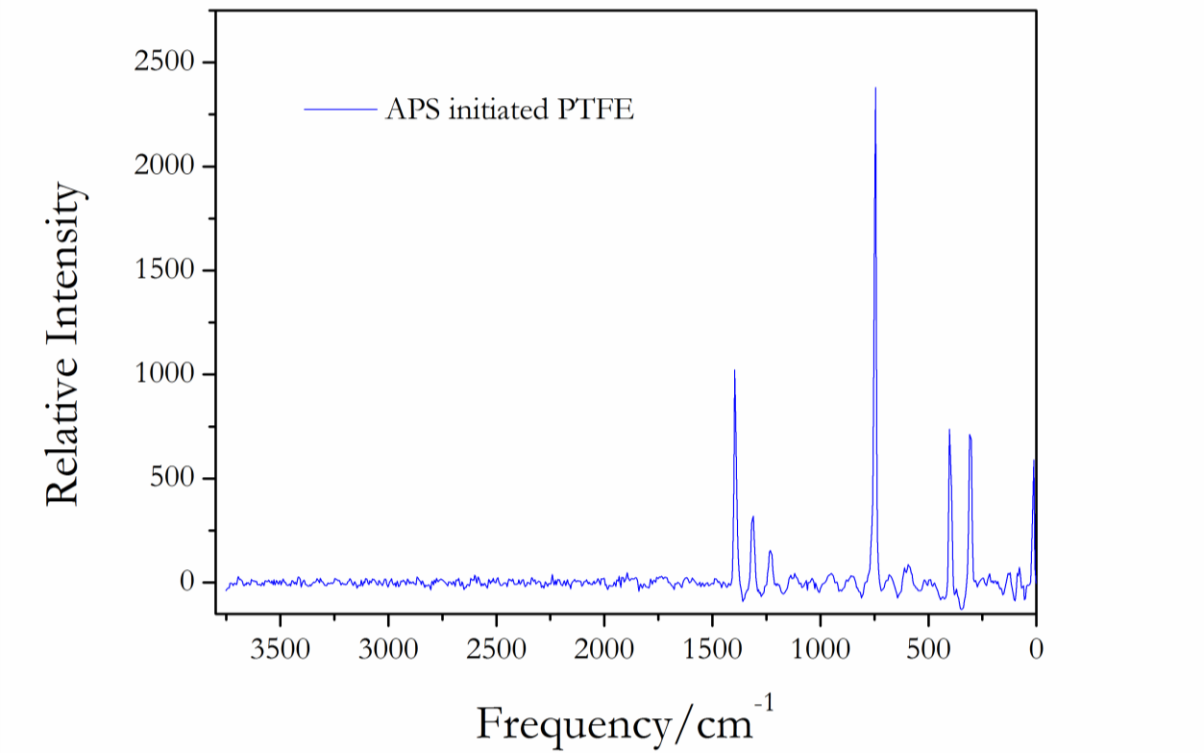

Figure 61: *Raman spectrum of APS initiated PTFE.*

The APS initiated PTFE samples proved troublesome when it came to collecting Raman spectra. Most of the spectra were poorly defined. It is believed this was because of fluorescence of the sample. After attempting several samples under different parameters, the spectrum shown in Figure 61 was obtained. The first thing that is apparent is the intensity of the PTFE structural peaks. They are significantly higher (about 5 times) than the commercial PTFE sample. It is not clear whether this is because of fluorescence or another issue with the sample. No peaks indicating end groups are apparent. This could be because the intensity of the structural peaks is so high, that relative to them the end group peaks are all but invisible. However, when an enlarged section of the region between 1500 and 3000 cm^{-1} is observed, as shown in Figure 62, no discernible peaks are visible. This would seem to indicate that there are indeed no peaks in this area.

The absence of a peak in the ~2100 to 2500 cm^{-1} region suggests that there are no C≡C or C≡N bonds present in this sample, because this is the region where these vibrations usually appear. The lack of any distinguishable peaks other than those of PTFE in this spectra makes the identification of end groups in this sample solely reliant on IR and NMR spectra.

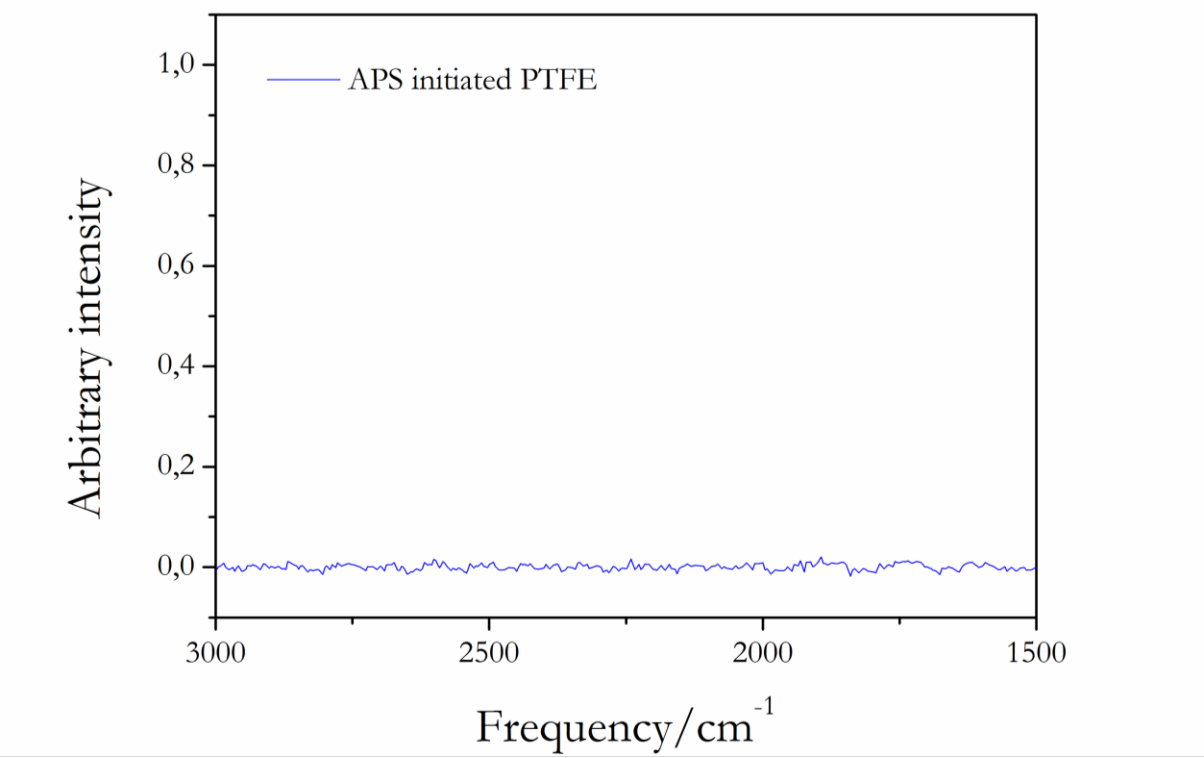

Figure 62: *Enlarged section of the region between 1500 and 3000 cm^{-1} for APS initiated PTFE. Note that no discernible peak can be seen, only noise.*

Figure 63 shows a comparison between Raman spectra of commercial PTFE and the APS initiated sample shown in Figure 61. From this it is clear that the APS initiated sample's PTFE peaks are of a much higher intensity than those of the commercial sample. Two more things are also apparent from this comparison: the lack of any peaks in the 1500 to 3500 cm^{-1} region for the APS sample and how *noisy* the APS sample is. The commercial sample shows a much smoother spectra. This could be because the sample fluoresced more than the commercial sample. The specific sample used was APS experiment 10, which used 5.5 % initiator and is believed to have a much lower molecular mass than the commercial sample. Whether the molecular mass influences fluorescence is unclear at this stage.

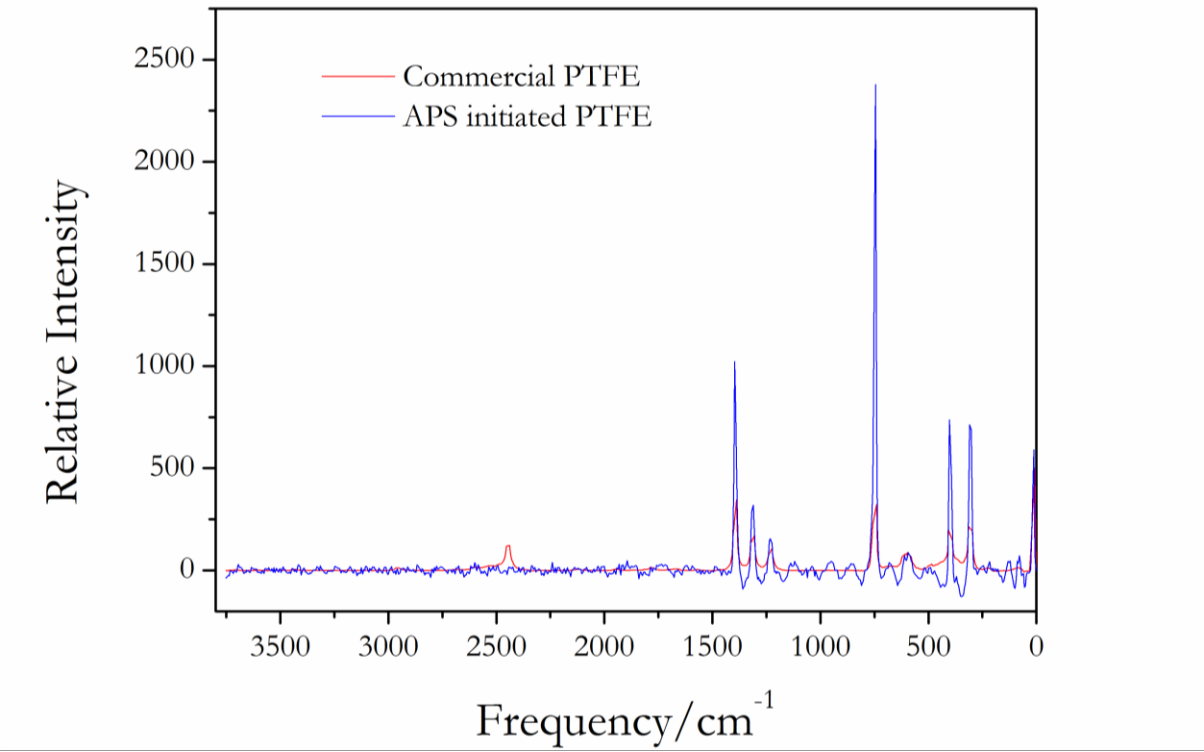

Figure 63: *Overlaid Raman spectra of APS initiated PTFE and commercial PTFE.*

Figure 64 shows the TGA curves obtained for the different APS initiated PTFE samples, using different buffering agents. What is interesting to see is that even though the three samples all had the same amount of initiator and the same experimental conditions, they still ended up with different molecular masses. This is evident from the curves in Figure 64. The samples that used borax and potassium carbonate as buffers had very similar molecular weights and decomposed in very similar fashions. However, the sample which had no buffer during synthesis took slightly longer to start decomposing, which indicates it had a slightly higher molecular mass. This sample also had some residual mass left until approximately 950 °C.

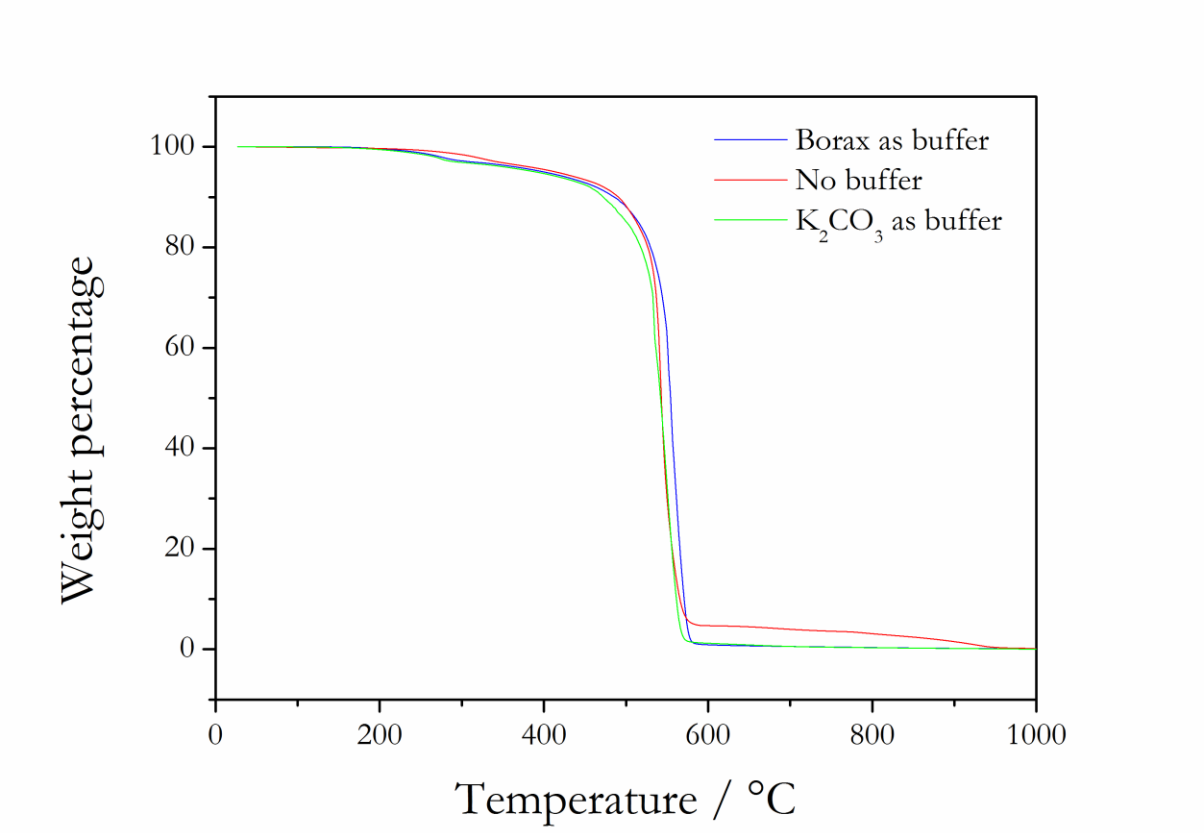

Figure 64: *TGA curves for APS initiated PTFE using different buffers.*

Figure 65 shows that while the heat of crystallisation for the borax and potassium carbonate buffered samples are very similar, the value for the buffer-less sample is higher. The same applies to the melting point. This seems to support the TGA result which shows that the buffer-less sample is of a higher molecular weight than the samples that were synthesised with a buffering agent. The calculated molecular mass values can be seen in Table 7.

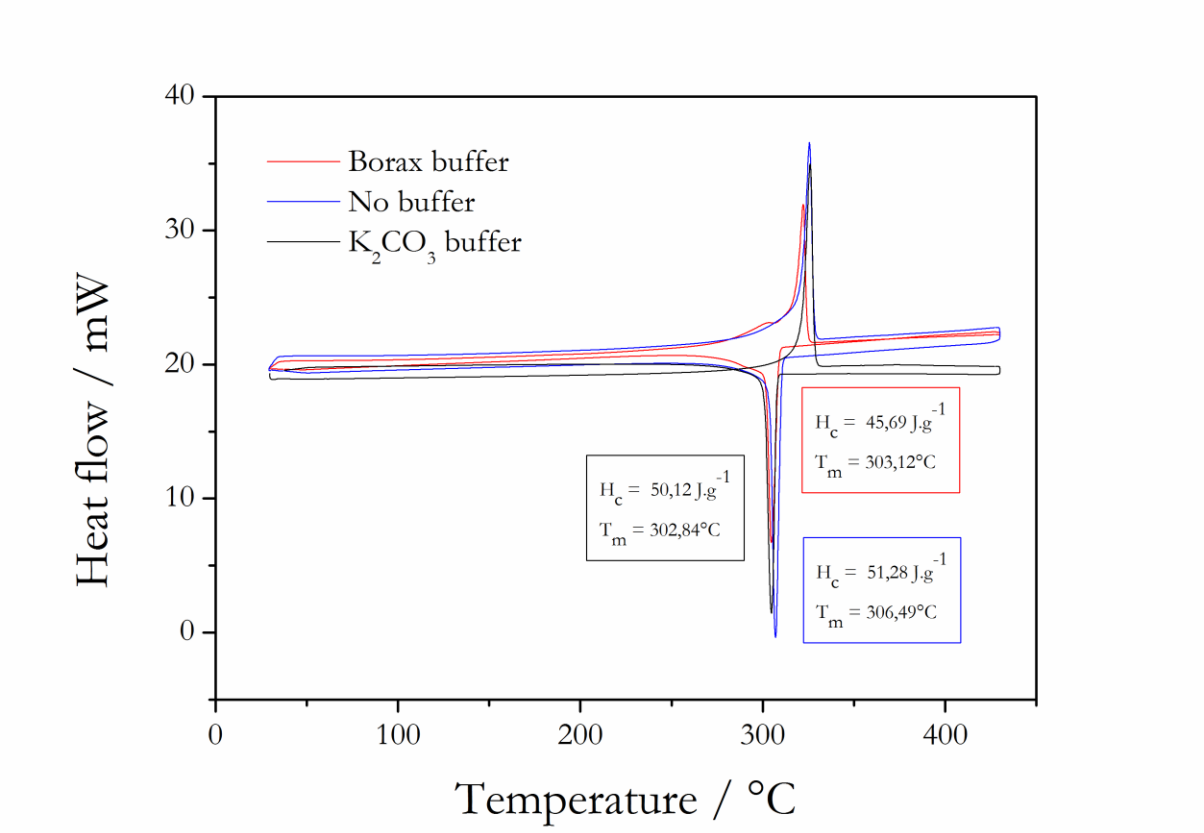

Figure 65: *DSC curves for APS initiated PTFE samples synthesised with different buffering agents.*

Experiments were conducted where sodium persulfate was used as the initiator instead of ammonium persulfate to compare the visual and structural differences between the two products formed. The resultant spectra can be seen in Figure 66.

From Figure 66 it can be seen that the sodium persulfate initiated sample's spectrum differs from that of the commercial and APS samples. Whereas the APS initiated sample showed three peaks at 3512, 3435, and 3555 cm^{-1} the SPS initiated sample only shows a single peak at 3557 cm^{-1}. It also shows an additional peaks at 1813 cm^{-1}. The peak at 1775 cm^{-1} is also of much higher intensity.

The peak at 1813 cm^{-1} corresponds to Pianca's predictions for COOH end groups and the sharp, high intensity peak at 1775 cm^{-1} corroborates this. The peak at 3557 cm^{-1} corresponds to COOH end groups, unlike the 3555 cm^{-1} peak shown by the APS initiated sample, which indicates $CONH_2$ end groups. The absence (or at least significant reduction) in the broad peak at approximately 1670 cm^{-1} indicates that if there is a COO^-X^+ group present, it is present in reduced amounts compared to the APS initiated sample.

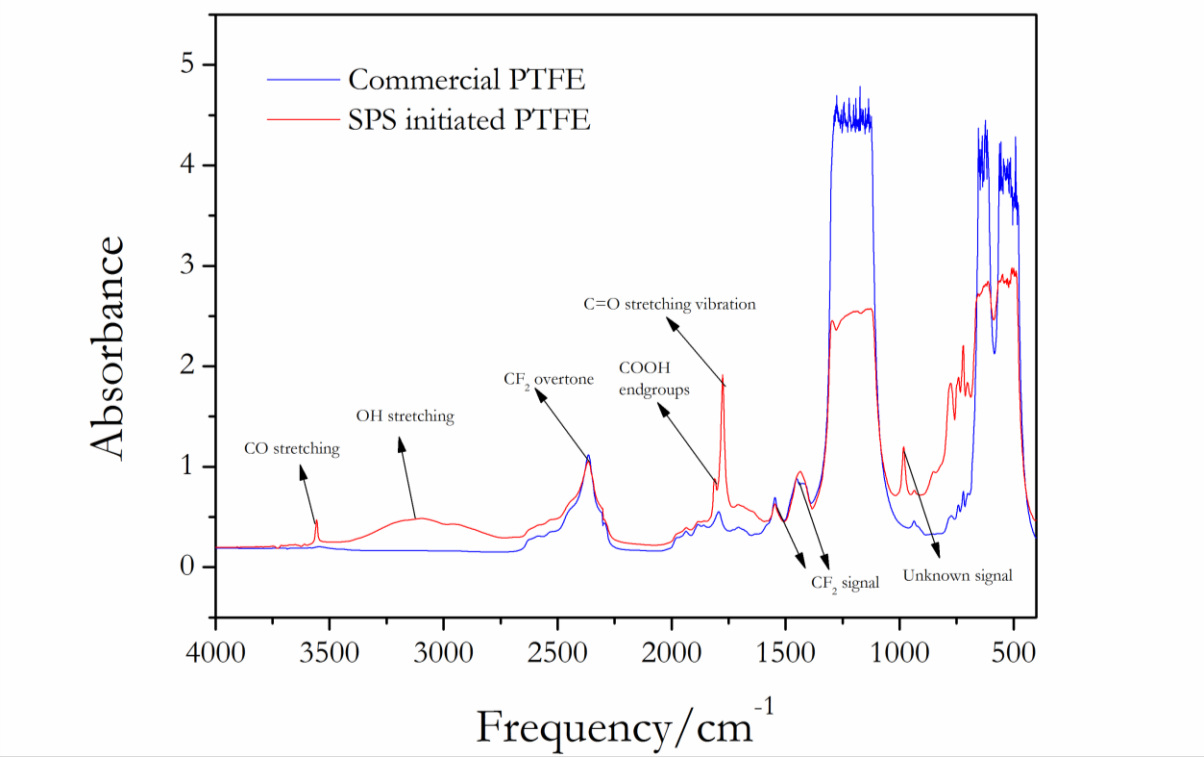

Figure 66: *Overlaid transmission FTIR spectra of PTFE initiated with sodium persulfate.*

A high initiator concentration of 30 % was used in order to lower the molecular mass of the produced PTFE as much as possible. A lower molecular mass polymer means that the end groups are in a higher concentration, which makes them easier to detect with spectroscopic methods.

From Figure 67 it is clear that the SPS initiated PTFE possesses all the same PTFE structural peaks as the commercial sample, albeit in a lower intensity. The lower intensity can be attributed to the lower molecular weight of the SPS initiated sample. The peak indicating the alkyne end group at ~ 2450 cm also matches that of the commercial sample, indicating a similar if not identical end group is present. Interestingly, the SPS initiated sample has a very sharp, distinctive peak at ~ 500 cm^{-1}. If one looks closely at the spectra, the commercial sample also possesses a peak at the same location, but it is much less intense and partially masked by other bands in the region. The sharpness and intensity of this peak in the SPS sample indicates that the group which is causing it, is in a much higher concentration than in the commercial sample. This is also likely due to the lower molecular mass of the SPS sample. Upon further investigation, it is believed that the band at 500 cm^{-1} is due to the deformation vibrations of the alkyne group bonded to an F atom. This makes sense, as the lower molecular weight would lead to increased concentrations of this group, leading to more intense spectra.

Figure 67 also shows several peaks which were identified as signals emanating from carbon, the significance of which will become clear in due course. The signals for carbon are only present in the Raman spectra of the samples, no trace of any carbonaceous signals were found in the IR spectra.

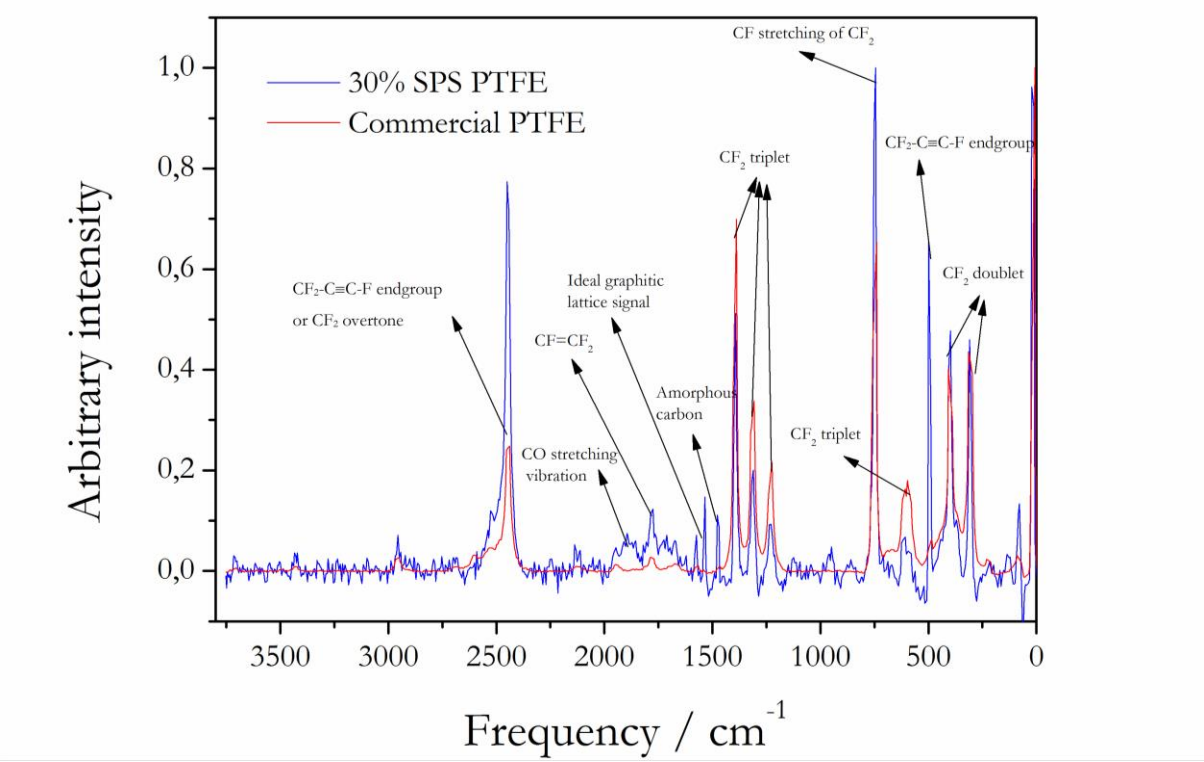

Figure 67: *Overlaid Raman spectra of SPS initiated PTFE and commercial PTFE.*

From Figure 68 it can be seen that the lower molecular weight sample has a much earlier onset of decomposition at ~250 °C as opposed to ~430 °C for the higher molecular weight sample. This is likely because of the shorter length chains of the lower molecular weight sample being decomposed first at the lower temperatures. However, once the lower molecular weight sample reaches ~430 °C, it decomposes rapidly in a very similar fashion to the other sample. This suggests that even the lower molecular weight sample has some very long chains. This in turn would suggest that the lower molecular weight sample has a higher polydispersity index (PDI). Lastly, it can be seen that some residual mass is left in the sample container until ~800 °C. It is believed this residual mass is some form of carbon that was eliminated from the end groups and was deposited into the crucible.

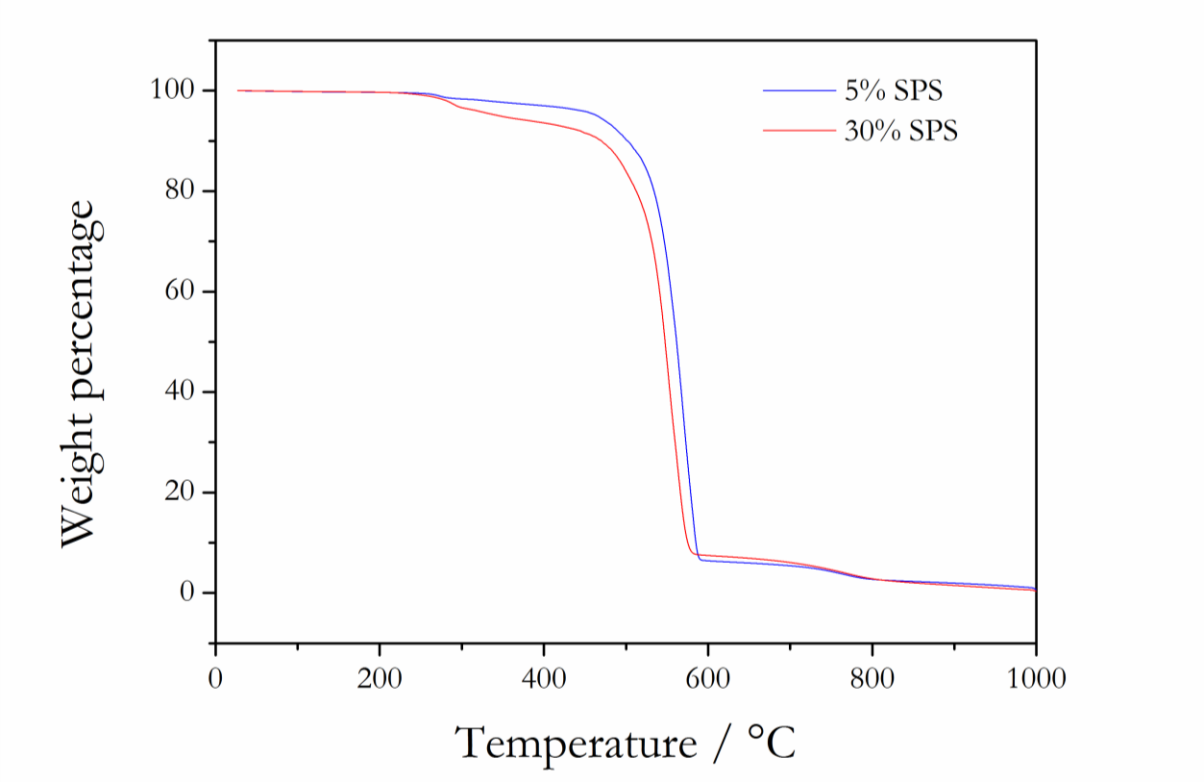

Figure 68: *TGA curves for SPS initiated PTFE using different initiator concentrations.*

From Figure 69 it can be seen that the crystallisation peak is smaller and broader for the lower molecular weight sample than for the higher molecular weight sample. This is completely contradictory to what was reported by Suwa *et al.* Therefore, it seems that Suwa's correlation is not valid for these samples, because the underlying assumption has been proved invalid. However, it should be noted that Suwa's correlation is only valid over a narrow range of values.

It can also be seen that the melting temperature for the lower molecular weight sample is several degrees lower than for the higher molecular weight sample, which makes sense, because melting temperature should increase with increasing molecular weight.

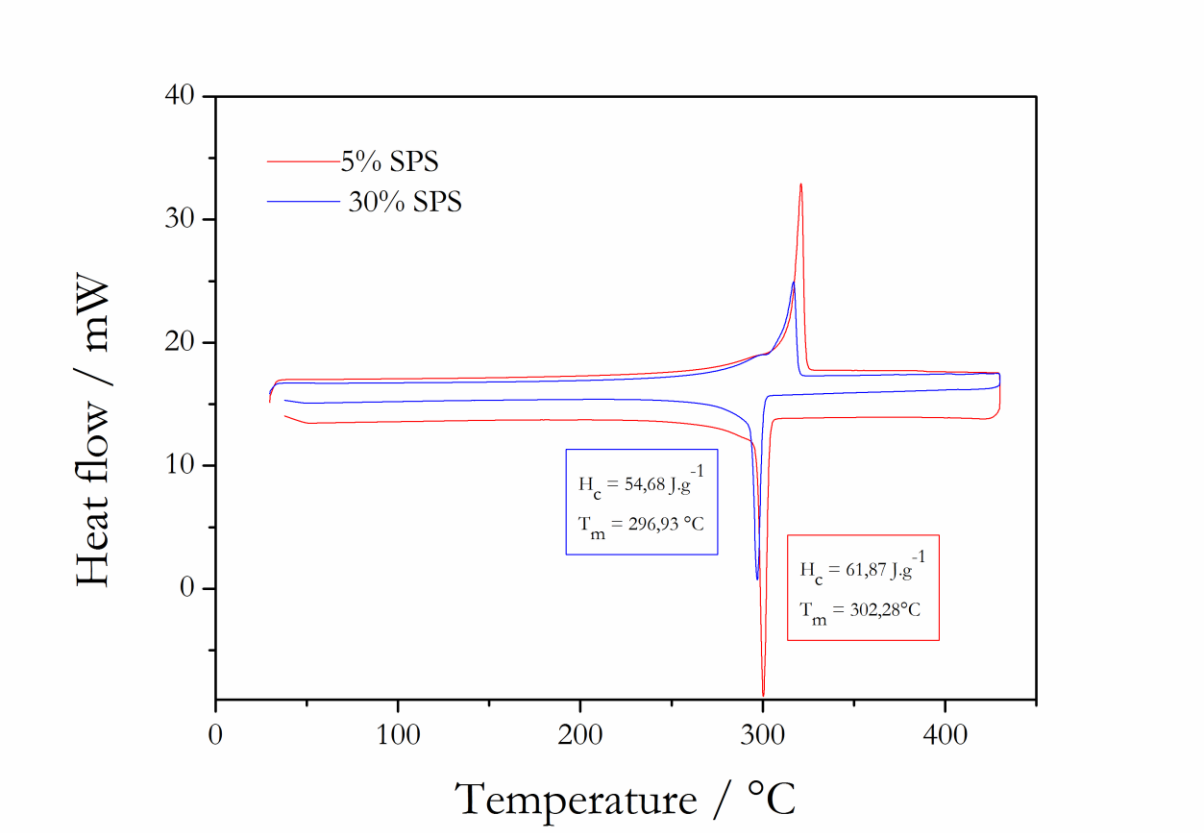

Figure 69: *DSC curves for SPS initiated PTFE.*

Experiments were conducted where potassium permanganate was used as the initiator to compare its visual and structural differences to commercial PTFE. The resultant spectra of experiment 24 from Table 6 can be seen in Figure 70.

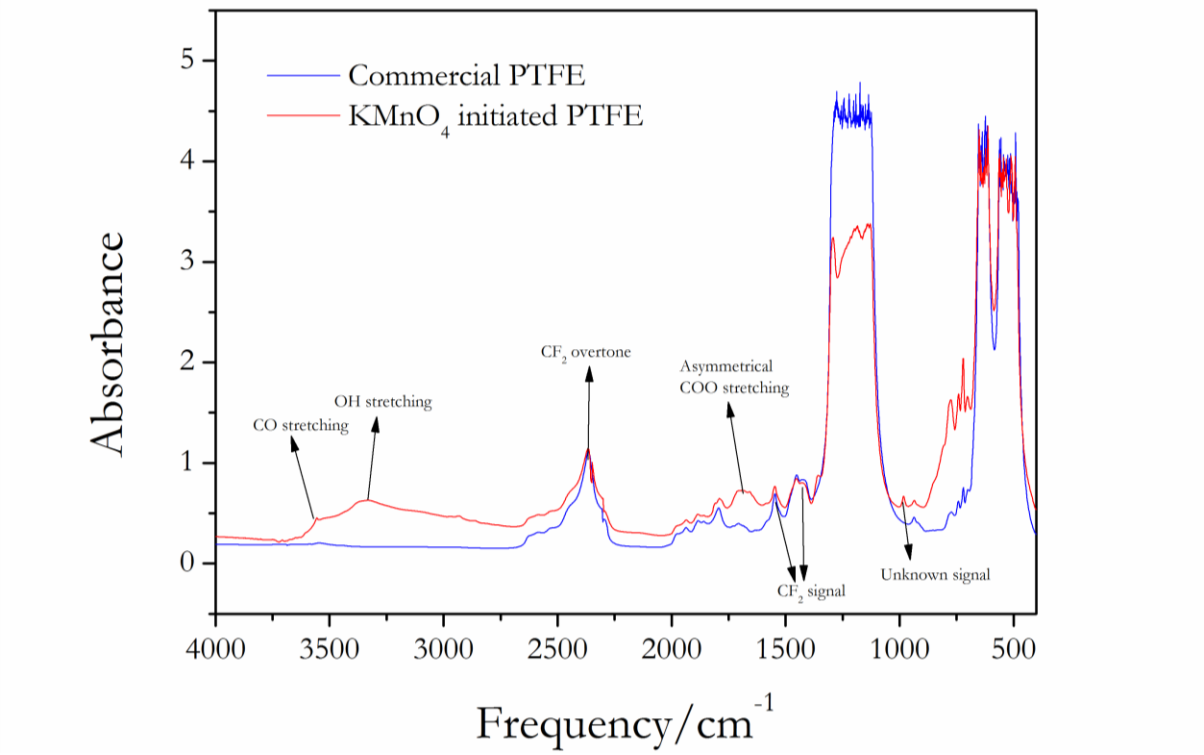

Figure 70: *Overlaid transmission FTIR spectra of PTFE initiated with potassium permanganate.*

The spectra of the $KMnO_4$ initiated sample appears mostly similar to the commercial sample. Similarly to the commercial sample, but unlike the APS initiated sample, the $KMnO_4$ initiated sample does not show a sharp peak at 1775 cm^{-1}, as well as any peak at 1813 cm^{-1}, which indicates it does not possess COOH end groups. Another notable difference is the lack of a broad peak at 1670 cm^{-1}. This indicates either an absence or a much lower concentration of carboxylic salt end groups in the $KMnO_4$ initiated sample. A broad peak from approximately 3400 cm^{-1} to 3300 cm^{-1} is present and likely results from OH stretching, indicating OH end groups. The absence of the 3512 cm^{-1} and 3435 cm^{-1} peaks indicate that there are no $CONH_2$ groups present, which makes sense, because there was no ammonium group present in the reaction which could form such groups (no buffer was used in the $KMnO_4$ initiated polymerisations).

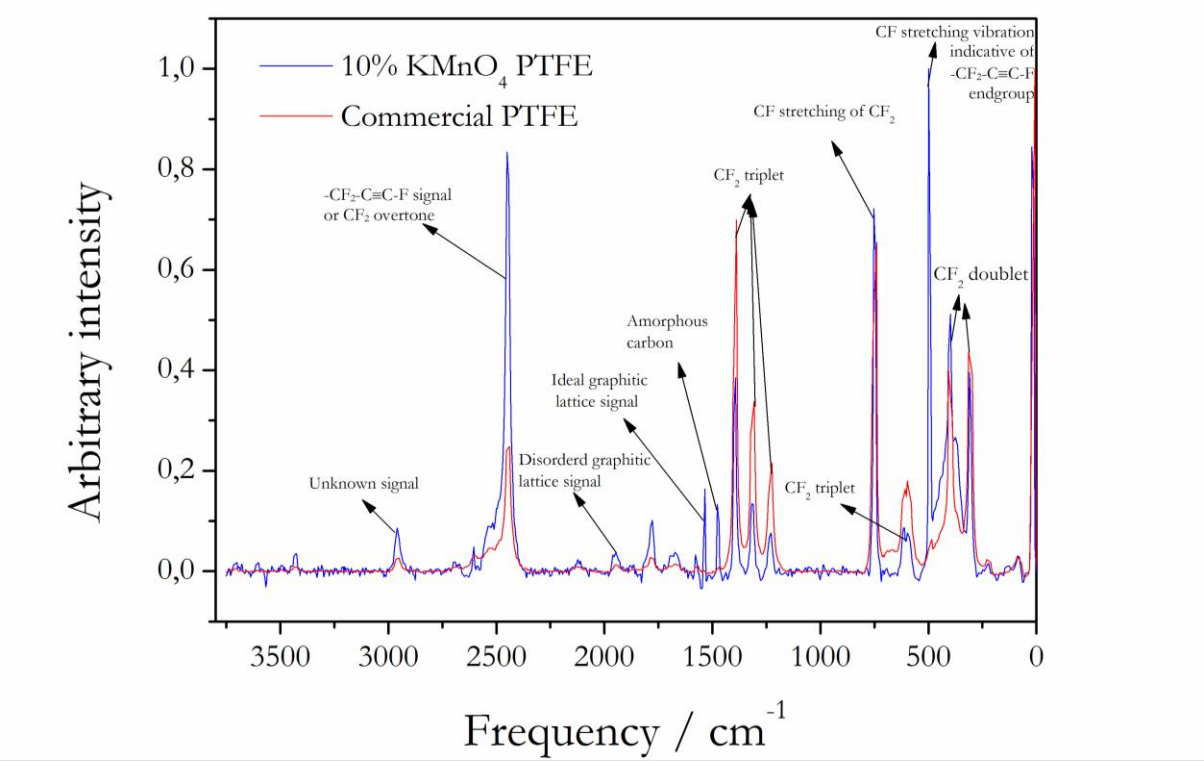

Figure 71: *Overlaid Raman spectra of $KMnO_4$ initiated PTFE and commercial PTFE.*

Similarly to the SPS initiated sample, a higher concentration of initiator was used for the $KMnO_4$ initiated samples. A 30 % initiator sample was prepared and analysed, but the sample fluoresced rather severely and a usable Raman spectra could not be obtained. However, the 10 % initiator sample delivered a very usable spectra that can be seen in Figure 71. The comparison is very similar to the previous one. All the expected PTFE peaks are visible, albeit in lower intensities than the commercial sample and the peak at ~2450 cm^{-1} is more intense than for the commercial sample. Once again this can be prescribed to the lower molecular mass of the in-house produced sample. Similarly to the SPS sample, the $KMnO_4$ sample's spectra shows a sharp, distinctive peak at 500 cm^{-1} which, along with the more intense peak at ~2450 cm^{-1}, is most likely indicative of the increased concentration of the alkyne-F bond. It also clearly shows the signals that indicate the presence of carbon in the samples.

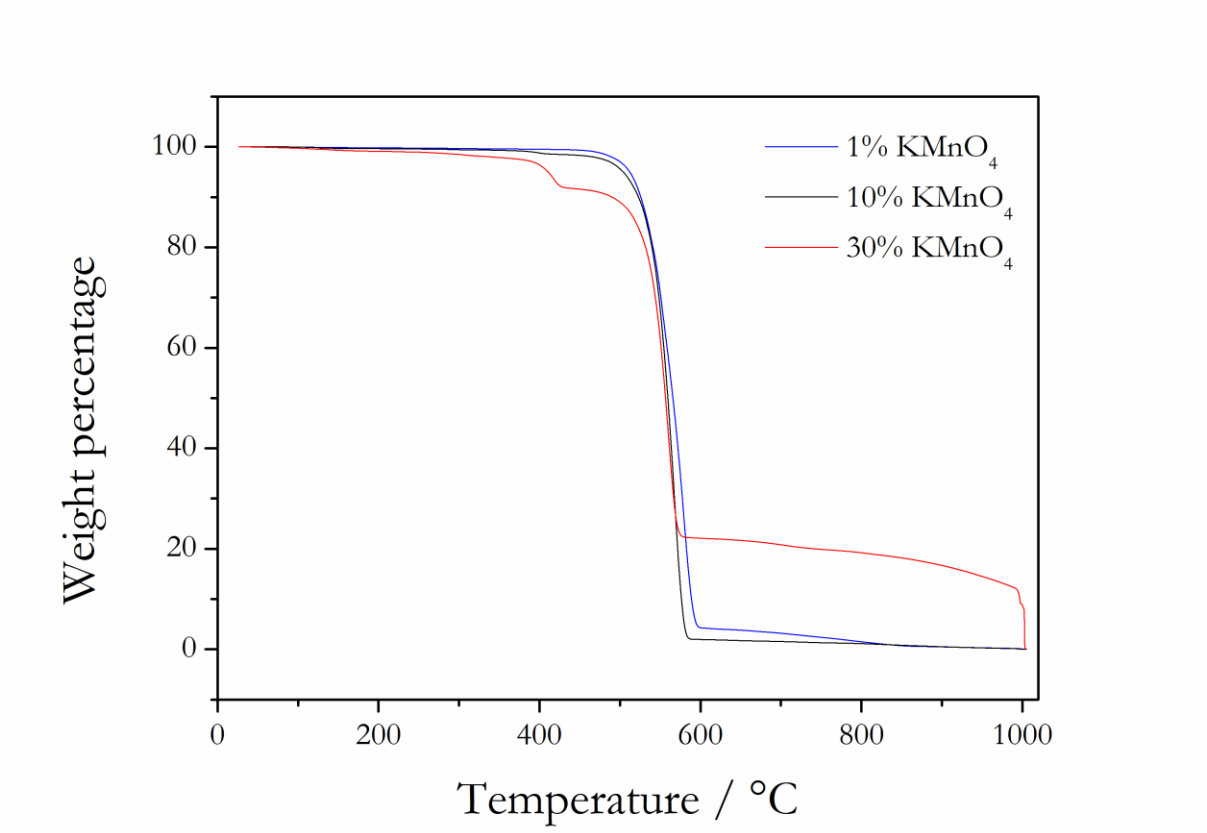

Figure 72: *TGA curves for $KMnO_4$ initiated PTFE using different initiator concentrations.*

The TGA curves for the potassium permanganate initiated samples are shown in Figure 72. For the 1 % and 10 % initiator samples, the expected results are obtained, with the 1 0% sample showing slightly earlier onset of its decomposition and reaching full decomposition at lower temperature due to its lower molecular weight. An interesting result was obtained for the 30 % initiator sample. The sample had a much earlier onset for its decomposition which was expected due to its lower molecular weight. What was not expected was to see different decomposition stages. The sample had an initial weight loss of ~10 % at ~400 °C after which it continued to decompose until ~20 % of the sample weight remained. Instead of continuing to decompose to destruction like the other two samples, it remained at ~20 % mass before abruptly decomposing to destruction at 1000 °C. The earlier onset of the decomposition can be attributed to shorter PTFE chains that evaporate before the bulk of the longer chain start to decompose. The residual mass can be attributed to amorphous carbon which decomposes at 1000 °C under oxygen. It is believed this amorphous carbon is deposited into the polymer matrix when the end groups are eliminated at elevated temperatures and could be responsible for the colour change seen in the sample post-sintering.

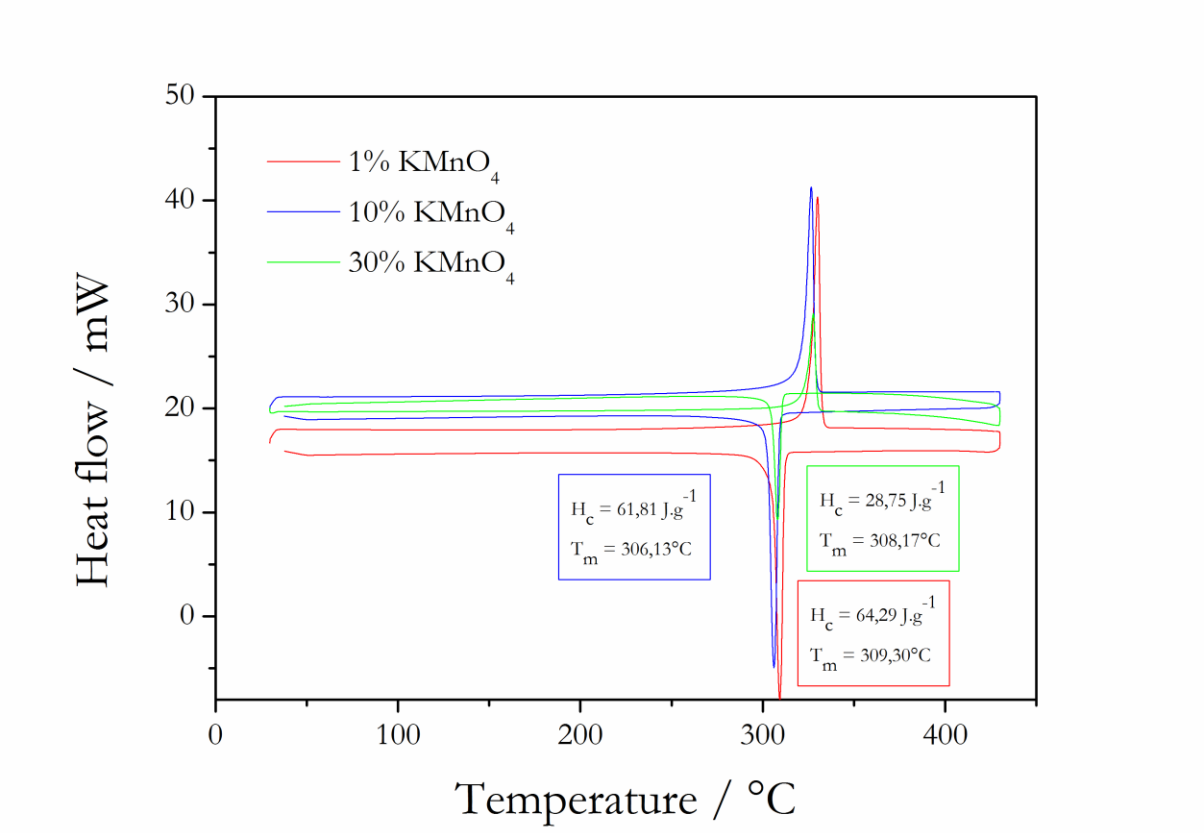

Figure 73: *DSC curves for $KMnO_4$ initiated samples.*

Figure 73 shows unsurprising results. The heat of crystallisation decreases with decreasing molecular weight. It can also be seen that the lower the molecular weight, the lower the melting temperature. What is interesting is that with decreasing molecular weight, the crystallisation peaks seem to become smaller and broader, once again in direct contradiction with what was reported in the literature.

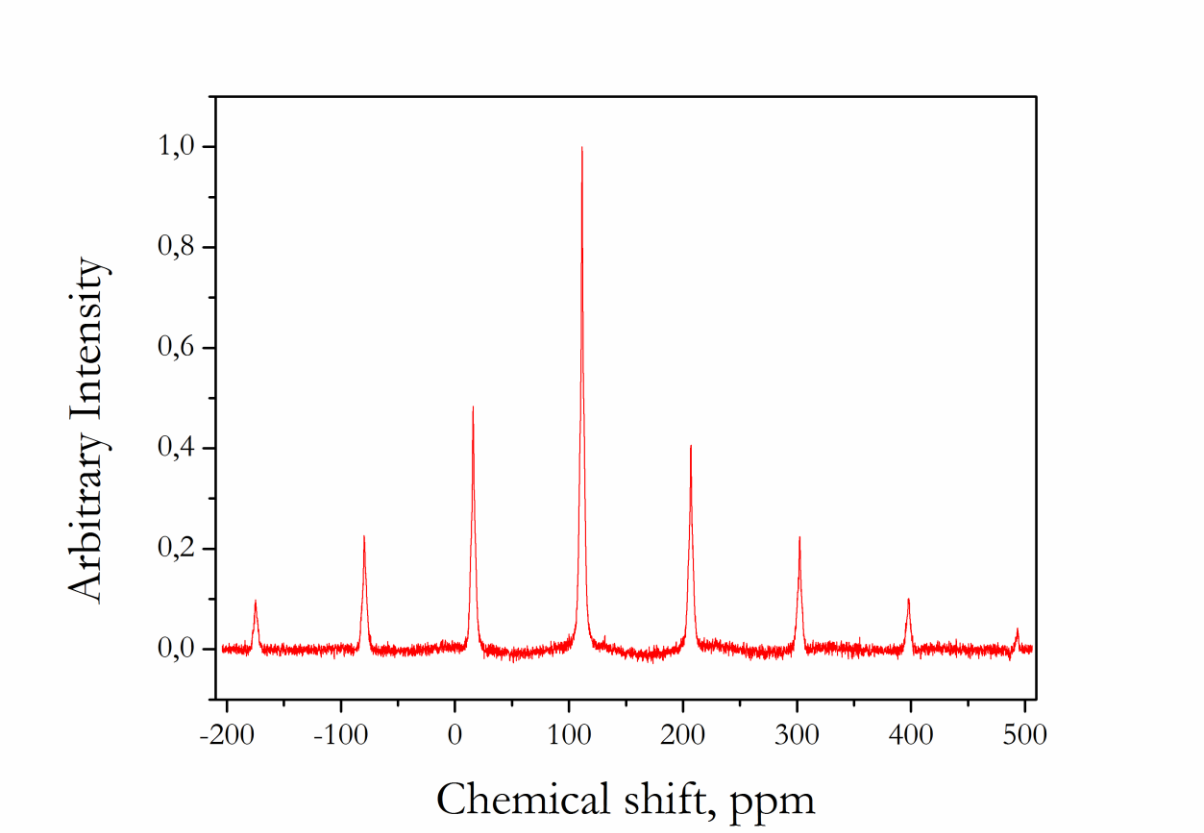

Figure 74: *^{13}C NMR DP spectrum of 30 % $KMnO_4$ sample.*

Figure 74 shows the ^{13}C NMR spectrum for the 30 % $KMnO_4$ sample obtained by running a Direct Pulse experiment at 12 MHz MAS rotor speed. The main signal in this sample appears at approximately 110 ppm and is assigned to the $-CF_2-CF_2-$ backbone structure of the polymer chain. Alkyne groups chemical shift is usually in the region of 80-90 ppm, but no signal is visible in this region. This could be because the instrument is not sensitive enough to pick up the concentration of end groups due to the low spinning rate of 12 MHz (it is believed at least 32 MHz is required). Either that, or the assumption that there are alkyne end groups present is incorrect.

The presence of alkyne end groups would have been easier to test had a solid state NMR with ^{19}F probe been available, because ^{19}F is 4763 times more sensitive than ^{13}C. However, a solid state NMR instrument that is capable of recording ^{19}F spectra with ^{13}C decoupling is not available in Africa.

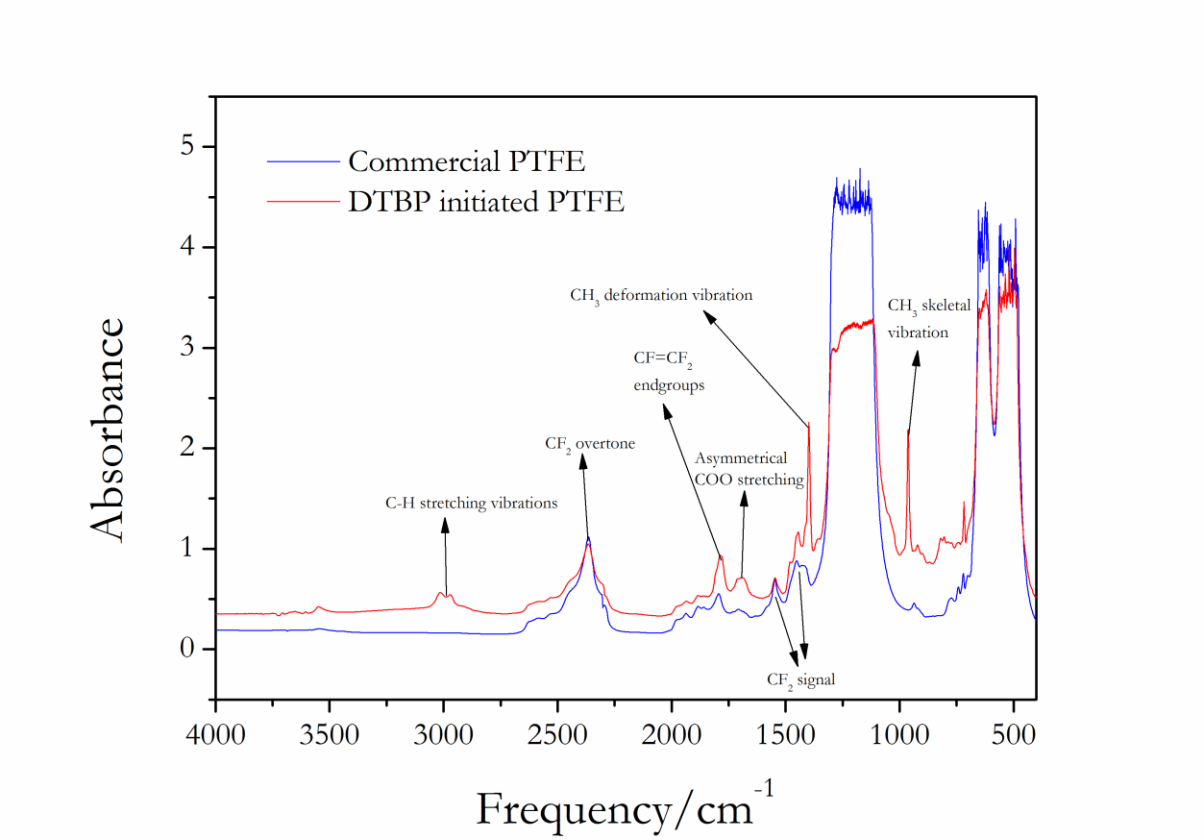

Figure 75: *Overlaid transmission FTIR spectra of PTFE initiated with DTBP.*

From Figure 75 it can be seen that while the structural bands that indicate PTFE are clearly present in both the DTBP and commercial samples, there are clear differences. The most striking of these is the presence of two previously absent, very sharp peaks at ~1398 cm^{-1} and ~963 cm^{-1}. It is believed that these two peaks are caused by symmetric CH_3 deformation vibrations and skeletal vibrations respectively and consequently indicate the presence of tertiary butyl end groups with an oxygen atom attached. Unfortunately the strong band caused by C-O stretching which should be visible at ~1200 cm^{-1} is obscured by the strong PTFE bands present in that region. There is also a doublet with broad, low intensity peaks at 2970 cm^{-1} and 3005 cm^{-1}. According to Pianca's paper [105] these two peaks are caused by C-H stretching vibrations and could indicate difluoromethyl groups. However, tertiary butyl groups also possess the C-H stretching vibrations present in this region and this together with the previous observations indicates strongly that there are tertiary butyl end groups present.

The DTBP initiated samples were troublesome to analyse using Raman spectroscopy. The 1 % and 10 % samples gave rather noisy spectra, while the 30 % sample fluoresced to such an extent that a usable spectra could not be obtained, even after varying the instrument's parameters. The

spectra of the 10 % sample was used to compare to commercial PTFE and can be seen in Figure 76.

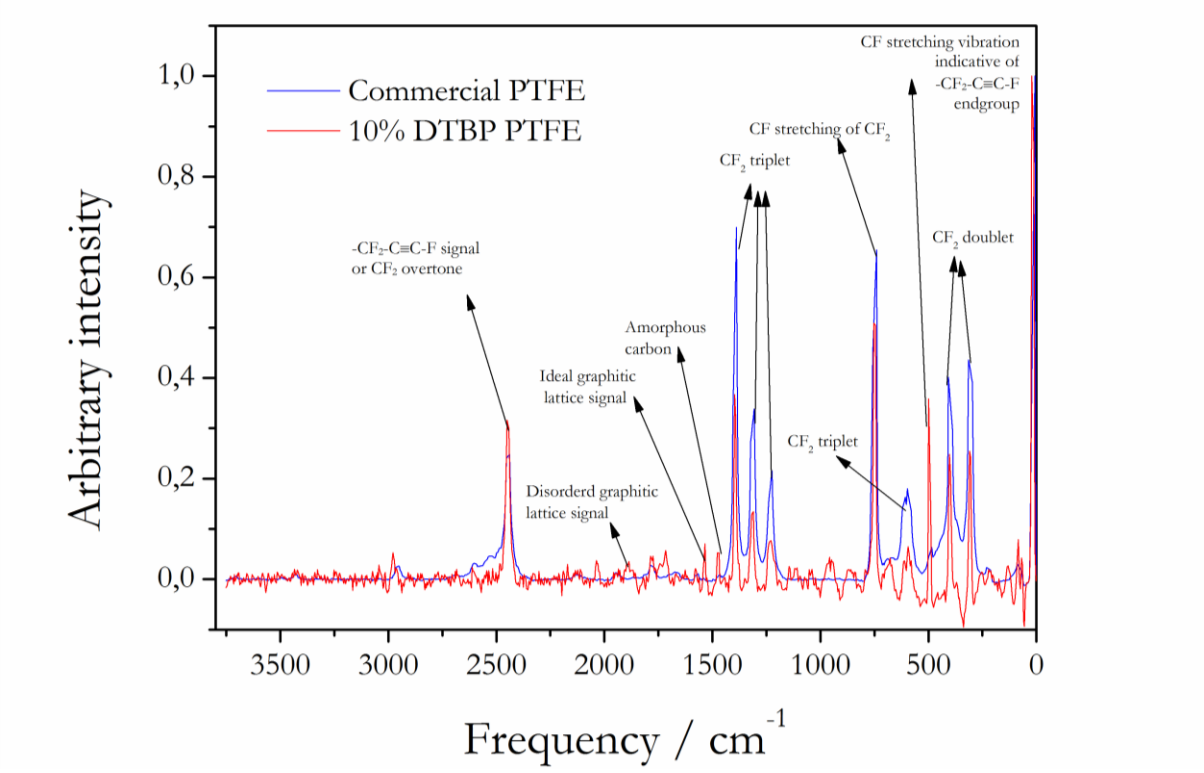

Figure 76: *Overlaid Raman spectra of DTBP initiated PTFE and commercial PTFE.*

From this it is clear that the expected PTFE curves are present in the DTBP sample and similarly to the previous in-house produced samples, the curves at ~2450 cm^{-1} and 500 cm^{-1} are clearly visible and more intense than those of the commercial sample, owing to the DTBP sample's lower molecular mass.

The TGA results shown in Figure 75 show the lower molecular weight samples starting to decompose at much lower temperatures of ~200 °C. The lower molecular weight samples had some residual weight remaining after 600 °C, which could indicate the presence of amorphous carbon, similar to the result obtained for the low molecular weight potassium permanganate initiated sample. The earlier onset of decomposition at ~200 °C shows that the DTBP initiated samples are of lower molecular weight than the $KMnO_4$ initiated samples. The decomposition also shows that these samples decomposed over a wider range of temperature when compared to the other samples, indicating a higher PDI, especially in the case of the 10 and 30 % initiator samples.

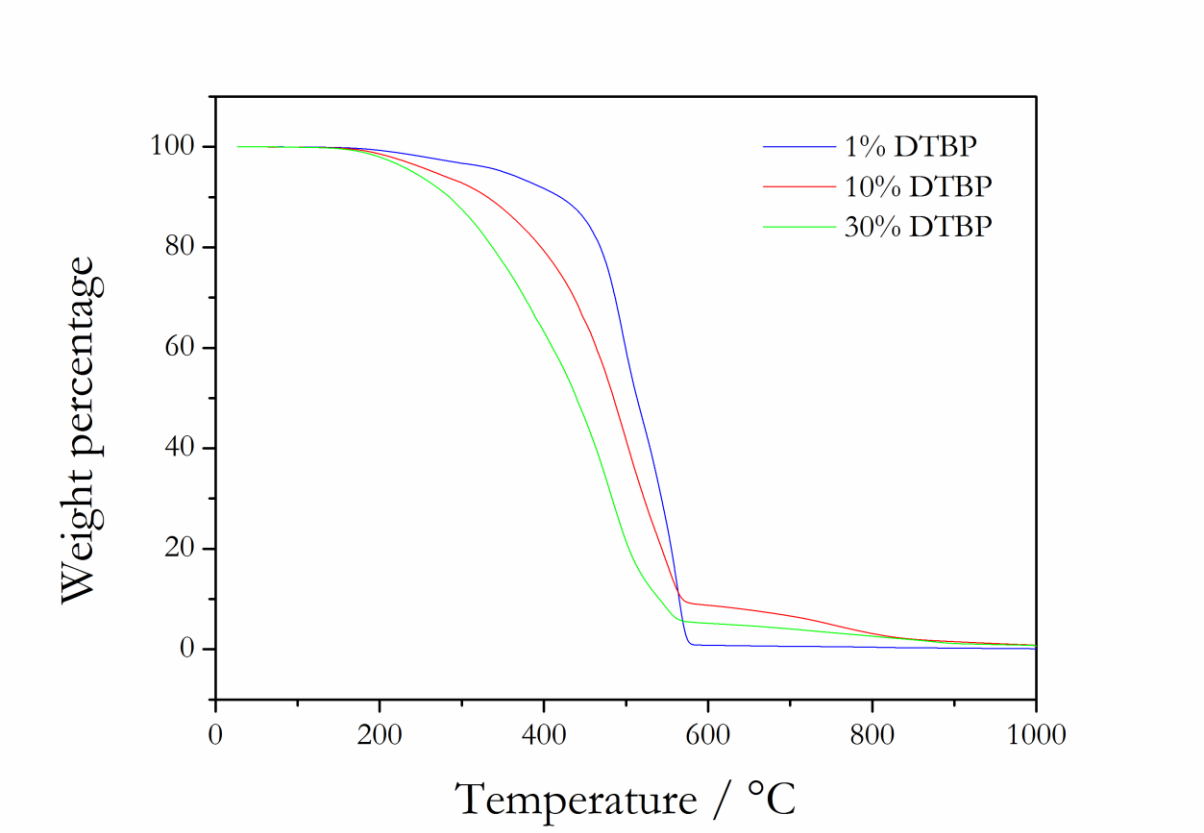

Figure 77: *Comparative TGA curves for DTBP initiated PTFE using different initiator concentrations.*

Figure 78 shows the heat of crystallisation for the lower molecular weight sample is lower than that of the higher molecular weight sample. It can also be seen that the lower the molecular weight, the lower the melting temperature. From these curves, it is obvious that the DTBP initiator delivers lower molecular weight polymer than any of the other samples, the 30 % sample being of particularly low M_n, evidenced by its very low heat of crystallisation.

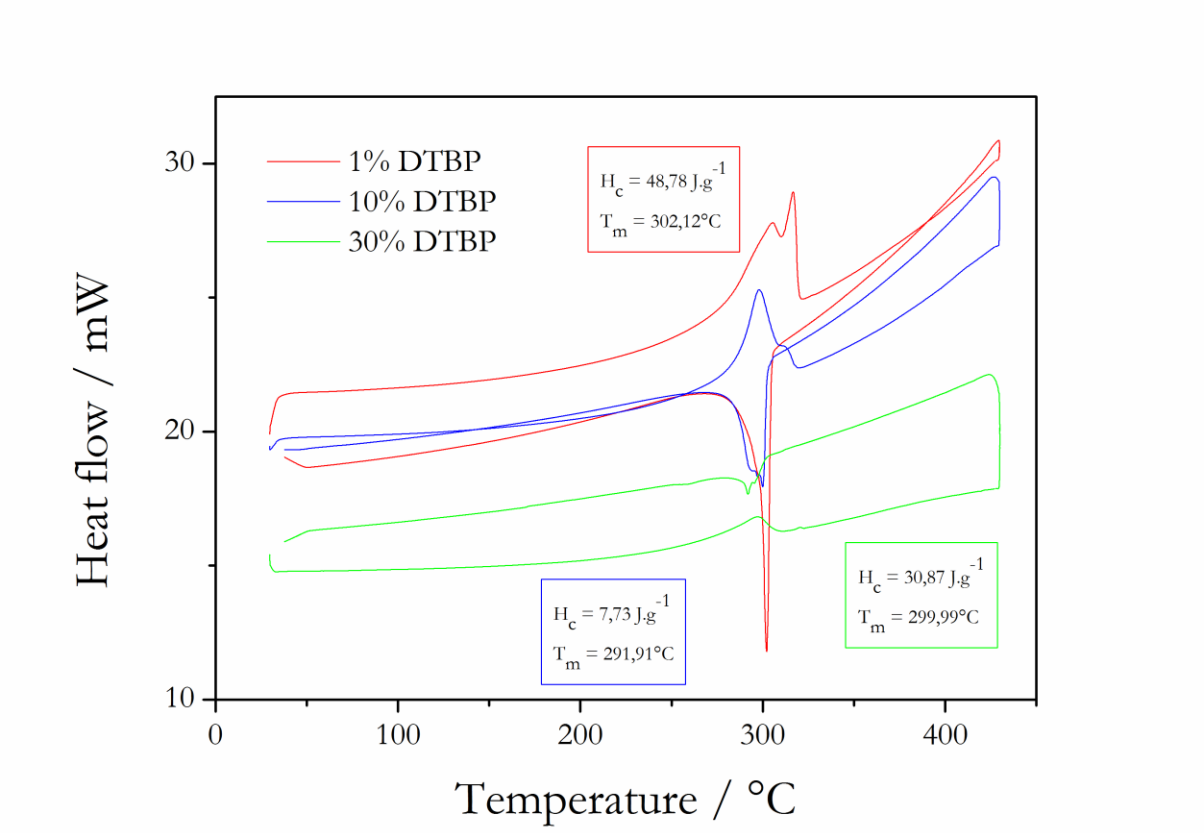

Figure 78: *DSC curves for DTBP initiated samples.*

Yields and M_n

The yields and molecular weights of the in-house produced PTFE samples that were thermally initiated can be seen in Table 7.

Table 7: *Yields and M_n of thermally initiated PTFE samples.*

Sample	Yield (mg)	Yield (%)	M_n as per Suwa's method	M_n as per Wiegel's method	Melting temperature (°C)
Commercial	n/a	n/a	2.19×10^6	3.65×10^7	313.94
1 % $KMnO_4$	1.9277	38.55	1.98×10^5	3.30×10^6	309.3
10 % $KMnO_4$	2.5783	51.57	2.83×10^5	4.72×10^6	306.13
30 % $KMnO_4$	1.3836	27.67	9.83×10^6	1.64×10^8	308.17
1 % DTBP	2.8508	57.02	1.17×10^6	1.95×10^7	302.12
10 % DTBP	2.8572	57.14	1.57×10^7	2.62×10^8	299.99
30 % DTBP	1.3836	27.67	2.60×10^{10}	4.33×10^{11}	291.91
5.5 % SPS	4.4068	88.136	2.32×10^5	3.86×10^6	300.28
30 % SPS	3.3382	66.764	4.19×10^5	6.99×10^6	296.93
K_2CO_3 buffer	3.7679	75.36	n/a	n/a	

From the results in Table 7 it can be seen that there is not necessarily an inverse correlation between initiator concentration and yield. While it seems to hold generally true that with increasing initiator concentration the yield decreases, as is the case with the SPS samples, in the case of DTBP initiator the yield stays approximately the same up to a certain initiator concentration and then drops off sharply. With $KMnO_4$ the yield actually increases when the initiator concentration is increased, but then decreases sharply again with further increases of the initiator concentration. These results are shown in Figure 79. These results would seem to suggest that there is a critical concentration where optimal yield can be obtained, with higher concentrations leading to decreased yields.

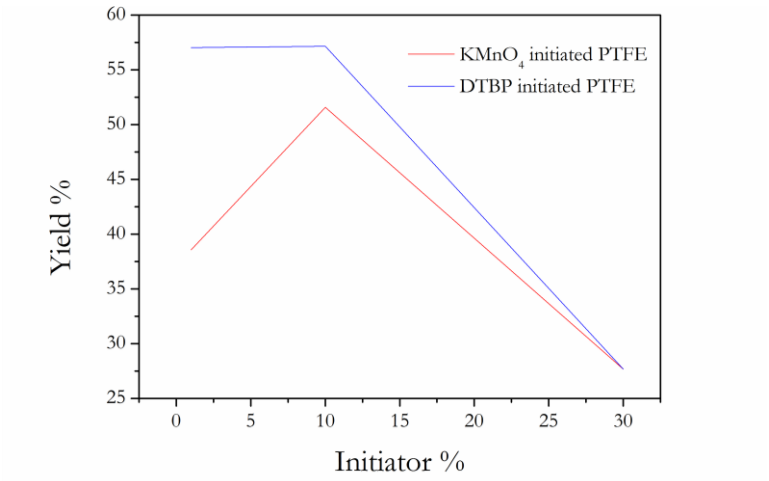

Figure 79: *Yield as a function of initiator concentration.*

With regards to the calculated M_n values seen in Table 7, the results obtained would seem to suggest that both Suwa and Wiegel's methods cannot be applied to these results in the hopes of getting accurate results. From the results tabulated, the trend seems to suggest that with increasing initiator concentration, the M_n values increase as well. This is the case for the samples initiated by $KMnO_4$, DTBP and SPS. This is contradictory to what has been discussed in the literature, as well as the TGA results obtained. Suwa and Wiegel's methods are only valid for a narrow range of molecular weights and it seems that the large differences in initiator concentrations have rendered most of the samples produced unable to be used in these methods because of their very low molecular weights. Therefore, when making observations about the molecular weights of the samples, TGA results would give a better qualitative indication of these properties for the given samples than DSC results applied to Suwa or Wiegel's methods.

Summary

Besides the expected signals that are reported by the literature, the FTIR and Raman spectra contain a strong signal which could not be definitively identified. It is believed this signal is either caused by an overtone signal because of a conformational aspect of the PTFE molecules, or if the ab initio calculations are to be believed, it is caused by alkyne end groups. At this point in the study it was still unclear which explanation was the correct one. It will be discussed again in the results regarding the processed samples.

The TGA and DSC results indicated that the commercial polymer is of a very high molecular weight and starts to decompose at a very high temperature. However, once this decomposition starts, it occurs very quickly.

The FTIR results shows that even with differing reaction conditions leading to different molecular weights, the structure of the synthesised PTFE samples were identical when the same initiator was used. The APS initiated samples that used borax as a buffering agent appear to have had multiple termination reactions, with the FTIR spectra indicating several different end group configurations. These end groups included: carboxylic acid end groups, amide end groups, carboxylic salt end groups with NH4+ and possibly alkyne containing end groups. The sample that did not include a buffering agent appears to also have had multiple termination reactions, with the spectra supporting the presence of carboxylic acid end groups, lower concentrations of carboxylic salt end groups and also possibly alkyne containing end groups. No evidence for the presence of amide end groups was found in this spectra for the buffer less sample. The spectra for the sample where potassium carbonate was used as the buffering agent showed very similar results to those of the borax sample, except for the absence of a peak to indicate carboxylic salt groups. It therefore seems that the potassium carbonate sample contained no carboxylic salt end groups, but did contain terminal alkyne end groups, carboxylic acid end groups and amide end groups.

The Raman spectra was not very useful in this regard as the spectra obtained for the borax sample was very noisy and did not show any peaks relating to end groups. Usable Raman spectra could not be obtained for the buffer less and potassium carbonate buffer samples.

The TGA results indicated that the buffering agent, or lack thereof, had an influence on the molecular weight of the polymer. Where borax and potassium carbonate were used as buffering agents, very similar molecular weights were obtained. However, when no buffering agent was used, the polymer was of a higher molecular weight, as evidenced by the later onset of its decomposition. These findings were supported by the DSC results.

From the FTIR spectra it is clear that the SPS initiated sample also had multiple termination modes. The spectra shows evidence for a high concentration of carboxylic acid end groups, a smaller concentration of carboxylic salt end groups and the terminal alkyne end group. The Raman spectra shows strong evidence of the presence of the terminal alkyne end group. The TGA results show that the higher initiator concentration clearly lead to a lower molecular weight polymer with a higher PDI. Both samples had residual mass up to approximately 800 °C. The DSC results showed that the lower molecular weight sample had a lower melting temperature and a lower heat of crystallisation. However, the lower molecular weight sample had a smaller, broader crystallisation peak, contrary to what was reported in the literature. The Hc values were used to calculate the molecular weight of the polymer according to Suwa and Wiegel's methods and will be discussed later.

The FTIR results of the potassium permanganate initiated sample indicate that the potassium permanganate initiated PTFE sample is similar to the commercial sample, with the exception being some evidence of OH end groups. The Raman spectra shows strong evidence of the terminal alkyne end group. The TGA analysis indicated that the low molecular weight sample deposited what is likely amorphous carbon into the polymer matrix due to elimination of the end groups at elevated temperatures. The DSC results show that the Hc values decrease with molecular weight and that Suwa's correlation was not valid in that range. The NMR results showed no evidence of alkyne groups, though this was likely due to the instrument not being able to attain the required sensitivity.

The FTIR results indicate the presence of tertiary butyl end groups and the absence of carboxylic acid and carboxylic salt end groups. It also indicates the presence of terminal alkyne end groups. Likewise, the Raman results indicate the presence of the terminal alkyne end group. The DSC and TGA results show these samples are of very low molecular weight, lower than the previous samples. The TGA results show residual mass in the lower molecular weight samples, which could be amorphous carbon eliminated from the end groups.

Table 8: *Initiators used in PTFE syntheses and subsequent end-groups before sintering.*

Initiator	**Exp. #**						
End-groups		-COOH	$-COO^+X^-$	$-CONH_2$	-C≡C-F	$-COC(CH_2)_2$	OH
Commercial	-				✓		
APS (Borax)	1, 4-17	✓	✓	✓	✓		
APS	2	✓	✓		✓		
APS (K_2CO_3)	3	✓			✓		
SPS	18, 19	✓			✓		
$KMnO_4$	20-22				✓		✓
DTBP	23-25				✓	✓	

In terms of the yield, the results indicate there is a critical concentration where optimal yield can be obtained, with higher concentrations leading to decreased yields. The DSC and TGA results show that obtaining quantitative results remains problematic.

4.1.2 Photoinitiated PTFEs

This section shows the results obtained for the photoinitiated PTFE samples, initiated with APS and H_2O_2 respectively.

Results of spectroscopic and thermal analysis

It is immediately apparent from Figure 80 that the FTIR spectra of the photoinitiated sample that it is remarkably similar to commercial PTFE. Besides a few differences in intensities, the only difference between the spectra is the small peak of the photoinitiated PTFE at 3557 cm^{-1}. In addition the peak at 3557 cm^{-1}, a medium but sharp peak at 1775 cm^{-1}, small but broad peak from 3300 cm^{-1} to 3000 cm^{-1} and a small peak at 1813 cm^{-1} all indicate the presence of COOH groups. The peaks that suggest amide groups at 3438, 1768 and 1587 cm^{-1} are absent in the spectrum of the photoinitiated PTFE's spectra.

There is also an absence of any peaks between 1775 cm^{-1} and 1600 cm^{-1} in the photoinitiated sample, whereas the thermally initiated sample has a broad peak indicative of a COO^-X^+ group. From this, it could be surmised that the photoinitiated sample is free from ionic bonding with the ammonium ions, unlike the thermally initiated sample.

Figure 81 shows that similarly to the photoinitiated APS sample, the photoinitiated H_2O_2 sample's FTIR spectra is remarkably similar to commercial PTFE's. The H_2O_2 initiated sample shows no bands from 4000 cm^{-1} to 2680 cm^{-1}. This along with the absence of bands at 1813 and 1775 cm^{-1} indicates that there are no COOH groups present. There are also no bands between 1775 and 1600 cm^{-1}, indicating no COO^-X^+ groups. The strong band at ~2450 cm^{-1} suggests the presence of the terminal alkyne end group, similarly to the other samples. The absence of any other peaks indicate that either there are no other end groups present, or they are present in such small concentrations that they are not visible on the spectra.

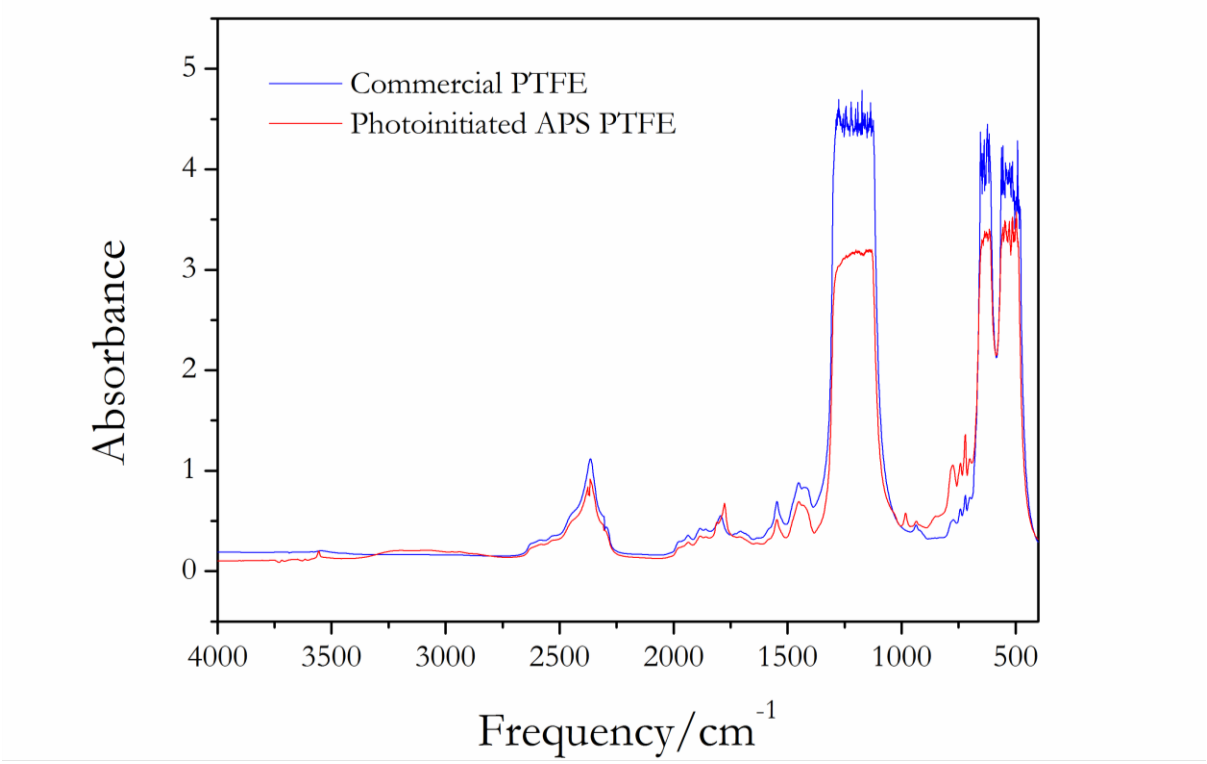

Figure 80: *Overlaid transmission FTIR spectra of commercial and photoinitiated APS PTFE.*

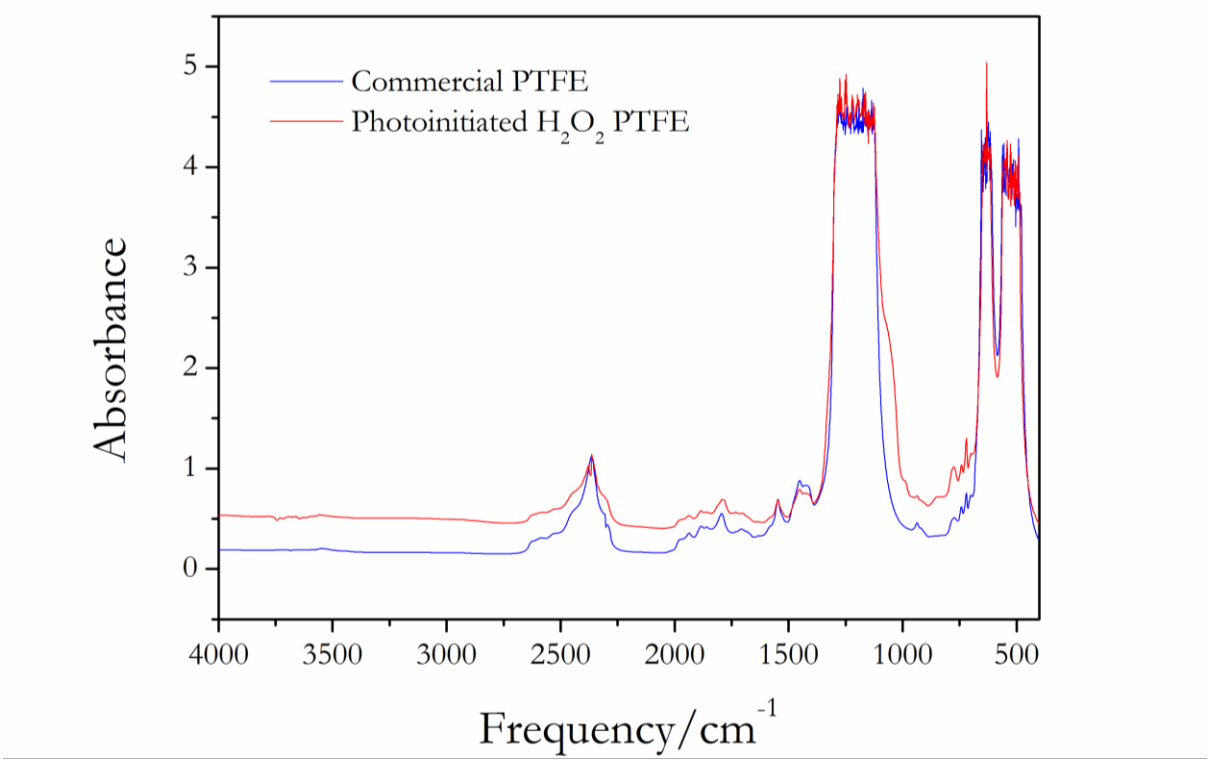

Figure 81: *Transmission FTIR spectra of photoinitiated PTFE, H_2O_2 as initiator.*

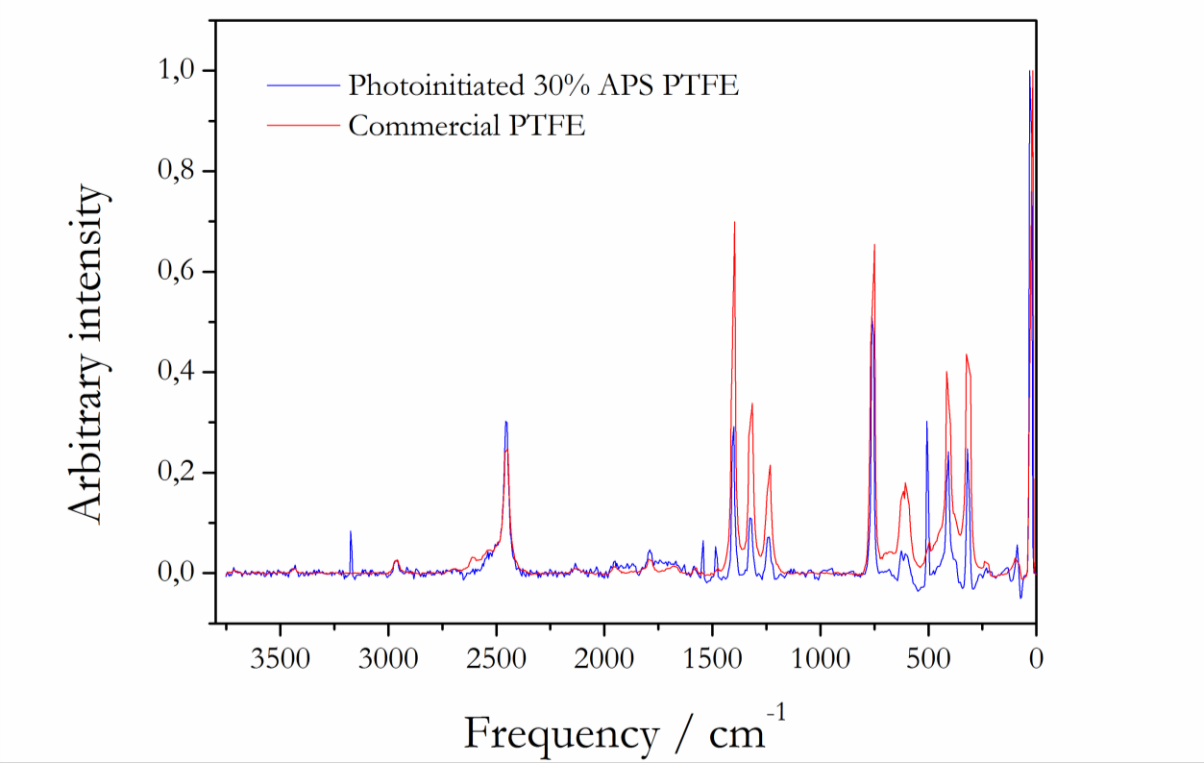

Figure 82: *Overlaid Raman spectra of APS photoinitiated PTFE and commercial PTFE.*

The spectra of a sample photoinitiated with 30 % APS can be seen in Figure 82. Interestingly, while it is clear that the expected PTFE curves are present in the in-house produced sample and similar to the $KMnO_4$ and DTBP samples, the spectra of the photoinitiated APS sample differs significantly from the spectra of the thermally initiated APS sample discussed previously in several regions. Firstly, the photoinitiated sample possesses a sharp peak at 500 cm^{-1} which the thermally initiated sample does not. This along with the presence of the peak at 2450 cm^{-1} in the photoinitiated sample and the lack thereof in the thermally initiated sample, seems to indicate that the photoinitiated sample possesses alkyne end groups in significant amounts, whereas the thermally initiated sample does not. Another interesting development is the presence of a medium-to-low intensity peak at ~3200 cm^{1} which is unassigned.

The spectra of photoinitiated H_2O_2 PTFE and the commercial sample can be seen in Figure 83. From this it can be surmised that the H_2O_2 is of a very high molecular mass, because of the low intensity of the PTFE peaks and the apparent absence of any of the aforementioned peaks that may indicate end groups. Interestingly, there is a sharp and rather intense peak (when compared to the other peaks of the H_2O_2 sample only) at ~2200 cm^{-1}, which has not been seen in any of the previous samples.

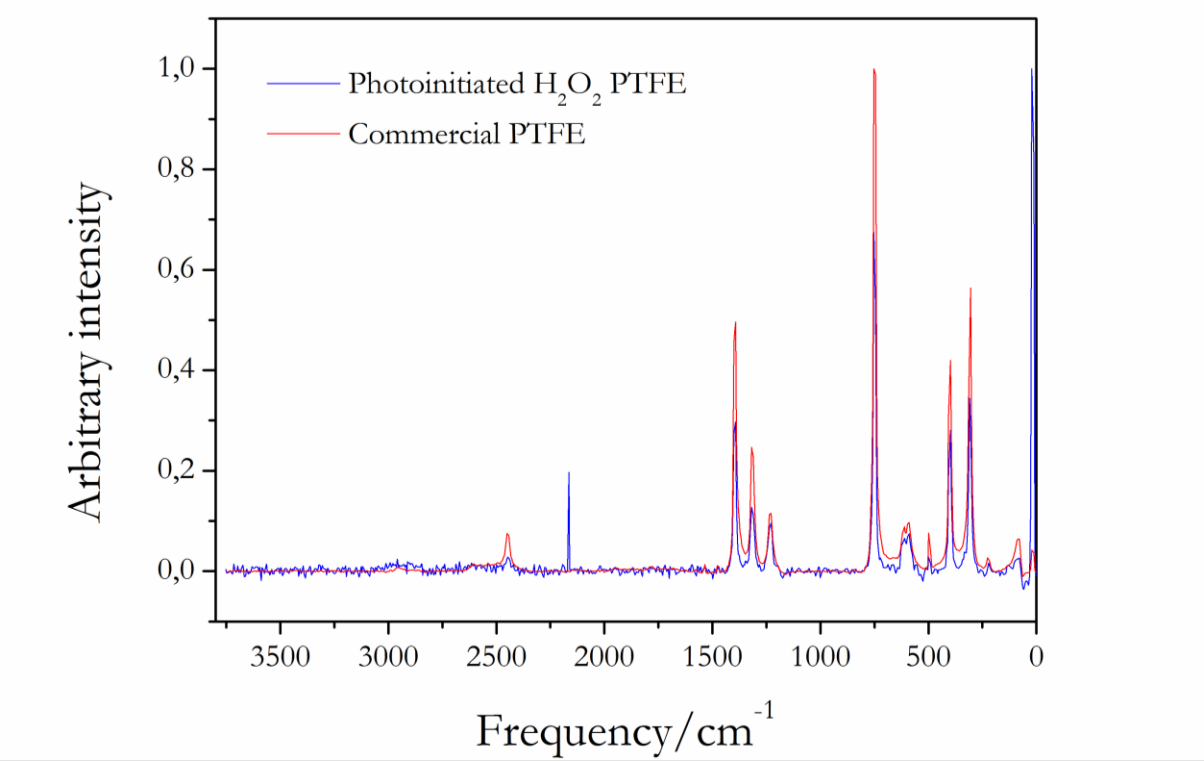

Figure 83: *Overlaid Raman spectra of H_2O_2 photoinitiated PTFE and commercial PTFE.*

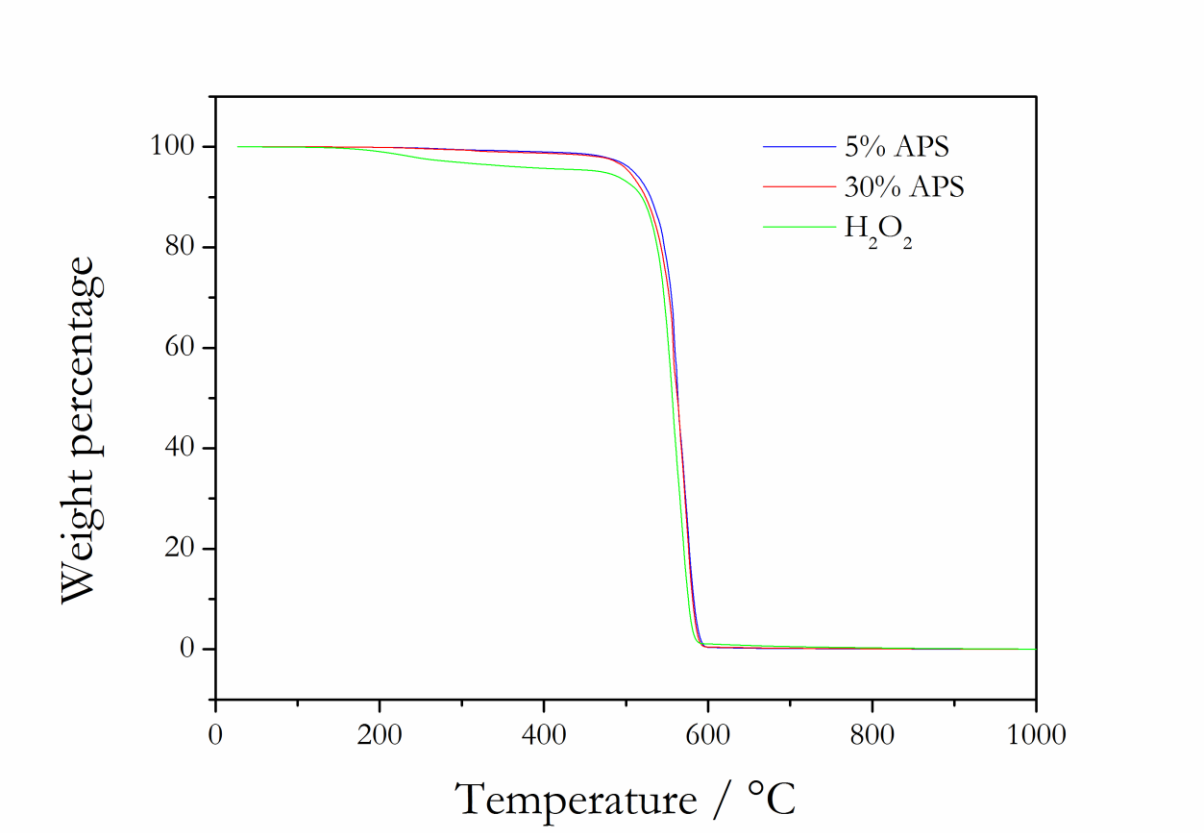

Figure 84: *TGA curves for photo-initiated polymerisations in sunlight using different initiators.*

The TGA results that can be seen in Figure 84 show that the photoinitiated samples are all of a high molecular weight, even the sample that had 30 % initiator. This is a very interesting result, as it was expected that this sample would have a much lower molecular weight than the 5 % sample due to increased initiator concentration. It is interesting to note that the H_2O_2 has an initial decomposition step that starts at a lower temperature than either of the APS samples. This could indicate some lower molecular weight chains that decompose first before the bulk of the chains, which are higher molecular weight, decompose in a similar fashion to the APS samples.

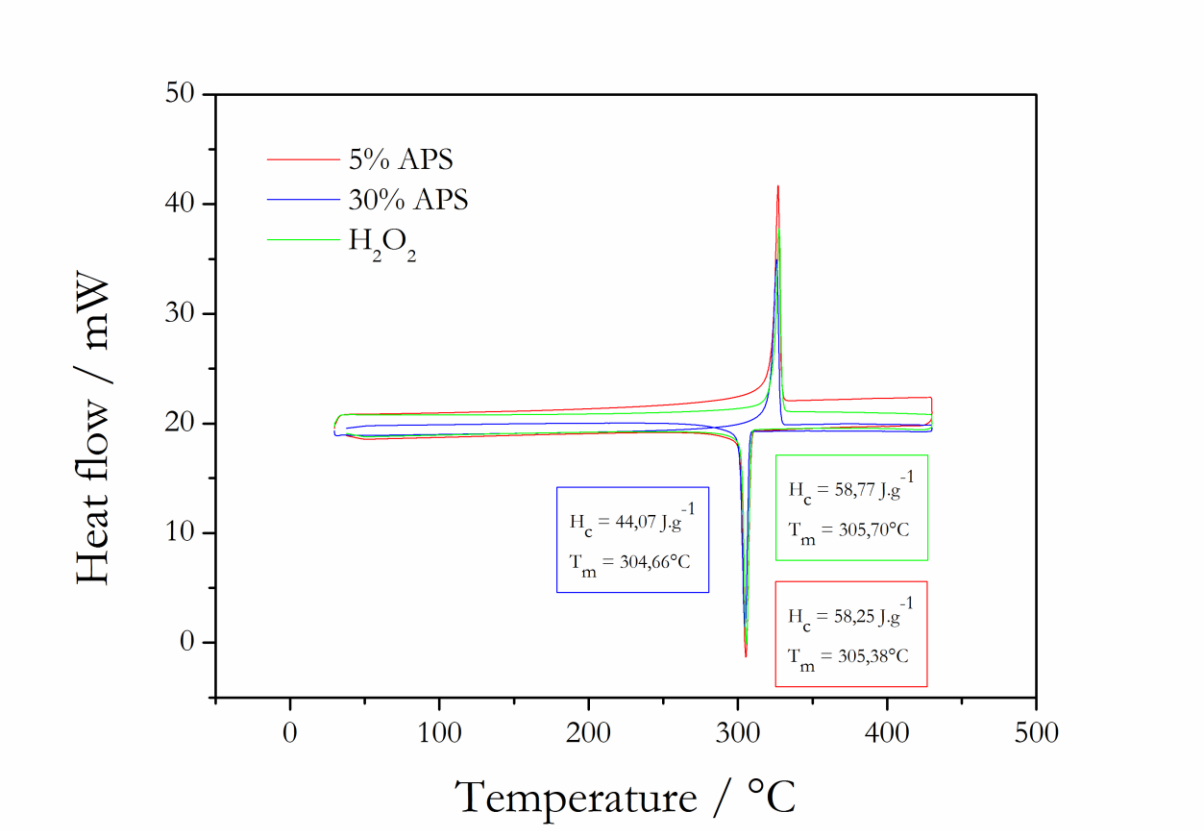

Figure 85: *DSC curves for photoinitiated samples, using APS and H_2O_2 as initiators.*

Yields and M_n

Table 9: *Yields of photoinitiated PTFE samples exposed to sunlight.*

Sample	Yield (mg)	Yield (%)	M_n as per Suwa's method	M_n as per Wiegel's method	Melting temperature (°C)
H_2O_2	369.0	73.80	2.53×10^5	4.21×10^6	305.7
5.5 % APS	347.4	69.50	2.64×10^5	4.40×10^6	305.38
30 % APS	332.9	66.58	1.12×10^6	1.86×10^7	304.66

From the results shown in Table 9 it can be seen that the 5.5 % APS sample and the H_2O_2 initiated sample have similar yields, as well as similar molecular masses as calculated by the correlations of Suwa and Wiegel. Though it has been shown that these correlations cannot be used outside a very narrow range of values, this still indicates that the two samples have very similar heats of crystallisation and from this it can be surmised that they have similar molecular weights, even if these values are not the values shown in Table 9.

It is also clear from Table 9 that when Suwa and Wiegel's correlations are used, the M_n value increases with increasing initiator concentration. This is counterintuitive, because increasing initiator concentration means shorter polymer chains and therefore lower M_n. This once again shows that the correlations are not valid for these ranges.

Summary

From the FTIR spectra of both the APS and H_2O_2 samples, it is clear both are very similar to the commercial PTFE. The APS sample shows evidence of carboxylic acid end groups in low concentrations, as well as a high concentration of the terminal alkyne end groups, suggesting two termination reactions. The H_2O_2 sample shows no evidence of carboxylic acid end groups, only a high concentration of the terminal alkyne end groups.

The Raman of the APS sample suggests the presence in high concentrations of the alkyne end group, which is strangely absent in the Raman spectra of the thermally initiated APS sample. There is also a sharp peak at 3200 cm^{-1} which is unassigned. The Raman of the H_2O_2 shows no evidence of the alkyne end group. The only peak which differs from the spectra of the commercial sample is a small sharp peak at 2200 cm^{-1}, which is unassigned.

The TGA results show that the APS samples have very similar molecular weights, which is strange considering the large difference in initiator concentrations. The H_2O_2 sample starts to decompose at a lower temperature, which suggests it has some lower molecular weight chains that decompose before the bulk of the chains which are of a higher molecular weight.

The DSC results again show that obtaining quantitative results for the M_n values remains problematic.

4.1.3 Controlled photo-initiated polymerisations

Results of spectroscopic and thermal analysis

Transmission FTIR measurements for the samples that were synthesised by exposure to UV only, IR only, visible only, and IR and visible could not be obtained, because there simply was not enough sample to be able to do this. However, because of the similar spectra of the other three samples, shown in Figure 86, it was assumed that these samples' spectra would be identical as well.

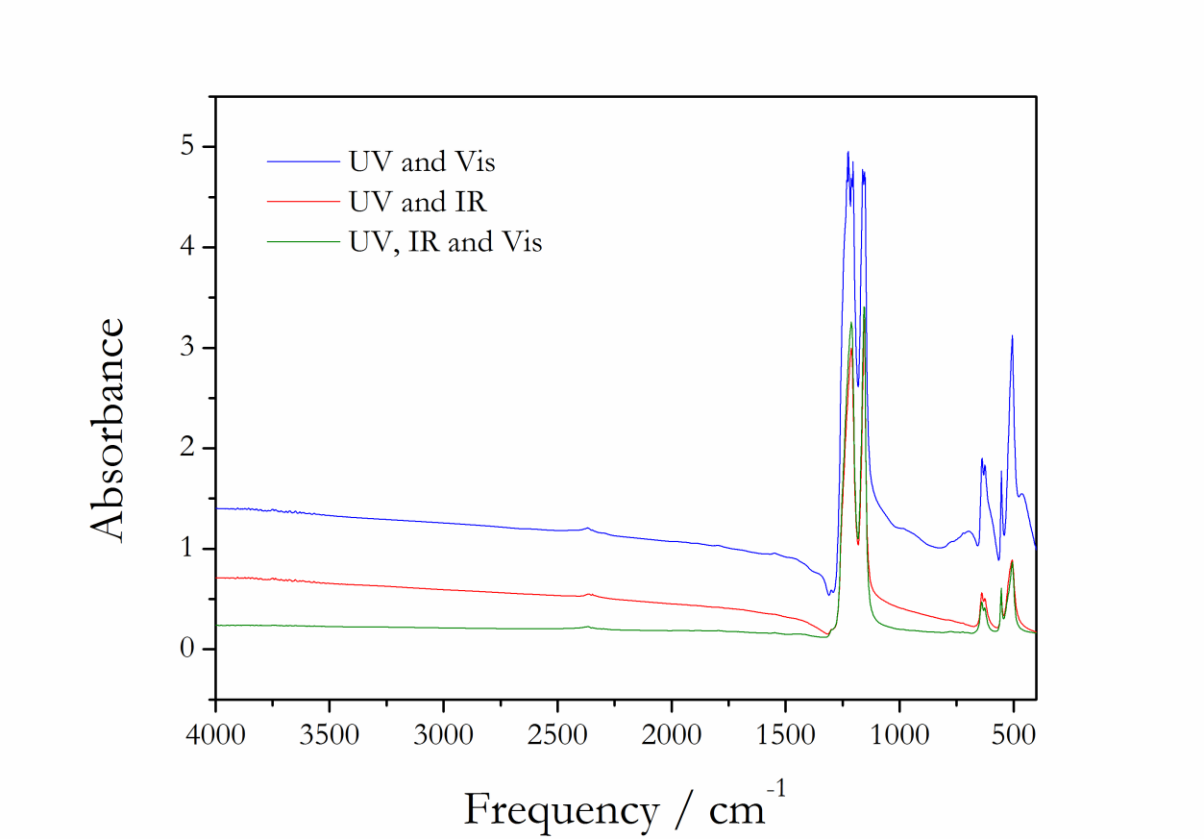

Figure 86: *Transmission FTIR spectra for photoinitiated PTFE samples.*

The TGA curves for the samples of which there was enough for analysis is shown in Figure 87. These results show that the samples are all of high molecular weight and follow the established trend of high molecular weight PTFE in that they start to decompose at ~500 °C and once decomposition starts, it occurs rapidly. Interestingly, none of these samples showed residual weight after 600 °C, unlike most of the thermally initiated samples.

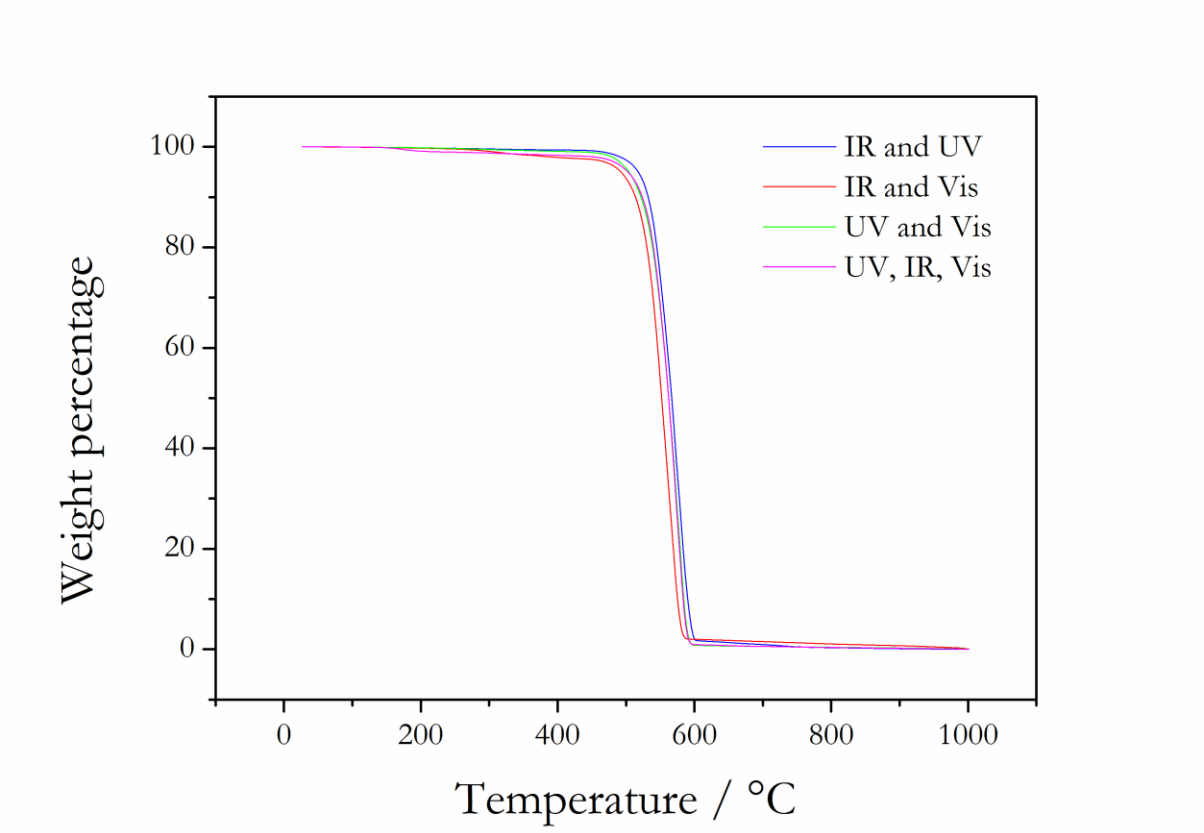

Figure 87: *Comparative TGA curves for controlled photo-initiated polymerisations using different regions of the electromagnetic spectrum.*

Figure 88 shows the DSC curves for some of the controlled photoinitiated polymerisations. It shows that the DSC curves for the four samples are very similar, with very similar heats of crystallisation and melting temperatures that only differ slightly. Interestingly, a definite trend appears where the lower the H_c value, the higher the melting point. These results are tabulated in Table 10. The results for Suwa and Wiegel's correlations are shown in Table 11 and will be discussed thereafter.

Table 10: *Heats of crystallisation and melting points for controlled photoinitiated samples.*

Sample	Heat of crystallisation ($J \cdot g^{-1}$)	Melting point (°C)
UV and Vis	57.91	306.10
UV, IR and Vis	50.90	306.18
UV and IR	50.28	307.73
IR and Vis	47.18	308.69

DSC measurements were not conducted on the IR only, visible only, UV only and IR and visible samples, because not enough sample was produced for analysis.

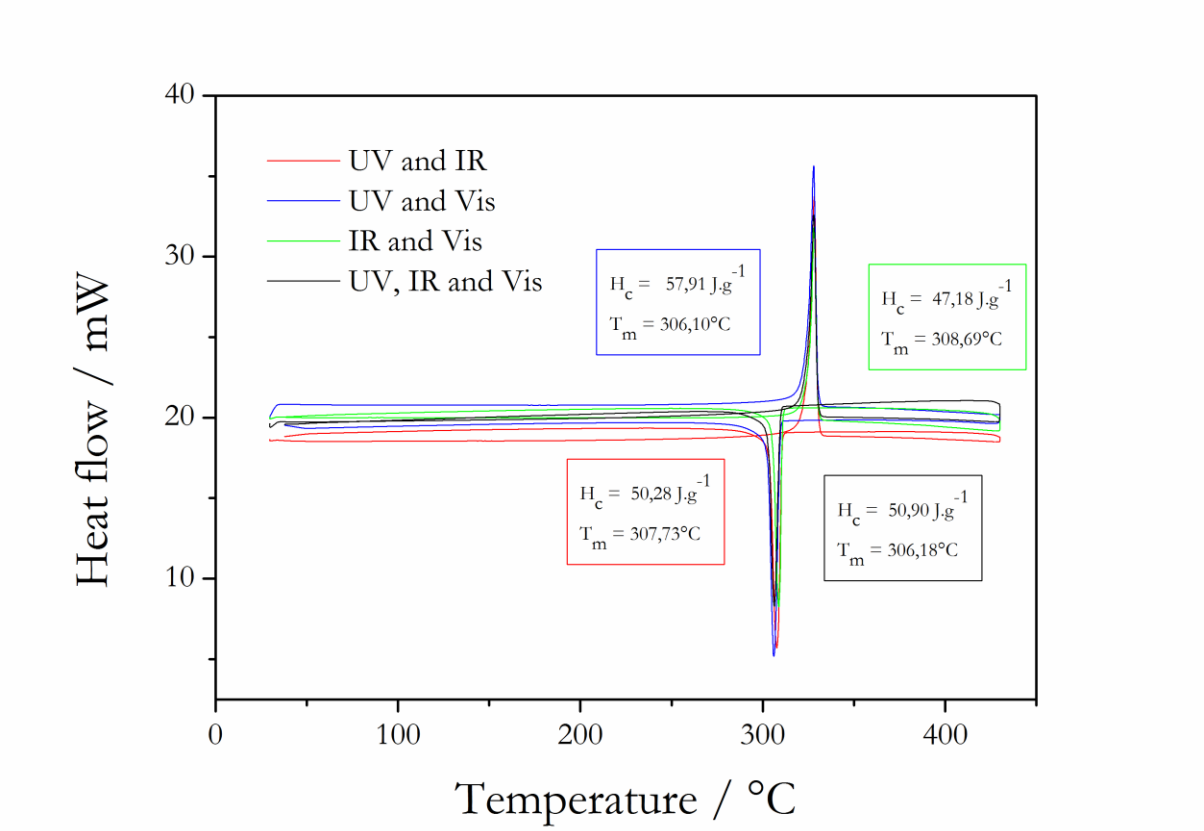

Figure 88: *DSC curves for controlled photoinitiated polymerisations.*

Yields and M_n

The results for the M_n values shown in Table 11, along with the results in Table 10 show that unlike the other polymers that were synthesised, these samples seem to fit Suwa's correlation in that higher molecular weight polymers have higher melting points. This is likely because their values fall into the narrow range in which Suwa's correlation is applicable.

Table 11: *Yields of the photoinitiated PTFE samples initiated with H_2O_2 exposed to controlled electromagnetic radiation spectra.*

Sample	Yield (mg)	Yield (%)	M_n as per Suwa's method (x 10^5)	M_n as per Wiegel's method (x 10^6)	Melting temperature (°C)
UV	53.8	10.76	n/a	n/a	n/a
IR	10.0	2.00	n/a	n/a	n/a
Visible light	15.2	3.04	n/a	n/a	n/a
UV + Vis	117	23.40	2.73	4.54	306.10
UV + IR	160.0	32.00	5.65	9.41	307.73
IR + Vis	93.0	18.60	7.84	13.1	308.69
UV + IR + Vis	162.4	32.48	5.3	8.84	306.18

Figure 89 shows the yield of the controlled photoinitiated polymerisations as a function of reaction time. The yield was only determined once the tubes were cut open after the full reaction time of six hours. To plot the results, it was assumed that the yield was a linear function of reaction time. From Figure 89 it is clear that there is some form of synergistic effect at work with the photo-initiation of PTFE. The yield when IR and visible light were used individually was very poor, 3 % or less. The yield when UV was used individually was also quite poor, though significantly better than visible and IR with a yield of just under 11 %.

Interestingly, when IR and visible were used in conjunction, the yield improved significantly from their individual yields to almost 19 %. This suggests synergistic effects between the two. The combination of UV and visible light gave a yield of just over 23 %, slightly higher than the combination of IR and visible light, but once again much higher than their individual yields.

UV and IR produced a yield of 32 %, significantly higher than that of the previous combinations. Interestingly, the combination of all three types of light only caused a very slight increase in yield, 32.5 % versus 32 %.

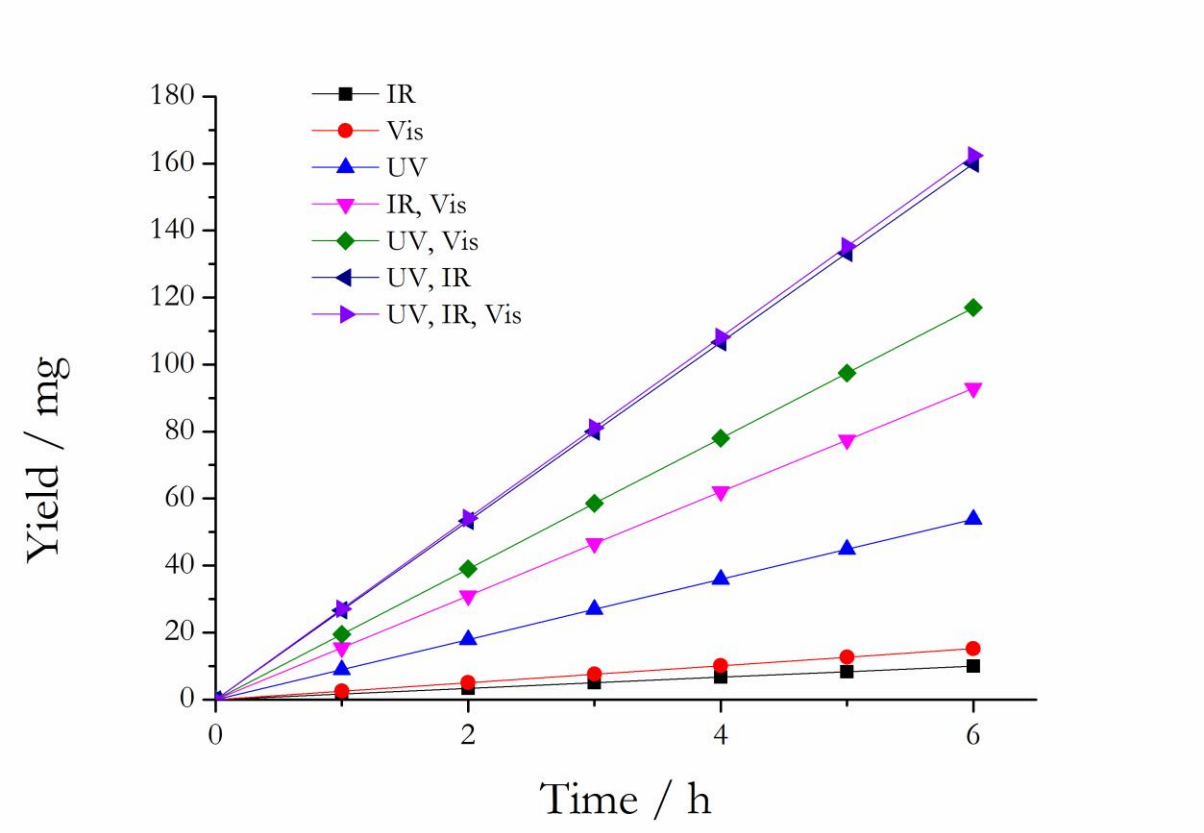

Figure 89: *Yields of controlled photo-initiated samples after 6h.*

Summary

These results seem to suggest that it is indeed a combination of the three regions of the electromagnetic spectrum that leads to successful photoinitiated polymerisation of PTFE. However, it seems that a combination of all three is only marginally better than the combination of UV and IR, which suggest these are the two parts of the spectrum that play the biggest role.

4.2 Processed PTFE results

All the previously mentioned samples were pressed into discs and heat treated (sintered) at 380 °C for a period of 30 min to ensure that the maximum colour change and therefore the maximum structural change took place. They were then analysed using FTIR and Raman spectroscopy to determine what changes the elevated temperature wrought to the structure and how these structural changes caused discolouration in the samples.

4.2.1 Thermally initiated PTFEs

Discolouration

The degree of discolouration for the experiments was rated on an arbitrary scale of 0-10, where 0 meant no discolouration and 10 meant complete discolouration (*i.e.* bright white at 0 and black at 10). The before-and-after photographs for the pressed discs are given in the supporting information and the degree of discolouration is summarised in Table 12 and Table 13.

As expected, commercial PTFE did not exhibit any colour change. The commercial sample became translucent at the sintering temperature, but reverted to an opaque white when cooled to ambient.

APS initiated samples were generally off-white to a light-yellow colour depending on the initiator concentrations before sintering and in most cases discoloured mildly to varying shades of brown. SPS initiated samples were white before sintering and discoloured significantly less than the APS samples when sintered. Control experiments using potassium persulfate (KPS) also did not discolour as much as the ammonium persulfate initiated polymers.

$KMnO_4$ initiated samples were pristine white in colour. The samples synthesised with lower initiator concentrations (1 % and 10 % respectively) showed no discolouration after sintering. However, the sample initiated with 30 % initiator showed the most pronounced discolouration of all the samples tested, going from pristine white to dark black when sintered. DTBP initiated samples were yellow to light brown in colour before sintering but underwent no change in colour when sintered. Lastly, PTFE synthesised by photo-initiation with H_2O_2 produced a pristine white polymer which underwent no colour change whatsoever during sintering.

The cause of discolouration in PTFE is not explicitly discussed in the literature. The literature indicates implicitly that the discolouration is due to chromophoric end-groups. Kurt Nassau [150] discussed the fundamental causes of colour and indicated that, for purely organic compounds (not

ligands), colouration arises from conjugated p-orbitals (*i.e.*, chains of alternating single and double bonds).

As stated previously, the literature regarding end-groups in fluoropolymers [105] indicates that APS, SPS and H_2O_2 initiated PTFE should exhibit end-groups which undergo thermolysis to produce C≡N or $CF=CF_2$ terminal moieties. Specifically, the nitrile end-groups are produced only by APS. Compounds such as DTBP do not produce end-groups which eliminate at sintering and should not produce any discolouration (this is confirmed by the lack of discolouration during sintering for this initiator, as reported in Table 13).

The known end-groups of PTFE are not conjugated systems and do not act as chromophores for visible light. For example, $CF_2=CF_2$, CF_3-$CF=CF_2$, CF_3-CF_2-$CF=CF_2$, *etc.*, are reported as colourless gasses. So too the homologues of CF_3-C≡N [151].

Furthermore, assuming the end-groups are the source of the discolouration, there should be a strong correlation between the concentration of the end groups and the degree of discolouration. From Tobolski's law [60, 152], the molecular weight decreases with the square root of the initial initiator concentration. As the end-group concentration increases with decreasing molecular weight, there should exist a strong correlation between the molecular weight and the degree of discolouration. The degree of discolouration is plotted as function of M_n in Figure 90. The figure indicates there is no correlation between degree of discolouration and molecular weight.

Table 12: *Results of the TFE polymerisations using APS as initiator.*

Exp. number	Temp. (°C)	Mass TFE (g)	Initiator (%)	Vol. water (mL)	Mass of buffer (g)	Degree of discolouration after sintering
1	65	5	5,5	100	0.48	5
2	65	5	5,5	100	-	2
3	50	5	5.5	100	0.48	5
4	55	5	2,3	100	0.48	7
5	55	5	5,5	100	0.48	8
6	55	5	8,7	100	0.48	8
7	65	5	1,0	100	0.48	8
8	65	5	2,0	100	0.48	7
9	65	5	5,5	100	0.48	6
10	65	5	8,7	100	0.48	7
11	65	5	10	100	0.48	6
12	65	5	20	100	0.48	2
13	75	5	2,0	100	0.48	7
14	75	5	5,5	100	0.48	4
15	75	5	8,7	100	0.48	5
16	75	5	10	100	0.48	3
17	80	5	5,5	100	0.48	3
18	80	5	10	100	0.48	3
19	50	5	5,5	100	0.18	6

Table 13: *Results of the TFE polymerisations using various other initiators, sans buffering agent.*

Exp. number	Initiator	Temp. (°C)	Mass TFE (g)	Initiator %	Vol. water (mL)	Yield (%)	Degree of discolouration after sintering
20	SPS	65	5	5.5	100	88.1	1
21	SPS	65	5	30	100	66.8	2
22	$KMnO_4$	35	5	1	100	38.6	0
23	$KMnO_4$	35	5	10	100	51.6	0
24	$KMnO_4$	35	5	30	100	27.7	10
25	DTBP	135	5	1	100	57.0	1
26	DTBP	135	5	10	100	57.1	1
27	DTBP	135	5	30	100	27.7	1
28	H_2O_2	80	5	10	100	73.8	0
29	ACPA	80	5	10	100	0	n/a
30	AAPH	80	5	10	100	0	n/a
31	BPO	85	5	10	100	0	n/a
32	LPO	85	5	10	100	0	n/a
33	ACPA	55	5	0.5	100	0	n/a
34	AAPH	55	5	0.5	100	0	n/a

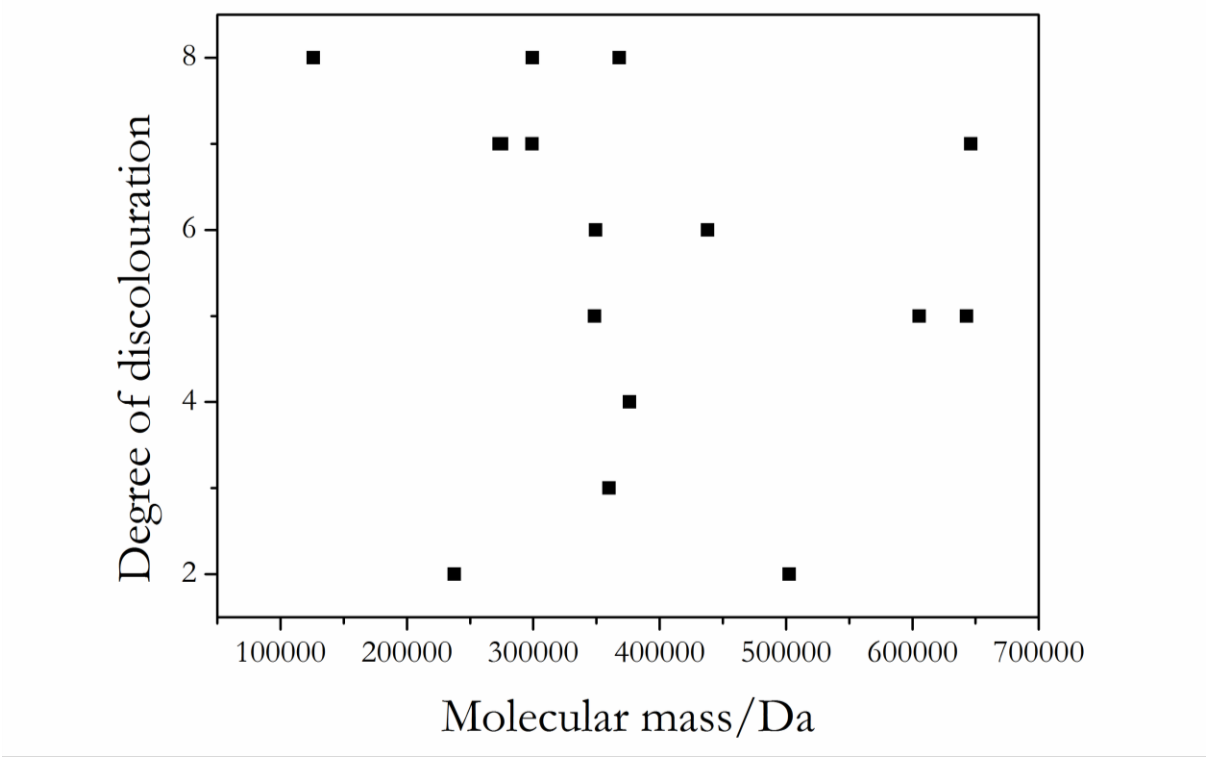

Figure 90: *Degree of discolouration of APS initiated PTFE samples as a function of the molecular mass according to Suwa's method.*

Spectroscopic results

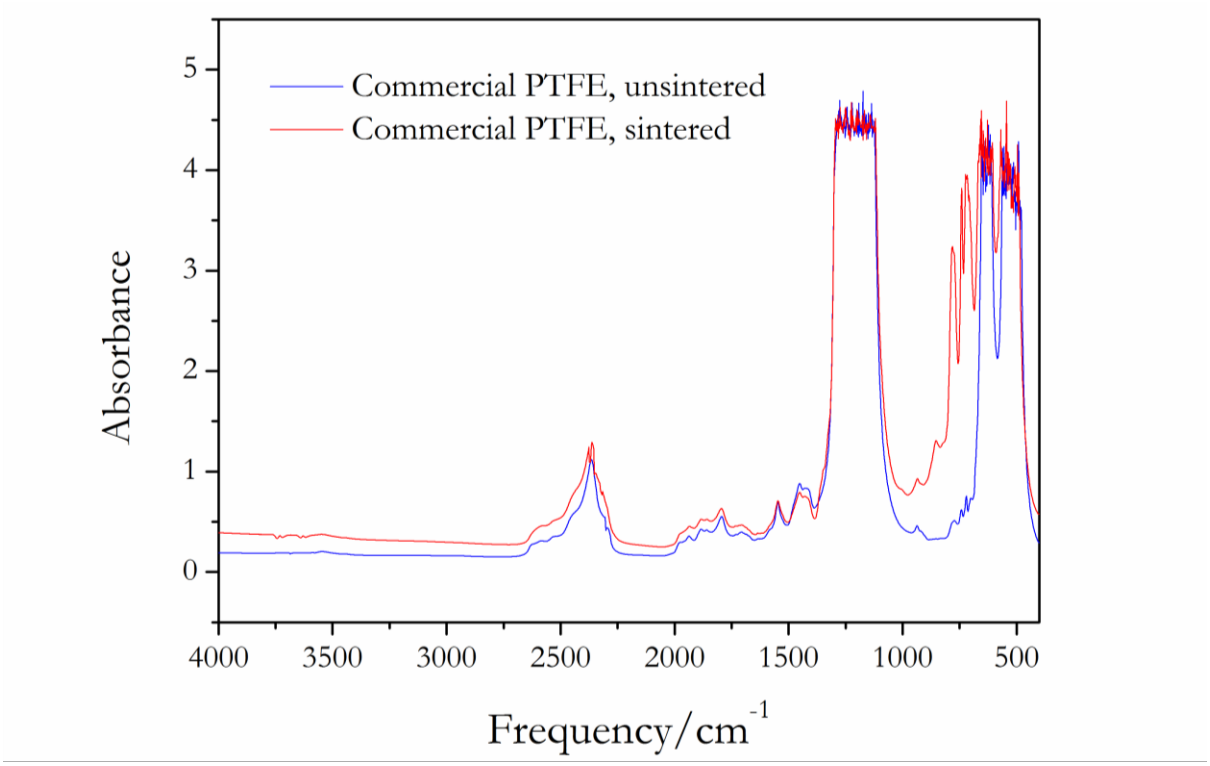

Figure 91: *Transmission FTIR spectra of unsintered and sintered commercial PTFE.*

From Figure 91 it can be seen that the structure of the commercial PTFE sample did not change upon sintering. The only change that can be seen is the increase in intensities of the peaks in the ~750 cm^{-1} region. This could be because of a change in conformation of the PTFE chains. An important point to note is that the peak at ~2450 cm^{-1}stays unchanged, which indicates that it is caused by a structural moiety and not by the alkyne end group, as previously believed. If the band were caused by alkyne end groups, the band would have disappeared or at least have lessened in intensity due to the end groups being eliminated during sintering. This confirms the proposition by Moynihan [131] that the peak at 2450 cm^{-1} is due to CF_2 overtones in the polymer chain. Commercial PTFE does not undergo a colour change upon sintering.

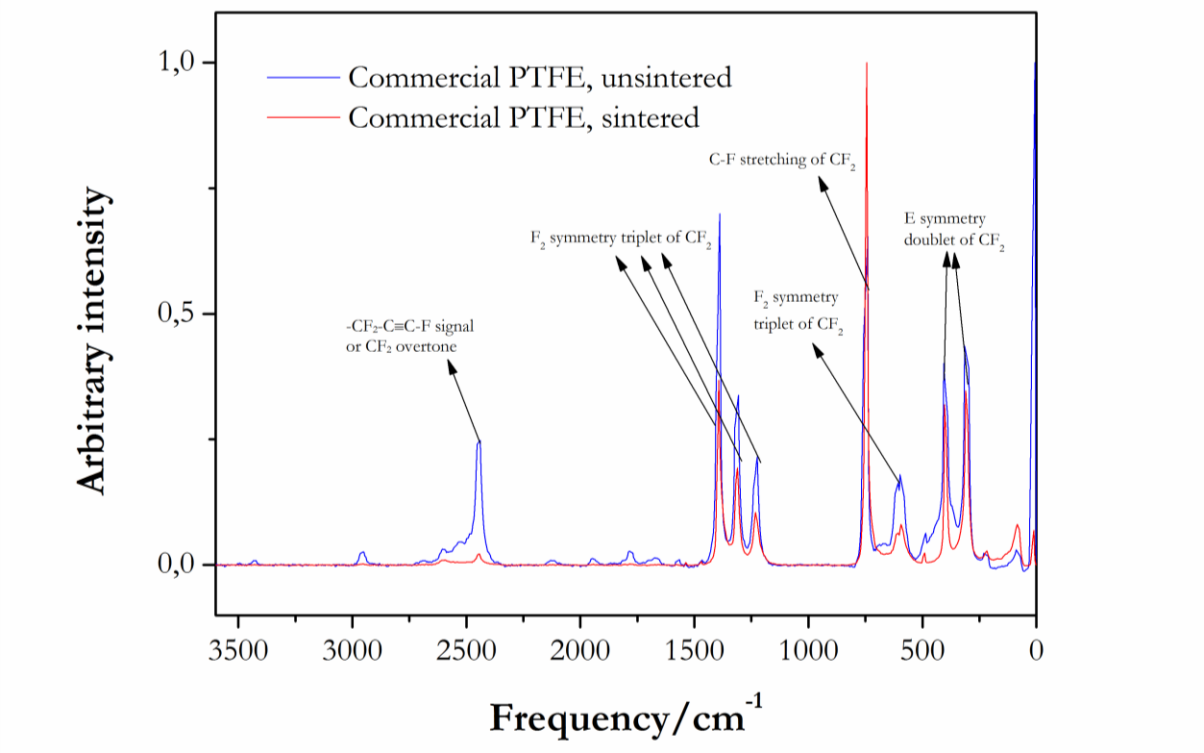

Figure 92: *Overlaid Raman spectra of commercial PTFE, pre-and post-sintering.*

From Figure 92 it can be seen that post sintering, the intensity of the peak at ~2450 cm^{-1} has significantly decreased, while the PTFE structural peaks' intensity have increased. This indicates that the change in the band at ~2450 cm^{-1} can be assigned to a change in the macro-structure, such as a change in the crystallinity of the polymer. There are no other changes in the Raman spectra that would suggest end groups being eliminated.

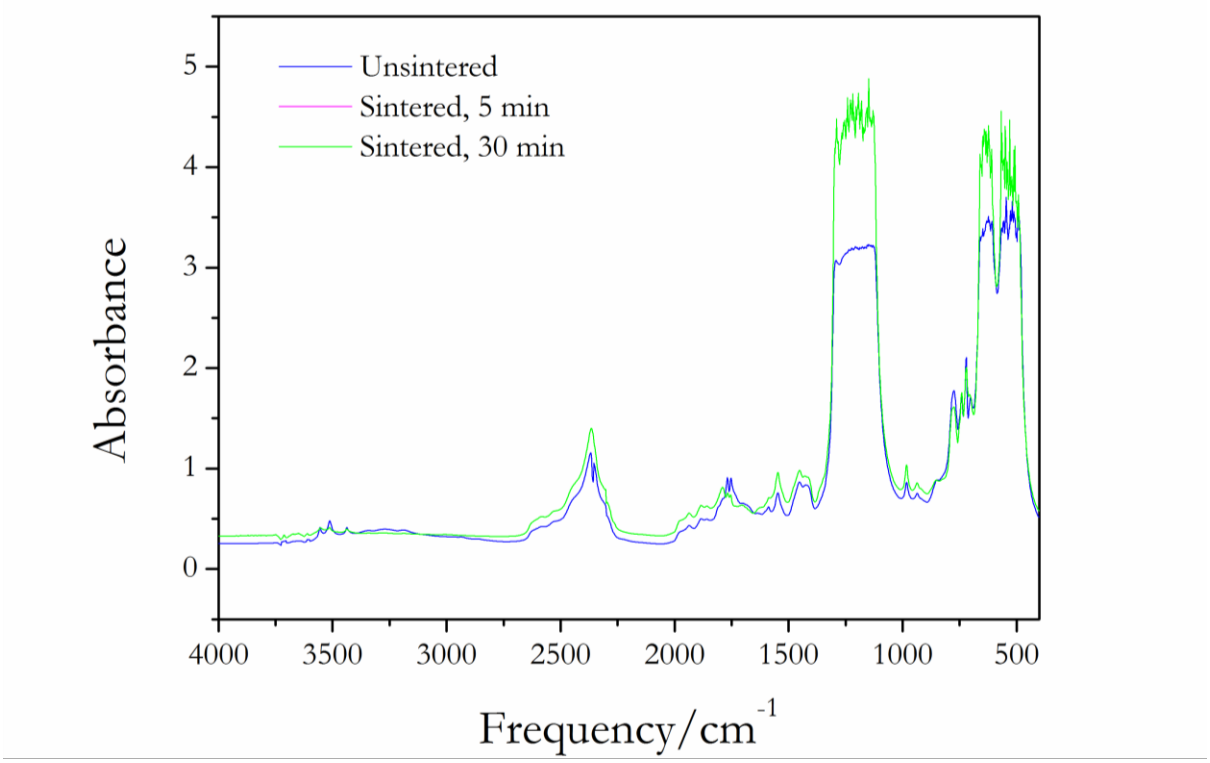

Figure 93: *Spectra of experiment 4 from Table 5, pre-sintering and after being sintered for 5 min and 30 min respectively.*

From Figure 93 some differences in the structure of the APS initiated PTFE sample pre- and post-sintering can be inferred. Firstly the three small peaks in the region of ~3500 cm^{-1} are still present, but their concentration seems to have decreased slightly. The peak at 1775 cm^{-1} which indicates COOH groups, changes in intensity, which could signify a change in concentration. This could be an indication of COOH groups reacting and being replaced by another group. The peak intensity seems to decrease the longer the sample was sintered, which supports the notion that at the increased temperature, the COOH groups are being removed *via* a reaction. Similar to the COOH peaks, the peaks indicating $CONH_2$ groups (1587cm^{-1} and 1768 cm^{-1}) also decrease in intensity. This would suggest that they are also experiencing a reaction. However, no new peaks appear at 1784 cm^{-1} or 1884 cm^{-1}, which suggests the COOH and $CONH_2$ groups are decomposing into something other than perfluorovinyl groups or acyl fluoride groups respectively. Either this, or the concentration of these newly formed groups is so low that it is not being picked up by the instrument or being masked by the other spectra.

This APS initiated sample experiences significant discolouration post sintering, going from a light yellow colour pre-sintering to very dark brown post-sintering.

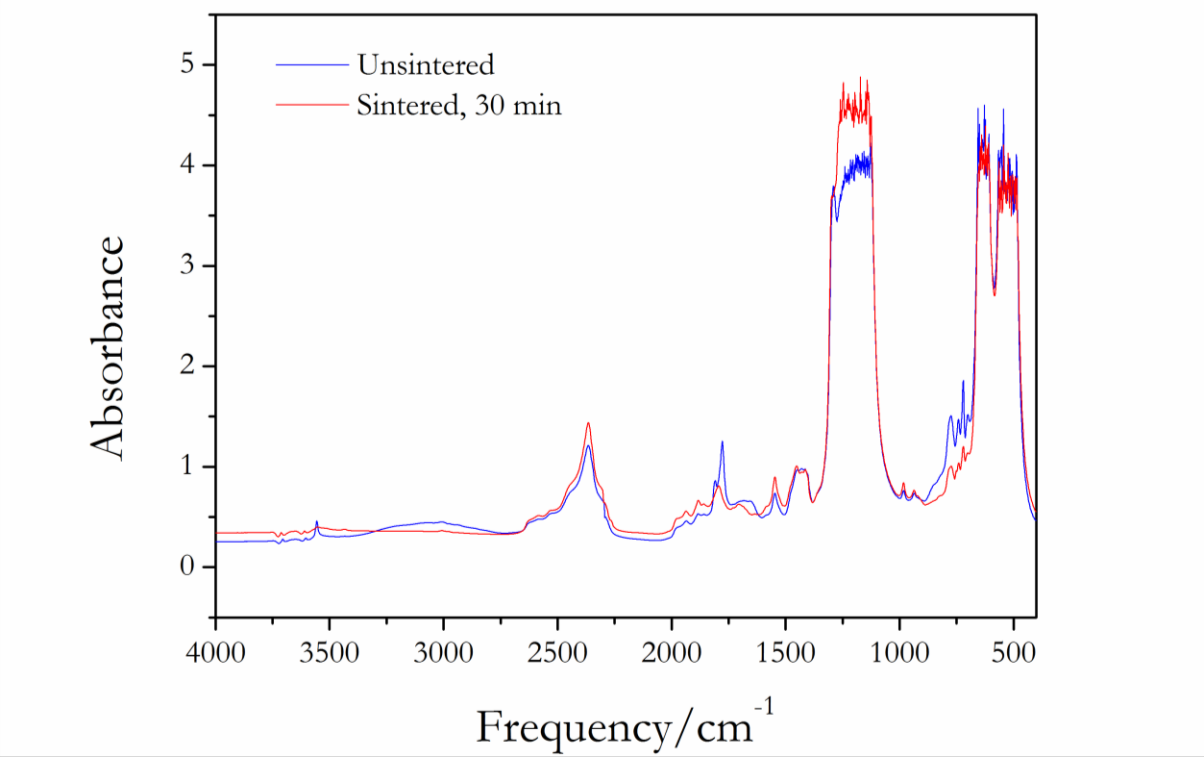

Figure 94: *Overlaid spectra of APS initiated PTFE with no buffer, pre- and post-sintering.*

Interestingly, the peaks at 3557 cm^{-1}, 1810 cm^{-1} and 1775 cm^{-1} seem to disappear or decrease in intensity post-sintering, which would suggest the decomposition of COOH groups. There appears to be a slight increase in the intensity of the peak at 1884 cm^{-1}, which could suggest some of the COOH groups have decomposed to COF groups. Other than that the structure appears unchanged.

The sample was white pre-sintering and experienced some discolouration post-sintering, with most of the polymer matrix being white but with brown spots interspersed throughout.

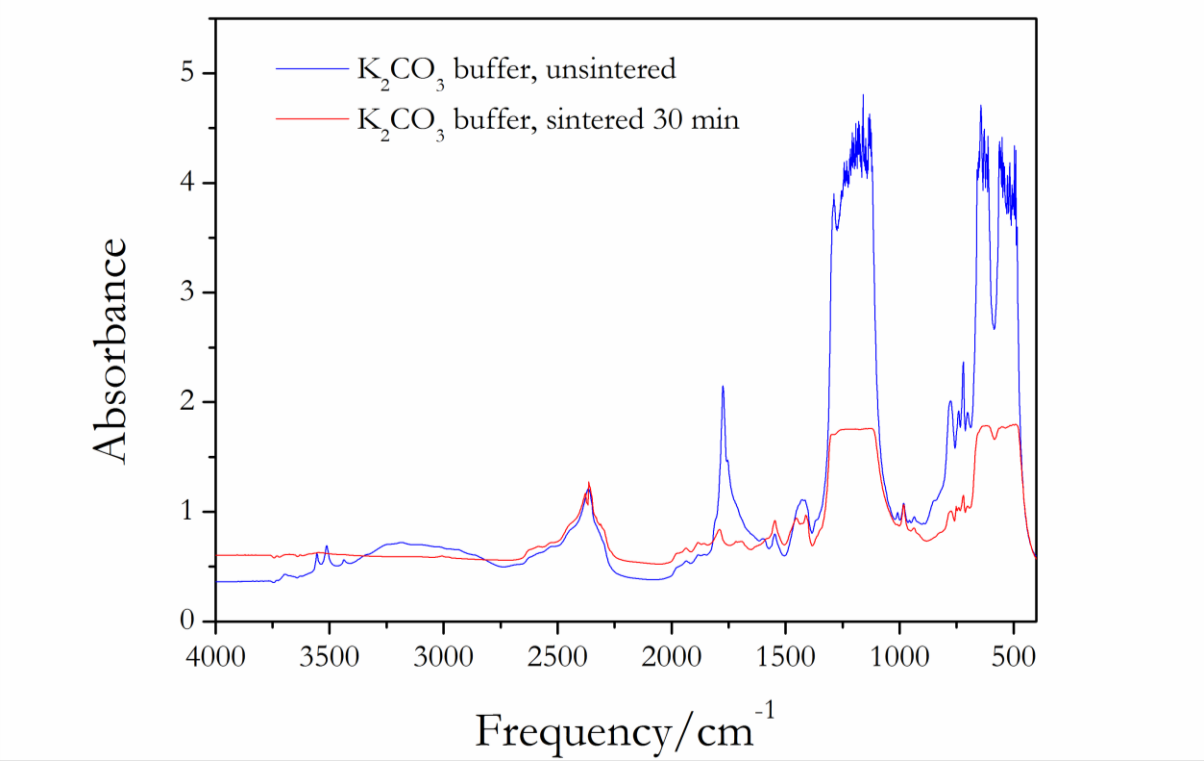

Figure 95: *Overlaid spectra of APS initiated PTFE where K_2CO_3 was used as buffer instead of borax, pre- and post-sintering.*

There are many differences between the spectra of the unsintered and sintered samples in this case, as can be seen in Figure 95. Starting from the left and moving towards the right, the first obvious difference is the absence of the three small peaks around 3500 cm^{-1} in the sintered sample. This could indicate that the COOH and $CONH_2$ groups are not present in the sintered sample, meaning they must have been eliminated at the elevated temperatures.

It also appears that the COOH indicative peak at 1775 cm^{-1} has disappeared and a small new band appears at 1790 cm^{-1}. This band was possibly present pre-sintering but was masked by the intense band at 1775 cm^{-1}. Then lastly, the somewhat broad peak at 1430 cm^{-1} seems to have split into two peaks at 1411 cm^{-1} and 1452 cm^{-1}.

The sample underwent significant discolouration from a slightly off-white colour pre-sintering to a mild brown colour post sintering.

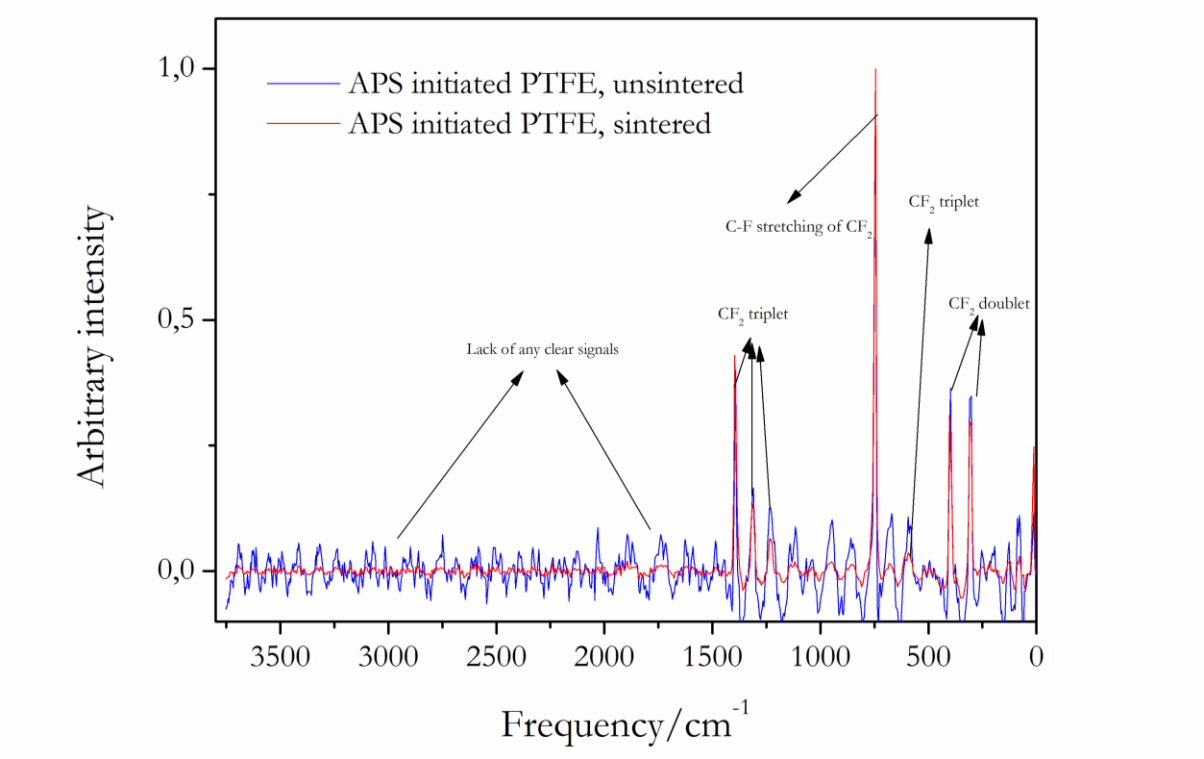

Figure 96: *Overlaid Raman spectra of APS initiated PTFE, pre-and post-sintering.*

From Figure 96 it is clear that even the sintered version of the APS initiated PTFE delivers very noisy spectra. This is strange, as most of the other in-house produced PTFE samples delivered very smooth spectra post-sintering. It is difficult to discern much from this spectra, but what can be surmised is that the PTFE structural peaks all seem to be unchanged. From this it can be deduced that the chains are unchanged by sintering. No information regarding the end groups can be gathered from this Raman spectra.

Usable Raman spectra could not be obtained for the samples that used no buffer and K_2CO_3 as buffer.

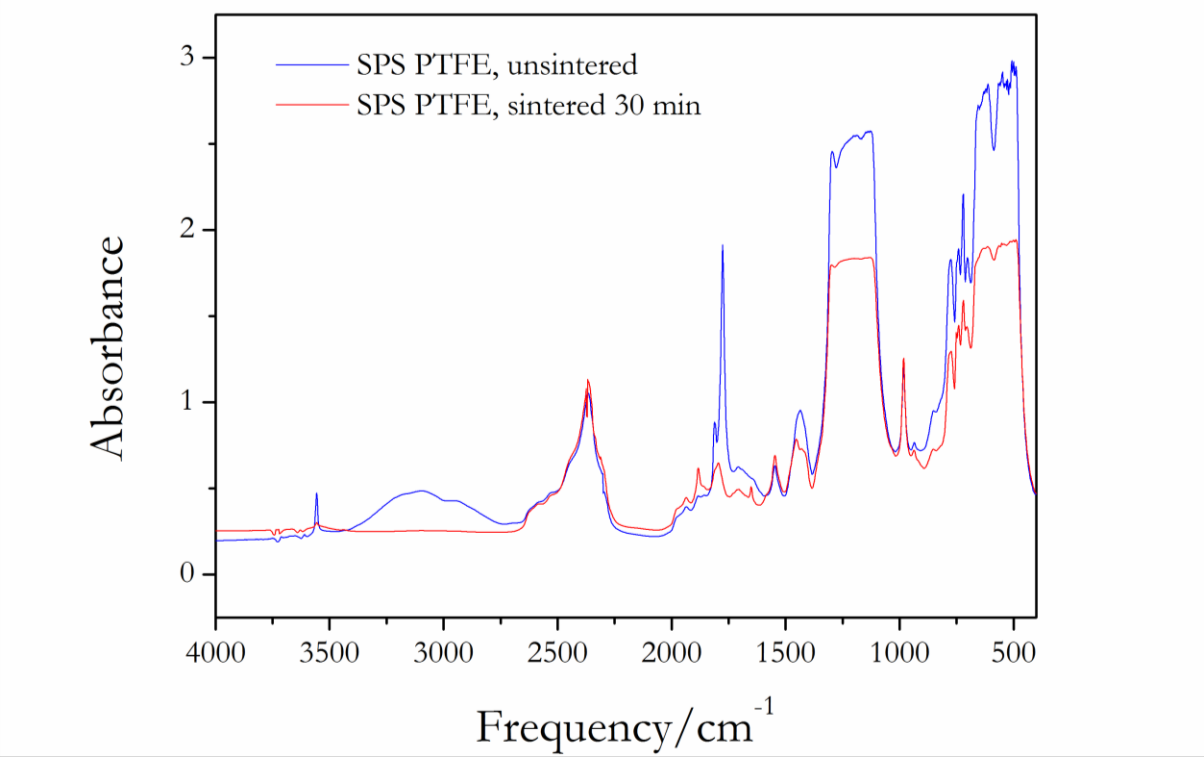

Figure 97*: Overlaid spectra of sodium persulfate initiated samples, pre- and post-sintering.*

Interestingly, no colour change takes place with this sample upon sintering. With regard to the FTIR spectra, seen in Figure 97, observing from left-to-right, the following changes take place post sintering: Firstly the sharp peak at 3557 cm^{-1} significantly lessens in intensity, but is still present, indicating a decrease in the concentration of COOH groups. The broad peak between 3400 cm^{-1} and 2800 cm^{-1}, which indicates the OH groups that are part of the COOH groups, disappears. Another peak at 1882 cm^{-1} seems to appear post sintering where before there was none. This new peak at 1882 cm^{-1} indicates the formation of acyl fluoride (COF) groups. Two well-defined peaks at 1811 cm^{-1} and 1775 cm^{-1} disappear. This supports the notion that the COOH groups have decomposed to COF. Next a small peak appears at 1650 cm^{-1} which was absent before. Lastly, the broad peak at 1436 cm^{-1} seems to retain its broad shape, while gaining an additional peak at 1454 cm^{-1}. Other than this, there do not seem to be any appreciable changes.

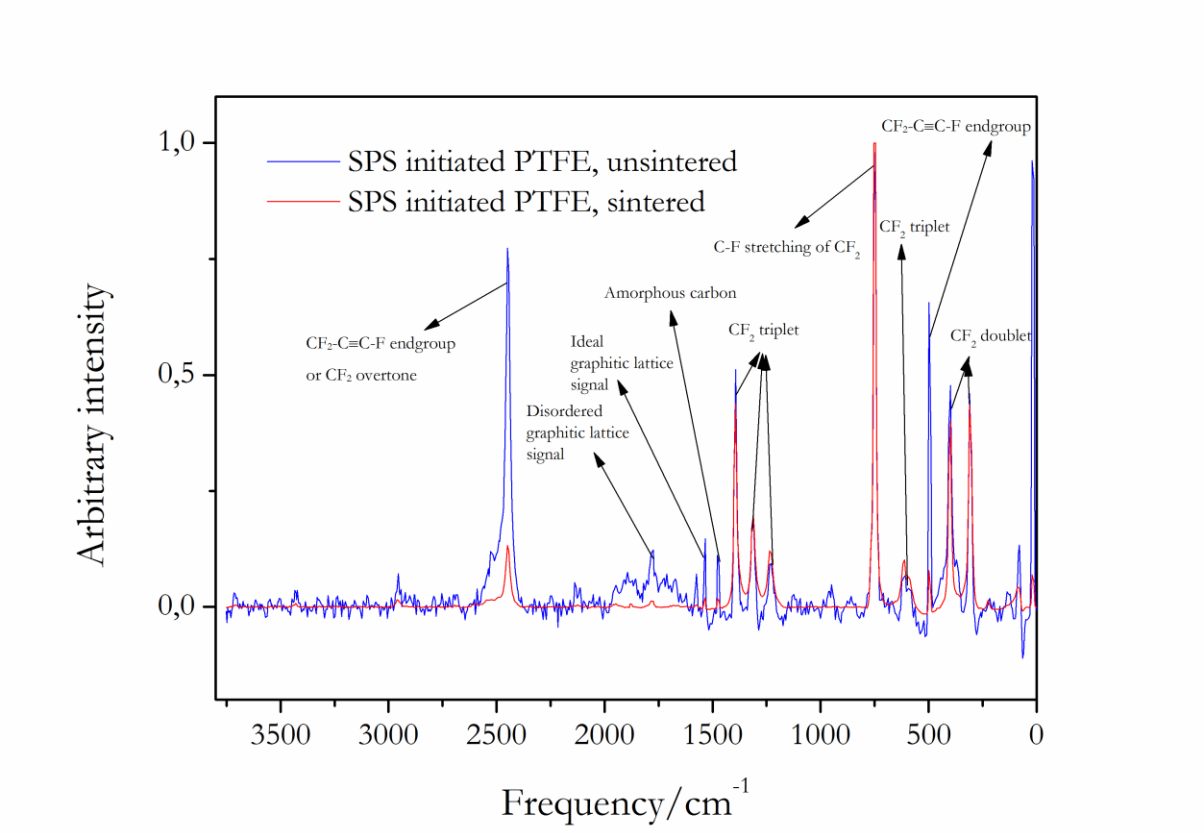

Figure 98: *Overlaid Raman spectra of SPS initiated PTFE, pre- and post-sintering.*

Figure 98 shows some interesting results. Apart from the obvious increase in intensities of the sintered sample, the bands that correspond to carbonaceous material seem to have disappeared. This is likely because the increased intensities of the other signals have made the carbon signals very small and therefore very difficult to spot on this scale. Other than this there appears to be no difference between the spectra. However, when it is taken into account that the sintered sample's intensity has increased dramatically, the peak at 2450 cm^{-1} has not increased concurrently. If the ratio between this peak and the PTFE structural peaks had stayed the same, this peak should have stretched to a relative intensity of approximately 1200. Other than this there appears to be no noticeable change to the Raman spectra post-sintering, which indicates that the PTFE chain structure is unchanged.

The spectra of two $KMnO_4$ initiated samples are shown in Figure 99 and Figure 100.

Figure 99 shows the overlaid spectra for unsintered and sintered samples initiated with 10 % $KMnO_4$. The virgin sample is transparent and white and did not discolour upon sintering. The first difference one notices here is the absence of the broad band between 3400 cm^{-1} and 2650 cm^{-1}. This indicates the absence in the sintered sample of hydroxyl groups. There is also a significant

reduction in the peak at ~1650 cm^{-1}. Furthermore, except for some small changes in intensity for certain peaks, the spectrum is largely unchanged.

The 30 % $KMnO_4$ sample, whose FTIR spectra is shown in Figure 100, experienced significant discolouration upon sintering, going from a slightly off-white colour to black after 30 min of sintering. There are only a few differences between the spectra of the unsintered and sintered 30 % $KMnO_4$, but these differences are significant, as can be seen in Figure 100. Firstly the broad band from ~3500 cm^{-1} to 3000 cm^{-1} disappears, indicating the absence of OH groups in the sintered sample. Secondly the single CF_2 overtone peak at 2350 cm^{-1} splits into a doublet. Then a very obvious difference is the disappearance of the intense, broad peak at ~1650 cm^{-1}. Lastly, the peaks at 1366 cm^{-1} and 805 cm^{-1} disappear in the sintered sample.

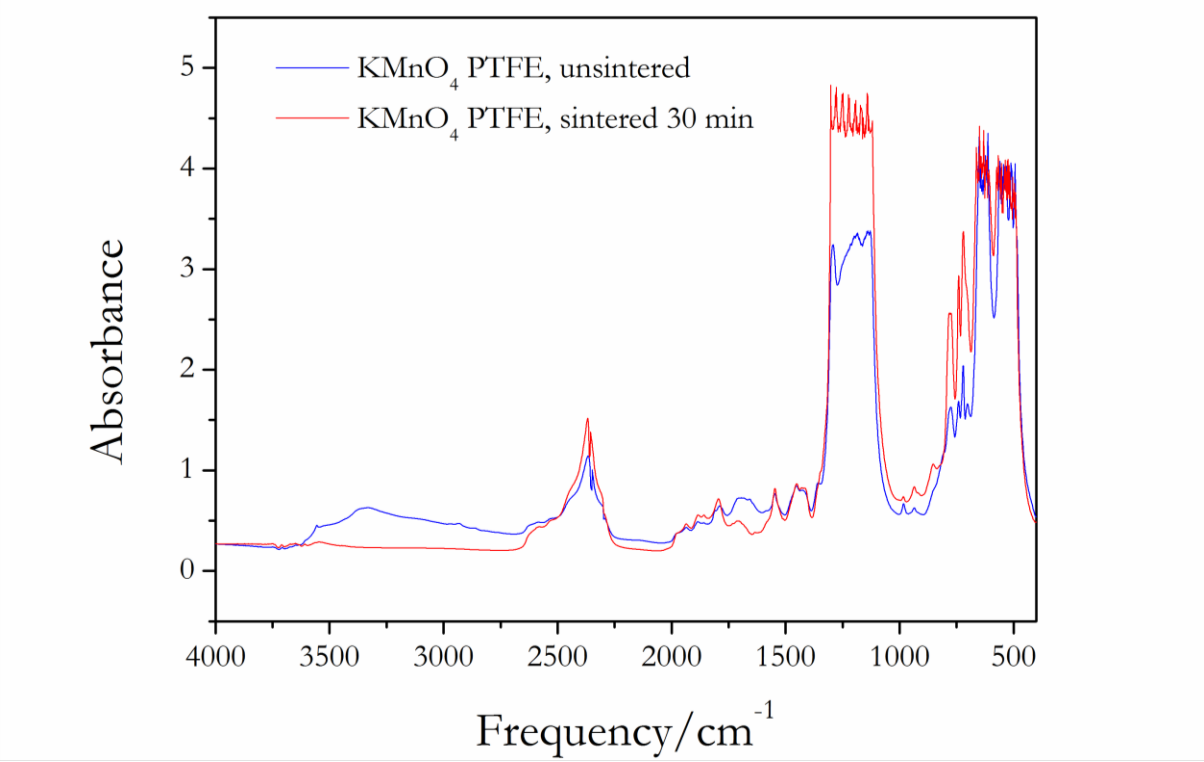

Figure 99: *Overlaid spectra of 10 % $KMnO_4$ initiated samples, pre- and post-sintering.*

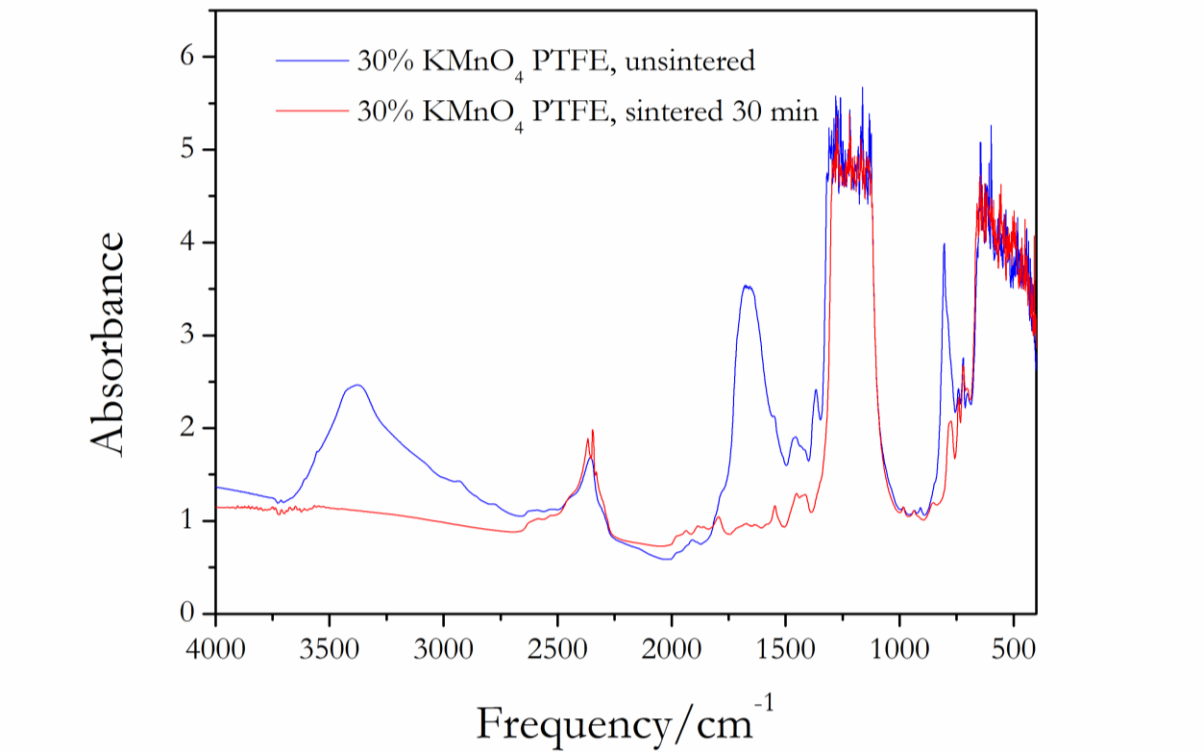

Figure 100: *Overlaid spectra of 30 % $KMnO_4$ initiated samples, pre- and post-sintering.*

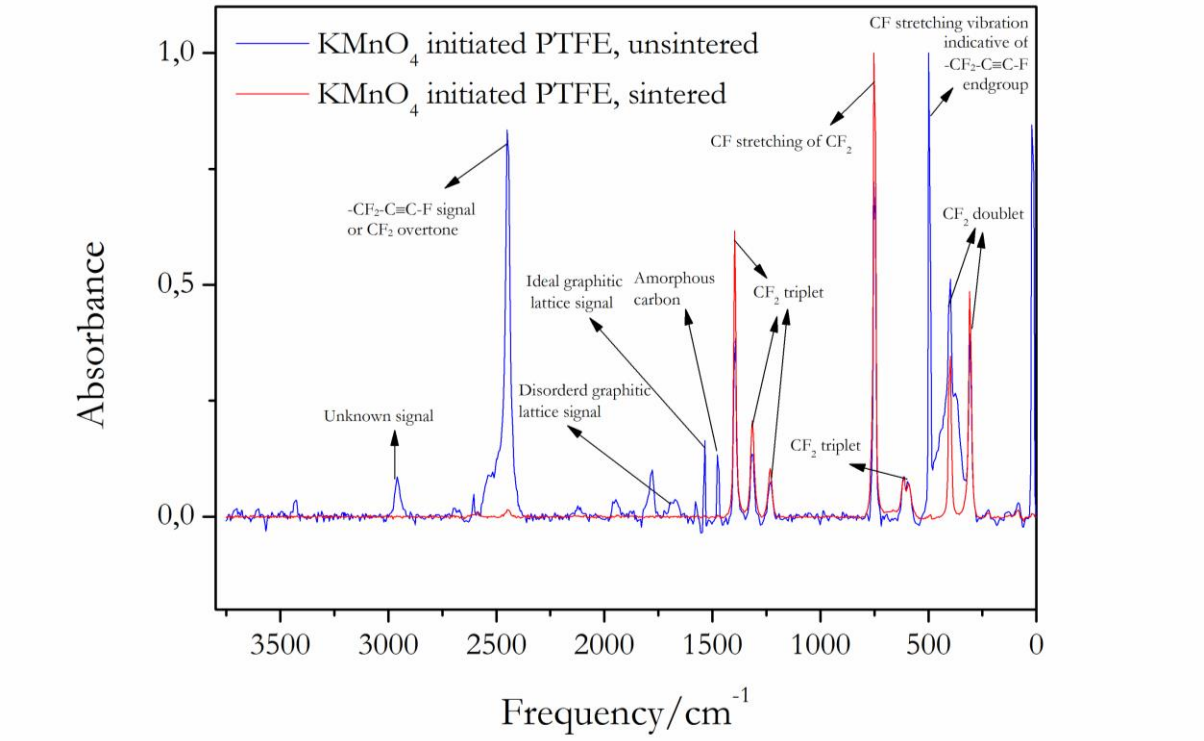

Figure 101: *Overlaid Raman spectra of $KMnO_4$ initiated PTFE, pre- and post-sintering.*

Figure 101 shows the expected sharp increase in intensities of the structural PTFE peaks and the decrease, or in this case, the almost complete disappearance, of the peaks at 2450 and 500 cm^{-1}

which were previously thought to have indicated alkyne end groups. It now seems that the disappearance of these peaks is indicative of a conformational change that PTFE undergoes during sintering. Other than this, there are no noticeable changes in the Raman spectra of the sample.

The sintered DTBP samples could not be analysed by FTIR because they melt when subjected to the sintering temperature of 380 °C and get stuck to the crucible in which they are placed. Sintering was attempted at a lower temperature of 340 °C, but the same problem ensued. Lowering the temperature further was not an option, as 340 °C is the lowest point at which sintering has been reported to have been implemented. The samples all had an off-white colour pre-sintering and did not experience any discolouration post-sintering.

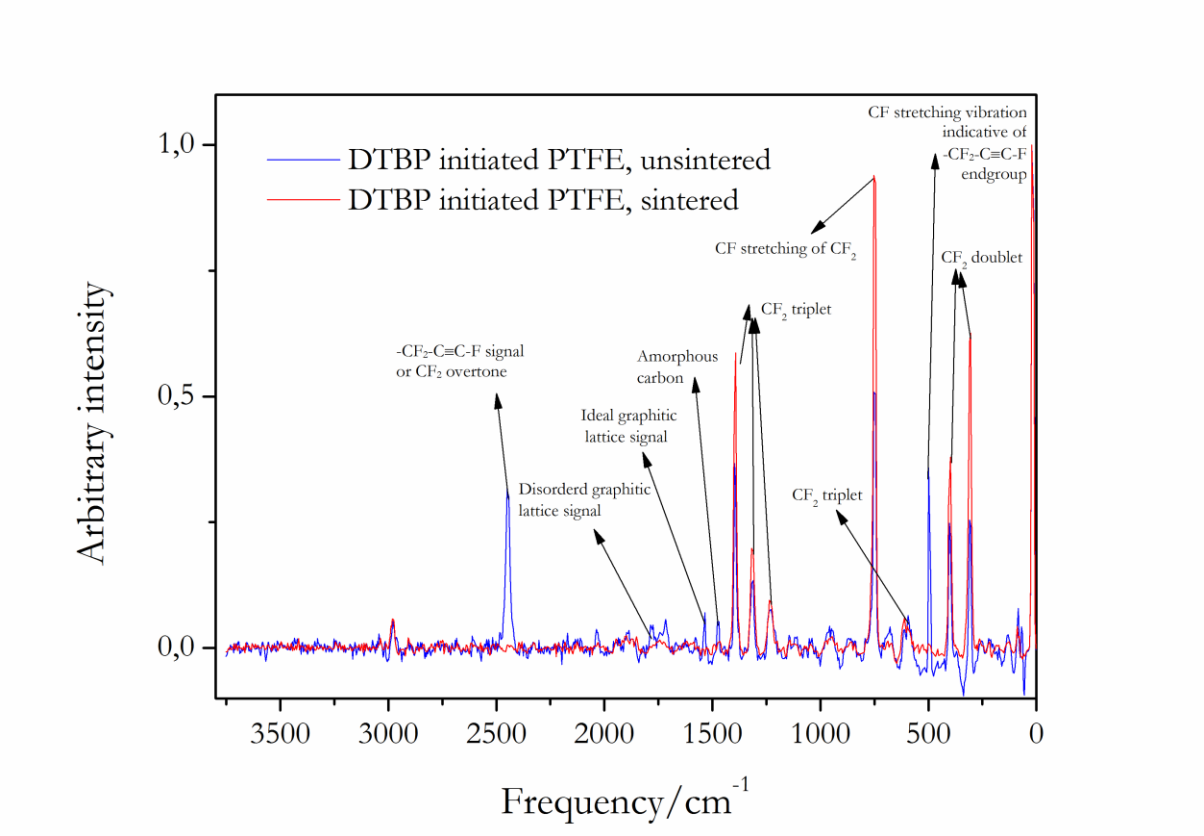

Figure 102: *Overlaid Raman spectra of DTBP initiated PTFE, pre- and post-sintering.*

Figure 102 shows the same expected increase in intensity of PTFE structural peaks and the disappearance of the peak at 2450 cm^{-1} which indicates the previously discussed conformational change. No new peaks that would indicate the structure of the newly formed end groups are apparent.

Summary

The IR and Raman spectra of commercial PTFE showed evidence of acyl fluoride (COF), $CF=CF_2$ and COO^+X end-groups. After sintering it showed no changes in the structure of commercial PTFE, except for an increase in crystallinity as evidenced by an increase in intensity of the signals in the region of 700 cm^{-1}.

The IR and Raman spectra for PTFE initiated with APS indicated that the synthesised samples possessed several different end-groups. The samples synthesised with borax as buffering agent contained carboxylate, ionic carboxylate and amidic end-groups. This suggests multiple termination reactions. APS initiated samples that used potassium carbonate as buffering agent had no ionic carboxylate end-groups and no amidic end-groups. The APS initiated sample that did not include a buffering agent in the reaction also had multiple termination reactions, with the IR and Raman spectra indicating the presence of carboxylic and carboxylic salt end-groups in lower concentrations, but no amide end-groups.

The APS initiated sample that used borax as buffering agent experienced significant discolouration during sintering. The FTIR results of the sintered samples showed that the carboxylic acid and amidic end-groups were at least partially eliminated during sintering. The disappearance of two bands at ~1750 cm^{-1} and the appearance of a new signal at ~1780 cm^{-1} indicated the elimination of carboxylic end-groups and the formation of $CF=CF_2$ end-groups. Similarly, the sample where potassium carbonate was used as buffering agent underwent significant discolouration and shows no evidence of the carboxylic acid or amidic end-groups after sintering, meaning these end-groups must have undergone an elimination reaction. The sample where no buffering agent was used discoloured upon sintering, though significantly less than the other two samples. The FTIR results suggest that some of the carboxylic acid end-groups of this sample decomposed into acyl fluoride groups. The end-group assignments for the sintered samples can be seen in Table 14.

Unlike the APS initiated samples, the SPS initiated samples were a translucent white colour before sintering. After sintering, they did not experience any significant discolouration. The FTIR spectra also indicated multiple termination modes for SPS initiated PTFE. The spectra showed evidence for high concentrations of carboxylic acid end-groups, and smaller concentrations of carboxylic salt end-groups. These samples did not discolour upon sintering. The post-sinter spectroscopic results show elimination of carboxylic end-groups and the formation of acyl fluoride end-groups.

The PTFE samples initiated by low concentrations of $KMnO_4$ (1 % and 10 %) were white and translucent before sintering and did not exhibit any discolouration during sintering. This was not

the case for the high initiator concentration (30 %) sample, which blackened completely after sintering. The $KMnO_4$ initiated samples had similar end-groups to the commercial sample, with the addition of OH end-groups. The spectroscopic results of the $KMnO_4$ initiated samples showed elimination of the OH end-groups after sintering. It is unclear which end-groups formed after this elimination, because no new peaks were present in the spectroscopic results after sintering.

The spectroscopic results of the DTBP initiated samples indicated the presence of tertiary butyl end-groups and the absence of carboxylic acid and carboxylic salt end-groups. The DTBP initiated samples showed little to no discolouration during sintering, which indicated the tertiary butyl end-groups were stable and not easily eliminated at elevated temperatures.

The FTIR and Raman spectra indicate that there are no moieties which could correspond to a conjugated p-orbital system. It seems the terminal structures are the same for both uncoloured samples and samples which exhibited pronounced discolouration. This indicates that the end-groups themselves are not the cause, or at least, not the sole cause of the discolouration of PTFE.

There exists a possibility that the elimination reactions which occur during sintering produce chromophoric compounds that are not part of the PTFE chains, but are trapped in the PTFE matrix and thus give rise to the discolouration.

Table 14: *Initiators used in PTFE syntheses and subsequent end-groups after sintering.*

Initiator	**Exp. #**							
End-groups		-COOH	$-COO^+X^-$	$-CONH_2$	-C≡C-F	$-COC(CH_2)_2$	OH	-CFO
Commercial	-				✓			
APS	1, 4-17	✓						✓
SPS	18, 19	✓						✓
$KMnO_4$	20-22						✓	
DTBP	23-25							

The commercial PTFE sample did not exhibit any mass loss up to the bulk decomposition temperature. Importantly, the TGA-curves for commercial PTFE did not exhibit any evidence for post-pyrolysis residues. The APS initiated samples did not show any residual masses until an initiator ratio of 30 %. Similarly, for SPS initiated PTFE, some post-pyrolysis residual mass remained in the crucible up to approximately 800 °C. At an initiator ratio of 30 %, the $KMnO_4$ initiated samples exhibited a residual mass of over 20 %. This residual masses remained

approximately constant up to 1000 °C. When the gas was switched to oxygen, the residual mass rapidly disappeared.

A TGA experiment was conducted for PTFE initiated with 30 % $KMnO_4$ in which the run was stopped at approximately 800 °C. Visual inspection of the crucible revealed a black, glassy substance. This observation, along with the previously discussed disappearance of the mass under oxygen at 1000 °C suggested that the substance was carbon. Due to the fact that no evidence of graphitic or diamond-like signals in the Raman spectra was found, it is assumed that it was amorphous carbon that formed. There exists a possibility that the residue may be manganous, but none of the oxides of manganese which are stable up to 1000 °C will evaporate upon exposure to oxygen at that temperature [153].

There exists some correlation between the ratio of initiator and the post-pyrolysis residual mass, evidence for this can be seen in Figure 103. There exists also some correlation between the degree of discoloration and the post-pyrolysis residual mass. This can be seen in Figure 104.

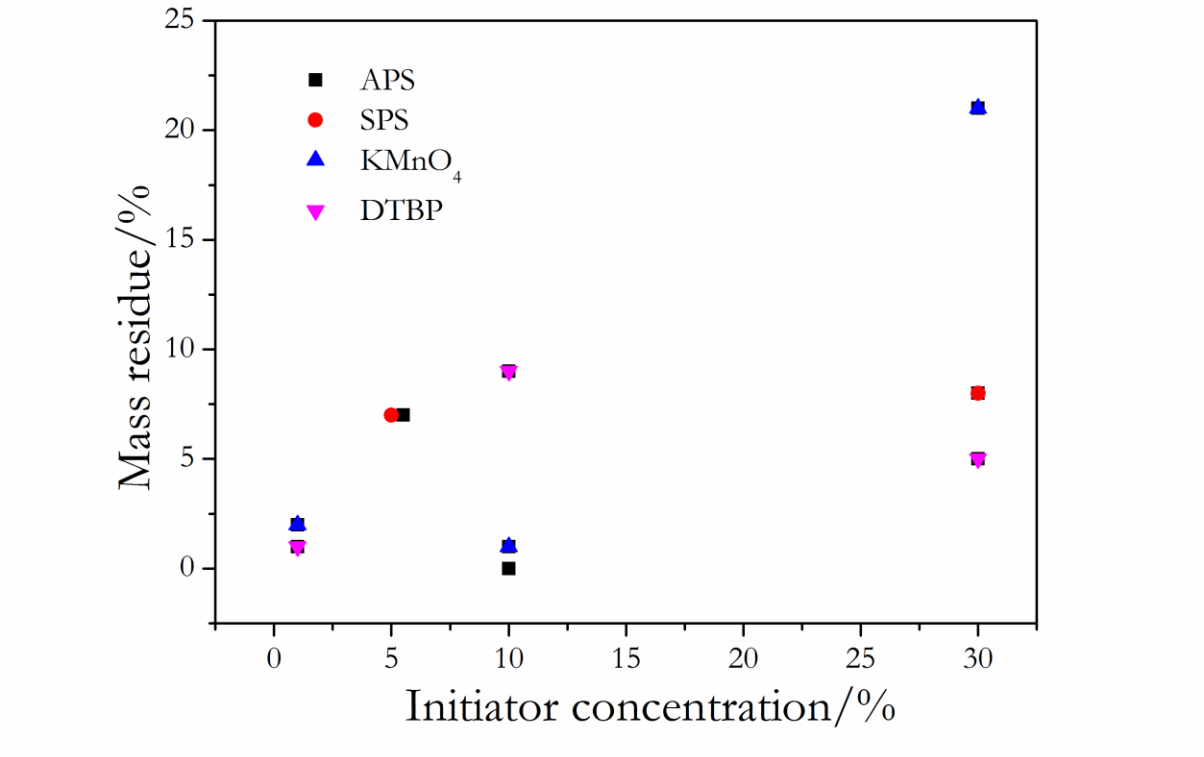

Figure 103: *Mass residue of samples after TGA analysis as a function of initiator concentration.*

These results seem to indicate that the discolouration of PTFE during sintering is due to the deposition of non-volatile elimination products within the polymer matrix. The mass of residue is insufficient for further analysis by XPS or SEM-EDX, but the thermogravimetric behaviour seems to indicate that this residue is amorphous carbon. No mechanism can yet be proposed to explain

how elemental carbon can form from the end-groups observed in PTFE that may undergo elimination.

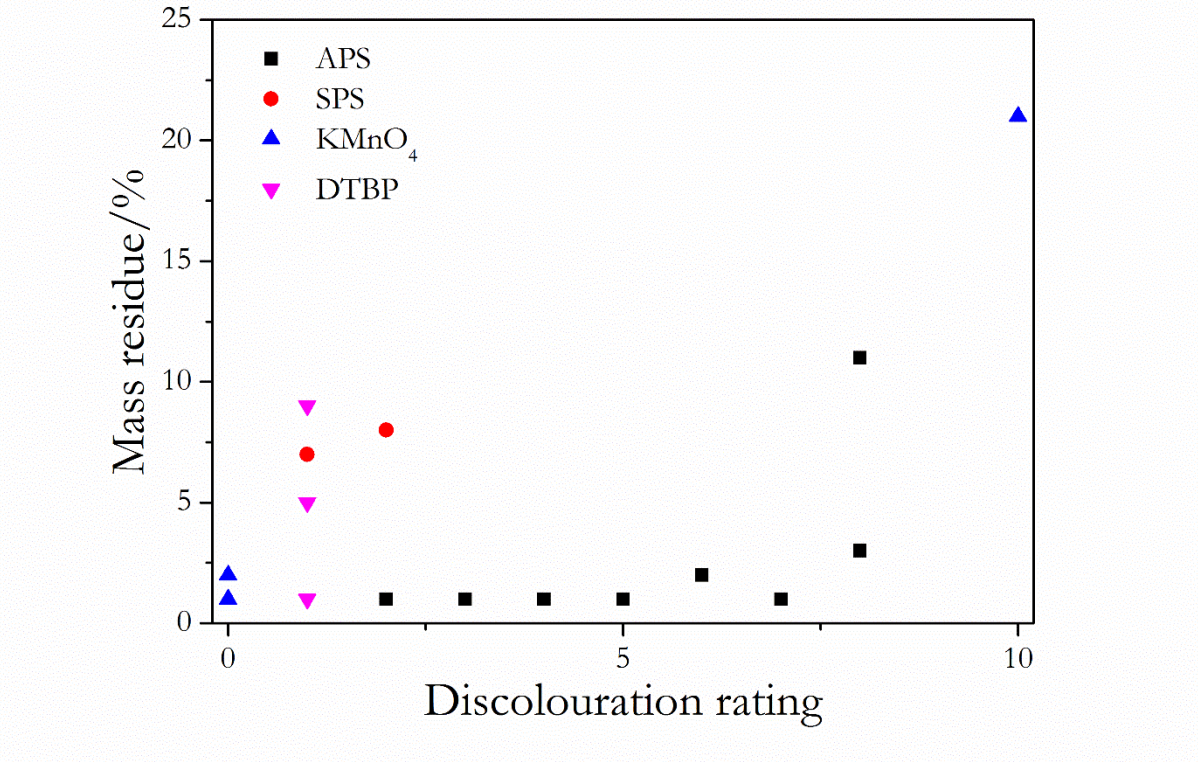

Figure 104: *Discolouration of samples as a function of the mass residue left over after TGA analysis.*

4.2.2 Photoinitiated PTFEs

Discolouration

Generally, the photoinitiated PTFEs showed little to no discolouration after sintering, which indicates that high molecular weight polymers were formed by this polymerisation method.

The photoinitiated APS sample showed discolouration similar to that of the thermally initiated APS PTFE samples, albeit to a lesser extent. The H_2O_2 initiated sample showed no discolouration upon sintering.

Spectroscopic results

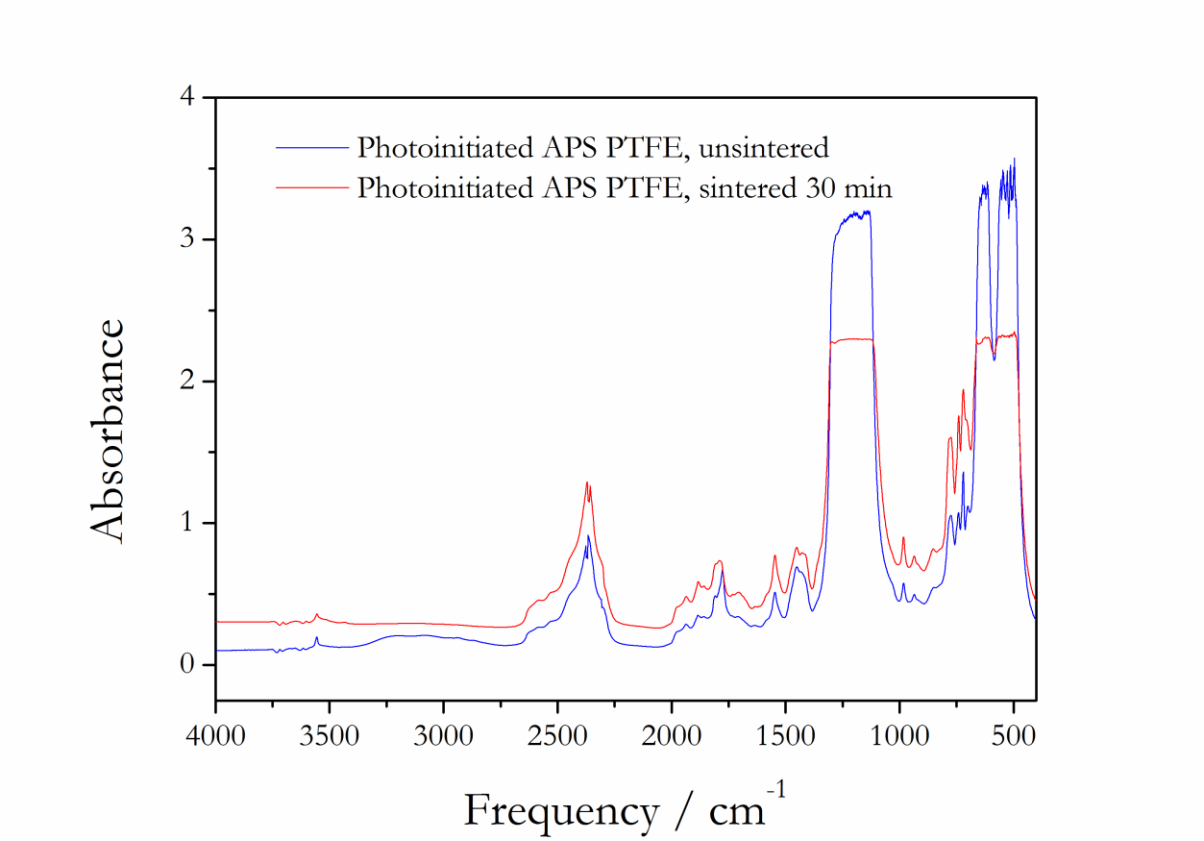

Figure 105: *Overlaid spectra of unsintered and sintered photoinitiated PTFE, using APS as initiator.*

Other than an increase in intensities across the spectrum, no easily discernible differences are visible in the spectra comparing unsintered and sintered APS photoinitiated PTFE shown in Figure 105. The peak indicating COOH groups at 3557 cm^{-1} is still present but has decreased slightly in intensity, which suggests that some of the COOH groups were decomposed by sintering.

Similarly to the photoinitiated APS PTFE samples, only some changes in intensities can be observed from the spectra of H_2O_2 initiated PTFE that can be seen in Figure 106.

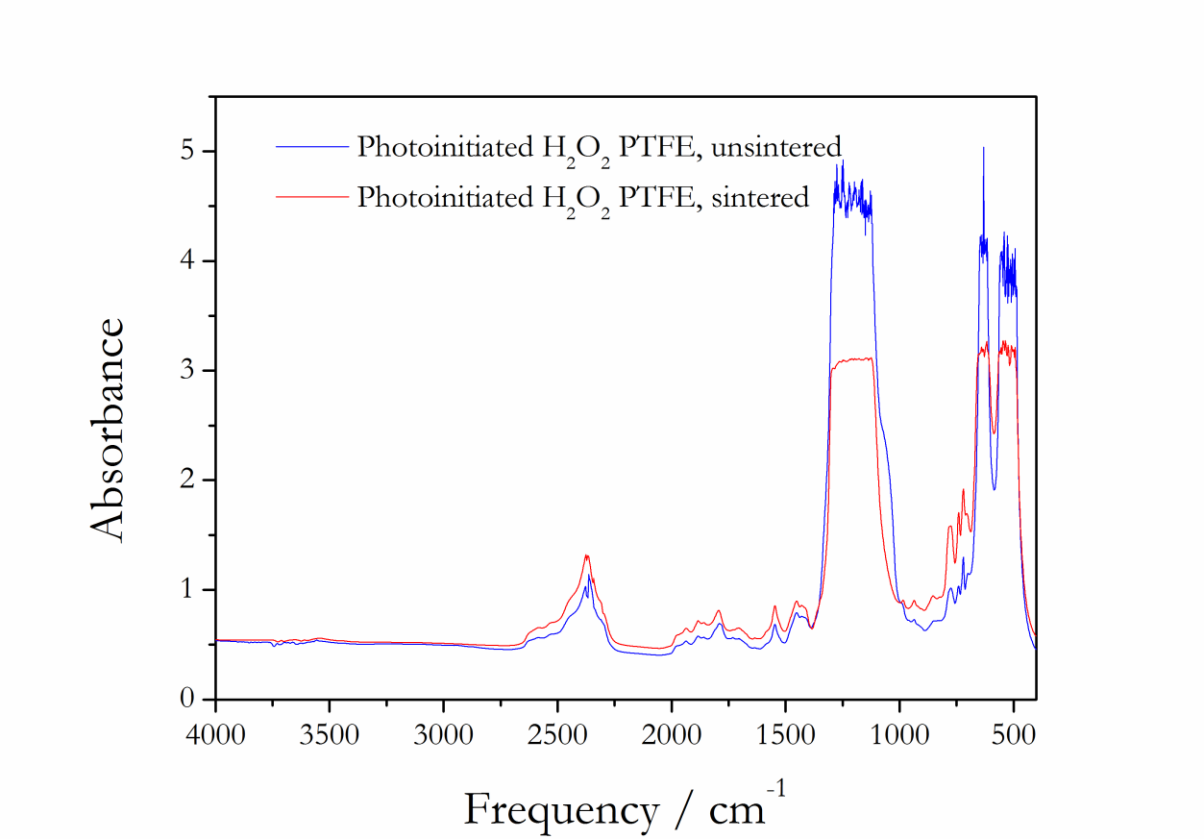

Figure 106: *Overlaid spectra of unsintered and sintered photoinitiated PTFE, using H_2O_2 as initiator.*

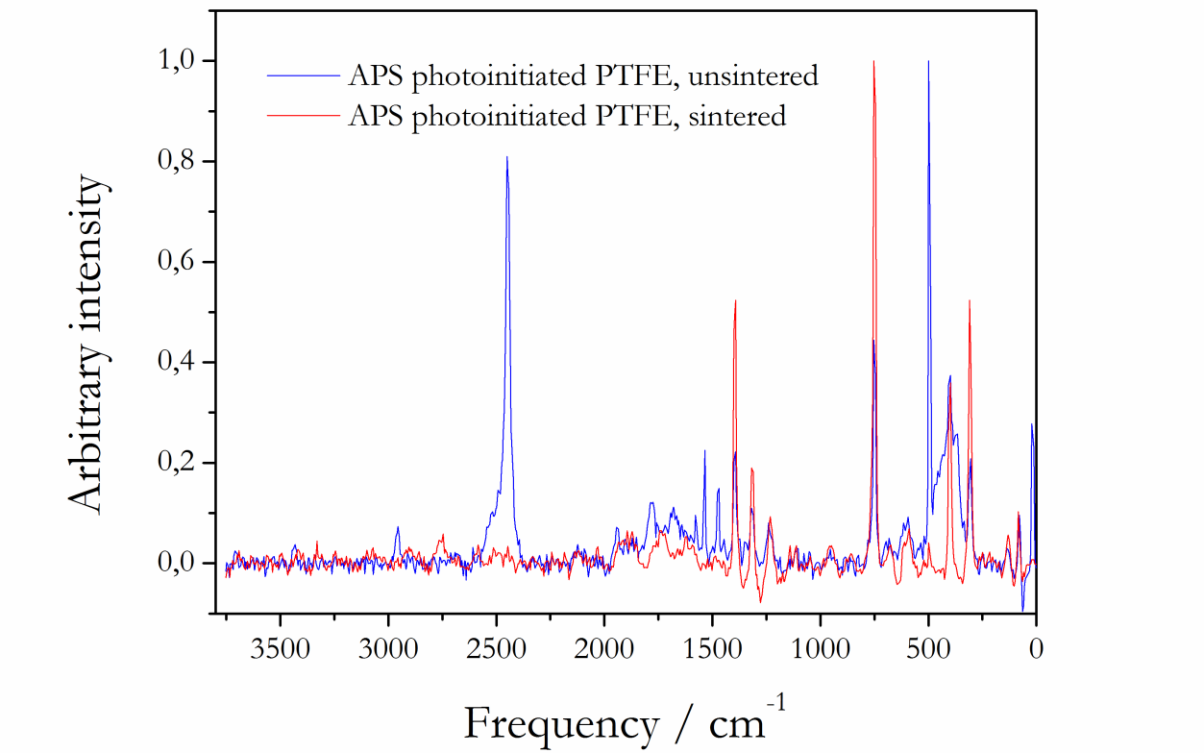

Figure 107: *Comparative spectra of APS photoinitiated PTFE, pre- and post-sintering.*

Figure 107 shows for comparison the spectra of pre-and post-sintered photoinitiated APS PTFE. Similarly to the previous examples, the peak at 2450 cm^{-1} disappears post-sintering. This indicates the conformational change as previously discussed.

Figure 108 shows for comparison the spectra of pre-and post-sintered photoinitiated H_2O_2 PTFE. The Raman spectra here is a prime example of the unsintered sample being rather *noisy*, whereas the sintered sample shows a much smoother spectra. What is interesting about this sample's spectra, is the apparent absence of the peak at 2450 cm^{-1} in the unsintered sample's spectra and the appearance of this peak in the sintered sample's spectra.

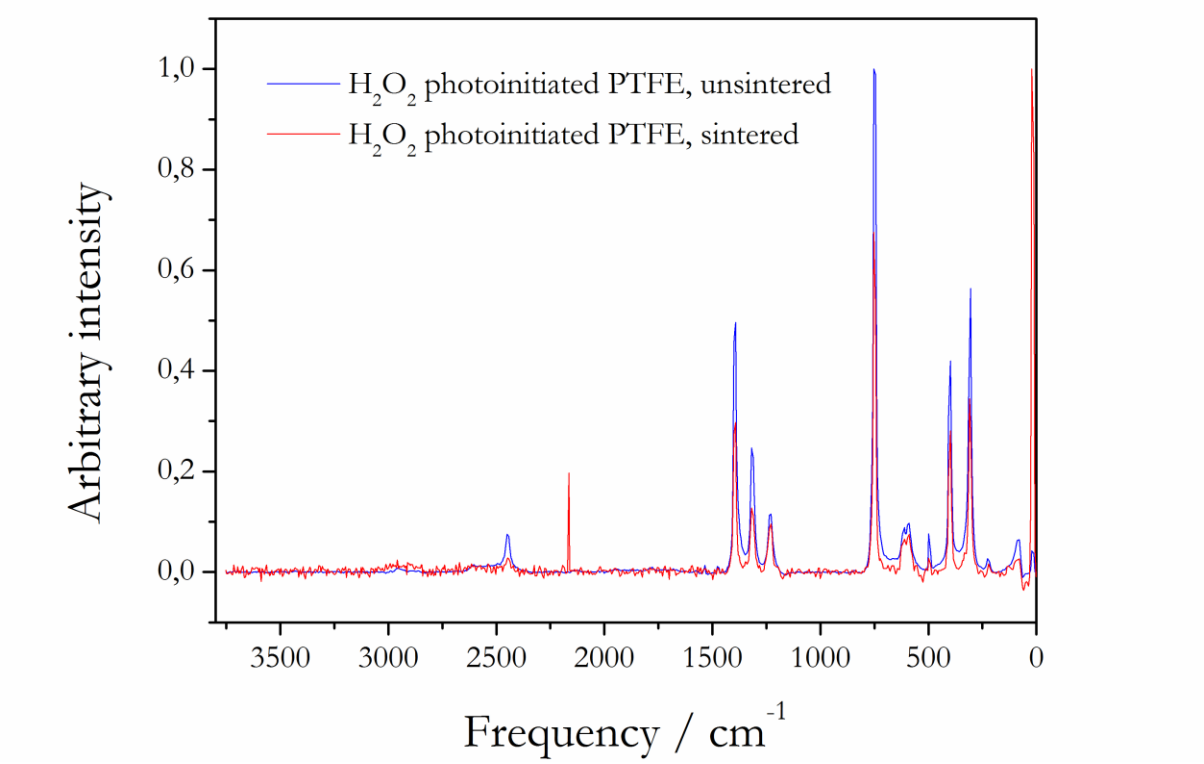

Figure 108: *Comparative spectra of H_2O_2 photoinitiated PTFE, pre- and post-sintering.*

Once again this comes down to the intensities of the peaks relative to each other. Upon closer inspection of the unsintered sample's spectra, there is a very small peak at 2450 cm^{-1} which is masked by *noise*. In the sintered sample's spectra, there is very little to no *noise*, so the peak is much more visible. As with all the previous examples, the intensity of the sintered sample is much greater than the unsintered sample, which also helps to make the peak that much more visible. The presence of the peaks at 2450 and 500 cm^{-1} in the sintered sample suggest that post-sintering no conformational change has taken place. This sample did not experience any discolouration whatsoever post-sintering. It is also believed to be of very high molecular mass. This leads to the

question of whether the molecular mass somehow influences the polymer's ability to undergo the conformational change at elevated temperatures and whether this has an effect on discolouration.

Summary

The photoinitiated APS sample showed discolouration, but to a lesser extent than the thermally initiated samples. This may be due to the lack of a buffering agent in this experiment. No noticeable changes in the spectra pre- and post-sintering were apparent. Similarly to the previous samples, the Raman spectra showed a conformational change post-sintering.

No noticeable changes in the spectra pre- and post-sintering were apparent. The lack of discolouration, coupled with the fact that the Raman spectra showed no conformational change post-sintering, poses the question of whether a conformational change has an influence on the discolouration of the polymer.

4.2.3 Controlled photo-initiated polymerisations

Discolouration

None of the photoinitiated samples showed discolouration or change in their respective FTIR spectra after sintering. This coupled with the lack of residual mass after TGA analysis suggests that whatever end groups were present and eliminated during sintering were not present in high enough concentrations to deposit enough carbon into the polymer matrix to cause any discolouration of the polymer.

Since these samples showed no discolouration after sintering, spectroscopy was not performed on them.

Chapter 5
Conclusions

5.1 Thermally initiated PTFEs

The synthesised samples all had multiple termination reactions which lead to multiple end-groups forming which included: carboxylic end-groups, amide end-groups, carboxylic salt end-groups with NH_4^+ and alkyne containing end-groups. The use of different buffering agents influenced the type and concentration of end-groups that formed, subsequently influencing discolouration at sintering temperatures and indicating that the phenomenon was not solely dependent on the initiator used.

The synthesised PTFE samples underwent discolouration at temperatures of approximately 380 °C. The pressed discs discoloured noticeably at these temperatures. With a few exceptions, the lower molecular weight samples were the ones which experienced the most discolouration. This lead to the conclusion that the lower molecular weight samples experience more discolouration, because of their higher concentration of end-groups.

The spectroscopic results showed that the carboxylic end-groups decomposed into acyl fluoride and perfluorovinyl groups during sintering. The alkyne, amidic, hydroxyl and carboxylic salt groups also decomposed, though it was not clear which new end-groups formed in their place. It is believed the discolouration was caused by amorphous carbon that was deposited into the polymer matrix after being eliminated from the end-groups. This was evidenced by the fact that low molecular weight samples showed residual weight up to 1000 °C. Once exposed to oxygen at this temperature, this mass quickly disappeared, indicating that this was in fact carbon. This was only evident with the high initiator concentration samples, as well as the samples that showed several termination modes and contained multiple end-groups.

Therefore, we conclude that the discolouration of PTFE during sintering is due to the elimination reactions from the chain ends producing carbonaceous deposits. This does not occur when initiators that produce stable end-groups, such as tertiary butyl groups or perfluorinated end-groups, are used.

Real-time examination of the decomposition reaction in a solid state NMR may yield better information regarding the reactions and fate of the end-groups as well as the exact mechanism by which carbon is generated.

5.2 Photoinitiated PTFEs

The results show that the photoinitiated APS PTFE is very similar to the commercial sample. The photoinitiated sample does not contain amide or carboxylic salt end groups, unlike the thermally

initiated version, though this is likely because no buffering agent was used in its synthesis. It does contain carboxylic acid end groups.

The sample showed discolouration to a lesser extent than its thermally initiated version. With only COOH end groups that decomposed during sintering, less carbon was deposited into the polymer matrix.

The photoinitiated H_2O_2 sample showed no discolouration post-sintering. The spectroscopic results indicated that the sample possessed no COOH end groups pre-sintering. For this reason not enough carbon was deposited into the matrix to cause discolouration. The H_2O_2 sample was of a very high molecular weight and unlike all the other samples, did not undergo a conformational change during sintering. Therefore it seems that with very high molecular weight, the polymer chains are of sufficient length that the forces required to cause a conformational change are not reached during sintering at 380 °C.

5.3 Controlled photoinitiated polymerisations

All the samples that could be analysed were of high molecular weight, so high that no end groups could be identified. None of these samples discoloured once sintered. Polymerisation was successfully carried out with all individual regions of the electromagnetic spectra, though the yields were very poor for all the individual regions. However, once the regions were combined, the yields improved dramatically with especially the combination of UV and IR proving to be the most effective. It would indeed seem that there are significant synergistic effects at play with photoinitiation of polymerisation. The yield of UV and IR only reached 32 %, far less than the 70 % yield obtained when the same experiment was carried out in complete sunlight, which would suggest more significant synergistic effects occur with sunlight than the simulated conditions that were used in the course of these experiments.

Chapter 6

References

References

1. Medupe, S., *Media Statement by the South African Government on the Establishment of a Pharmaceutical Manufacturing Plant in South Africa*. 2012, Department of Trade and Industry: Cape Town.
2. Plunkett, R.J., *Tetrafluoroethylene polymers*. 1941, Google Patents.
3. Boday, D., *The State of Fluoropolymers.* Advances in Fluorine Containing Polymers, 2012.
4. Ebnesajjad, S., *Fluoroplastics, Volume 1 - Non-Melt Processible Fluoroplastics*. 2001: William Andrew Publishing/Plastics Design Library.
5. Gangal, S.V., *Process for reducing adhesions during suspension polymerization*. 1980, Google Patents.
6. Hyatt, T., *Chemical Economics Handbook: Fluoropolymers*. 2016, IHS Markit: London, United Kingdom.
7. Wood, L., *Global Fluoropolymers Products, Technologies and Applications Market Report 2016 - Research and Markets*. 2016, Research and Markets: Dublin, Republic of Ireland. p. 588.
8. Brubaker, M.M., *Process for polymerizing tetrafluoroethylene*. 1946, E I du Pont de Nemours and Co: US.
9. Joyce, J.R.M., *Process for polymerizing tetrafuloroethylene*, U.P. Office, Editor. 1946, E.I. du Pont de Nemours and Company.
10. Hanford, W.E. and R.M. Joyce, *Polytetrafluoroethylene.* Journal of the American Chemical Society, 1946. **68**(10): p. 2082-2085.
11. Harmon, J. and R.M. Joyce, *Sulfur-dioxide modified tetrafluoroethylene polymer*, U.P. Office, Editor. 1946, E.I. du Pont de Nemours and Company.
12. Dorough, G.L., *Catalytic polymerization of monoolefinic organic compounds*, U.P. Office, Editor. 1946, E.I. du Pont de Nemours and Company.
13. Anonymous, *Improvements in or relating to the polymerisation of tetrafluorethylene*, B.P. Office, Editor. 1946, E.I. du Pont de Nemours and Company: United Kingdom.
14. Renfrew, M.M., *Polymerization of tetrafluoroethylene with dibasic acid peroxide catalysts*, U.P. Office, Editor. 1950, E.I. du Pont de Nemours.
15. Feiring, A.E., et al., *Hydrofluorocarbon solvents for fluoromonomer polymerization*, U.P. Office, Editor. 1993, E.I. du Pont de Nemours and Company.
16. Carlson, D.P., *Tough stable tetrafluoroethylene-fluoroalkyl perfluorovinyl ether copolymers*, U.P. Office, Editor. 1972, E.I. du Pont de Nemours and Company.
17. DeSimone, J.M. and T. Romack, *Nonaqueous polymerization of fluoromonomers*, U.P. Office, Editor. 1997, University of North Carolina.

18. Du, L., et al., *Fluoropolymer synthesis in supercritical carbon dioxide.* The Journal of Supercritical Fluids, 2009. **47**(3): p. 447-457.
19. Berry, K.L. and J.H. Peterson, *Tracer studies of oxidation—Reduction polymerization and molecular weight of "Teflon" tetrafluoroethylene resin.* Journal of the American Chemical Society, 1951. **73**(11): p. 5195-5197.
20. Bankoff, G.S., *Polymeric tetrafluoroethylene dispersions*, U.P. Office, Editor. 1952, E.I. du Pont de Nemours.
21. Berry, K.L., *Process for obtaining dispersions of polyfluorethylenes*, U.P. Office, Editor. 1953, E.I. du Pont de Nemours and Company.
22. Myers, R.L., *Method for polymerizing tetrafluoroethylene*. 1952, General Electric Co US.
23. Robb, E.L. and F.J. Lontz, *Process for producing tetrafluoroethylene polymer compositions*, U.P. Office, Editor. 1952, E.I. du Pont de Nemours and Company.
24. Nakagawa, S., et al., *Process for preparing tetrafluoroethylene/fluoro(alkyl vinyl ether) copolymer*, U.P. Office, Editor. 1985, Daikin Kogyo Company Ltd.
25. Benning, A.F., *Fluorinated aliphatic phosphates as emulsifying agents for aqueous polymerizations*, U.P. Office, Editor. 1951, E.I. du Pont de Nemours.
26. Hercules, D.A., C.A. Parrish, and J.S. Thrasher, *Chapter 9: Research and Non-major Commercial Co- and Terpolymers of Tetrafluoroethylene*, in *RSC Polymer Chemistry Series*. 2017. p. 206-264.
27. Duck, E.W., *Improvements in or relating to the preparation of Fluorine-Containing Polymeric Materials by the Catalytic Polymerisation of Fluorine-Containing Unsaturated Compounds and the resulting Polymeric Materials.*, B.P. Office, Editor. 1960, Petrochemicals Limited.
28. Goerrig, D., H. Jonas, and W. Moschel, *Process for the polymerisation of low-molecular-mass aliphatic halogenated olefins, Part 1*, G.P. Office, Editor. 1955, Farbenfabriken Bayer.
29. Goerrig, D. and H. Jonas, *Process for the polymerisation of low-molecular-mass aliphatic halogenated olefins, Part 2* G.P. Office, Editor. 1956, Farbenfabriken Bayer.
30. Weisz, P.B. and R.D. Goodwin, *Gaseous polymerization by electrical discharge*, U.P. Office, Editor. 1954, Socony-Vacuum Oil Company.
31. Golub, M.A., T. Wydeven, and L.S. Finney, *Plasma homo- and copolymerizations of tetrafluoroethylene and chlorotrifluoroethylene.* Plasmas and Polymers, 1996. **1**(2): p. 173-194.
32. Golub, M.A. and T. Wydeven, *Relative rates for plasma homo- and copolymerizations of a homologous series of fluorinated ethylenes.* Plasmas and Polymers, 1998. **3**(1): p. 35-42.
33. Golub, M.A., T. Wydeven, and A.L. Johnson, *Similarity of plasma-polymerized tetrafluoroethylene and fluoropolymer films deposited by RF sputtering of poly(tetrafluoroethylene).* Langmuir, 1998. **14**(8): p. 2217-2220.

34. Ferrero, F., et al., *On the minimum ignition temperature for the explosive decomposition of tetrafluoroethylene on hot walls: Experiments and calculations.* Journal of Loss Prevention in the Process Industries, 2012. **25**(2): p. 293-301.
35. Puts, G., *Synthesis of novel low-molecular weight polytetrafluoroethylene for pyrotechnic applications*, in *Chemical Engineering*. 2017, University of Pretoria: Pretoria.
36. Duus, H.C., *Thermochemical studies on fluorocarbons - heat of formation of CF_4, C_2F_4, C_3F_6, C_2F_4 dimer, and C_2F_4 polymer.* Industrial & Engineering Chemistry, 1955. **47**(7): p. 1445-1449.
37. Patrick, C.R., *Thermal Stability of Polytetrafluoroethylene.* Nature, 1958. **181**(4610): p. 698-698.
38. Renfrew, M.M. and E.E. Lewis, *Polytetrafluoroethylene. Heat Resistant, Chemically Inert Plastic.* Industrial & Engineering Chemistry, 1946. **38**(9): p. 870-877.
39. Furukawa, G.T., R.E. McCoskey, and M.L. Reilly, *Heat capacity, heats of fusion and vaporization, and vapour pressure of tetrafluoroethylene.* Journal of Research of the National Bureau of Standards, Section A: Physics and Chemistry, 1953. **51**(2): p. 69-72.
40. Lentz, D., et al., *Crystal and Molecular Structures and Experimentally Determined Charge Densities of Fluorinated Ethenes.* Chemistry – A European Journal, 2004. **10**(20): p. 5059-5066.
41. Ruff, O. and O. Bretschneider, *Die Bildung von Hexafluoräthan und Tetrafluoräthylen aus Tetrafluorkohlenstoff.* Zeitschrift für anorganische und allgemeine Chemie, 1933. **210**(2): p. 173-183.
42. Yaws, C.L., *Yaws' Handbook of Thermodynamic and Physical Properties of Chemical Compounds: Physical, Thermodynamic and Transport Properties for 5,000 Organic Chemical Compounds*. 2003, New York: McGraw-Hill.
43. Veretennikof, N.V., L.I. Reshetova, and T.A. Fil'chakova, *Solubility of different fluorine-containing compounds in water and aqueous solutions of fluoro-organic sufactants.* Fizika Khimiya, 1984. **1984**(4): p. 112-114.
44. Von Tress, W.R., *Preparation of Tetrafluoroethylene*, U.P. Office, Editor. 1964, Dow Chemical Company.
45. Farlow, M.W., *Method for the preparation of tetrafluoroethylene*, U.P. Office, Editor. 1963, E. I. du Pont de Nemours and Company.
46. Hercules, D.A., et al., *Preparation of tetrafluoroethylene from the pyrolysis of pentafluoropropionate salts.* Journal of Fluorine Chemistry.
47. Drobny, J.G., *Technology of Fluoropolymers*. 2014, Boca Raton, Florida: CRC Press.
48. Siegemund, G., et al., *Fluorine compounds, organic*, in *Ullmann's Encyclopedia of Industrial Chemistry*. 2000, Wiley-VCH Verlag GmbH & Co. KGaA: Weinheim, Germany.

49. Smith, D.W., S.T. Iacono, and S.S. Iyer, *Handbook of Fluoropolymer Science and Technology*. 2014: Wiley.
50. Hercules, D.A., et al., *Evolution of academic barricades for the use of tetrafluoroethylene (TFE) in the preparation of fluoropolymers*, in *Handbook of Fluoropolymer Science and Technology*, D.W. Smith, S.T. Iacono, and S.S. Iyer, Editors. 2014, John Wiley & Sons, Inc.: Hoboken, New Jersey. p. 413-431.
51. Ferrero, F., et al., *Analysis of the self-heating process of tetrafluoroethylene in a 100-dm³-reactor.* Journal of Loss Prevention in the Process Industries, 2012. **25**(6): p. 1010-1017.
52. Babenko, Y.I., Y.A. Lisochkin, and V.I. Poznyak, *Explosion of tetrafluoroethylene during nonisothermal polymerization.* Combustion, Explosion and Shock Waves, 1993. **29**(5): p. 603-609.
53. Lacher, J.R., G.W. Tompkin, and J.D. Park, *The Kinetics of the Vapor Phase Dimerization of Tetrafluoroethylene and Trifluorochloroethylene1*. Journal of the American Chemical Society, 1952. **74**(7): p. 1693-1696.
54. Ferrero, F., et al., *Self-ignition of tetrafluoroethylene induced by rapid valve opening in small diameter pipes.* Journal of Loss Prevention in the Process Industries, 2013. **26**(1): p. 177-185.
55. Ferrero, F., et al., *Study of the spontaneous ignition of stoichiometric tetrafluoroethylene–air mixtures at elevated pressures.* Journal of Loss Prevention in the Process Industries, 2013. **26**(4): p. 759-765.
56. Abusleme, J.A., *(Co)Polymerisation process of fluorinated olefinic monomers in aqueous emulsion.*, E.P. Organisation, Editor. 1995, Ausimont S.p.A.: Italy.
57. Felix, B., et al., *Process for the preparation of tetrafluoroethylene polymer in aqueous suspension*. 1992, Hoechst AG: US.
58. Felix, B., G. Lohr, and R. Hengel, *Process for the preparation of tetrafluoroethylene polymer in aqueous suspension*, U.P. Office, Editor. 1992, Hoechst Aktiengesellschaft
59. Plyusnin, A.N. and N.M. Chirkov, *Use of stable radicals for the determination of rate constants of elementary processes.* Theoretical and Experimental Chemistry, 1966. **2**(6): p. 563-566.
60. Tobolsky, A.V., *Dead-end Radical Polymerization.* Journal of the American Chemical Society, 1958. **80**(22): p. 5927-5929.
61. Xu, A., et al., *Low-molecular-weight polytetrafluoroethylene bearing thermally stable perfluoroalkyl end-groups prepared in supercritical carbon dioxide.* Polymer International, 2012. **61**(6): p. 901-908.
62. Kroll, A.E. and D.A. Nelson, *Polymerization of tetrafluoroethylene with tertiary butyl peroxide or peracetate*, U.P. Office, Editor. 1956, E.I. du Pont de Nemours and Company.

63. Anonymous, *Process for Polymerizing Perfluorinated Monomers*, B.P. Office, Editor. 1958, E.I. du Pont de Nemours and Company.
64. Brubaker, M.M., *Process for polymerizing tetrafluoroethylene*, U.P. Office, Editor. 1946, E.I. du Pont de Nemours and Company.
65. Halliwell, R.H., *Low Pressure Tetrafluoroethylene Polymerization Process*, U.P. Office, Editor. 1963, E.I. du Pont de Nemours and Company.
66. Felix, B., K. Hintzer, and G. Lohr, *Preparation of a Modified Polytetrafluoroethylene and use thereof*, U.P. Office, Editor. 1996, Hoechst Aktiengesellschaft.
67. Anderson, L.R., W.B. Fox, and F.J. Gefri, *Fluorinated peroxides*, U.P. Office, Editor. 1974, Allied chemical Corporation.
68. Felix, B., K. Hintzer, and G. Lohr, *Preparation of a modified polytetrafluoroethylene and use thereof*. 1996, Hoechst AG: US.
69. Bro, M.I. and C.A. Sperati, *Endgroups in tetrafluoroethylene polymers*. Journal of Polymer Science, 1959. **38**(134): p. 289-295.
70. Berry, K.L., *Aqueous colloidal dispersions of polymers*. 1951, Google Patents.
71. Sperati, C.A. and H.W. Starkweather, *Fluorine-containing polymers. II. Polytetrafluoroethylene*, in *Fortschritte Der Hochpolymeren-Forschung*. 1961, Springer Berlin Heidelberg: Berlin, Heidelberg. p. 465-495.
72. Franck, J. and E. Rabinowitsch, *Some remarks about free radicals and the photochemistry of solutions*. Transactions of the Faraday Society, 1934. **30**: p. 120-130.
73. Rabinowitch, E. and W. Wood, *The collison mechanism and the primary photochemical process in solutions*. Transactions of the Faraday Society, 1936. **32**: p. 1381-1387.
74. Chanda, M., *Introduction to polymer science and chemistry: a problem-solving approach*. 2013: CRC Press.
75. Denisov, E.T., *Cage effects in a polymer matrix*. Die Makromolekulare Chemie, 1984. **8**(S19841): p. 63-78.
76. Herk, L., M. Feld, and M. Szwarc, *Studies of "cage" reactions*. Journal of the American Chemical Society, 1961. **83**(14): p. 2998-3005.
77. Braden, D.A., E.E. Parrack, and D.R. Tyler, *Solvent cage effects. I. Effect of radical mass and size on radical cage pair recombination efficiency. II. Is geminate recombination of polar radicals sensitive to solvent polarity?* Coordination Chemistry Reviews, 2001. **211**(1): p. 279-294.
78. Noyes, R.M., *A treatment of chemical kinetics with special applicability to diffusion controlled reactions*. The Journal of Chemical Physics, 1954. **22**(8): p. 1349-1359.

79. Noyes, R.M., *Effects of diffusion rates on chemical kinetics.* Progress in reaction kinetics and mechanism, 1961. **1**: p. 129-160.
80. Cavanaugh, R.J., *Process for the suspension polymerization of tetrafluoroethylene*, U.P. Office, Editor. 1985, E.I. du Pont de Nemours and Company.
81. Joyce, J.R.M., *Process for polymerizing tetrafuloroethylene*. 1946, Google Patents.
82. Bhanu, V. and K. Kishore, *Role of oxygen in polymerization reactions.* Chemical Reviews, 1991. **91**(2): p. 99-117.
83. Edgar, K.A. and N.D. Albert, *Polymerization of tetrafluoroethylene with tertiary butyl peroxide or peracetate*. 1956, Google Patents.
84. George, K.C., *Polymerization of tetrafluoroethylene with selected metal fluorides*. 1960, Google Patents.
85. Scoggins, L.E. and J.E. Mahan, *Polymerization of tetrafluoroethylene*. 1971, ConocoPhillips Co: US.
86. Nakagawa, S., et al., *Process for preparing tetrafluoroethylene/fluoro(alkyl vinyl ether) copolymer*. 1985, Google Patents.
87. Carlson, N.G., *Polymerization of fluoroethylene monomers*. 1959, Google Patents.
88. Roberts, H.L., *Process for Polymerizing Tetrafluoroethylene with Sulfur Chloride Pentafluoride and Ultraviolet Radiation*, U.P. Office, Editor. 1962, Imperial Chemical Industries.
89. Vogh, J.W., *Process for Polymerizing Tetrafluoroethylene*, U.P. Office, Editor. 1966, The Dow Chemical Company.
90. Clocker, E.T., *Preparation of halogenated olefin polymers using gaseous phase polymerization in the presence of a carbonyl Initiator*, U.P. Office, Editor. 1969, Ashland Oil & Refining Company.
91. Coffman, D.D., *Polymerization process using polyfluoroazoalkanes as initiators*, U.P. Office, Editor. 1962, E.I. du Pont de Nemours and Company.
92. Brothers, P.D., *Polymerization of fluoromonomers in carbon dioxide*. 2000, Google Patents.
93. Sheppard, C.S. and V.R. Kamath, *The selection and use of free radical initiators.* Polymer Engineering & Science, 1979. **19**(9): p. 597-606.
94. Teumac, F.N., *Polymerization of Tetrafluoroethylene and preparation of Fluorocarbon Waxes*, U.P. Office, Editor. 1965, Fred N. Teumac.
95. Jesse, H. and R.M. Joyce Jr, *Sulfur-dioxide modified tetrafluoroethylene polymer*. 1946, US Patent 2,411,722.
96. Dorough, G.L., *Catalytic polymerization of monoolefinic organic compounds*. 1946, Google Patents.
97. George, B.S., *Polymeric tetrafluoroethylene dispersions*. 1952, Google Patents.

98. Mackenzie, R.M., *Polymerization of tetrafluoroethylene with dibasic acid peroxide catalysts*. 1950, Google Patents.

99. Carlson, D.P., *Tough stable tetrafluoroethylene-fluoroalkyl perfluorovinyl ether copolymers*. 1972, Google Patents.

100. Feiring, A.E., et al., *Hydrofluorocarbon solvents for fluoromonomer polymerization*. 1993, Google Patents.

101. Miller, W., *Copolymers of perfluoropropene and tetrafluoroethylene and method of making same*. 1952, Google Patents.

102. Edgar, K.A. and N.D. Albert, *Polymerization of tetrafluoroethylene with tertiary butyl peroxide or peracetate*. 1956, E I du Pont de Nemours and Co: US.

103. Anderson, R.F., W.L. Edens, and H.A. Larsen, *Polytetrafluoroethylene molding powder and its preparation*, U.P. Office, Editor. 1966, E.I. du Pont de Nemours and Company.

104. Fluon. *The Moulding of PTFE Granular Powders*. n.d. [cited 2016 17 February]; Available from: http://www.agcchem.com/newsroom/articles/finish/13-fluon-ptfe-resins/41-processing-note-f1-molding-of-ptfe-granular-powders.

105. Pianca, M., et al., *End groups in fluoropolymers*. Journal of Fluorine Chemistry, 1999. **95**(1–2): p. 71-84.

106. Socrates, G., *Infrared and Raman characteristic group frequencies: tables and charts*. 2004: John Wiley & Sons.

107. Skoog, A., F. Holler, and S. Crouch, *Principles of Instrumental Analysis*. 2007, Belmont, CA 94002-3098: Brooks/Cole.

108. Kuptsov, A. and G.N. Zhizhin, *Handbook of Fourier transform Raman and infrared spectra of polymers*. Vol. 45. 1998: Elsevier.

109. Firsov, S., et al., *Raman spectra and structure of polytetrafluoroethylene subjected to elastic deformation grinding*. Journal of Applied Spectroscopy, 1993. **59**(3): p. 644-647.

110. Koenig, J. and F. Boerio, *Raman scattering and band assignments in polytetrafluoroethylene*. The Journal of Chemical Physics, 1969. **50**(7): p. 2823-2829.

111. Katoh, E., et al., *Structures of polytetrafluoroethylene oligomers as studied by high-resolution solid-state 19F NMR and their properties*. Journal of Molecular Structure, 1995. **355**(1): p. 21-26.

112. Dec, S.F., R.A. Wind, and G.E. Maciel, *Solid-state fluorine-19 NMR study of fluorocarbon polymers*. Macromolecules, 1987. **20**(11): p. 2754-2761.

113. Wilson, C.W. and E.R. Santee, *Polymer analysis by high-resolution NMR, with applications to poly(vinylidene fluoride) and poly(vinyl fluoride)*. Journal of Polymer Science Part C: Polymer Symposia, 1965. **8**(1): p. 97-112.

114. English, A.D. and O.T. Garza, *Composition and Microstructure of Fluoropolymers. High-Temperature High-Resolution FT NMR.* Macromolecules, 1979. **12**(2): p. 351-353.

115. Smith, P. and K.H. Gardner, *Dissolution of poly(tetrafluoroethylene).* Macromolecules, 1985. **18**(6): p. 1222-1228.

116. Li, L., et al., *NMR Study of the Chain End and Branching Units in Poly(vinylidene fluoride-co-tetrafluoroethylene).* Macromolecules, 2013. **46**(18): p. 7146-7157.

117. Twum, E.B., et al., *Characterization of end groups and branching structures in copolymers of vinylidene fluoride with hexafluoropropylene using multidimensional NMR spectroscopy.* European Polymer Journal, 2014. **51**: p. 136-150.

118. Madorskaya, L., et al., *Role of end groups in polyvinylidene fluoride.* Polymer Science USSR, 1983. **25**(10): p. 2490-2496.

119. in *Modern Fluoropolymers, High Performance Polymers for Diverse Applications*, S. J, Editor. 1997, Wiley: New York.

120. Hauptschein, M., *Process for polymerizing vinylidene fluoride*. 1965, Google Patents.

121. Buckmaster, M.D., *Process for the stabilization of fluoropolymers*. 1992, E I du Pont de Nemours and Co: US.

122. Colaianna, P., J.A. Abusleme, and N.D. Fanti, *Process for preparing tetrafluoroethylene copolymers with other perfluorinated monomers*. 1997, Solvay Specialty Polymers Italy SpA: European.

123. Fischer, D., et al., *FTi. r. spectroscopy on electron irradiated polytetrafluoroethylene.* Polymer, 1998. **39**(3): p. 573-582.

124. Fisher, W.K. and J. Corelli, *Effect of ionizing radiation on the chemical composition, crystalline content and structure, and flow properties of polytetrafluoroethylene.* Journal of Polymer science: Polymer chemistry edition, 1981. **19**(10): p. 2465-2493.

125. Gibbard, H.C., *Stabilization of fluoropolymers*, USPTO, Editor. 1993, Asahi Glass Fluoropolymers USA Inc: US.

126. Imbalzano, J.F. and D.L. Kerbow, *Stable tetrafluoroethylene copolymers*, USPTO, Editor. 1988, E I du Pont de Nemours and Co: US.

127. Morgan, R.A. and W.H. Sloan, *Extrusion finishing of perfluorinated copolymers*, USPTO, Editor. 1986, E I du Pont de Nemours and Co: US.

128. Pellerite, M.J., *Unusual reaction chemistry in thermal decomposition of alkali metal 2-alkoxy-2, 3, 3, 3-tetrafluoropropionate salts.* Journal of Fluorine Chemistry, 1990. **49**(1): p. 43-66.

129. Vanni, H. and J. Rabolt, *Fourier transform infrared investigation of the effects of irradiation on the 19 and 30° C phase transitions in polytetrafluoroethylene.* Journal of Polymer Science: Polymer Physics Edition, 1980. **18**(3): p. 587-596.

130. Courtenay, S.R., *Stabilized tetrafluoroethylene-fluoro-olefin copolymers having-cf2h end groups*. 1963, Google Patents.

131. Moynihan, R.E., *The Molecular Structure of Perfluorocarbon Polymers. Infrared Studies on Polytetrafluoroethylene1*. Journal of the American Chemical Society, 1959. **81**(5): p. 1045-1050.

132. Legeay, G., et al., *AF fluoropolymer for optical use: spectroscopic and surface energystudies; comparison with other fluoropolymers.* European Polymer Journal, 1998. **34**(10): p. 1457-1465.

133. Beg, M.A.A. and H.C. Clark, *CHEMISTRY OF THE TRIFLUOROMETHYL GROUP: PART V. INFRARED SPECTRA OF SOME PHOSPHORUS COMPOUNDS CONTAINING CF3*. Canadian Journal of Chemistry, 1962. **40**(3): p. 393-398.

134. Puts, G., *Conjugated double bonds possible cause of discolouration in sintered PTFE*, W. Venner, Editor. 2017: University of Pretoria.

135. Wavefunction, I., *Spartan'06*. Wavefunction, Inc.: Irvine, CA.

136. Suwa, T., M. Takehisa, and S. Machi, *Melting and crystallization behavior of poly(tetrafluoroethylene). New method for molecular weight measurement of poly(tetrafluoroethylene) using a differential scanning calorimeter.* Journal of Applied Polymer Science, 1973. **17**(11): p. 3253-3257.

137. Mark, H.F., *Encyclopedia of Polymer Science and Technology: Step-reaction polymerization to Thermoforming*. Vol. 13. 1970: Interscience Publishers.

138. Sherratt, S., *Polytetrafluoroethylene.* Kirk-Othmer Encyclopedia of Chemical Technology, ed, 1966. **2**: p. 805-31.

139. Lappan, U., et al., *The estimation of the molecular weight of polytetrafluoroethylene based on the heat of crystallisation. A comment on Suwa's equation.* Macromolecular Materials and Engineering, 2004. **289**(5): p. 420-425.

140. Koch, E.C., *Metal-Fluorocarbon Based Energetic Materials*. 2012, New York: Wiley.

141. Ikeda, S., et al., *Formation of crosslinked PTFE by radiation-induced solid-state polymerization of tetrafluoroethylene at low temperatures.* Radiation Physics and Chemistry, 2008. **77**(4): p. 401-408.

142. Mehta, A. *Introduction to the Electromagnetic Spectrum and Spectroscopy*. 2011 [cited 2017 11 July]; Analytical Chemistry Notes].

143. NASA. *Sun: By the Numbers*. n.d. [cited 2017 11 July].

144. Anon. *Spectrum of Solar Radiation*. 2013 [cited 2017 11 July]; Available from: http://commons.wikimedia.org/wiki/File:Solar_spectrum_ita.svg.

145. MacAdam, D.L., *Color measurement: theme and variations*. Vol. 27. 2013: Springer.

146. Wyszecki, G. and W. Stiles, *Color Science: Concepts and Methods, Quantitative Data and Formulas*. 1967, John Wiley and Sons, Inc., New York, London, Sidney.

147. Anon. *Spectral composition of sunlight at Earth's surface*. 2014 [cited 2017 12 July]; Available from: https://en.wikipedia.org/wiki/File:Spectrum_of_Sunlight_en.svg.

148. Puts, G., *Non-reactivity of HFP*, W. Venner, Editor. 2016.

149. Lappan, U., et al., *Number-average molecular weight of radiation-degraded poly(tetrafluoroethylene). An end group analysis based on solid-state NMR and IR spectroscopy*. Polymer, 2002. **43**(16): p. 4325-4330.

150. Nassau, K., *The fifteen causes of color: The physics and chemistry of color*. Color Research & Application, 1987. **12**(1): p. 4-26.

151. Lewis, R.J., *Hawley's Condensed Chemical Dictionary*. Fifteenth ed. 2007, Hoboken, New Jersey: John Wiley & Sons, Inc.

152. Tobolsky, A.V., C.E. Rogers, and R.D. Brickman, *Dead-end Radical Polymerization. II*. Journal of the American Chemical Society, 1960. **82**(6): p. 1277-1280.

153. Terayama, K. and M. Ikeda, *Study on Thermal Decomposition of MnO_2 and Mn_2O_3 by Thermal Analysis*. Transactions of the Japan Institute of Metals, 1983. **24**(11): p. 754-758.

Appendix A

Polymer analysis techniques

A.1 FTIR spectroscopy

The Mid-IR range consists of wavenumbers between 4000 and 200 cm^{-1}. IR absorption, emission and reflection spectra can all be rationalised by the assumption that all these arise from various changes in energy brought about by transitions of molecules from one vibrational or rotational energy state to another [107]. IR radiation is not energetic enough to bring about the kinds of electronic transitions that ultraviolet and visible radiation are capable of. Absorption of IR radiation is therefore confined largely to molecular species that have small energy differences between various vibrational and rotational states. To absorb IR radiation, a molecule must undergo a net change in dipole moment as it vibrates or rotates. Only under these circumstances can the alternating electric field of the radiation interact with the molecule and cause changes in the amplitude of one of its motions. As a molecule vibrates, a regular fluctuation in its dipole moment occurs and a field is established that can interact with the electric field associated with radiation. If the frequency of the radiation exactly matches a natural vibrational frequency of the molecule, absorption of the radiation takes place that produces a change in the amplitude of the molecular vibration. Similarly the rotation of asymmetric molecules around their centres of mass results in periodic dipole moment fluctuations that allow interaction with the radiation field. No net change in dipole moment occurs during the vibration or rotation of homonuclear species such as O_2, N_2 or Cl_2. As a result, compounds such as this cannot absorb IR radiation [107].

The relative positions of atoms in a molecule are not fixed but instead fluctuate continuously as a consequence of a multitude of different types of vibrations and rotations about the bonds in the molecule. Analyses of large molecules becomes increasingly difficult. Not only do large molecules have a large number of vibrating centres, but also interactions among several centres can occur and must be taken into account for a complete analysis. Vibrations fall into two basic categories of stretching and bending. A stretching vibration involves a continuous change in the interatomic distance along the axis of the bond between two atoms. Bending vibrations are characterised by a change in the angle between two bonds and are of four types: scissoring, rocking, wagging and twisting [107]. These can be seen schematically in Figure 109. All these vibration types may be possible in a molecule containing more than two atoms. In addition, interaction or coupling of vibrations can occur if the vibrations involve bonds to a single central atom. Coupling results in a change in the characteristics of the vibrations involved.

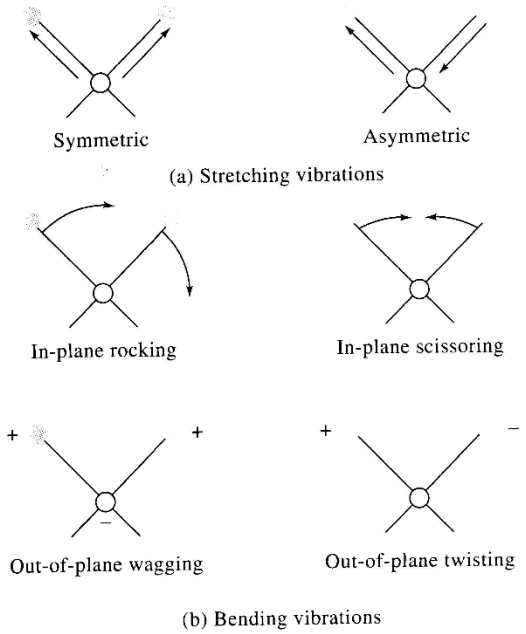

Figure 109: *Types of molecular vibrations. + indicates motion outwards from the page and – indicates motion into the page [107].*

Coupling of vibrations is a common phenomenon. As a result, the position of an absorption banc corresponding to a given organic functional group cannot be specified exactly. Although interaction effects may lead to uncertainties in the identification of functional groups contained in a compound, it is this very effect that provides the unique features of IR spectroscopy that are so important for the positive identification of a specific compound [107].

Fourier transform infrared spectrometers are commonly used because of their speed, reliability, signal-to-noise advantage and convenience.

According to Lappan *et al.*, [149] PTFE predominantly undergoes change scission when subjected to irradiation at room temperature in air or vacuum. The result is a dramatic drop in mechanical properties. This has been used to convert PTFE into low molecular weight micropowders which can be compounded into plastics, coatings and lubricants. They also report that high-speed MAS ^{19}F NMR provides detailed and quantitative information on structural changes in PTFE and that NMR and IR were used to calculate number-average molecular weight of irradiated PTFE.

IR spectroscopy is known to be very sensitive to formation of carbonyl species in perfluorinated polymers because bands of the C=O stretching vibrations are relatively strong and appear in a region of the spectrum where perfluorinated polymers have only weak overtones and combination bands [131].

One major advantage of the use of infrared spectra is that there is a vast base of reference spectra which can easily be referred to. The base of reference spectra for IR is much more well established than that of Raman spectra for example. This is one of several reasons why IR is still widely preferred to Raman spectroscopy. Some other reasons include but are not limited to:

- Raman spectrometers tend to be more expensive than IR spectrometers and are therefore less readily available to the analyst. IR is generally readily available and is a very versatile technique.
- Raman spectroscopy requires more skill by the operator, both in experimental and interpretational aspects.
- IR techniques are more established than Raman and therefore enjoy greater amount of support.
- Quantitative measurements are more involved in Raman spectroscopy. In IR spectroscopy, the concentration of a functional group is linearly dependent on the absorbance of its related band and therefore easily quantifiable.

However, Raman Spectroscopy does offer some advantage over IR spectra when identifying certain bands which are weak or inactive in IR, for example, those due to the stretching vibrations of C=C, C≡C, C≡N, C-S, S-S, N=N and O-O functional groups. These exhibit strong bands when examined by Raman spectroscopy and are often found in polymers. However, these bands are not expected to be found in PTFE, and therefore Raman spectroscopy should not be required. Although not always true, as a general rule, it can be assumed that bands that are strong in infrared spectra are often weak in Raman spectra and bands that are strong in Raman often tend to be weak in IR spectra. Bands due to the following groups: OH, C=O, C-O, S=O, SO_2, P=O, PO_2, NO_2, *etc.* are strong in IR [106].

In general, the IR spectra of very large molecules are broad and so it is often difficult to identify the origins of particular bands. It would be expected that, similarly to many large natural molecules, the spectra of synthetic polymers would consist of broad absorptions with few discernible features. Fortunately for polymer analysts, the fundamental vibrations occur in relatively narrow ranges [106]. Therefore, unlike the spectra of many large, naturally occurring molecules, the spectra of most synthetic polymers usually consist of sharp bands to which the normal group frequency approach may be applied.

To put it simply, the polymer chains are so long that the vast majority of functional groups experience very similar environments and interactions and therefore their vibrational motions are very similar. Consequently, they occur over narrow ranges, which makes them easy to distinguish

on FTIR spectra. However, in order to make such a statement, various assumptions and/or approximations must be made. These include, but are not limited to:

- chain folding does not have an influence on the vibrations of the group
- that interactions between the chains do not occur

To simplify matters further, it should be considered that each polymer molecule is isolated from its neighbours or, alternatively, that all polymer molecules (therefore the repeat unit and functional groups) experience an averaged-out environment or interaction [106]. Therefore, a change in the electric dipole or polarizability induced in one part of the polymer molecule may be cancelled by the opposite effect elsewhere in the chain. Consequently, it is only when the vibrations of the functional groups are in phase that a net change in dipole or polarisibility would occur and the vibration would be Raman or IR active and a band observed. As a result of this, the IR and Raman spectra of polymers generally consist of sharp bands [106].

Generally, crystalline substances have spectra that contain sharp discrete bands whereas non-crystalline materials contain broad, diffuse bands. The vibrational spectra of crystalline polymers also exhibit a high degree of definition (high peak intensity) because of the aforementioned in-phase vibrational motions that result in active spectral bands in the IR spectrum.

The vibrational modes of crystalline polymers may be considered in terms of their unit cell and the symmetry associated with this cell. The number of atoms in the unit cell determines the maximum number of fundamental vibrations that may occur, rather than the number of atoms in the polymer repeat unit. Therefore, because more than one polymer chain is often involved as part of the unit cell, the number of fundamental vibrations that may occur is almost always greater than that determined by considering the number of atoms in the isolated repeat unit. The vibrational motions of a crystalline polymer may be considered as having two origins, internal and lattice. Lattice modes of vibration are those due to polymer chains moving relative to each other and occur at low wavenumbers, generally below 150 cm^{-1} [106]. Internal vibrational modes are those due to the motions of the atoms of a chain relative to each other. Generally, these occur between 150 cm^{-1} and 4000 cm^{-1}. In a crystalline polymer, more internal modes of vibration can occur than if a polymer molecule were considered as an isolated entity. The number is dependent on the structure of the unit cell, *i.e.* it is dependent on the number of chains involved in the unit cell. The internal vibration modes may be in or out-of-phase with each other. Due to intermolecular interactions of the chains, in-phase and out-of-phase vibrations occur at different frequencies and so their associated internal vibrations occur at definite and fixed values. This can lead to

phenomena such as a doublet band appearing in the crystalline phase where a single band would be expected [106]. The intensities of these components of the doublet may not be equal because the absorptivities for the two vibrations may differ.

The observation that crystalline polymers display more bands than expected can be explained by crystallinity results in a perturbation of the vibrational modes. This leads to the conclusion that the intensity ratios of bands is related to the degree of crystallinity of the polymer. If the crystallinity of a sample is decreased, the bands become broader and often new bands appear [106]. These new bands are due to the vibrational motions of different conformations and/or rotational configurations of the parts of the polymer chains present in the disordered phases.

The most pronounced changes in the spectrum with regards to crystallinity in PTFE occur in the 850 – 700 cm^{-1} region and at 384 cm^{-1}. Several bands were found in these regions which decrease regularly in intensity with increasing crystallinity [131]. If it is assumed that a polymer can be treated as a two component mixture of amorphous and crystalline regions with no regards for the boundary material, both density and the amorphous band intensities are linear functions of volume fraction crystallinity and therefore, of each other [131]. In practice the ratio of the 778 and 2367 cm^{-1} band intensities are measured and used to determine the crystallinity.

The intensities of bands are related to the concentrations of the functional groups producing them, allowing quantitative analysis if required [106].

Socrates [106], provides flowcharts that can be used to assist in the identification of polymers. Such a flowchart can be seen in Figure 110. The flowcharts are based on strong bands that occur in relatively interference free regions. Unfortunately it is very uncommon that identifying polymers or more specifically their end groups is as straightforward as following a simple flowchart. The spectra of polymers may differ from those on which the flowcharts are based and polymers prepared by different methods or using different initiators *etc.*, may have different spectra. If polymers are examined spectroscopically without removing additives such as fillers, plasticisers *etc.*, then their infrared spectra may be drastically affected. Fortunately this was not a problem during the course of the experimental work completed for this document, as all the produced polymer was virgin PTFE, which was examined *as polymerised*.

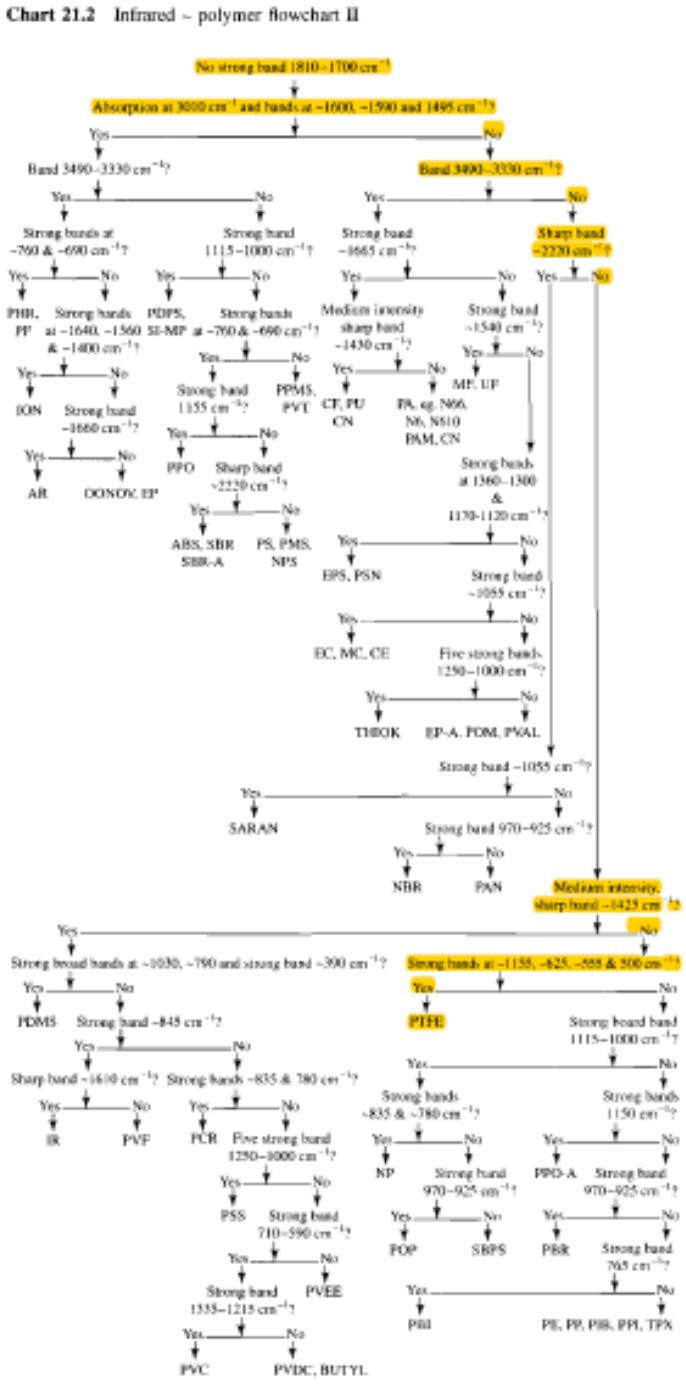

Figure 110: *Flowchart to aid in the identification of polymers using IR spectrum [106]. The path to PTFE is highlighted for the reader's convenience.*

A.2 Raman spectroscopy

Raman spectroscopy is a spectroscopic technique used to observe vibrational, rotational, and other low-frequency modes in a system. Raman spectroscopy is commonly used in chemistry to provide a structural fingerprint by which molecules can be identified. Infrared spectroscopy yields similar, but complementary, information.

The Raman effect occurs when electromagnetic radiation interacts with a solid, liquid, or gaseous molecule's polarizable electron density and bonds. The spontaneous effect is a form of inelastic light scattering, where a photon excites the molecule in either the ground (lowest energy) or excited rovibronic state (a rotational and vibrational energy level within an electronic state). This excitation puts the molecule into a virtual energy state for a short time before the photon scatters inelastically. Inelastic scattering means that the scattered photon can be of either lower or higher energy than the incoming photon, compared to elastic, or Rayleigh, scattering where the scattered photon has the same energy as the incoming photon. After interacting with the photon, the molecule is in a different rotational or vibrational state. This change in energy between the initial and final rovibronic states causes the scattered photon's frequency to shift away from the excitation wavelength (that of the incoming photon), called the Rayleigh line [108].

For the total energy of the system to remain constant after the molecule moves to a new rovibronic state, the scattered photon shifts to a different energy, and therefore a different frequency. This energy difference is equal to that between the initial and final rovibronic states of the molecule. If the final state is higher in energy than the initial state, the scattered photon will be shifted to a lower frequency (lower energy) so that the total energy remains the same. This shift in frequency is called a Stokes shift, or downshift. If the final state is lower in energy, the scattered photon will be shifted to a higher frequency, which is called an anti-Stokes shift, or upshift.

For a molecule to exhibit a Raman effect, there must be a change in its electric dipole-electric dipole polarizability with respect to the vibrational coordinate corresponding to the rovibronic state. The intensity of the Raman scattering is proportional to this polarizability change. Therefore, the Raman spectrum, scattering intensity as a function of the frequency shifts, depends on the rovibronic states of the molecule.

Typically, a sample is illuminated with a laser beam. Electromagnetic radiation from the illuminated spot is collected with a lens and sent through a monochromator. Elastic scattered radiation at the wavelength corresponding to the laser line (Rayleigh scattering) is filtered out by either a notch

filter, edge pass filter, or a band pass filter, while the rest of the collected light is dispersed onto a detector.

Spontaneous Raman scattering is typically very weak, and as a result the main difficulty of Raman spectroscopy is separating the weak inelastically scattered light from the intense Rayleigh scattered laser light. Historically, Raman spectrometers used holographic gratings and multiple dispersion stages to achieve a high degree of laser rejection. In the past, photomultipliers were the detectors of choice for dispersive Raman setups, which resulted in long acquisition times. However, modern instrumentation almost universally employs notch or edge filters for laser rejection and spectrographs either axial transmissive (AT), Czerny–Turner (CT) monochromator, or FT (Fourier transform spectroscopy based) detectors.

A.3 NMR spectroscopy

Nuclear Magnetic Resonance Spectroscopy, or NMR, is based on the measurement of absorption of electromagnetic radiation in the radio frequency region of approximately 4 to 900 MHz. In contrast to IR spectroscopy, the nuclei of atoms rather than outer electrons are involved in the absorption process. To cause nuclei to develop the energy states required for absorption to occur, it is necessary to place the analyte in an intense magnetic field. NMR spectroscopy is one of the most powerful tools available to chemists and biochemists for elucidating the structure of chemical species [107].

The theoretical basis for NMR spectroscopy was proposed by W. Pauli in 1924. He suggested that certain atomic nuclei have the properties of spin and magnetic moment and that exposure to a magnetic field would lead to splitting of their energy levels. In the years following the discovery of NMR, chemists became aware that the molecular environment influences the absorption of radio frequency radiation by a nucleus in a magnetic field and that this effect can be correlated with molecular structure [107]. Two general types of NMR spectrometers are currently in use namely, continuous-wave (CW) and Fourier transform (FT-NMR). Currently, the FT-NMR dominates the market. In FT-NMR instruments, the sample is irradiated with periodic pulses of RF energy that are directed through the sample right angles to the magnetic field. These excitation pulses elicit a time-domain signal that decays in the interval between pulses. This signal is then converted to a frequency domain signal by using a Fourier-transformation to give an absorption spectrum [107].

To account for the properties of certain nuclei, it must be assumed that they possess the property of spin. Nuclei with spin have angular momentum, p. This maximum observable component of

this angular momentum is quantised and must be an integral or a half-integral multiple of $h/2\pi$, where h is Planck's constant. The maximum number of spin components or values for p for a particular nucleus is its spin quantum number, I. A spinning, charged nucleus creates a magnetic field analogous to the field produced when electricity flows through a coil of wire. The resulting magnetic moment, μ, is oriented along the axis of spin and is proportional to the angular momentum p. Therefore:

$$\mu = \gamma\rho$$

where the proportionality constant, γ, is the magnetogyric or gyromagnetic ratio which has different values for each type of nucleus. The relationship between nuclear spin and magnetic moment leads to a set of observable magnetic quantum states m given by:

$$m = I, I-1, I-2, \ldots, -I$$

Therefore, the nuclei to be considered will have two magnetic quantum numbers, $m = +\frac{1}{2}$ and m = -½.

The nuclei that have the greatest use to organic chemists are ^{1}H, ^{13}C, ^{19}F and ^{31}P. The spin quantum number for these nuclei is ½.

In a FT-NMR measurement, nuclei in a strong magnetic field are subjected periodically to very brief pulses of intense RF radiation. The interval between pulses is usually one to several seconds. During these intervals, a time domain radio frequency (RF) signal is emitted by the excited nuclei as they relax. This signal is known as the free-induction decay (FID) signal and can be detected with a radio receiver coil perpendicular to the static magnetic field. The FID signal is digitised and stored in a computer for data processing. The FID signals from numerous successive pulses are added together to improve the signal-to-noise ratio. The resulting summed data is then converted to a frequency domain signal by a Fourier transformation [107].

There are several kind of NMR spectra, depending on the kind of instrument used, the type of nucleus involved, the physical state of the sample, the environment of the analyte nucleus and the purpose of the data collection. However, most NMR spectra can be classified as either wide line or high resolution [107]. Wide line spectra are those in which the bandwidth of the source of the lines is large enough that the fine structure due to chemical environment is obscured. They are useful for the quantitative determination of isotopes and for studies of the physical environment of the absorbing species. Wide line spectra are usually obtained at relatively low magnetic field strength [107].

Most NMR spectra are high resolution and are collected by instruments capable of differentiating between very small frequency differences 0.01 ppm or less. The frequency of RF radiation that is absorbed by a given nucleus is strongly affected by its chemical environment, *i.e.* by nearby electrons and nuclei. This means that even simple molecules provide a wealth of spectral information that can be used to determine the chemical structure.

There are two main types of environmental effects present when performing NMR spectroscopy, namely chemical shift and spin-spin splitting. Chemical shift is caused by small magnetic fields generated by electrons as they circulate around nuclei. Without delving too much into the mathematics thereof, suffice it to say that these small magnetic fields oppose the applied magnetic field. This means that the nuclei of the atoms are exposed to an effective field that is smaller than the applied field, therefore the nucleus is said to be shielded from the full effect of the primary applied field. This in turn means that the strength of the applied magnetic field must be higher than the theoretical strength required to induce nuclear resonance [107].

Spin-spin splitting causes chemical shift resonance peaks to split into more peaks. It occurs as the magnetic moment of a nucleus interacts with the magnetic moments of immediately adjacent nuclei [107]. A spinning nucleus creates a magnetic field which affects the distribution of electrons in its bonds to other nuclei. This change in electron distribution then produces changes in the magnetic fields of the adjacent nuclei and causes splitting of energy levels and hence multiple transitions. This magnetic coupling of nuclei that is transmitted by bonding electrons is often referred to as a polarization interaction. Therefore, the fine structure of split resonance peaks of a specific group can be attributed to the effect of the spins of the adjacent groups. This effect, known as coupling, are independent of the applied field and are superimposed on the effects of the chemical shift [107]. The coupling effect is quantified by the coupling constant, *J*.

Both the chemical shift and spin-spin splitting are important in structural analysis. Experimentally the two are easily distinguished, because the peak separations resulting from a chemical shift are directly proportional to the field strength or to the oscillator frequency. Therefore, if the field strength is increased, the distance horizontal distance between any set of resonances is increased proportionally to the increase in field strength. In contrast, the distance between the fine structure peaks within a group, caused by spin-spin coupling, is not altered by this frequency change [107].

The chemical shift is used to identify functional groups and to aid in in determining structural arrangements of groups. These applications are based on empirical correlations between structure and shift. A number of correlation charts and tables have been published [107].

The absorption bands of many groups consist of several narrow resonances that can be routinely separated with a high-resolution instrument.

The magnetic effect transmitted to the receiving group on the adjacent carbon atom is determined by the instantaneous spin combinations in the donating group. If the spins are paired and opposed to the external field, the effective applied field on the receiving group is slightly decreased. Therefore a higher field strength is needed to bring them into resonance, which results in an upfield shift. Spins that are paired and aligned with the applied field result in a downfield shift. The combinations where the spins are opposed have no effect on the resonance, because they cancel each other out. The area under the peaks is proportional to the amount of spin combinations involved, *i.e.* the middle peak of a triplet is twice that of the other two peaks, because two spin combinations are involved. A triplet occurs when there are two of the donating group that affect the receiving group. When there are three of the same donating group, there are eight possible spin combinations. However, among these are two groups containing three combinations that have equivalent magnetic effects. Therefore this peak will be split into a quartet having areas in the ratio 1: 3: 3: 1. This gives rise to the general rule that the number of peaks in a split band in a first-order spectrum is equal to the number n of magnetically equivalent protons on adjacent atoms plus one. The number of such peaks is referred to as the multiplicity [107].

The following rules given by Skoog et al., govern the appearance of first-order spectra:

1. Equivalent nuclei do not interact with one another to give multiple absorption peaks.
2. Coupling constants decrease significantly with separation of groups and coupling is seldom observed at distances greater than four bond lengths.
3. The multiplicity of a band is determined by the number, n, of magnetically equivalent protons on the neighbouring atoms and is given by the quantity $n + 1$.
4. If the protons on atom B are affected by protons on atoms A and C that are non-equivalent, the multiplicity of B is equal to $(n_A + 1)(n_C + 1)$, where n_A and n_C are the number of equivalent protons on A and C respectively.
5. The approximate relative areas of a multiplet are symmetric around the midpoint of the band and are proportional to the coefficients of the terms in the expansion $(x + 1)^n$.
6. The coupling constant is independent of the applied field, therefore multiplets are readily distinguished from closely spaced chemical-shift peaks by running spectra at two different field strengths.

Appendix B

Photos of pressed PTFE discs, pre and post-sintering

B.1 APS initiated PTFE

Experiment number	Unsintered	Sintered 2 min	30 min
1			n/a
2	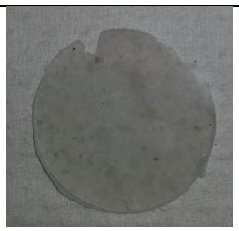		
3			
4			
5	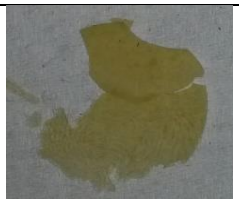		n/a
6		n/a	n/a
7			

8			
9			
10	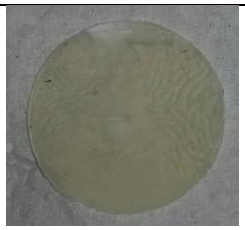		
11			
12			n/a
13			n/a
14			

15			
16			
17		n/a	
18	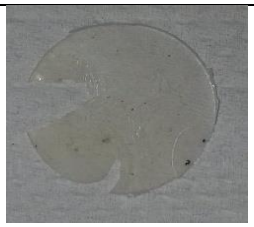	n/a	
Commercial PTFE		n/a	
K_2CO_3		n/a	

B.3 Photoinitiated PTFE

Experiment	Unsintered	Sintered 5 min	Sintered 30 min
H_2O_2 in sunlight #1		n/a	
H_2O_2 in sunlight #2			
APS in sunlight		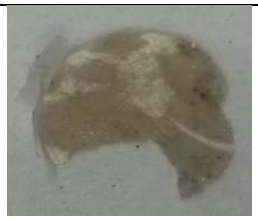	
H_2O_2 exposed to Vis, IR, UV			n/a
H_2O_2 exposed to Vis, IR	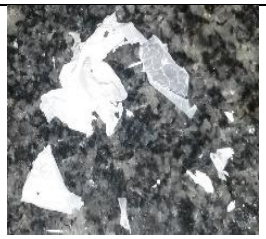		n/a
H_2O_2 exposed to IR, UV		n/a	n/a
H_2O_2 exposed to UV, Vis		n/a	n/a

B.4 Thermally initiated PTFE

Initiator	Unsintered	Sintered 30 min
1 % DTBP		
10 % DTBP		
30 % DTBP		
1 % $KMnO_4$		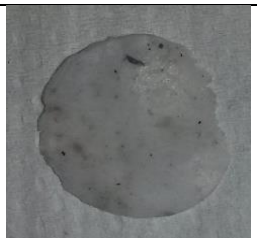
10 % $KMnO_4$		
30 % $KMnO_4$	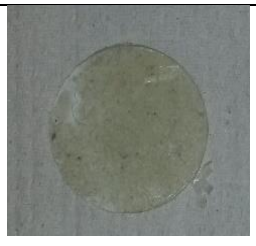	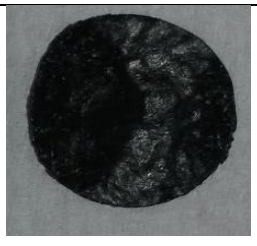

Sodium persulfate	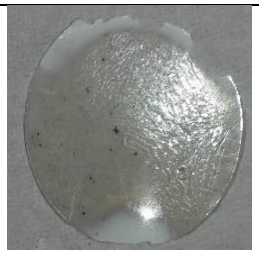	
30 % $KMnO_4$ after additional 24 h wash.